The University of
Nottingham

Development of Continuous Microbial Fuel Cell for renewable energy production from wastewater

By

Huaining Hu, MSc., BEng.

Thesis submitted to the University of Nottingham

for the degree of Doctor of Philosophy

October 2009

Summary

There is around 9.5 kJ/L of energy contained in UK wastewater which is wasted through traditional aeration treatment. Microbial fuel cell (MFC) technology provides a new approach to carry the promise of both treating wastewater without aeration and producing renewable energy in the form of electricity and H_2. This work has contributed to making this a reality.

In this work, MFC designs were developed and constructed to test their energy performances. The power densities ranged from 13.3 mW/m^2 to 30 mW/m^2. The coulombic efficiency based on the contained substrates is in the range of 1 % to 7 %. The Chemical Oxygen Demand (COD) removal conversion per pass of MFCs arrived at 3.0 %. The H_2 recovery rate was about 14 % with H_2 yield of 11.6 mg/g COD. Comparative study suggested that continuous flow, no membrane and single chamber design can be used effectively in MFC for further application.

The high temperature CO_2 oxidation treatment of carbon anode materials resulted in an improvement of power by a factor of 2 when applied to MFC. Scanning Electron Microscopy (SEM) study and the textural property measurements based on Brunauer Emmett Teller (BET) theory suggested that treatments help bacteria to grow on the material surface resulting in power improvement. Graphite as cathode decreased the MFC power density by around 50 % compared to that of MFC with Pt contained cathode, but the cost is 1/1000 that of the Pt makes it a very attractive alternative.

A typical industry case study for implementation of MFC were carried out that considerable energy cost savings and water disposal savings can offset the installation within 1-2 year. It shows that the MFC technology has a promising future for the sustainable development of the world with further research.

Acknowledgement

I would hereby like to acknowledge the following people and groups who have contributed towards to this thesis.

My supervisor Dr John Andresen to whom I am indebted for his patience concerning the accomplishment of this thesis and passing on his knowledge of the dark art of microbial fuel cells and for all of his enthusiastic support.

All of the members past and present of our research group under the supervision of Dr. John Andresen deserve a big thank you to help and support my research work.

I am eternally grateful to all the collaborators I have worked with over the past 3 years in both L4 and L3, especially Mahmud Maythem, Bin Gao, Dong Liu, Ziyan Li, Sujing Li, Chuang Peng and Junru Li who help me to do the potential harmful work and heavy labor work during my pregnant period.

I would like to thank my partner Yunfeng Gu and family to give me the strongest spiritual and academic support.

Finally I want to thank my baby girl Yinuo Gu who gives me endless energy to carry on my research.

Affirmation

The work presented in this dissertation was undertaken at the Department of Chemical and Environmental Engineering, University of Nottingham, between October 2005 and March 2009. This dissertation is the result of my own work and some of the work done in collaboration was indicated in the text. Neither the present dissertation, nor any part thereof, has been submitted previously for a degree to this or any other university.

Table of Contents

Chapter 1 Introduction 1

1.1 Sustainability challenges 1

1.2 Aim and Objectives 3

1.2.1 Aim 3

1.2.2 Objectives 3

1.3 Thesis outline 4

Chapter 2 Background 5

2.1 Global issues for sustainability 5

2.1.1 Energy Demand 5

2.1.2 Water Demand 8

2.2 Principles of Microbial Fuel Cells 10

2.2.1 History and classification 10

2.2.2 Basic principles 12

2.2.3 MFC materials 15

2.2.4 Types of MFCs 17

2.2.4.1 MFC feed: actual vs. artificial wastewater 17

2.2.4.2 MFC operation: Single vs. mixed microbial culture 19

2.2.4.3 MFC built design 20

2.2.5 Microbiological aspects of MFCs 21

2.2.5.1 Transport mechanisms of substrate to bacteria 21

2.2.5.2 Bacteria metabolism 21

2.2.5.3 Electron migration out of bacteria 25

2.2.5.4 Proton migration out of bacteria 25

2.2.6 Electrochemical aspects of MFCs 25

2.2.6.1 Open Circuit Potential 25

2.2.6.2 Electrode potentials 26

2.2.7 Hydrogen production from MFCs 27

2.2.7.1 Hydrogen production from conventional MFCs 27

2.2.7.2 Anaerobic MFC with additional voltage 28

2.3 Performance and Developmental aspects of MFCs 30

2.3.1 MFCs performance expressions 30

2.3.1.1 Energy output 31

2.3.1.1.1 Power density 31

2.3.1.1.2 Polarization curve 33

2.3.1.1.3 H_2 production 34

2.3.1.2 Energy conversion efficiency 35

2.3.1.2.1 Coulombic efficiency 35

2.3.1.2.2 Energetic efficiency 37

2.3.1.2.3 H_2 recovery rate 38

2.3.1.3 Substrate consumption 40

2.3.2 MFC design developments 41

2.3.3 Materials involved in MFCs 46

2.3.3.1 Anode Materials 46
2.3.3.2 Cathode materials 50
2.4 Current MFC limitations 52
2.4.1 Limitations Related to microbiology 52
2.4.1.1 Diffusion of substrate towards bacteria 52
2.4.1.2 Bacteria metabolism and activation energy 53
2.4.1.3 Mixed species versus single species limitations 53
2.4.2 Limitations related to electrochemistry 54
2.4.2.1 Energy conversion efficiency 54
2.4.2.2 Energy losses 56
2.4.2.2.1 Activation losses 56
2.4.2.2.2 Ohmic losses 57
2.4.2.2.3 Concentration diffusion losses 57
2.4.2.2.4 Identifying energy losses 58
2.4.3 Limitations related to materials 58
2.4.3.1 Anode 58
2.4.3.2 Cathode 58
2.4.3.3 Membrane 59
2.4.3.4 Medium 59
2.4.4 Limitations related to construction conditions and costs 60
2.5 Related technologies 61
2.5.1 Traditional water treatment approaches 61
2.5.2 Anaerobic digestion 63
2.5.3 Sludge removal and MFC 63
2.6 Summary 64
Chapter 3 Experimental 66
3.1 Microbes and feed 66
3.1.1 Procurement 66
3.1.2 Incubation 66
3.1.3 Substrates 66
3.1.4 Artificial wastewater 67
3.2 Reactor manufacture and running conditions 67
3.2.1 Reactor factors 67
3.2.1.1 Operating conditions 67
3.2.1.2 Reactor setup 68
3.2.1.3 Cation exchange membrane 68
3.2.1.4 Polydimethylsiloxane material fabrication 68
3.2.2 Electrode materials and connections 69
3.2.2.1 Anode materials 69
3.2.2.2 Cathode materials 70
3.2.2.3 Flow and wiring connections 71
3.2.2.4 Gas sampling 71
3.3 Testing procedures and instruments 72
3.3.1 Tests related to wastewater 72

3.3.1.1 COD 72
3.3.1.2 BOD 72
3.3.2 Scanning Electron Microscopy 73
3.3.3 Performance of MFC 73
3.3.3.1 Micro GC for gas composition 73
3.3.3.2 GC for organic in wastewater 75
3.3.3.3 Cell voltage data logger 75
3.3.3.4 External resistance system 76
3.3.3.5 Potentiostat 77
3.3.3.6 Surface properties tests 77
3.3.3.7 Calorific value test 78
3.3.3.8 Anode treatment procedures 79
Chapter 4 Development of continuous MFC reactor setup 80
4.1 Main reactor setup parameters 80
4.2 Miniature MFC 80
4.2.1 Micro-channel MFC 81
4.2.1.1 Geometry 81
4.2.1.2 Polarization curves and power output 84
4.2.1.2 Coulombic efficiency and energetic efficiency 86
4.2.1.3 COD removal rate 87
4.2.1.5 H_2 production 88
4.2.1.6 Design evaluation 89
4.2.2 Stacked MFC 90
4.2.2.1 Geometry 90
4.2.2.2 Polarization curves and power output 92
4.2.2.3 Coulombic efficiency and energetic efficiency 93
4.2.2.4 Fixed voltage control 94
4.2.2.5 Substrate consumption 96
4.2.2.6 Design evaluation 97
4.3 Hexagonal tube MFC 98
4.3.1 Geometry 98
4.3.2 Aerobic hexagonal tube MFC application 100
4.3.2.1 Polarization curves and power output 101
4.3.2.2 COD Removal 103
4.3.3 Anaerobic MFC application 105
4.3.3.1 Power output, coulombic and energetic efficiency 106
4.3.3.2 COD removal and substrate supply 108
4.3.3.3 H_2 production 109
4.3.3.3.1 Anaerobic MFC and fermentation process 109
4.3.3.3.2 H_2 production profiles 111
4.3.3.3.3 H_2 production versus power generation 112
4.3.3.3.4 H_2 recovery rate from substrate and H_2 yield 114
4.4 Comparative study 114
4.4.1 Power production 115

4.4.2 Coulombic efficiency 116
4.4.3 COD or substrate removal 117
4.4.4 H_2 production 118
4.5 Design configuration 119
4.5.1 Electrode performance 119
4.5.2 External conditions 121
4.5.3 Design factors 122
4.6 Summary of major findings 122
Chapter 5 Electrode materials 124
5.1 Characteristics of materials 124
5.1.1 SEM 124
5.1.2 Textural properties measurement 127
5.2 Physical treatment of anode materials 129
5.2.1 Experimental methods 129
5.2.2 MFC performance 131
5.2.2.1 Performance based on the star rack anode setting 131
5.2.2.2. Performance based on the separated anodes setting . 133
5.2.2.2.1 Cell voltage data 133
5.2.2.2.2 Electrochemical analysis 134
5.2.3 SEM results of materials 138
5.2.4 BET results of materials 142
5.2.5 Summary of physical treatment 144
5.3 Chemical treatment of anode materials 145
5.3.1 Experimental methods 145
5.3.2 MFC performance 146
5.3.2.1 Performance based on the star rack anode setting 146
5.3.2.2 Performance based on the separated anode setting 148
5.3.3 SEM investigation of chemical treatment 153
5.3.4 Summary of chemical treatment 154
5.4 Graphite granules as cathode materials 154
5.5 Summary 157
Chapter 6 Barriers 160
6.1 MFCs barriers 160
6.2 Rate limiting steps 164
6.2.1 Substrate uptake by bacteria 164
6.2.2 Bacteria metabolism 166
6.2.3 Electron transfer to the anode 166
6.2.3.1 Electron transfer efficiency 166
6.2.3.2 Electrons transfer onto anode 172
6.2.4 Electrons through external circuit to cathode electrode 176
6.2.5 Proton concentration and transfer activities 177
6.2.5.1 Proton transfer in anode 177
6.2.5.2 Proton transfer to cathode 179
6.2.6 Protons on the surface of cathode 181

6.2.6.1 Different proton concentrations in cathode 181
6.2.6.2 Bacteria in cathode versus cell voltage 186
6.2.7 H_2 production in cathode electrode 189
6.3 Summary of MFC internal barriers 194
Chapter 7 MFC solutions for industry applications 196
7.1 Sustainable organic removal 196
7.2 Power redeem 198
7.3 H_2 production 198
7.4 Outline of industrial implementation of MFC 199
7.4.1 Industrial setting 199
7.4.2 Mass balance 200
7.4.3 Energy balance 201
7.4.4 Cost balance 202
Chapter 8 Conclusions and Outlook 204
8.1 Conclusions 204
8.2 Suggestions for further development 208
8.2.1 Reactor designs and electrodes structures 209
8.2.2 Electrode materials treatment 210
8.2.3 Bacteria behaviour 211
8.2.4 Combining MFC with other technologies 211

List of Figures

Figure 2.1 The scenarios of various energy options in 2050 6
Figure 2.2 World marketed energy use by fuel type, 1980-2030 7
Figure 2.3 Domestic use of water from different nations in average per capita 9
Figure 2.4 Scheme of double-chamber MFCs 14
Figure 2.5 Scheme of FC 14
Figure 2.6 A simplified view of bacteria metabolism 22
Figure 2.7 Typical polarization curves for a MFC where triangle symbol for power density data and cubic symbol for voltage data 34
Figure 2.8 Cylindrical based MFC with inner cathode adjusted from 42
Figure 2.9 Upflow based MFCs composed in the a single chamber 43
Figure 2.10 Tubular reactor with outer cathode and inner packed bed anode 44
Figure 2.11 Types of MFCs for batch mode application 45
Figure 2.12 Types of MFCs for continuous mode application 46
Figure 2.13 Comparison of the ideal and actual conversion losses for combustion systems versus electrochemical system 56
Figure 2.14 Wastewater treatment process diagram 62

Figure 3.1 Carbon cloth materials designation B (right) and D (left) 70
Figure 3.2 Schematic diagram of a GC 74
Figure 3.3 Circuit diagram of the external resistor system 77

Figure 4.1 Schematic of Micro-channel MFC, (A) Top view and (B) side view 82
Figure 4.2 Actual Micro-channel MFC 82
Figure 4.3 Flow sheet of Micro-channel MFC set 83
Figure 4.4 Brief polarization curve of the Micro-channel MFC during early incubation 85
Figure 4.5 Partial polarization curve of Micro-channel MFC during late incubation 85
Figure 4.6 Power densities gained from Micro-channel MFC under continuous flow condition 86
Figure 4.7 Actual assembly of stacked MFC 91
Figure 4.8 Schematic diagram of the stacked MFC setup 91
Figure 4.9 Flow sheet of stacked MFC 92
Figure 4.10 Polarization curve of stacked MFC 93
Figure 4.11 Current and power densities as the functions of fixed cell voltages for stacked MFC 95
Figure 4.12 Configuration of the Hexagonal tube MFC 100
Figure 4.13 Flow sheet of the hexagonal tube MFC 100
Figure 4.14 Polarization curve for batched aerobic hexagonal tube MFC 102
Figure 4.15 Polarization curve for continuous aerobic hexagonal tube MFC 103

Figure 4.16 power densities of aerobic tube MFC versus influent COD 105
Figure 4.17 Power generated under initial anaerobic hexagonal tube MFC.. 106
Figure 4.18 Power densities produced under high COD anaerobic hexagonal tube MFC conditions..... 108
Figure 4.19 H2 productions by MFC and Fermentation processes 112
Figure 4.20 H2 productions by MFC and Fermentation processes 2 112
Figure 4.21 Energy versus hydrogen generation from anaerobic tube MFC. 113
Figure 4.22 Log CE% as a function of the log (m2/l)..... 117

Figure 5.1 SEM images of plain carbon cloth B (left) & D (right)..... 125
Figure 5.2 SEM EDAX spectrum of plain carbon cloth B 125
Figure 5.3 SEM EDAX spectrum of plain carbon cloth D 126
Figure 5.4 SEM images of woven web with 2.5 g/m2 Pt at magnifications 3000 times meg. (left) and 31000 times meg. (right) 127
Figure 5.5 SEM EDAX spectrum of woven web with 5g/m2 Pt..... 127
Figure 5.6 Nitrogen adsorption curve of plain B and D anode materials 128
Figure 5.7 Cell voltages of B materials with thermal treatments at different temperatures with star rack anode setting 131
Figure 5.8 Cell voltages of D materials with thermal treatments at different temperatures with star rack anode setting 132
Figure 5.9 Cell voltages of B materials with thermal treatments at different temperatures with separated anode setting 133
Figure 5.10 Cell voltages of D materials with thermal treatments at different temperatures with separated anode setting 134
Figure 5.11 Polarization curves of different B materials 137
Figure 5.12 polarization curves of different D materials..... 138
Figure 5.13 Single fibres from B material before (left) and after (right) treatment at 800°C in CO2 139
Figure 5.14 Single fibres from D material before (left) and after (right) treatment at 800°C in CO2 140
Figure 5.15 SEM images of microbes attached to the 800°C CO2 treated B material (above) and D material (below) after using them in MFC..... 141
Figure 5.16 Nitrogen adsorption isotherm of plain B and 600 °C B treated materials..... 142
Figure 5.17 Nitrogen adsorption isotherm of plain D and 800 °C D treated materials..... 143
Figure 5.18 Cell voltages of different treated B materials during one cycle. 147
Figure 5.19 Cell voltages of different treated D materials during one cycle 147
Figure 5.20 Cell voltages of B materials with different treatments 149
Figure 5.21 Cell voltages of D materials with different chemical treatment 150
Figure 5.22 Comparison of the polarization curves of the B materials before and after chemical treatments..... 152
Figure 5.23 Comparison of the polarization curves of the D materials before

and after chemical treatments 153
Figure 5.24 SEM photos of KOH treated B (left) and D (right) materials 154
Figure 5.25 Polarization curves in stacked MFC with and without Pt in cathode 156
Figure 5.26 Fixed voltage control in stacked MFC with and without Pt in cathode 157

Figure 6.1 Overview of the seven transfer steps during the MFC process ... 161
Figure 6.2 Cell voltages of three batch MFCs during incubation period..... 168
Figure 6.3 Cell voltages of three batch MFCs during stable period..... 169
Figure 6.4 Cell voltages of continuous MFC5 & MFC6 during growing period170
Figure 6.5 Cell voltages of two continuous MFC4 &MFC6 during stable period 171
Figure 6.6 cell voltages of MFCs with 2 different electron acceptors added in anodes compare with normal batch MFC..... 174
Figure 6.7 MFC4 with air bubbled in anode compared with normal batch MFC3 175
Figure 6.8 Cell voltage polarization curve of the stacked MFC..... 177
Figure 6.9 Adding acid in MFC1 cathode or alkaline in MFC2 anode..... 179
Figure 6.10 Adding acid in cathode and alkaline in anode at the same MFC 181
Figure 6.11 Cell voltages of four MFCs where MFC1, MFC2 and MFC3 contained 500ml of 0.5 M H2SO4, 1 M H2SO4 and 2 M H2SO4 in cathodes, respectively, and MFC4 contained plain wastewater in cathode 184
Figure 6.12 Cell voltages as a function of proton concentration at the cathode 186
Figure 6.13 Cell voltages for three MFCs with different cathode medium ... 188
Figure 6.14 Hydrogen recovery and average power density as a function of applied voltage..... 192
Figure 6.15 Applied voltages as a function of the produced current density and the input power density..... 193

Figure 7.1 Outline of typical industrial setting 200
Figure 7.2 Daily mass balances for MFC 201
Figure 7.3 Daily energy balances for MFC 202
Figure 7.4 Annual estimated energy generation and cost savings from MFC transfer pipe 203

List of Tables

Table 2.1 Maximum power densities performance reported in literatures 32
Table 2.2 Anode material treatments and their MFC performance from literature 49
Table 2.3 Different alternative cathode materials and their MFCs performance from literature 51

Table 4.1 COD removal in 5 repeated experiments in Micro-channel MFC..... 88
Table 4.2 Substrate consumptions during the stacked MFC runs 97
Table 4.3 COD and BOD removal in continuous aerobic hexagonal tube MFC 104
Table 4.4 COD removal rate as a function of inlet COD 104
Table 4.5 COD removal rates under in anaerobic hexagonal tube MFC..... 108
Table 4.6 Energy contained in COD 109
Table 4.7 Comparison of the anaerobic MFC and the fermentation processes 110
Table 4.8 Power densities performance for the three MFCs..... 115
Table 4.9 The relationship of anode (cm^2/ml) and the coulombic efficiency..116
Table 4.10 COD or substrate removal in three continuous MFCs and their flow rates 118
Table 4.11 Electrode materials used in three MFCs 119
Table 4.12 External conditions for three MFCs 121
Table 4.13 Effective factors in three MFCs..... 122

Table 5.1 Material density decreases after physical treatment 129
Table 5.2 OCPs of B and D materials before and after physical treatment .. 135
Table 5.3 Electrode potentials of B materials with physical treatment..... 136
Table 5.4 Electrode potentials of D materials with physical treatment..... 136
Table 5.5 BET results and their maximum power densities..... 144
Table 5.6 Material density changes after chemical treatment..... 146
Table 5.7 OCPs of the plain and chemical treated B and D materials 151
Table 5.8 Electrode potentials of B materials..... 151
Table 5.9 Electrode potentials of D materials..... 151

Table 6.1 MFCs with different substrate concentrations and COD removal rates 165
Table 6.2 Coulombic efficiencies of MFCs with different conditions 167
Table 6.3 The additions of H2SO4 and NaOH in MFCs..... 179
Table 6.4 Changes of pH values before and after MFCs experiment..... 182
Table 6.5 Comparison of the COD removal in anode chamber and coulombic efficiency of H2SO4 doped MFCs experiments 185
Table 6.6 Change in pH before and after experiment..... 187
Table 6.7 COD removal before and after and coulombic efficiency of MFCs. 187
Table 6.8 Daily H2 production and daily recovery rates from stacked MFC.. 190

List of nomenclature

$\eta_{energetic}$	Energetic efficiency	
$\eta_{coulombic}$	Coulombic efficiency	
η	Energy efficiency	
ΔS	The unavailability of a thermodynamic reaction system's energy	J/K
ΔH	Enthalpy difference between reagents and reaction products	J
ΔG	Gibbs free energy	J
ΔCOD_s	COD removal rate within a single pass of MFC reactor	mg/l
ΔCOD	COD difference between influent and effluent	mg/l
A	Effective anode surface area	m^2
F	Faraday's constant 96485	C/mol
I	Current generated in MFCs	A
M	Molecule weight of material	
n	Number of electrons exchanged during the reaction	
P	power density	W/m^2
R_{ext}	External resistance	
R_{total}	Total resistance	
R_{H2}	Hydrogen recovery rate	
T	Temperature	K
t	total period of experiment	s
t_{exp}	Time of experiment in seconds	s
V_{cell}	Cell voltage	V
V_e	Effective volume of anode chamber	
V_{MFC}	Total volume of MFC compartment	m^3
Y_{H2}	H_2 yield	g H_2/g-COD

List of Abbreviations

AD	Anaerobic Digestion	
ATP	Adenosine triphosphate	
BOD	Biological Oxygen Demand	mg O_2/L
CEM	Cation Exchange Membrane	
COD	Chemical Oxygen Demand	mg O_2/L
COD_{in}	Influent COD value	mg/L
COD_{out}	Effluent COD value	mg/L
CV	Caloric Value	
DADP	nicotinamide-adenine dinucleotide-phosphate	
DNA	Deoxyribo Nucleic Acid	
DO	Dissolved Oxygen	
E. Coli	Escherichia Coli	
EDAX	Energy dispersive analysis by X-rays	
EPA	Environmental Protection Agency	
EU	European Union	
FCs	Fuel Cells	
GC	Gas Chromatography	
HHV	Higher Heating Value	
HRT	Hydraulic retention time	
IEA	International Energy Agency	
IPCC	The Intergovernmental Panel on Climate Change	
kWh	Kilowatthour	
MFCs	Microbial Fuel Cells	
NAC	Net Anodic Compartment Volume	
NADH	Nicotinamide Adenine Dinucleotide	
NADPH	Nicotinamide Adenine Dinucleotide Phosphate	
NHE	Normal Hydrogen Electrode	
NR	Neutral Red	
OCP	Open Circuit Potential	
PDMS	Polydimethylsiloxane	
PEM	Proton exchange membrane	
PE	person equivalent	
ppm	Parts per Million	
PTFE	Polytetrafluoroethylene	
RNA	Ribo Nucleic Acid	
rpm	Rotations per Minute	
RSC	Royal Society of Chemistry	
SHE	Standard Hydrogen Electrode	
TAC	Total Anodic Compartment volume	
VFA	Volatile Fatty Acid	
WBCSD	World Business Council for Sustainable Development	
WW	Wastewater	

Chapter 1 Introduction

1.1 Sustainability challenges

The world is facing serious sustainability challenges. Natural resources such as fresh water and fossil fuels are rapidly becoming in short supply. The heavy reliance on fossil fuels is further resulting in environmental concerns, especially global warming. Wastewater is also a growing issue. Current wastewater treatment technology is energy intensive requiring about 3 % of the energy consumption of a developed nation (EPA, 2008). This is resulting in a great carbon footprint for water treatment companies. Furthermore, this energy intensive solution is preventing water treatment in developing countries, where typically less than 1% of the water is treated (WBCSD, 2004).

In the UK alone, there are more than 347,000 km of sewers for both domestic and industrial use (Forster, C.F., 2003). These sewers feed a daily volume of 11 billion liters to about 9000 sewage treatment works with a treatment cost of £9 million per day in 2003 (Forster, C.F., 2003). Wastewater contains a significant amount of energy in the form of organic matter and a significant proportion of the cost is involved in removing this organic content. Traditional water treatment processes may therefore not be the best route forward towards sustainable water treatment. There are several biological processing strategies that not only accomplish satisfactory treatment of wastewater, but also utilise wastewater as energy source to produce alternative fuel at the same time. These include fermentation processes, biogas production and microbial fuel cells (MFCs). Depending on the organic content of the wastewater, different bio-processing strategies can be used to treat industrial or agricultural wastewater. Some of the bio-processing strategies are designed to produce bio-energy, such as methane, hydrogen or electricity and MFCs is one of the most promising technologies to be applied.

MFCs provide a novel bio-processing strategy to produce sustainable energy and water treatment. It produces electricity and, under certain conditions, biogas from biodegradable compounds and simultaneously reduces carbohydrates and complex substrates in domestic and industrial wastewater. In order to convert bio-convertible energy to electricity directly, a MFC consists of an anode and a cathode and an external load connecting the two electrodes. During MFC operation the bacteria switch their electron donating direction from the natural electron acceptor in the bulk wastewater, mainly oxygen or nitrate, directly to the anode via a redox reaction of electron mediators on the anode surface. Another function of MFCs is the capability to clean the wastewater in terms of reducing the level of organic materials. Recovery of energy from wastewater might help to redeem the cost of wastewater treatment, and help reduce our current dependence on fossil fuels. To reach this goal there is a need to show that the MFCs can be scaled up and applied to industries.

This work focuses on the optimisation of the built design of MFCs towards scale up to treat domestic and industrial wastewater. A variety of complex geometry MFCs were developed to understand the electron transfer mechanisms and to optimize the process parameters. A unique single chamber, non-membrane, continuous and high flow rate configuration MFC was developed that open the possible engineering solutions to current industrial wastewater treatment. Particular emphasis was directed toward the electrode materials treatments to optimize electricity production, where improved anode materials structure for enhanced interaction with anaerobic bacteria and alternative cathode materials to replace the expensive catalyst component Platinum currently used. It was found that a simple oxidation treatment of the anode material, significantly improved power production performance of the MFCs and that graphite granules on their own can act as cathode materials. This work also identified and addressed the barriers and limitations of MFCs as well as the current and potential applications of MFCs technologies. In summary, it is concluded that with proper configuration of the MFC

technology, based on detailed understanding of its intricate principles and barriers, MFC hold a great potential to convert bio-energy by reducing the organic content in wastewater to supply sustainable fuels and improve water quality. The deep knowledge of the MFCs processes established in this work is essential to develop the stainable energy production in the near future.

1.2 Aim and Objectives

1.2.1 Aim

The aim of this work was to establish the scale up potential of MFC by studying different construction configurations of MFC, where particular attention was paid to improving interaction between bacteria and carbon materials, optimizing parameters such as electrode materials to increases the power density, coulombic efficiency and the yield of hydrogen in MFCs, that maximize energy generation and removal of COD from wastewater. A future scale-up of the MFC identified and its application towards industrial and developing countries, will be calculated in terms of sustainability and cost savings.

1.2.2 Objectives

The specific objectives of this work were:

- Construct new MFC reactors with relatively high efficiency and compatible electrode materials that can be implemented by industry;
- Compare the performance of several MFCs including power densities, coulombic efficiencies, COD removals and H_2 productions;
- Evaluate electrode materials treatment to improve the power performance of MFCs;

- Define and test importance of the main barriers of MFCs to predict scale up issues; and
- Identify an executable industrial implementation scenario based on this study.

1.3 Thesis outline

MFC might provide a solution to several of the bottlenecks in traditional wastewater treatment processes such as high energy cost, complicated procedures and large operational requirements. Hence, this study was initiated with the objective of generating energy from the wastewater to offset the energy and operational costs. Three research pathways were followed in this work:

- Optimization through reactor design development and operational knowledge augmentation (Chapter 4)

- Technological optimization of electrodes through increased knowledge towards the interaction between anode materials and bacteria and the alternative cathode materials, in order to increase MFC power performance and decrease investment costs (Chapter 5)

- Identification and addressing the embedded MFC barriers to further understand the MFC principles and limitations for further improvements of the MFC performance (Chapter 6)

- Outlining a industrial MFC solution based on this work (Chapter 7)

Chapter 2 Background

2.1 Global issues for sustainability

Global industrialization and rapid rise in the non-sustainable use of fossil resources is increasing the amount of carbon dioxide and other greenhouse gases that enter the atmosphere leading to a warming of the planet and resulting in climate changes (Bilen, K. et al., 2008; Martinot, E., 2006; WBCSD, 2004). Moreover, rising population and increasing consumption, and land use, have caused a rapid acceleration of climate change over the past twenty years (EIA, 2008; IPCC, 2001). Parallel to the global warming issues, the rapid depletion of fossil fuels is leading to increased global tension towards resource availability. For instance, the UK currently relies heavily upon electricity produced from fossil fuels, especially North Sea gas which will be depleted shortly, and alternative sources located in other parts of the world are less stable (ESD, 2003). Reduced availability of fossil fuels will raise energy prices globally and consequently increase water treatment costs. It is therefore important to focus on sustainable technologies, such as Microbial Fuel Cell, to cover these needs.

2.1.1 Energy Demand

The world is faced with an immense challenge as the global population continuous to grow. Most of the human race is striving for growth, development and urbanization, with a corresponding increasing demand for energy. According to forecasts by the International Energy Agency (IEA), by 2030 the global energy consumption will have increased by another 60 % compared to 2001 (Bilen, K. et al., 2008). It is also predicted that by the middle of this century, the energy demand could even double or triple based on the anticipated increase in population, the expanding economies of developing countries and the changes in global living

standards. At the same time it will become more and more difficult to meet these energy demands from fossil resources. The IPCC scenario shown in Figure 2.1 indicates that various energy options will be used in 2050, and it is clear that renewables will play an increasing role (IPCC, 2001).

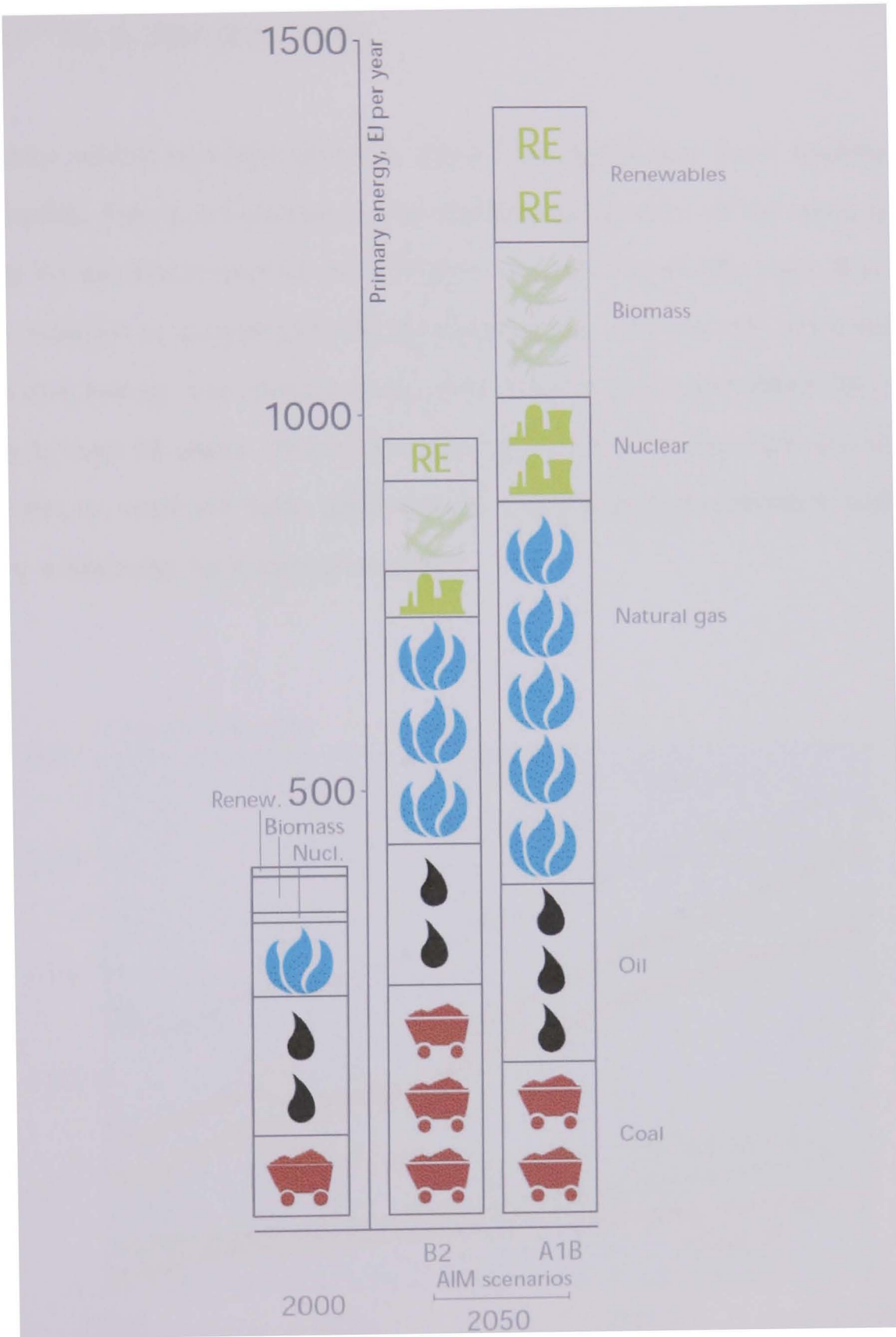

Figure 2.1 The scenarios of various energy options in 2050 (IPCC, 2001)

Figure 2.2 suggests that the world's hunger for energy shows no sign of stopping

and within the next 20 years the demand on primary energies such as oil, coal, natural gas, nuclear, biomass and other renewable energies will be doubled. The rapid growth prediction is based on actual total primary energy consumption in the past 25 years that increased 1.9 % annually from $290*10^{15}$ Btu in 1980 to over $460*10^{15}$ Btu in 2005 (EIA, 2008).

It is now widely accepted that the world's energy supply must become more sustainable. Figure 2.2 compares the global consumptions of the main types of energy for the past 25 years and future prediction for the next 25 years. It suggests a fast increase in consumption of all energy types. Despite the consumption of renewable energy rise continuously, fossil fuels will still dominate the energy supply in next 25 years. This means that limited natural resources are still very important to meet the basic global needs, but the use of renewable sources of energy is essential for future generations.

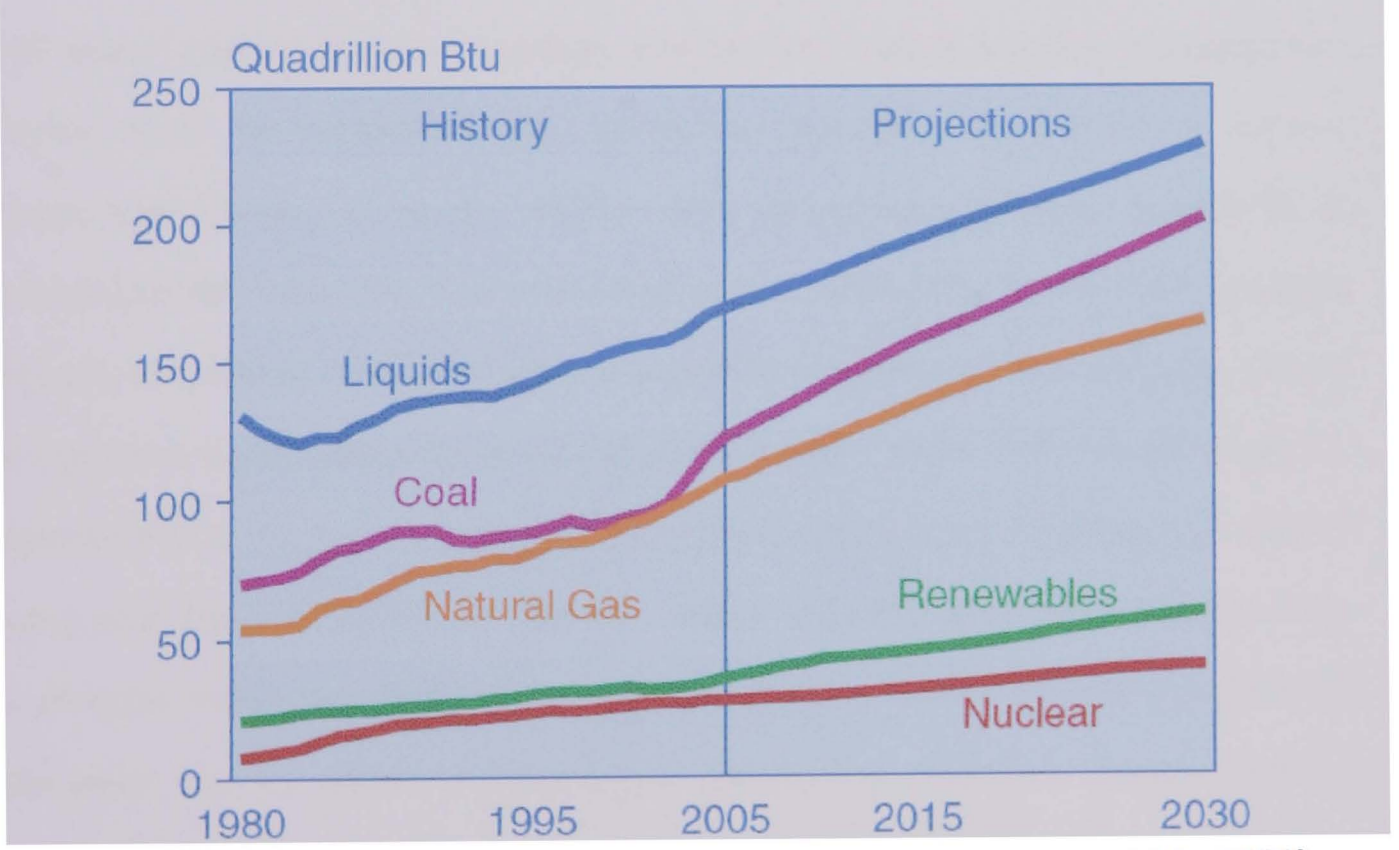

Figure 2.2 World marketed energy use by fuel type, 1980-2030 (EIA, 2008)

At present, renewable energy account for less than 7.8 % of the global primary

energy supply including wind power, hydropower, solar energy, geothermal energy and biomass. It is predicted that about half of the global energy demand could be met by renewable sources by the year 2050 (EIA, 2008; Martinot, E. et al., 2002). Organics in wastewater used in MFCs could be an important renewable resource in the transition from fossil to sustainable fuels as shown below.

2.1.2 Water Demand

Water is a precious resource in short supply globally (White, S. et al., 2007). More than 97 % of the water on earth is seawater which is non-potable without energy intensive desalination technology. For the remaining 3 % of freshwater, two thirds is locked in glaciers and polar ice. Therefore human needs must be met with only 1 % of the Earth's total water resource.

Global water use for human purposes can be split into three major categories, normally 70 % for agriculture use, 20 % for industry use, and 10 % for the domestic use (White, S. et al., 2007). MFC technology is highly applicable to industrial and domestic use. The amount of water used varies widely from one type of industry to another. The basic uses of water in industries are generally as cooling water, process water, water for products and even as a medium for waste disposal. The remaining 10 % used for domestic activities include water for drinking, cooking, cleaning and flushing toilets. In the UK, water industry provides 18,000 million litres of water every day to 60 million people. Figure 2.3 shows water withdrawals for domestic use for different nations per capita. The minimum human need of drinking water per day to survive is two liters, which is less than one cubic meter per year (WBCSD, 2005b).

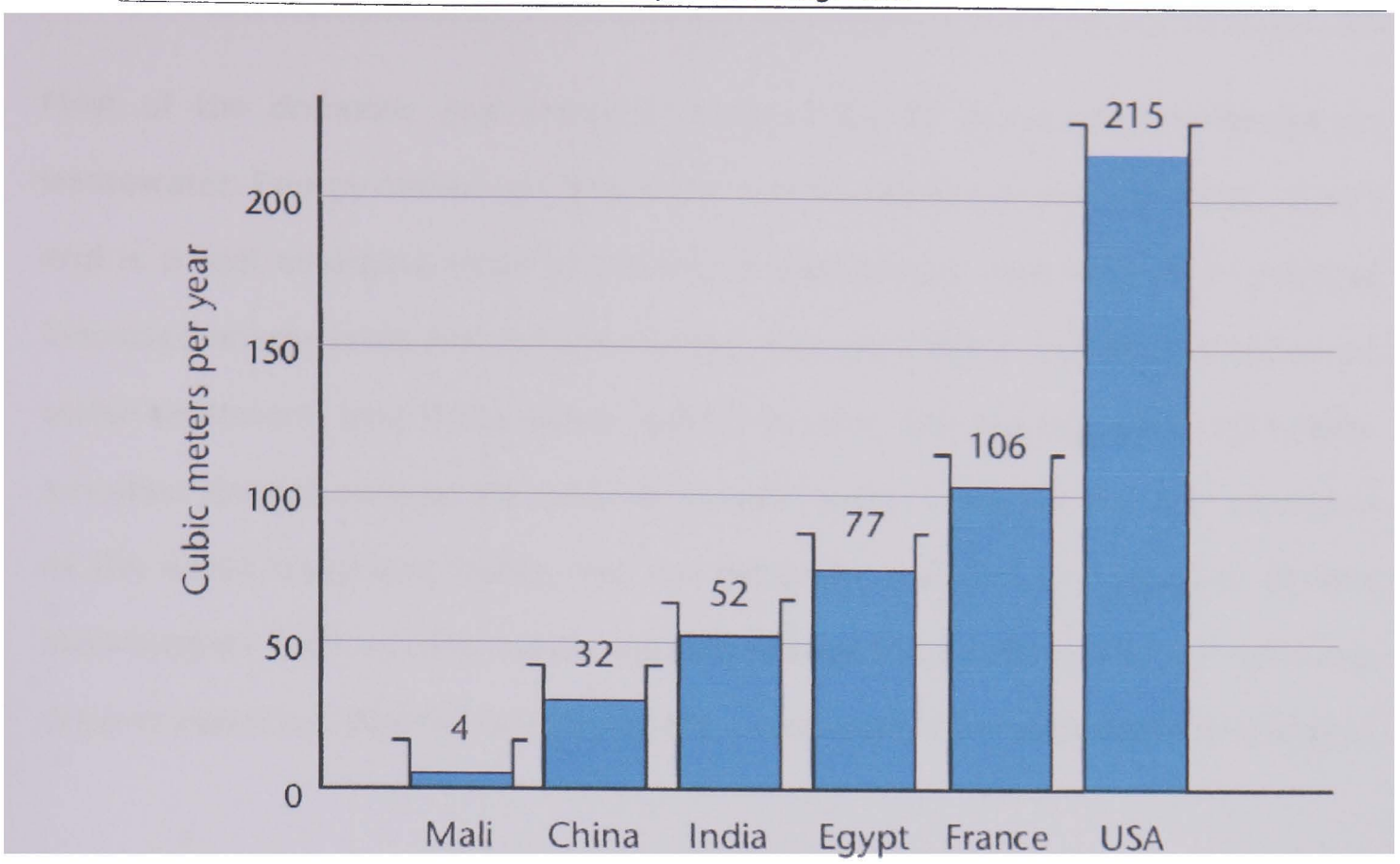

Figure 2.3 Domestic use of water from different nations in average per capita (WBCSD, 2005b)

Demand for water will increase as the global population grows and as developing countries become more industrialized. In 2000, the world population was 6.2 billion. It is estimated that by 2020 more than 4 billion of the world's population will be living in water stressed countries (WBCSD, 2005a). It occurs when there is not enough water for all uses, including agricultural, industrial and domestic. Currently, it has been proposed that when annual per capita renewable freshwater availability is less than 1,700 cubic meters, a nation begins to experience periodic or regular water stress. Below 1,000 cubic meters per capita, water scarcity begins to hamper economic development and human health and well-being (WBCSD, 2005b).

The availability of freshwater is threatened by four dominant mechanisms that contribute to water stress: (1) Excessive withdrawal from surface waters and underground aquifers; (2) Pollution of fresh water resources; (3) Inefficient use of freshwater; and (4) Climate change which affects water precipitation. Recently, changes in global temperature, precipitation patterns, solar radiation, humidity and wind have significant increased water stress for a number of countries.

Most of the domestic and industrial used water is eventually discharged as wastewater. Energy makes up 28 % of the cost of treating wastewater (RSC, 2007) and is a real emerging issue in water and wastewater treatment as a result of increased energy costs and climate change. New regulations may require improved water treatment, and if the water quality is poor, the energy costs will further increase. Energy savings are possible through better management and operation of the water treatment works, but are generally marginal. Introduction of new technologies such as MFC which extract energy from wastewater by removing organic waste can significantly improve the sustainability of wastewater treatment.

2.2 Principles of Microbial Fuel Cells

2.2.1 History and classification

The history of MFC starts with the discovery of the relationship between biology and electricity (Bullen, R.A. et al., 2006; Davis, F. and Higson, S.P.J., 2006; Shukla, A.K. et al., 2004). In 1791, Galvani observed that electric current was generated by twitching a frog's leg. It was found that biological reactions and electric current are closely related. Fifty years later, the first fuel cell was created by Mr William R. Grove in 1839 (Grove, W.R., 1839). In his experiment, Grove reversed the process of electrolysis of water, where hydrogen and oxygen were also combined back to water and electricity produced during the process.

After these discoveries, in 1910, a Professor Michael Cresse Potter in botany at the University of Durham, UK, described the electricity production gained from cultures of yeast and Escherichia coli (E. coli). It was the first time that biological process was observed producing bioelectricity (Bullen, R.A. et al., 2006; Davis, F. and Higson, S.P.J., 2006; Shukla, A.K. et al., 2004). Further progress made by Cohen in 1931 showed that a batch-biological fuel cell could produce more than 35V of

voltage (Cohen, B., 1931). During 1960s, biological fuel cell was a hot topic due to the space race. The USA space program was interested in this technology since it could convert the organic waste in space flights to power. But it was soon replaced by other energy source such as photovoltaic panels (Bullen, R.A. et al., 2006; Davis, F. and Higson, S.P.J., 2006).

In 1969, Rao and Yao showed that using platinum as the working electrode, dextrose and glucose can both be used as fuel to produce power (Rao, M.L.B. and Drake, R.F., 1969; Yao, S.J. et al., 1969). However, it was not until 1976 that Rao identified the clear principle of the biological fuel cell (Rao, J.R. et al., 1976). It was establish that bacteria transferred electrons onto the anode which was used as an electron acceptor. Electrons subsequently produced electricity through an external resistance and protons migrated through a proton exchange membrane to the cathode where electrons and protons recombined to complete the circuit. The name and concept of microbial fuel cells (MFCs) was first explored from 1980s (Roller, S.D. et al., 1984). The concept of combining wastewater treatment and MFCs was introduced in 1991 (Habermann, W. and Pommer, E., 1991).

It is common to distinguish between microbial fuel cells and enzymatic fuel cells (Davis, F. and Higson, S.P.J., 2006; Shukla, A.K. et al., 2004). The MFCs use microorganisms as the biocatalyst to split electrons and protons. For enzymatic fuel cells, enzymes are required to be isolated individually from microorganisms and then applied to the system to produce electricity similar to MFCs. Although enzymatic fuel cells have higher efficiency with the help of enzymes, it is more conveniently and economically to simply apply bacteria in a microbial fuel cell and supply mixed substrates, such as wastewater to fuel the system. Currently researches are more focused on MFCs rather than enzymatic fuel cells.

MFCs, can be roughly classified into three types based on the way electrons are produced and transported within the bacteria, namely (1) Mediated electron

transfer MFCs, (2) Direct electron transfer MFCs, i.e. mediator-less MFCs and (3) Photoheterotrophic MFC. Most of the research interest has been paid towards mediator-less MFCs (Kim, H.J. et al., 2002; Bond, D.R. and Lovley, D.R., 2003; Chaudhuri, S.K. and Lovley, D.R., 2003; Liu, H. et al., 2004; Rabaey, K. et al., 2004; He, Z. et al., 2005; Moon, H. et al., 2006). Some groups also have focused on photoheterotrophic MFCs (Rosenbaum, M. et al., 2005) and mediated electron transfer MFCs (Park, D.H. and Zeikus, J.G., 1999; Bond, D.R. et al., 2002; McKinlay, J.B. and Zeikus, J.G., 2004). Mediated electron transfer MFCs rely on the extracellular redox mediators, such as neutral red (Park, D.H. and Zeikus, J.G., 1999; McKinlay, J.B. and Zeikus, J.G., 2004) or thionin (Choi, Y. et al., 2003) that are costly chemicals and cannot be recycled once added into MFCs system. Some of these chemicals also poison some bacteria as well as contaminate the wastewater. For the photoheterotrophic MFCs, an extra light source is needed to add extra energy into the MFCs system. The mediator-less MFCs is therefore more environmental friendly, with no concerns towards the effects of mediators and no extra energy needed for completing the process.

2.2.2 Basic principles

Compared to the relative long history of the traditional Fuel Cells (FCs) from 1830s, MFCs has a relatively short history going back to the 1980s. Although MFCs transfer the chemical energy into electricity directly similar to traditional FCs, there are great differences in their principles, prototype structures, materials, fuels and products generated. Hydrogen can be biologically produced in the MFC from biomass and other renewable resources alongside electricity generation (Angenent, L.T. et al., 2004). The fuels for MFCs are flexible in that they can be different kinds of biodegradable waste, reduced carbohydrates, glucose, sucrose, acetate, lactate, starch and some other complex substrates in municipal or industries wastewaters, and in the form of liquid or sludge (Lovley, D.R., 2006b; Rabaey, K. and Verstraete,

W., 2005; Logan, B.E. et al., 2006; Logan, B.E. and Regan, J.M., 2006).

Typical two chamber MFCs and traditional FCs schemes are shown in Figure 2.4 and 2.5, respectively. As Figure 2.4 demonstrates, the essence of MFCs is to convert organic materials directly into electricity under room temperature and normal pressure. The process can be achieved using specific strains of bacteria in the anode chamber to gain electrons from biomass and transport to either the anode via electron acceptors (Rabaey, K. and Verstraete, W., 2005) or directly transport onto the anode electrode itself, i.e., the bacteria on the anode surface can directly transfer electrons onto anode electrodes. Electron acceptors can be self-produced intracellular redox mediators by bacteria such as soluble quinones, proteins and phenazines (Kim, H.J. et al., 2002; Nevin, K.P. and Lovley, D.R., 2002; Bond, D.R. and Lovley, D.R., 2003). Alternatively, electron acceptors can be extracellular mediators added to the water such as neutral red (Park, D.H. and Zeikus, J.G., 1999; McKinlay, J.B. and Zeikus, J.G., 2004) thionin (Choi, Y. et al., 2003) or ferricyanide (You, S. et al., 2006). This process is in essence similar as in traditional FCs shown in Figure 2.5. Hydrogen is here the fuel compared with organics in MFC. The Pt splits H_2 into H^+ and e^-, where as in MFCs the bacteria splits the organic to a cation (H^+) and e^-. The e^- travels to the cathode through an external route and the H^+ travels through the membrane. These are recombined at the cathode to create current in the system.

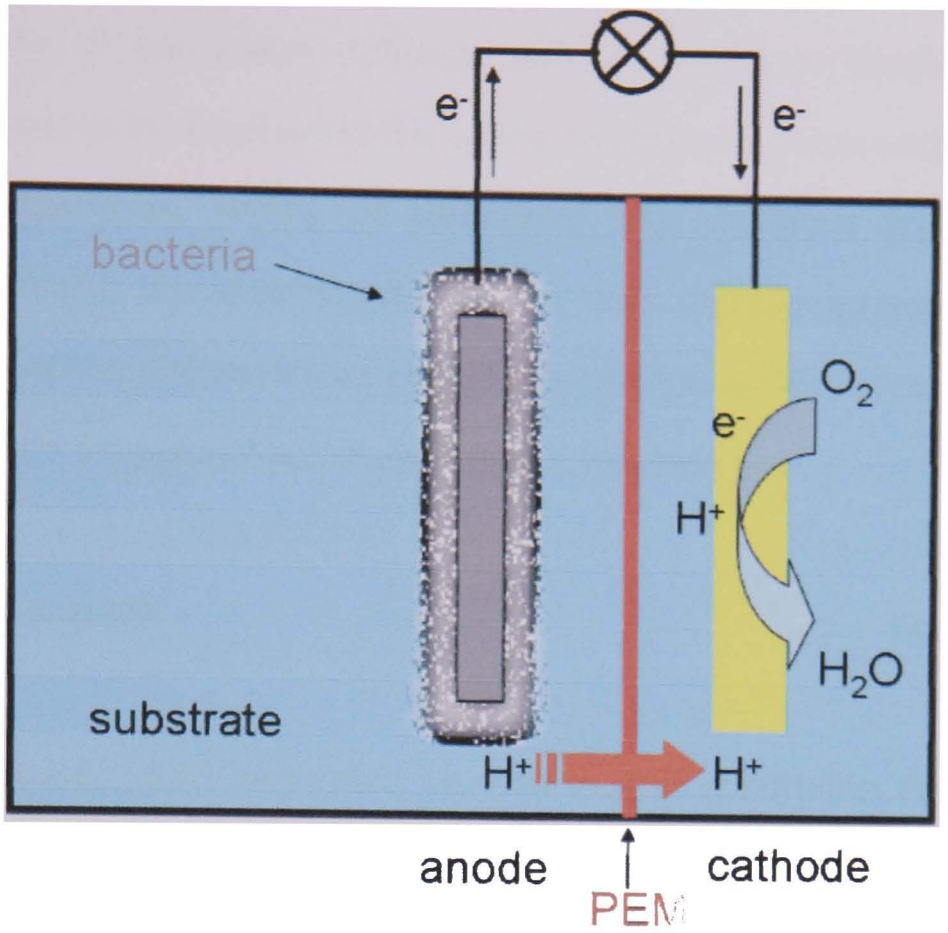

Figure 2.4 Scheme of double-chamber MFCs (adapted from Angenent, L.T. et al., 2004)

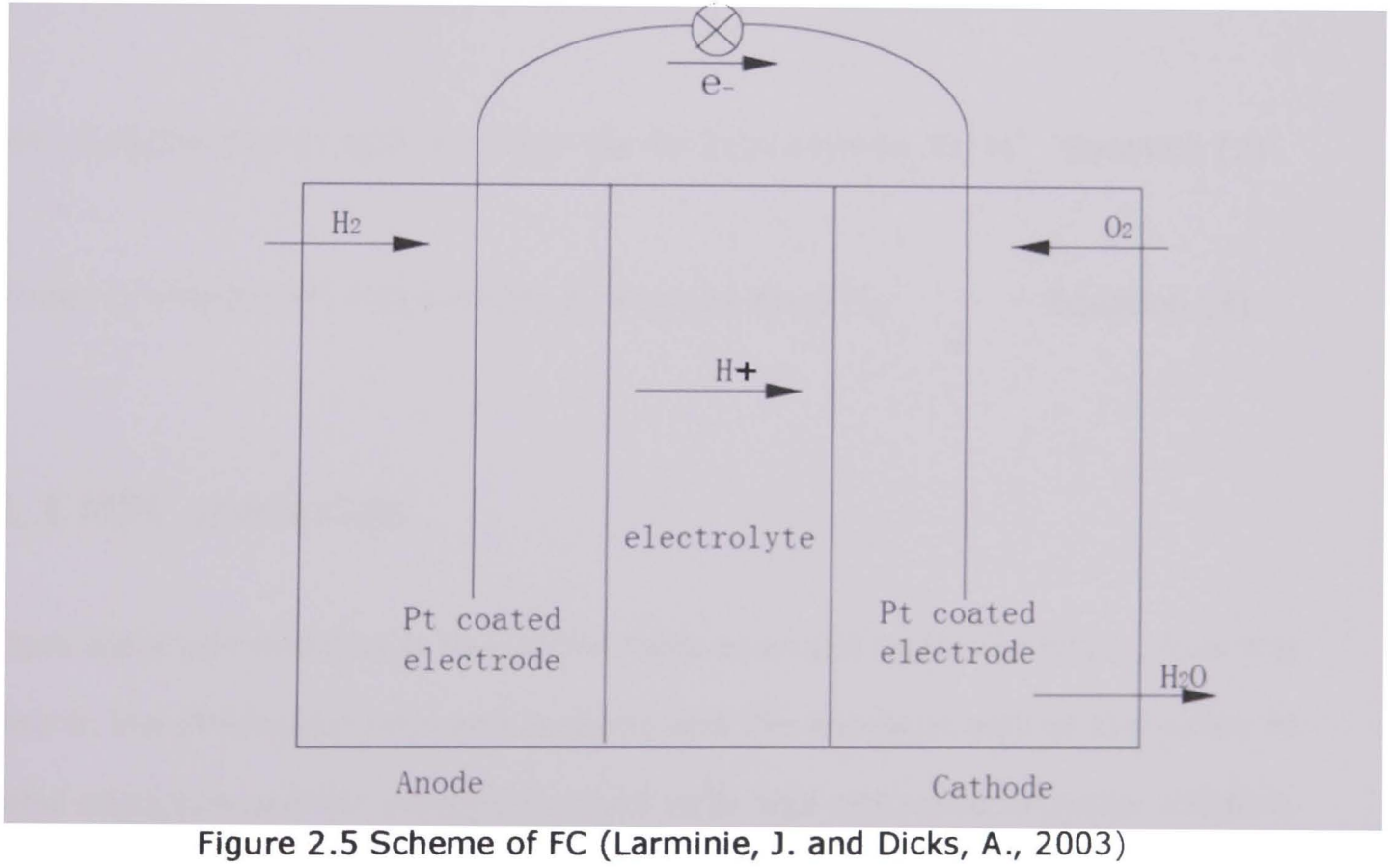

Figure 2.5 Scheme of FC (Larminie, J. and Dicks, A., 2003)

Biofilm is another factor that affects the MFC electron transfer. It is formed as a layer of bacteria, or organics precipitating from wastewater, that attached itself on

the anode surface. It can utilize different electron acceptors biochemically or physically transporting the electron to the anode electrode surfaces which works as a biocatalyst. Afterwards, similar to traditional FCs, electrons on the anode electrode travel along the external conductive wire to the cathode electrode. During aerobic conditions the cathode chamber is open to air to use oxygen as the proton and electron acceptor. The overall aerobic reaction is:

$$4H^+ + O_2 + 4e^- \rightarrow 2H_2O \qquad \text{Equation (1)}$$

MFCs can also operate under anaerobic, i.e. non-oxygen conditions. For anaerobic MFC, oxygen cannot be the proton and electron acceptor in the cathode and MFCs has the potential to produce hydrogen instead of water at the cathode. Hence, anaerobic MFC has the potential to extract energy in forms of both electricity and H_2 from the organic content. Equations (2) and (3) show this concept:

Anode: $C_xH_yO_z + (2x-z)\ H_2O \rightarrow xCO_2 + (y+4x-2z)e^- + (y+4x-2z)\ H^+$ Equation (2)

Cathode: $(y+4x-2z)\ H^+ + (y+4x-2z)\ e^- \rightarrow (y/2+2x-z)\ H_2$ Equation (3)

2.2.3 MFC materials

Suitable electrode material is one of the most essential factors in MFCs, since it is related to the interaction between bacteria and the anode as well as the ability to transfer electrons and for protons to react with high reduction potential matters, such as oxygen at the cathode. Anode materials should have high conductivity, be chemical stable in the wastewater streams, have good biocompatibility with no toxicity towards microorganism, high surface area for microorganism to easily anchor and grow on the surface, good adaptability, stability at room temperature, pressure and pH between 5-7, resistant to biofouling and have low costs. The most

versatile anode material in MFCs applications is carbon, available as carbon cloth, carbon fibres, graphite plates or rods and graphite granules.

Cathode materials should have high conductivity, good adaptability, stable at room temperature, pressure and pH between 5-7, high electro-catalytic activity towards the redox reaction of protons and electrons on the surface, resistant to poisoning by chemicals contained in wastewater streams and other biological by-products during the MFCs process and low costs as well. To increase the rate of oxygen reduction effect in the cathode chamber, the most effective cathode materials in MFCs applications at the moment are carbon materials containing certain amount of Pt which acts as the high performance catalyst for the redox reaction on the surface. Since Pt is a precious metal material with very high costs, and it is easily poisoned by MFC by-products such as hydrogen sulphide, alternative cathode materials with low cost and high resistance to deactivation are urgently needed to solve the poisoning and capital investment issue for MFCs.

Besides electrode materials, some MFCs rely on other materials to complete the MFCs circuit, such as membranes used to separate anode and cathode chambers, and mediators for electron transfer in the anode chamber. The most common used membrane materials are cation exchange membrane (CEM) or proton exchange membrane (PEM). The membrane functions as a separator to isolate the anode and cathode chambers, as well as to selectively transfer cation from anode to cathode chamber. Most of the membranes are water impermeable but gas permeable. Some membranes allow substrates to penetrate through them as well. These properties may result in oxygen penetrating from cathode to anode chamber leading to reduced efficiency for electrons transport onto the anode electrode. Also, cation migration might be a rate limiting steps especially for continuous MFCs as investigated in Chapter 6.

For MFCs using mediators, see Section 2.2.2, electron transfer from bacteria to the

anode is promoted. Besides the mediators that the bacteria produce themselves, external chemical mediators are used in some MFC applications to assist and improve the electrons transfer rate. The chemicals include K_2HPO_4, KH_2PO_4, KCl, $CaCl_2.2H_2O$, NH_4Cl, $MgSO_4.7H_2O$ and a range of trace elements (Madigan, M.T. and Martinko, J., 2006). These chemicals also act as culture medium for the bacteria, and are consumed and therefore need to be continuously supplied. In some studies, ferricyanide or permanganate were used in the cathode chamber to act as electron acceptor instead of the commonly used oxygen (You, S. et al., 2006). The advantage is that this can adjust the open circuit potential between anode and cathode. The drawback is that most of the mediators are toxic to microorganisms. Also, they are consumed during the process and creating an unrenewable system. Recent efforts are focused on avoiding these chemicals application in MFCs to simplify MFC conditions.

For the electrode connections and data collection, graphite rods are the most common used materials since they have good conductivity, non-corrosive and low cost.

2.2.4 Types of MFCs

Research activities on MFCs have generated much interest, and a great number of different MFCs designs and operation conditions have come forth, and these can be categorised depending on the types of feed streams, bacteria cultures and built design.

2.2.4.1 MFC feed: actual vs. artificial wastewater

There are three general substrates used to categorise MFCs:

(1) Wastewater fed MFCs. Actual wastewater is used, which is collected from

wastewater treatment company or industries, such as the urban wastewater, swine wastewater, food processing wastewater, corn waste, brewage waste or even oil refining waste. In these non-buffered streams the power densities obtained are generally low. But as long as there is enough organic nutrients contained in the substrate to sustain bacteria growth, the MFCs can be used to produce energy (Angenent, L.T. et al., 2004; Liu, H. et al., 2004; Min, B. et al., 2005b; Oh, S.E. and Logan, B.E., 2005; Ditzig, J. et al., 2007; Rodrigo, M.A. et al., 2007).

(2) Artificial wastewater fed MFCs. Salts such as potassium phosphate are used as growth medium for bacteria and act as a buffer solution, and acetate, sucrose or other organic materials are added as the substrate for bacterial activity (Chaudhuri, S.K. and Lovley, D.R., 2003; He, Z. et al., 2005; Moon, H. et al., 2006). These MFCs produce high power density but require substantial chemical monitoring and maintenance.

(3) Sediment fed MFCs. The principle of sediment MFCs is slightly different from wastewater fed MFC (Hasvold, Ø. et al., 1997; Reimers, C.E. et al., 2001; Bond, D.R. et al., 2002). Sediment MFC uses the potential differences between sediment underneath a water body and the upper water of the system. The principle of this type of MFCs is the use of bacteria contained in sediments to split electrons and protons and then release them to the anode and the water system, respectively. Electrons go through the anode to the external load, and then to the cathode electrode which is immersed in the water. Electricity is produced from this process although in a limited water system the power densities produced might be much lower than wastewater fed MFCs due to poor ion transport. If the boundary of the system extends to a large water body and a large number of these MFCs are used for power production, sediment MFCs could have considerable application and potential market for ships or oil field at sea.

2.2.4.2 MFC operation: Single vs. mixed microbial culture

There are two types of MFCs based on the bacteria species employed in MFCs. One type employs a single species of bacteria (Kim, H.J. et al., 2002; Bond, D.R. and Lovley, D.R., 2003; Ieropoulos, I.A. et al., 2005; Liu, Z.-D. et al., 2006; Prasad, D. et al., 2006; Zhang, E. et al., 2006) and another is based on a mixed microbial cultures.

Those bacteria used as single species include the anodophilic bacteria from the families of *Geobacteraceae, Desulfuromonaceae, Alteromonadaceae, Enterobacteriaceae, Pasteurellaceae, Clostridiaceae, Aeromonadaceae, and Comamonadaceae* (Hoggers, G., 2002; Park, D.H. and Zeikus, J.G., 2002; Chaudhuri, S.K. and Lovley, D.R., 2003). It has been found that the electricity generation from a mix culture performs better than single species (Park, D.H. and Zeikus, J.G., 2002). It is claimed that when using mixed bacteria culture from wastewater to inoculate MFCs, they act as suitable biocatalysts for electricity production (Liu, H. et al., 2004). Hence, wastewater can be used both as the inoculums and the substrates. This mixed cultures application is preferable for future MFCs developments due to decreased costs and time for purchasing and incubating compared to single bacteria culture.

Most studies claim that MFCs operating with mixed cultures achieved substantially higher power productions compared to single cultures (Rabaey, K. et al., 2004; Rabaey, K. et al., 2005a). However, some studies on single cultures such as Shewanella Oneidensis DSP10, generated 3 W/m^2, though no comparable work had done based on the same reactor with mixed culture (Ringeisen, B.R. et al., 2006). A range of bacteria species are used in MFCs depending on its operation conditions. When the anode potential is low and the concentration of mediators and other electron acceptors are low in the anode chamber, the main MFC process is fermentation, where electrons are transferred intensively internally in the bacteria

to reduce organic compounds (Rabaey, K. and Verstraete, W., 2005). The bacteria used for fermentation to generate hydrogen include the genus *Clostridium, Alcaligenes, Enterococcus, Geobacter* and other species from families such as *Streptococcaceae, Sporolactobacillaceae, Lachnospiraceae and Thermoanaerobacteriacea* (Fang, H.H.P. et al., 2002; Rabaey, K. and Verstraete, W., 2005). When the anode potential is high, the electricity production is the main process and the anaerobic microorganisms are expected to oxidize the organic materials in the anode chamber and transfer the electrons to the anode electrode. The consortia typically used include *Pseudomonas aeruginosa, Enterococcus faecium, and Rhodoferrireducens* (Fang, H.H.P. et al., 2002; Rabaey, K. and Verstraete, W., 2005), Metal-reducing bacteria, such as *Shewanella Putrefaciens* and *Geobacter Sulfurreducens*, can transfer electrons to anode either directly or by producing the electron mediators themselves (Kim, H.J. et al., 2002; Nevin, K.P. and Lovley, D.R., 2002; Bond, D.R. and Lovley, D.R., 2003).

Besides the bacteria species used in MFC systems, it is necessary to briefly introduce the concept of biofilm as mentioned before under Section 2.2.2. Biofilm is a small ecosystem consisting of different species of bacteria with different thickness on the solid anode surfaces. Frequently, they will form small attached colonies rather than close layers of uniform thickness. The thickness of the biofilm is a function of bacteria growth rate and depends on the stability of the biofilm and the shear stress of the influent flow. For a thick biofilm with a few cells in depth, cells at the bottom may die due to the lack of substrate for energy and growth (Logan, B.E., 1999; Wiesmann, U. et al., 2007). This can affect MFCs performance mainly due to the decreased transport of electrons to the anode.

2.2.4.3 MFC built design

Several MFC designs have been reported, including single and double chambers

design, vertical and horizontal design, continuous flow and batch mode design, and using a series of MFCs with electricity collection in series or in parallel mode (Liu, H. and Logan, B.E., 2004; He, Z. et al., 2005; Min, B. et al., 2005a; Aelterman, P. et al., 2006). The various configurations are aimed at optimising the environment for bacteria growing, increasing energy extraction efficiency, and aligning lab scale design with industrial application in the future. Detailed MFC designs are further described in Section 2.3.2.

2.2.5 Microbiological aspects of MFCs

2.2.5.1 Transport mechanisms of substrate to bacteria

Bacteria are prokaryotic cells due to their lack of a karyon or cell nuclens (Madigan, M.T. and Martinko, J., 2006). Bacteria are normally around 0.5 μm to 1.5μm in size and can be rod, spherical or spiral shaped. Some bacteria are motile, since they have a special structure of flagella, allowing the microorganisms to regulate their position through flagella movement in aquatic environments. Other immobile bacteria have to wait for the diffusion of substrates onto their position. In the MFCs anode chamber environment, the motile bacteria in the wastewater can easily seek out nutrition rich locations, and then degraded the matters to a form from which they can gain energy. This is one of the reasons that the MFCs can show high organic removal but low generation of electricity due to partial or fully mobile bacteria consuming organic matters without contributing electrons to the anode. MFC technology that can transport substrate to immobile bacteria on anode surface, such as continuous flow MFC, could address this issue.

2.2.5.2 Bacteria metabolism

Understanding the principles of bacteria metabolism is crucial in order to increase

the energy production and improve the energy transformation efficiency of MFC. The energy production in MFCs strongly depends on the bacteria activity and the oxidation-reduction reactions in the MFCs. A simplified view of the bacteria metabolism is shown in Figure 2.6, highlighting the main processes of degrading nutrition to supply energy to bacteria (catabolism) and synthesising cell components from external organic matters (anabolism) (Madigan, M.T. and Martinko, J., 2006). In MFCs applications, the focus is on the catabolism process that degraded chemicals for both bacteria energy and extra electrons and protons for MFCs application.

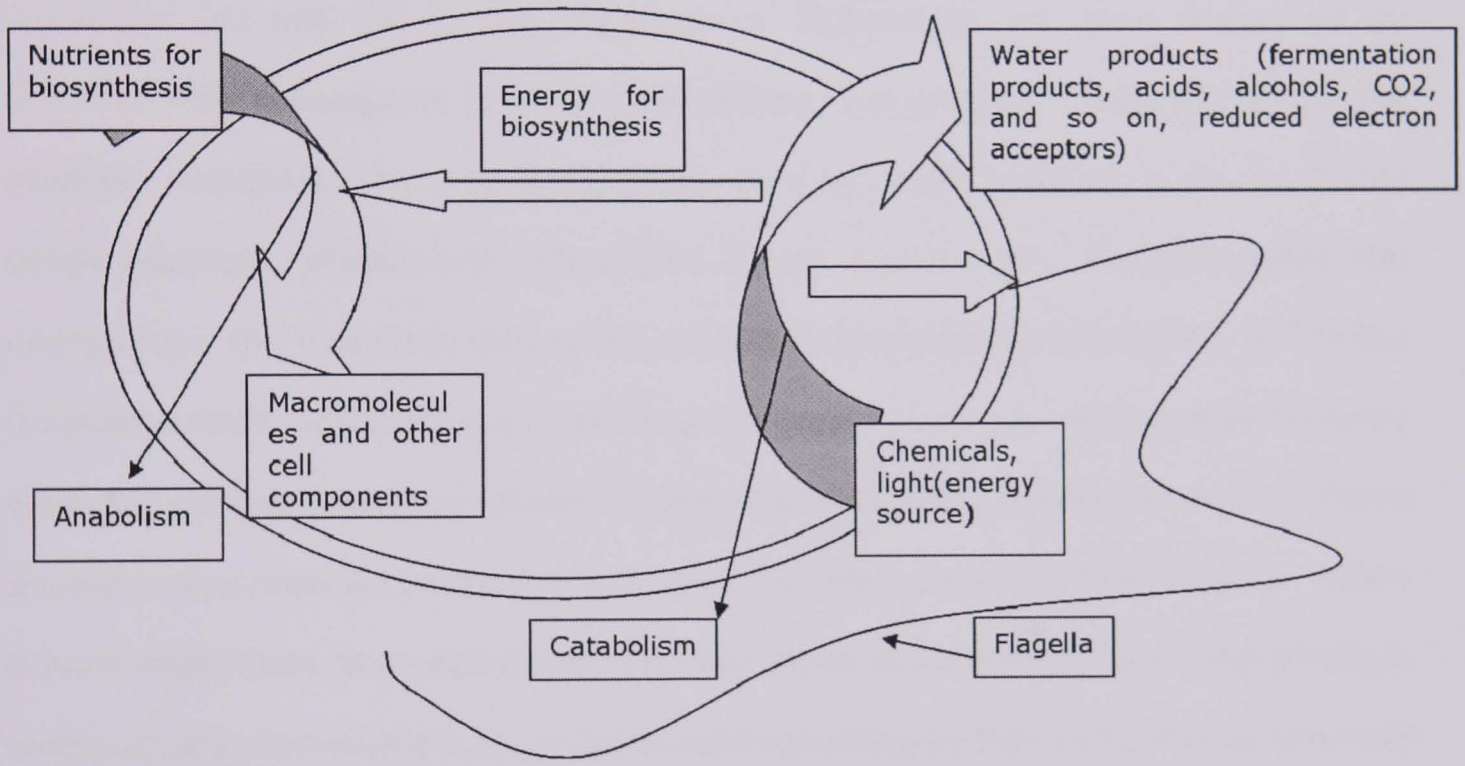

Figure 2.6 A simplified view of bacteria metabolism (Madigan, M.T. and Martinko, J., 2006)

Most reactions in living organisms would not occur at a proper rate without the use of catalysts, which is commonly known as enzymes in microorganisms. Enzymes are proteins that can break bonds of reactants and combine with them to form complex middle states that lead to their degradation (Madigan, M.T. and Martinko, J., 2006). After the degrading reactions, the enzymes are returned to their original state by releasing degradation products, such as electrons and protons. Thus substrates contained in wastewater are consumed with subsequent release of

electrons and protons and the overall process is enhanced by MFCs.

The next steps occur internally in the bacteria. Oxidation-reduction reactions take place where electron donors and acceptors as well as electron carriers are playing a role during the electron transfer processes in the cell. The reaction can be considered as a three stage process; (1) removal of electrons from primary donor; (2) transfer of electrons to one or a series of electron carriers; and (3) delivery to terminal acceptors. Electron carriers, such as nicotinamide adenine dinucleotide (NAD+) and nicotinamide adenine dinucleotide phosphate ($NADP^+$) transfer one proton and two electrons when reduced to NADH or NADPH which shown in Equations (4) and (5) below, respectively. Substrates are then converted by bacteria with subsequent release of electrons and protons. Electrons follow the electron transport chain to pass down through intermediates such as NADH dehydrogenase, ubiquinone (coenzyme Q) or cytochrome. Bacteria store the energy from the substrate conversion in Adenosine triphosphate (ATP). ATP is the most important high energy phosphate compound in living organisms and normally serves as the prime energy carrier in living organisms for conserve of energy. There are two redox reaction pathways for bacteria to keep alive: (1) fermentation, which occurs when there is no additional terminal electron acceptor, and (2) Respiration, which occurs when there is O_2 or other electron acceptor that can serve as terminal electron acceptors.

$NAD^+ + H^+ + 2e^- \rightarrow NADH$ Equation (4)

$NADP^+ + H^+ + 2e^- \rightarrow NADPH$ Equation (5)

Fermentation occurs when there is no existing electron acceptors presented in bacterial environment and the anode cannot be the electron acceptor, i.e. the potential is low (Rabaey, K. and Verstraete, W., 2005). Only partial oxidation of carbon atoms of the substrates occurs and a small amount of the potential energy

is released available to use. Bacteria will transfer their spare electrons to the oxidized substrates hence form reduced metabolites such as acetate, ethanol, H_2 or methane. These fermentation products can be further oxidized by some anaerobic bacteria and withdraw more energy to support electricity production in MFCs (Bond, D.R. and Lovley, D.R., 2003).

Respiration occurs when the anode potential is high and the bacteria oxidizes surrounding compounds during the metabolism process (Rabaey, K. and Verstraete, W., 2005; Logan, B.E. et al., 2006; Lovley, D.R., 2006b). A process by which a compound is oxidized and uses O_2 as external electron acceptor is called aerobic respiration. It produces a greater amount of electrons than fermentation due to the carbon atoms can be completely oxidized to CO_2 and the potential difference is larger. The electrons and protons librated from substrates are then transferred through internal electron acceptors of the bacteria and used for the further growth of the bacteria. The electrons that have not been captured by bacteria are delivered to the external electron acceptors O_2. When there is no oxygen present in the environment, other chemicals with relatively high reduction potential can act as electron acceptors, such as Fe^{3+}, NO_3^-, or SO_4^{2-}, or the anode electrode in itself.

Bacteria can gain energy and conserve it for bacterial activities by transferring the electrons and protons from reduced substrates at low potential to electron acceptors at higher potential. The higher the potential difference, the more energy are available for bacteria to use (Rabaey, K. and Verstraete, W., 2005). If anode potential is higher than other alternative electron acceptors, the bacteria are likely to transfer electrons to anode rather than other acceptors. But if anode potential is lower than other electron acceptors, bacteria preferentially deliver electrons to these alternative electron acceptors (respiration), or to form more reduced complexes (fermentation). So the potential of the anode is very important to the electron transfer route and hence the whole MFCs process.

2.2.5.3 Electron migration out of bacteria

Electron transport systems within the bacteria are composed of a series of membrane-associated electron carriers such as from NADH to Flavoprotein and from quinine to cytochrome (Madigan, M.T. and Martinko, J., 2006). The carriers are bound to membrane proteins and the transfer orders are arranged according to their reduction potentials, from lower potential to higher potential. At the last stage, excess electrons, not captured by bacteria for growth use can theoretically be transport by the carriers with higher reduction potential to external electron acceptors in the environment.

2.2.5.4 Proton migration out of bacteria

Protons are separated from electrons during the internal transport process, such as hydrogen atoms removed from NADH, that are separated into electrons and protons i.e. Equation (4) in reverse. Protons extrude from the membrane with the help of the pH gradient and potential differences across the cell membrane and then proton motive fore produced in bacteria to be conserved in ATP (Madigan, M.T. and Martinko, J., 2006).

2.2.6 Electrochemical aspects of MFCs

2.2.6.1 Open Circuit Potential

The open circuit potential (OCP) indicates the potential difference between the anode and the cathode. The anode potential depends on the coulombic efficiencies and the surface characteristics of the anode electrode. The cathode potential mainly depends on the electron acceptors deposited on the cathode as well as the reaction rate in the cell. High OCP combined with low surface area and total resistance will increase the power density of the MFCs as according to Equation (6)

(You, S. et al., 2006):

$$P = \frac{OCP^2}{AR_{total}} \qquad \text{Equation (6)}$$

Where:

P = power density of the system, W/m^2;

A = the effective anode surface area, m^2;

OCP = Open circuit potential of the cell, V, and;

R_{total} = the total resistance of MFC including internal and external resistances, Ω.

2.2.6.2 Electrode potentials

The electrode potential is formed by measuring the individual potential of a half cell reaction, either as the anode or cathode potential. The standard electrode potentials are given at standard conditions of 25° C, 1 bar and a solution concentration of 1 mol/kg. The potentials vary with temperature, concentration, pressure as well as pH values (Logan, B.E. et al., 2006). A reference electrode, for which the potential is defined or agreed upon by convention, is commonly used to be introduced in the measurement. Electrodes, for which the electrode potential is not yet known, can then be paired with the reference electrode to give the value of the unknown potential. For MFCs, a Ag/AgCl reference electrode with potential of 0.197V corrected to a normal hydrogen electrode (NHE) is typically used.

Presently, the anode potentials and cathode potentials reported in literatures is roughly around -0.275V or -0.285V (NHE) at pH 7 or lower (Liu, H. and Logan, B.E., 2004; Liu, H. et al., 2005b). Cathode potential of around 0.43V to 0.51V (NHE) were reported when no PEM membrane was used (Liu, H. and Logan, B.E., 2004; Liu, H. et al., 2005b). As discussed in Section 2.2.4.2, a strong negative anode

potential is essential for MFC, since the anode potential effects the microbiological reactions in the anode chamber and therefore indicates the amount of electrons that can be used in the MFC process. The cathode potential is another crucial factor governing the power production and it depends on the choice of the cathode electron acceptors (Logan, B.E. et al., 2006).

2.2.7 Hydrogen production from MFCs

Hydrogen production from MFCs has received significant attention since hydrogen can be used as a fuel for road transport, and generate heat and electricity with virtually no pollutants (Scottish-Executive, 2006). It has been shown that hydrogen and electricity can be generated from organic compounds in water simultaneously using MFCs (Angenent, L.T. et al., 2004). The process of hydrogen production from MFCs will be introduced in terms of conventional MFCs and MFC set with additional applied voltage.

2.2.7.1 Hydrogen production from conventional MFCs

Conventional MFCs may produce hydrogen from fermentation processes depending on the abundance or shortage of electrons acceptors in the anaerobic environment. Reducing the electron to the oxidized substrates form reduced secondary substrate where H_2 can be produced during this biological process. The feed is not limited to carbohydrates, virtually any biodegradable dissolved organic matters can be used to generate H_2. However, the H_2 conversion efficiency based on fermentation is low and has limitations. Fermentation of glucose, by all known biological routes, can only produce up to 4 mol H_2 /mol glucose, which corresponds to one-third of the hexose substrate electrons (Rabaey, K. and Verstraete, W., 2005). Equations (7) and (8) show some reactions that would happen during the fermentation of glucose. In literature, typically 60 %-68 % of the sugar is reported to be fermented into

butyrate. This means that typically around 1 to 2.5 moles H_2 production per mole glucose has been observed (Liu, H. and Fang, H.H.P., 2003; Angenent, L.T. et al., 2004). The average conversion efficiency of H_2 from the energy stored in the organic substrate is only around 15 % (Logan, B.E. et al., 2002).

$$C_6H_{12}O_6 + 2H_2O \rightarrow 4H_2 + 2C_2H_4O_2 + 2CO_2 \qquad \text{Equation (7)}$$

$$C_6H_{12}O_6 \rightarrow 2H_2 + C_4H_8O_2 + 2CO_2 \qquad \text{Equation (8)}$$

The H_2 production during the fermentation process reported in literatures has generally been poor and not economic enough to collect and purified for further applications. Some specific process designs have been reported where the bacteria consortia or enzyme studied have achieved H_2 conversion efficiencies of 96.7% by using enzymes (Woodward, J. et al., 2000). However, the economic potential and biochemical routes for this H_2 production aspect have not yet been confirmed.

A bio-gas producing technology competing with MFC is Anaerobic Digestion (AD). Although the methanogenic anaerobic digestion process is mature and reliable, it might not be viable on its own since more or less 15% of the energy is recovered from feedstock depending on their types (Ileleji, K.E. et al., 2008). The economic comparison between hydrogen, methane and electricity production shows that it is more cost effective if the organic matter can also be recovered in the form of electricity (Logan, B.E., 2004). This suggests that bio-hydrogen production combined with electricity production by MFCs can improve energy recovery and thus make the technology more favorable for industrial implementation.

2.2.7.2 Anaerobic MFC with additional voltage

Hydrogen production can be promoted by applying additional voltage to the MFCs

by using electrochemical active micro-organisms in a process called biocatalyzed electrolysis. This has been reported both by Bruce Logan's group in America (Liu, H. et al., 2005c) and Wageningen's group in Netherlands (Rozendal, R.A. et al., 2006). An additional voltage is applied to decrease the cathodic potential below the theoretical potential of -420 mV at pH 7.0, at which $2H^+ + 2e^- \rightarrow H_2$ occurs. Bacteria produce electrons and protons from substrates through the NADH mechanism in the anode chamber, where the potential of NADH formation is -320 mV (Madigan, M.T. and Martinko, J., 2006). Theoretically, H_2 production can then be promoted with an additional voltage of -0.1 V [-420mV-(-320mV)]. This is much more economical than traditional H_2 production with water electrolysis which typically requires a theoretical applied cell voltage of around 1.8 V to 2.0 V (Cheng, H. et al., 2002).

Because of the electrochemical losses, mainly due to overpotential losses at the cathode and the range of bacteria metabolism pathways, more than 0.1 V is needed to be applied for actual H_2 production using MFC. Normally, bench scale experiments require a voltage range from 0.3 V to 0.9 V and it can produce 8-9 mol H_2 /mol glucose in the cathode chamber (Liu, H. et al., 2005c; Rozendal, R.A. et al., 2006). This was achieved in two steps. First glucose was fermented to $C_2H_4O_2$ to generate 2-3 mol H_2 /mol glucose. Then voltage was applied to convert the fermentation by-products according to Equations (9) and (10). The $C_2H_4O_2$ produced 6 mol H_2 /mol glucose based on the electrochemical method above and combined produced 8-9 mol H_2/mol glucose (Liu, H. et al., 2005c). The half reactions occurring at the anode and cathode, respectively, are as follows:

Anode: $C_2H_4O_2 + 2H_2O \rightarrow 2CO_2 + 8\ e^- + 8H^+$ Equation (9)

Cathode: $8H^+ + 8e^- \rightarrow 4H_2$ Equation (10)

Combining Equations (9) and (10) gives a theoretical overall conversion of:

$C_2H_4O_2 + 2H_2O \rightarrow 4H_2+2CO_2$ Equation (11)

Combining Equations (7) and (11) gives the theoretical overall conversion of

$C_6H_{12}O_6 + 6H_2O \rightarrow 12H_2+6CO_2$ Equation (12)

For the sucrose as substrate, the theoretical overall conversion is:

$C_{12}H_{22}O_{11} + 13H_2O \rightarrow 24H_2+12CO_2$ Equation(13)

For the biocatalysed electrolysis, the high yield of H_2 can be generated based on the reactions of Equations (12) or (13) if glucose or sucrose was used as substrate. The main disadvantage of this technology is that external power is needed to be added into the system. This questions the sustainability of this process unless the excess voltage is generated from another MFC or within the MFC itself. Equations (12) and (13) can also be used as the theoretical reactions for the fermentation process if glucose or sucrose was used as substrate in the MFC.

2.3 Performance and Developmental aspects of MFCs

Common expressions describing the performance of MFCs related to energy production and efficiencies have been formulated in literature to compare MFC data generated from different MFC designs under development.

2.3.1 MFCs performance expressions

The most common expressions used to assess MFCs performance are related to its

energy output, energy conversion efficiency and substrate conversion.

2.3.1.1 Energy output

Energy output expressions and performances included power density, polarization curve and hydrogen production of MFCs.

2.3.1.1.1 Power density

The power density is normally reported as the produced power based on per unit of anode surface area, effective volume of anode chamber or total MFCs volume. This makes it possible to compare power production of different MFCs systems. The power density largely depends on the anode materials applied in the system due to the tremendous influence of bacteria on anode surface towards the power densities of the MFCs. If carbon cloth or graphite felt is used, power density based on the overall anode surface area is the most used expression. If graphite granule is used in the anode chamber, it is not convenient to calculate the total effective surface area of granules, thus power densities based on the volume of the chamber is used. Equations (14) and (15) shown the expressions of power density based on the anode surface area and power density based on the total volume of MFC chamber, respectively.

$$P = \frac{V_{cell}^{\ 2}}{R_{ext} A} \qquad \text{Equation (14)}$$

$$P = \frac{V_{cell}^{\ 2}}{R_{ext} V_{MFC}} \qquad \text{Equation (15)}$$

Where:

P= power density, W/m^2;

V_{cell}= cell voltage recorded with a data logger, V;

R_{ext}= external resistance, Ω;

A= anode surface area, m^2, and;

V_{MFC}= total volume of MFC chamber, m^3.

A wide range of power densities have been reported in literature using several different types of MFCs. Some of these power density data are compared in Table 2.1.

Table 2.1 Maximum power densities performance reported in literatures

Inoculum	Substrate	Anode materials	Max power density, mW/m^2	Reactor types	References
Geobacter	Acetate	Plain grap. [4]	13	Two-cham.	a
An. S[1]	Glucose	Plain grap.	3600	Stacked	b
AS[2]	Glucose	Plain grap.	78	Single	c
WW[3]	Glucose	Woven grap	26	Single	d
WW	Glucose	Woven grap	494	Single	d
WW	WW	Woven grap	146	Single	d
An. S	WW	RVC[5]	170	Tubular upflow	e
An. S	Glucose	Plain grap.	4310	stacked	f
AS	Glucose	Grap. Granules	50.2 W/m^3	Tubular	g
Geobacter	WW	Grap. rods	26	Single	h
AS	WW	Grap.	25	Two-cham.	i
WW	WW	Carbon paper	38	Two-cham. Salt bridge	j
An. S	Acetate	Grap. granules	258 W/m^3	Stacked	k
An. S	Acetate	Grap. granules	90 W/m^3	Tubular	l

1 Anaerobic Sludge, 2 Activated sludge, 3 Wastewater, 4 graphite, 5 Reticulated vitreous carbon

a (Bond, D.R. and Lovley, D.R., 2003), b (Rabaey, K. et al., 2003), c (Park, D.H. and Zeikus, J.G., 2003), d (Liu, H. and Logan, B.E., 2004), e (He, Z. et al., 2005), f (Rabaey, K. et al., 2004), g (You, S. et al., 2007), h (Liu, H. et al., 2004), i (Rodrigo,

M.A. et al., 2007), j (Min, B. et al., 2005a), k (Aelterman, P. et al., 2006), l (Rabaey, K. et al., 2005b)

2.3.1.1.2 Polarization curve

The polarization curve represents the cell voltages as a function of the produced current or current densities. It is a powerful tool to analysis and characterize the properties of fuel cells (Hoggers, G., 2002). It can be recorded for the anode, the cathode or the whole MFC using either a variable external resistor unit and data logger or electrochemical equipment, known as a potentiostat. A variable load test, involves a periodical decrease or increase in the cell load, and the different voltage data are measured. The corresponding current can be calculated by Ohms law shown in Equation (16) and a voltage curve can be plotted. For the potentiostat examination, a scan rate of around 1 mV/s is typically chosen. The voltage and corresponding produced current data are calculated and a linear polarization curves is shown as a V-I plot. Besides the V-I plot, another curve plotting the power density as a function of current or current density is usually presented in the same plot. An example from literature is shown in Figure 2.7.

$$I = V/ R_{ext} \qquad \text{Equation (16)}$$

Where:

I= current generated in the MFCs, A;

V_{cell}= cell voltage generated in the MFCs, V; and

R_{ext}= external resistance of the MFCs, Ω.

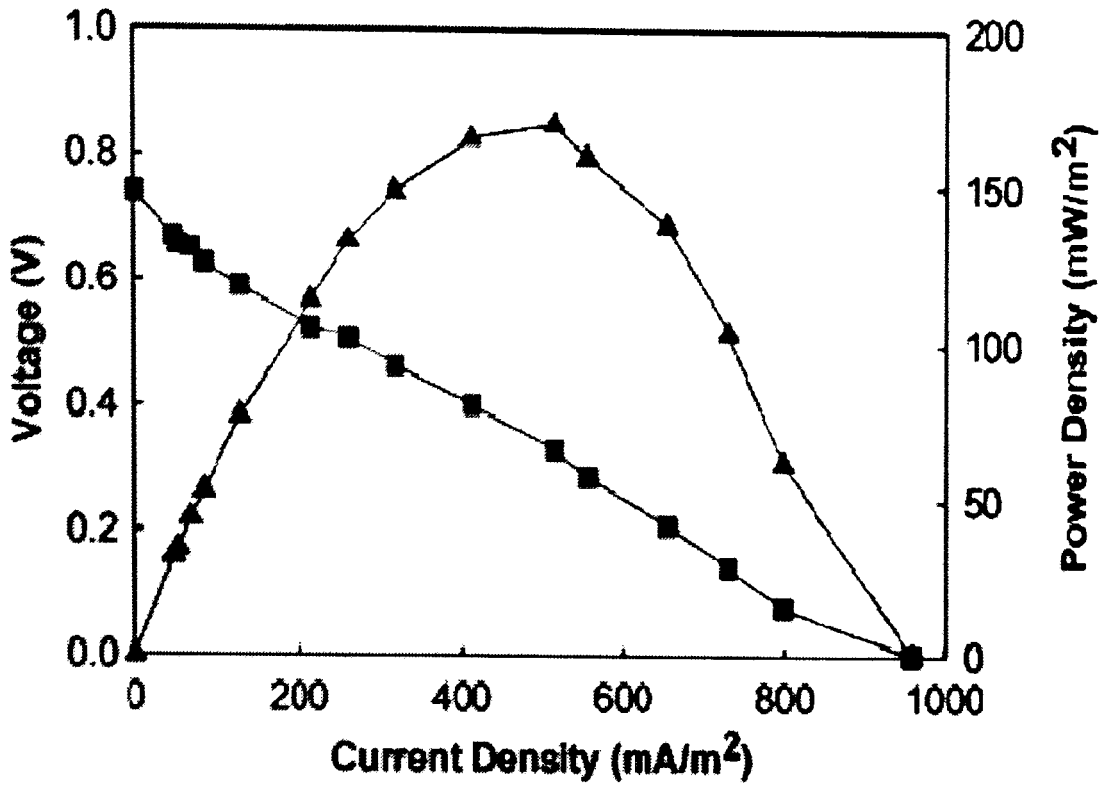

Figure 2.7 Typical polarization curves for a MFC (He, Z. et al., 2005) where triangle symbol for power density data and cubic symbol for voltage data

The cell voltage curve represented the polarization curve of the MFC. The peak in the power density curve indicates the maximum power density that can be generated in a particular MFC system. Accordingly, the corresponding current and voltage data based on the maximum power density can be used to calculate the optimal external resistance by Ohms law to operate the system at its optimal state. The value of the internal resistance of the MFC system can be obtained from the slope in the cell voltage polarization curve (Logan, B.E. et al., 2006).

2.3.1.1.3 H_2 production

The H_2 yield for a MFC is typically expressed as the total amount of H_2 produced in the MFCs per unit of COD removal. It can be calculated according to Equation (17):

$$Y_{H_2} = \frac{n_{H_2} \times M_{H_2}}{V_e \times (COD_{in} - COD_{out})} \times 1000 \qquad \text{Equation (17)}$$

Where:

Y_{H2}=hydrogen yield, g H_2/g-COD;

M_{H2}= the molecular weight of hydrogen which is 2 g/mol;

n_{H2}= the total mol of H_2 produced in the test, mol;

V_e= the effective volume of influent involved in the work, L;

COD_{in}= the influent COD at the beginning of experiment, mg/L;

COD_{out}= the effluent COD at the end point of experiments, mg/L.

In conventional MFCs studies, the focus has been placed on the power production in the system, and only a few publications have reported the actual hydrogen yield in the conventional MFCs.

2.3.1.2 Energy conversion efficiency

The MFC energy conversion efficiency can be expressed in several forms, but all link between the chemical energy contained in the substrates and the electric energy generated (Rabaey, K. and Verstraete, W., 2005). The energy conversion efficiency expressions and performances, including the coulombic efficiency and the H_2 recovery efficiency, are introduced in this section.

2.3.1.2.1 Coulombic efficiency

Coulombic efficiency deals with the electrons that are recovered from the substrate in the form of electric current. It expresses the rate of actual amount of electrons that is gained from the substrate in the form of electricity against the theoretical amount of electrons that the bacteria could deliver based on the COD removal or substrate removal. The coulombic efficiency is one of the most important indexes that were used to describe the MFC performance in terms of power generation. Efforts have been focused on coulombic efficiency improvement to promote MFCs for industrial applications. The coulombic efficiency expressing the transfer of substrates into e^- is calculated using Equation (18) if the substrate composition is

complex or extremely ill-defined (He, Z. et al., 2005) or Equation (19) if the substrate is well defined (Liu, H. et al., 2005c):

$$\eta_{coulombic} = \frac{\int_0^t I' dt_{exp}}{\frac{F \times n \times \Delta COD \times V_e}{M}} \times 1000 \times 100\% \qquad \text{Equation (18)}$$

Where:

$\eta_{coulombic}$= coulombic efficiency of the MFCs system, %;

I'= current generated in the MFCs system per unit time, for instance 60s;

t_{exp}= the recording interval time of the experiment in seconds (s), for instance 60s per data;

t= the total period of the experiment, sec;

F= the Faraday's constant which is 96485 C/mol;

n= the number of electrons exchanged per mol of substrate, which is 4 mol e- per mol O_2;

ΔCOD= the chemical oxygen demand difference between the beginning of the experiment and the end of the experiment, mg/L;

V_e= the effective volume of influent involved in the work, L; and

M= the molecule weight of substrates, g/mol.

$$\eta_{coulombic} = \frac{\int_0^t I' dt_{exp}}{\frac{F \times \Delta substrate \times n}{M}} \times 100\% \qquad \text{Equation (19)}$$

Where:

$\eta_{coulombic}$= coulombic efficiency of the MFCs system, %;

I'= current generated in the MFCs system per unit time, for instance 60s;

t_{exp}= the recording interval time of the experiment in seconds (s), for instance 60s

per data;

t= the total period of the experiment, sec;

F= the Faraday's constant which is 96485 C/mol;

Δ substrate= the weight of total substrate used during the MFC process, g;

n= the number of electrons exchanged per mol of substrate; which is 8 mol e- per mol CH_3COONa in the case of sodium acetate as substrate; and

M= the molecule weight of substrate, g/mol.

Equation (18) relates coulombic efficiency to the COD removal and Equation (19) calculates the total charges that can be converted from the consumption of the substrate. The numerators of both equations integrate current production over the entire experiment period. The use of these two equations depends on the method used for measuring the remaining substrate in the system. Current performance of coulombic efficiencies reported in literature vary from very low, such as 0.7-8.1 % (He, Z. et al., 2005), 3-12 % (Liu, H. et al., 2005a) and 9-12 % without PEM membrane (Liu, H. and Logan, B.E., 2004), to as high as 40-55 % (Liu, H. and Logan, B.E., 2004), 55 % (Min, B. et al., 2005a) and 75 % (Rabaey, K. et al., 2005b) with PEM membrane. The coulombic efficiency has been formed to mainly depend on the MFC design, the electrode materials, the anodic medium and the bacteria culture used.

2.3.1.2.2 Energetic efficiency

Another expression used is energetic efficiency. This expression compares the electric energy recovery over the chemical energy stored in the removed substrate (He, Z. et al., 2005). The formula is expressed in Equation (20) and is applied to all kinds of substrates, such as organics from wastewater.

$$\eta_{energetic} = \frac{\int_0^t V_{cell} I' dt_{exp}}{E_{added}} \times 100\% \qquad \text{Equation (20)}$$

Where:

$\eta_{energetic}$= energetic efficiency, %;

V_{cell}= cell voltage recorded with a data logger, V;

I'= current generated in the MFCs system per unit time, for instance 60s;

t_{exp}= the recording interval time of the experiment in seconds (s), for instance 60s per data;

t= the total period of the experiment, sec; and

E_{added}= the energetic content of the substrate consumed, J.

Scarce data have been published for the energetic efficiency when actual wastewater is used as substrate of MFCs. It is difficult to analysis the total chemical energy input into the system and this is usually estimated from the energy content in COD.

2.3.1.2.3 H_2 recovery rate

In conventional MFC, the H_2 recovery rate is a measure of the actual amount of H_2 generated by MFC compared to the theoretical amount of H_2 that could produced from the MFC based on the theoretical fermentation reactions of the substrate, depends on the substrate used in the system, for example glucose as substrate and the reaction as in Equation (12). Equation (21) expresses the H_2 recovery rate in MFCs.

$$R_{H_2} = \frac{H_2 Actual}{H_2 Theoretical} \times 100\% \qquad \text{Equation (21)}$$

Where:

R_{H2}= H_2 recovery rate, %;

H_2 Actual= the actual produced hydrogen molecules in the MFC, which can be calculated as the H_2 concentration multiply the total volume of MFC headspaces, mol; and

H_2 Theoretical= the theoretical amount of H_2 in MFCs, which is calculated based on the consumed amount of substrate with the theoretical fermentation reactions.

In the biocatalysed electrolysis system as described in Section 2.2.7.2, the H_2 recovery rate is a rate of the actual amount of H_2 generated in the cathode chamber versus to the theoretical amount of H_2 that can be converted from the current production with the application of additional voltage in the system. This is expressed in Equation (22).

$$R_{H_2} = \frac{H_2 Actual}{\frac{\int_0^t I' dt_{exp}}{2F}} \times 100\% \qquad \text{Equation (22)}$$

Where

R_{H2}= H_2 recovery rate, %;

H_2 Actual= the actual produced hydrogen molecules in the reactor, which can be calculated as the H_2 concentration multiply the total volume of the reactor headspaces, mol;

I'= current generated in the MFCs system per unit time, for instance 60s;

t_{exp}= the recording interval time of the experiment in seconds (s), for instance 60s per data;

t= the total period of the experiment, sec;

F= is Faraday constant 96485 C/mol; and

2= two electrons per mol of H_2.

The denominator in Equation (22) expresses the theoretical amount of H_2 that can

be produced by converting the amount of electrons based on the current production. The H_2 recovery rate is an important index that expresses the ability of MFC to recover H_2 from the current generation particularly for the biocatalysed electrolysis system with applied voltage.

2.3.1.3 Substrate consumption

The chemical oxygen demand (COD) and biological, or biochemical oxygen demand (BOD) tests are used to measure the extent of substrate consumption by bacteria in MFCs.

The COD test is commonly used to indirectly measure the amount of organic compounds in water in the area of environmental chemistry (Wiesmann, U. et al., 2007).The principle of the COD test is based on the fact that nearly all organic compounds can be fully oxidized to carbon dioxide with a strong oxidizing agent under acidic conditions. The amount of oxygen required to oxidize an organic compound can be tested and calculated. It can be used to measure the water quality, such as determine the amount of organic pollutants found in surface water, like lakes and rivers. The unit of COD is expressed in milligrams O_2 per litre, mg/L, which indicates the mass of oxygen consumed per liter of solution (Forster, C.F., 2003; Wiesmann, U. et al., 2007).

BOD is a test used to provide measure of the concentration of biodegradable organic matter present in a water sample. It is used to infer the general quality of the water and its degree of pollution. It should not be considered as an accurate quantitative method to indicate the quality of water. The BOD level of a water sample is determined from the amount of dissolved oxygen consumed after 5 days of water samples being sealed in a bottle.

The difference between COD and BOD is that COD relates to the total chemical conversion of organic matters into CO_2 rather than BOD test that only refers to the biodegradable substance level. Normally COD is higher than BOD for the same sample and generally the BOD is roughly 0.6 times that of COD which is a recognized empirical data. One limitation of COD is that it cannot tell the difference between biologically active organic substances levels and biologically inactive matter levels. However, COD has the advantage of requiring a relatively short test time of 3 hours, compared to BOD test which needs 5 days for one single sample.

For MFCs experiments, normally COD is measured to characterize the substrate consumption. There is an assumption in this work that the COD removal rate in MFCs is consistent for each passes of the reactor routes. The COD removal rate in a long term of MFC running follows the formula described in Equation (23).

$$COD_{in} \times (1 - \Delta\, COD_s\%)^x = COD_{out} \qquad \text{Equation (23)}$$

Where COD_{in}= the influent COD at the beginning of experiment, mg/L;

$\triangle COD_s$= COD removal rate within a single pass of MFC reactor,

x =total passes, and

COD_{out}= the effluent COD at the end point of experiments, mg/L.

2.3.2 MFC design developments

The MFCs technology has developed very rapidly in just a few years. One of the most fast developing areas is the MFCs designs. Based on the principles of the most simplified two-chamber MFC, many other designs have been developed and studied. In this section, several types of classic designs mainly capable of continuous flow applications with great MFCs performance are introduced.

A cylindrical chamber MFC reactor was developed by Liu et al. for treatment of wastewater (Liu, H. et al., 2004). In their system, both anode and cathode were placed in one cylinder chamber where the cathode was set in the centre of the reactor through which an air flow was imposed and eight anode graphite rods were located concentric around the cathode as shown in Figure 2.8. Compared to the two-chamber system shown in Figure 2.4, this structure can be used both in batch and continuous mode. The anode surface area is larger to increase the amount of bacteria and passive air transfer to the cathode requires extra energy.

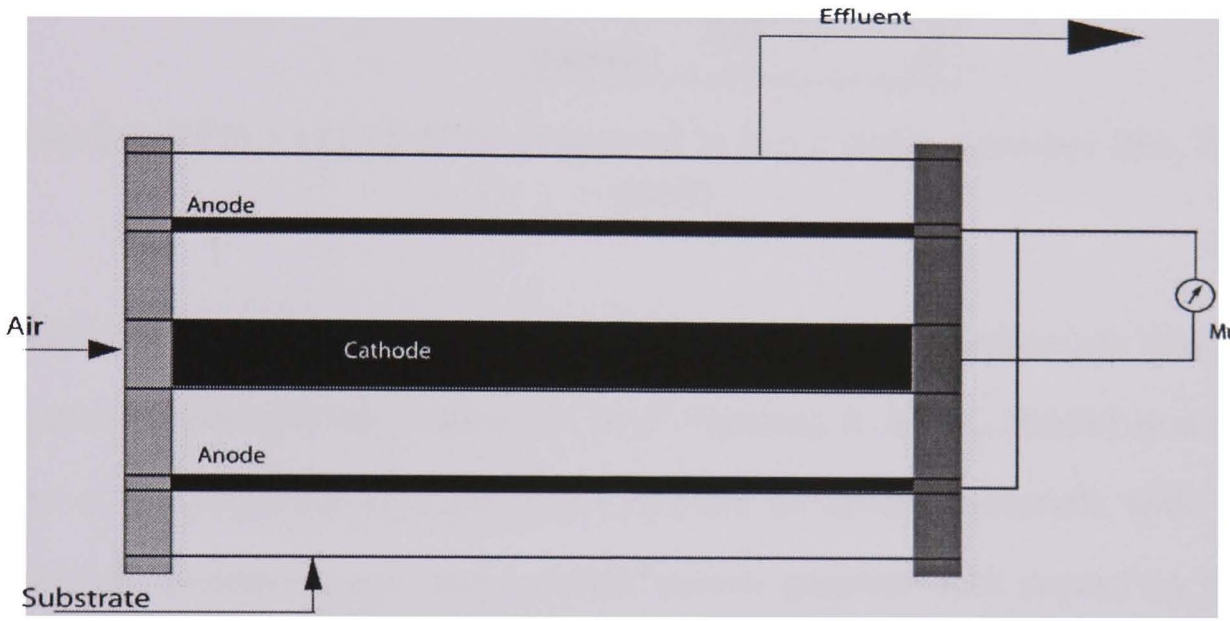

Figure 2.8 Cylindrical based MFC with inner cathode adjusted from (Liu, H. et al., 2004)

He, Z. et al. designed an upflow MFCs where the anode and cathode were physically present in the same reactor unit as shown in Figure 2.9 (He, Z. et al., 2005). Through the reactor, an upflow stream was imposed and the cathode was located at the top. Between the anode and the cathode chamber, a PEM membrane was installed to avoid oxygen penetration from the cathode area to the anode area. Due to long distance for protons to travel and a high internal resistance of 84 Ω, the MFC performance for this reactor was considerably lower than the reactor type shown in Figure 2.8. The anode surface area supplied by granular activated carbon is large and low cost, but air is needed to be pumped into the cathode chamber which is energy intensive.

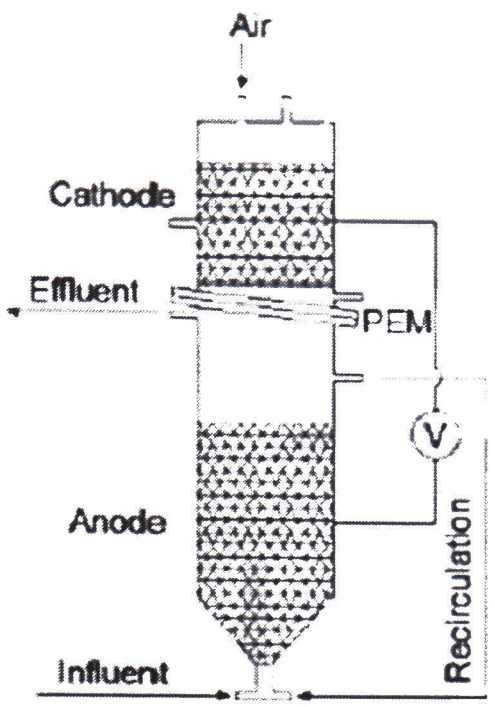

Figure 2.9 Upflow based MFCs composed in the a single chamber (He, Z. et al., 2005)

A tubular reactor with an inner granular packed bed graphite anode and an outer cathode was designed by Rabaey, K et al (Rabaey, K. et al., 2005b) and shown in Figure 2.10. Graphite granules were applied as anode materials with bacterial incubation. In this design, the cathode woven graphite mat served as the outer material and was wrapped around the anode separated by a Cation Exchange membrane (CEM). The internal resistance of the system was only 4 Ω, which indicates a good design for reducing internal voltage losses. The anode surface area was very high, and no pump was needed to supply O_2. An electron acceptor $K_3Fe(CN)_6$ was used, which is consumed and needed to be replenished.

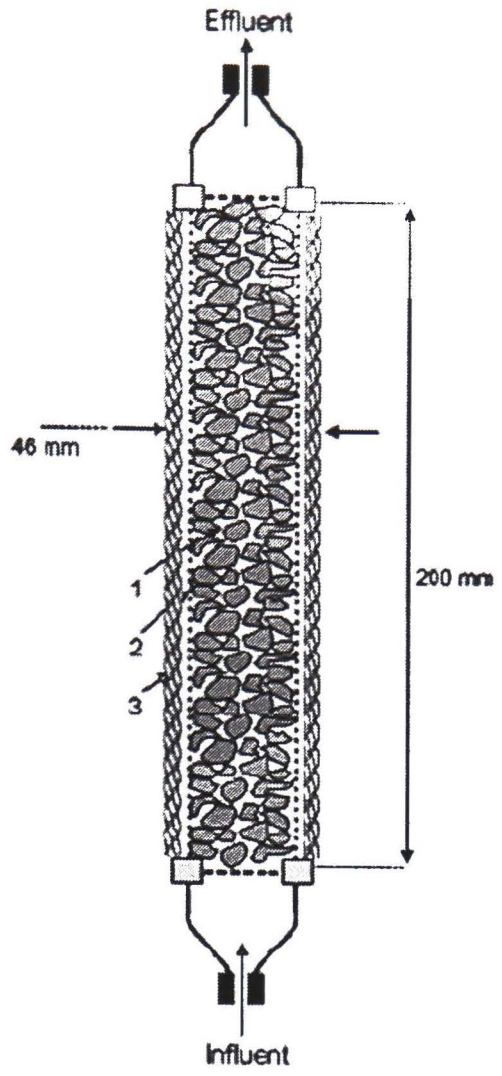

Figure 2.10 Tubular reactor with outer cathode and inner packed bed anode (Rabaey, K. et al., 2005b)

Figures 2.11 and 2.12 below show several types of batch and continuous MFCs, respectively, developed by Bruce Logan's group (Logan, B.E. et al., 2006). Picture A and F in Figure 2.11 show the simplest designs with two chambers connected with a PEM membrane bridges for proton transmission (Logan, B.E. et al., 2005; Min, B. et al., 2005a). Pictures B and C show two-chamber MFCs with membrane separation in stacked constructions (Rabaey, K. et al., 2005a; Rabaey, K. et al., 2005c). In these MFCs the anode materials were graphite granules resulting in high surface areas with relatively high power performance. Picture D shows a photoheterotrophic MFC where light was needed to support the power generation from substrate with photoheterotrophic bacteria (Rosenbaum, M. et al., 2005). Picture E shows a single chamber membrane MFCs with an open air cathode (Liu, H. and Logan, B.E., 2004). No cathode chamber and medium is needed since the oxygen in the open air was used as cathode electron acceptor.

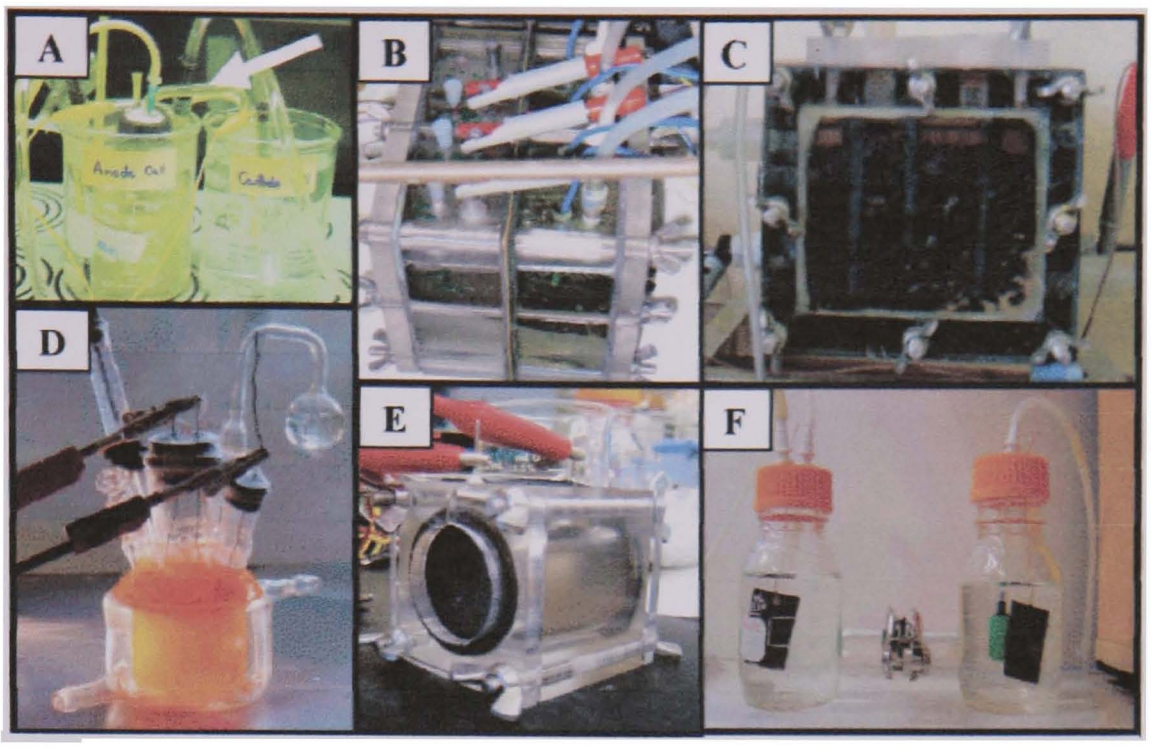

Figure 2.11 Types of MFCs for batch mode application (Logan, B.E. et al., 2006) (A) Salt bridge two chamber MFC; (B) Stacked four MFCs; (C) same as B but with a continuous flow-through anode; (D) photoheterotrophic type MFC;(E) single-chamber air-cathode MFC; (F) Two-chamber MFC

Figure 2.12 shows MFC design for continuous flow applications. Pictures A and B show both upflow MFCs that were described in detail in Section 2.3.2 (He, Z. et al., 2005; Rabaey, K. et al., 2005b). Picture A has an inner anode with an outer cathode. Picture B has an upper cathode with anode below. Picture C shows a flat plate MFC where two half channels were made on the blocks and the anode and cathode materials were located in between with a membrane separation and then sandwiched together (Min, B. and Logan, B.E., 2004). Picture D is a single chamber MFC with an anode rod and an air cathode tube as explained in Section 2.3.2 (Liu, H. et al., 2004). Picture E is a stacked continuous MFC containing six mini-MFCs jointed in a block to possible increase the power production (Aelterman, P. et al., 2006).

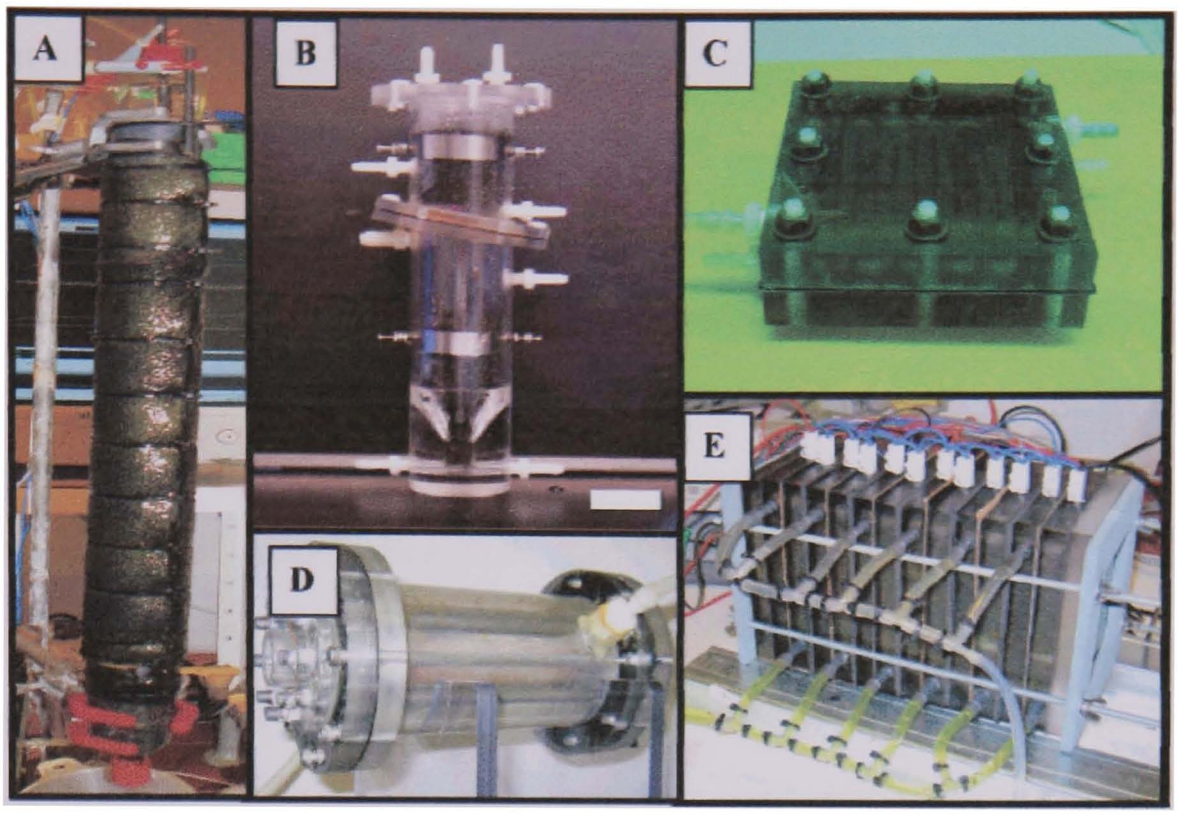

Figure 2.12 Types of MFCs for continuous application (Logan, B.E. et al., 2006) (A) upflow, tubular type MFC with inner graphite bed anode and outer cathode; (B)upflow, tubular type MFC with anode below and cathode above, the membrane is inclined; (C) flat plate design with two electrode channels separating with membrane ; (D) single-chamber with an inner concentric air cathode surrounded by graphite rods as anode; (E) stacked six separated MFCs

Since the MFC design can strongly affect the power production performance, the coulombic efficiency and the internal resistance, the most effective MFC design with high performance and low cost is still sought. At present, there is no strict definition of the optimum MFCs design, since most of the designs have their advantages and disadvantages. In particular, power density data are still very low. Although the power performance is affected by the MFC design, many other factors, such as bacteria species, electrode materials, mediums and separation membrane, influence the MFC performance as describe below.

2.3.3 Materials involved in MFCs

2.3.3.1 Anode Materials

Besides the MFCs structures and bacteria species used, there are many other

factors that affect the performance of MFCs. One of the most essential factors is a high-performance anode. The anode material and its structure can directly affect the bacteria behaviour, their attachment, the electron transfer and the metabolism process of the bacteria towards substrate consumption. To date, the most common used anode materials are carbon materials, such as solid graphite, carbon cloth, carbon papers, graphite felt, graphite granules and vitreous carbon (Kim, H.J. et al., 2002; Chaudhuri, S.K. and Lovley, D.R., 2003; He, Z. et al., 2005; Liu, H. et al., 2005b). They have good stability in a microbial environment, high surface area for bacterial attachment and high conductivity for the charge transfer. But the power productions from these materials are still low and not efficient, where the efficiencies barriers are not well understood at the moment.

While the exact molecules that act as electron mediators and transport electrons from the bacteria to the anode surface have yet to be identified (Cheng, S. and Logan, B.E., 2007), various concepts and mechanisms for electron transfer from microbial cells to the anode surface have been proposed (Rosenbaum, M. et al., 2007). Two main concepts have been suggested, namely (1) direct electron transfer from bacteria to anode surface; and (2) energetic electrocatalytic anode materials that directly oxidize the secondary products from fermented substrates. In both cases, electrons are captured by these anode materials.

The first concept suggests that the process is based on direct electron transfer from bacterial cell to the anode as described in the electron transfer mechanisms in Section 2.2.2. Some bacteria could produce electron shuttling compounds to facilitate the electron transfer onto the anode surface (Rabaey, K. et al., 2004). Some bacteria may have the ability to form conducting nanowires, such as bacterial pili, where electrons can be transported through the pili from bacteria directly to the anode. Geobacter Sulfurreducens (Reguera, G. et al., 2005; Reguera, G. et al., 2006) and Shewanella Oneidensis MR-1 (Gorby, Y.A. et al., 2006) have both been shown to support this concept.

The second concept is totally different from above. It suggests that the substrates contained in the anode chamber can be fermented and degraded by bacteria to secondary metabolic products, for instance H_2. They were then oxidized by an electrocatalytic anode material that performs efficient in-situ oxidation. For instance, anode material with platinum as electrocatalyst can be used for this concept to oxidize H_2 where the catalyst avoids large overpotential in the delivery of electrons. Several anode treatment technologies based on these two concepts have already been studied and developed, with the purpose to improve the power production performance of MFCs. Some of the outcomes of these studies are listed in Table 2.2.

The first four studies in Table 2.2 were focused on the concept of direct electron transfer. Ammonia gas treatment and Fe_2O_3 coated carbon were used to increase the positive charge and electrostatic charge of the anode surface to attract more bacteria with electrons to the surface. A range of compounds, including Mn^{4+}, Ni^{2+}; Fe_3O_4, Ni^{2+}; Fe_3O_4 and neutral red, were used to modify graphite to incorporate microbial oxidants or electron mediators to anode materials. This dramatically helped the electron transfer on the surface compared to non-treated carbon especially for ammonia where power densities close to 2 W/m^2 were produced. The bottom three studies in Table 2.2 used composited, carbonated or polymerized chemicals with conductive materials, to increase the anode electrocatalytic activity to oxidize substrates. Tungsten carbide and Pt materials were used to oxidize the H_2 from fermentation to further increase the capturing of electrons. Extremely high power densities close to 6 W/m^2 were produced.

Table 2.2 Anode material treatments and their MFC performance from literature

Anodes	Inoculation	Types of MFCs	Max PD,mW/m^2	Principles
Ammonia treated carbon cloth [a]	Domestic WW.	Single chamber	1970	Surface charge increased
Mn^{4+}, Ni^{2+}; Fe_3O_4, Ni^{2+}; Fe_3O_4 modified graphite [b]	marine seawater	Sediment	105	Microbial oxidants incorporated
Fe_2O_3 coated carbon [c]	Domestic WW.	Two chambers	30	Positive surface charge and electrostatic charge
Mn^{4+}; neutral red modified graphite [d]	Sewage sludge	Two chambers	788	Electron mediators incorporated
CNTs/polyaniline composite film [e]	E. coli K12	Not clear	42	Anode electrocatalytic activity increased
Tungsten carbide pressed on graphite [f]	E. coil	Not clear	5860	Anode electrocatalytic activity increased, hydrogen oxidation
Fluorinated polyaniline polymerized on Pt sheet [g]	E. coli K12	N/A	5.3A/m^2	Anode electrocatalytic activity increased, hydrogen oxidation

References: [a] (Cheng, S. and Logan, B.E., 2007); [b] (Lowy, D.A. et al., 2006); [c] (Kim, J.R. et al., 2005); [d] (Park, D.H. and Zeikus, J.G., 2003); [e] (Qiao, Y. et al., 2007); [f] (Rosenbaum, M. et al., 2007); [g] (Niessen, J. et al., 2004)

Both concepts appear to increase power density which might indicate that MFCs operate using both concepts in tandem. However, a breakthrough technology has not yet been identified and the present procedures of anode treatment are all based on complicated fabrication procedure resulting in high treatment and materials costs. Furthermore, the second concept of improvement of anode electrocatalytic activity, encountering with the reducing of H_2 production in MFCs, weakens the application of this anode treatment.

2.3.3.2 Cathode materials

Similar to anode materials, cathode materials can also substantially affect the MFC performance. The cathode in MFCs provides sites where electrons and protons transfer to their electron acceptors. It involves electron acceptors that are introduced into the cathode chamber, usually as added chemicals such as plain carbon cathode electrode in ferricyanide (Schroder, U. et al., 2003; Oh, S.E. et al., 2004) or permanganate solutions (You, S. et al., 2006). These chemicals act as redox mediators with good properties for redox activities and higher reduction potentials in cathode chambers. After use, the chemicals need to be supplemented, or recycled.

An oxygen cathode is most commonly used in MFCs (Rabaey, K. et al., 2003; Liu, H. et al., 2004; He, Z. et al., 2005; You, S. et al., 2007), where the cathode material is immersed in water and dissolved oxygen is used as electron acceptor (Hoggers, G., 2002). In order to help the reduction of O_2 in the cathode chamber, a gas-permeable electro-catalyst, such as platinum (Pt), is usually incorporated into the cathode material. Pt can be used successfully with loadings as low as 0.35 mg/cm^2 (Liu, H. et al., 2005b).

The advantage of using Pt as catalyst in the MFCs cathode is its high oxygen reduction properties (Zhao, F. et al., 2006). However, the main characteristic of Pt is its sensitivity to impurities, such as CO and H_2S, that can poison all known electro-catalysts including Pt (Palanker, V.S. et al., 1977). Concentrations as low as 100 ppm of CO in the system will reduce the current output of a hydrogen fuel cell by about 80%, since CO strongly adsorbs onto the active Pt sites and blocks further reaction on it (McIntyre, D.R. et al., 2002). Also, since Pt is a noble metal, the cost is high and there is a need to either decrease the content of Pt in the cathode, i.e. the catalyst loading rate or substitute Pt with cheaper, non-noble metal catalysts. The disadvantages of Pt have lead to increased attentions to find an alternative as

the catalyst for the MFC cathode. Several cathode alternatives have already been developed and studied, where comparable MFC performances to that of Pt contained cathodes were achieved as shown in Table 2.3.

Table 2.3 Different alternative cathode materials and their MFCs performance from literature

Cathodes	Inoculation	Types of MFCs	Max PD,mW/ m^2 anode	Principles
Fe^{3+} graphite [a]	Sewage sludge	Two-chamber	788	Electron mediators incorporated
Pyrolyzed iron phthalocyanine (pyr-FePc) [b]	E coli K12	Two chamber	230	Alternative O_2 reduction
Cobalt tetramethylpheny-lporphyrin (CoTMPP) [c]	Domestic WW	Single chamber	369	Alternative O_2 reduction
FePc [d]	Mixed culture	Single chamber	2011	Alternative O_2 reduction
Lead dioxide (pbO_2) [e]	Domestic WW	Two-chamber	25	Alternative O_2 reduction

References: [a] (Park, D.H. and Zeikus, J.G., 2003); [b] (Zhao, F. et al., 2006); [c] (Cheng, S. et al., 2006b); [d] (Yu, E.H. et al., 2007); [e] (Morris, J.M. et al., 2007)

Some research have been focused on substituting the Pt carbon cathode with stainless steel materials for marine sediment MFCs, where a maximum power density of 23 mW/m^2 was achieved by forming a biofilm to cover the metal to help oxygen reduction in the seawater (Dumas, C. et al., 2007). Graphite granules is another well investigated plain cathode material. Freguia et al., found that with nano-scale pores contained in granular graphite, the high surface area promoted

oxygen reduction that increased the power output up to 21 W/m^3 which is in the same order of magnitude as most catalyzed materials tested (Freguia, S. et al., 2007).

The cathode design configuration is another topic where MFC cathode performance can be improved. A rotating cathode design achieved a 40 % higher power density compare to a non-rotating cathode system for a sediment MFC (He, Z. et al., 2007). Simply by applying a PTFE layer to the air-side of the cathode, the coulombic efficiency was improved by 32 % due to the reduction of aerobic degradation of substrate in anode chamber by preveting O_2 diffusion from the cathode chamber (Cheng, S. et al., 2006a).

2.4 Current MFC limitations

2.4.1 Limitations Related to microbiology

2.4.1.1 Diffusion of substrate towards bacteria

For the mediator-less MFCs, it is essential that bacteria are attached on the surface of anode materials to form a biofilm. Bacteria can easily transfer electrons onto the anode surface through their pili structure as described in Section 2.2.4.2. However, a fixed position prevents bacteria from actively collecting nutrients i.e. organic substrate in wastewater. The only available substrate is that surrounding their position. For thick biofilms with multi-layers of cells in depth, cells at the bottom may die due to the lack of a source of substrate for energy and growth (Logan, B.E., 1999; Wiesmann, U. et al., 2007). Hence, the diffusion limitation of the substrate from bulk water to a position surrounding the anode surface is a main factor affecting the efficiency of the bacteria to produce electrons and protons to the external environment.

2.4.1.2 Bacteria metabolism and activation energy

Bacteria metabolism is a major MFC limitation caused by the slowness of the biological process taking place, especially surrounding the anode surface. This can be improved by maintaining an optimum temperature for biological activity, typically 20-30 ℃. Further, the bacteria metabolism requires a certain activation energy to activate its redox reactions, involving the reduction of a compound at the bacterial surface, and while the compound is oxidized directly at the anode surface. This activation energy requirement incurs a potential loss generally described as activation losses and it could unfavourable to the MFC process. Lowering of potential loss such as with the help of enzyme application could help to improve the MFC.

2.4.1.3 Mixed species versus single species limitations

The use of mixed bacteria species or a single species can lead to different limitations. When using single species in the anode, a detailed and specific effect can be well developed and analysed. Also, it is much easier to analyse the relationship between this species and some other MFC factors, such as the anode surface and external mediators. Some studies also implied that the coulombic efficiencies of certain single species are very high (Bond, D.R. et al., 2002; Bond, D.R. and Lovley, D.R., 2003; Chaudhuri, S.K. and Lovley, D.R., 2003). However, the application of single species needs a very complicated isolation procedure and care must be taken for non-contamination of other bacteria culture in the feed streams. This obviously is not achievable for wastewater treatment without sterilizing the water. The inoculums costs are high for individual species and they also need specific cultivation process and high environment requirements for both cultivation and MFC processes.

For mixed species, the main advantage is that they are appear everywhere in

natural sources, such as different kinds of wastewater, active sludge and pond sludge. Also, they are obtained at low or no cost, easy to manage and have few or no specific cultivation requirements. However, the main disadvantage of mixed species is that with different collection sources, the species and strains of bacteria are different, which makes the MFC performance unpredictable. Several studies of mixed microorganisms community have shown great diversity in their composition (Bond, D.R. et al., 2002; Phung, N.T. et al., 2004; Rabaey, K. et al., 2004; Logan, B.E. et al., 2005; Aelterman, P. et al., 2006). The intricate mutual effect and relationship between different species within a culture is not well established at present. This includes bacteria that self-produce redox mediators that are used by other species as electron shuttles. Also, there might be some bacteria species that have negative effect on the electron transport system, where they consume electrons rather than delivered them to the anode. Since the power performances of mixed cultures are generally higher compared to single species, a majority of the research is focus on using mixed culture as the inoculators for MFCs.

2.4.2 Limitations related to electrochemistry

2.4.2.1 Energy conversion efficiency

The overall energy conversion in MFC can be limited both by Gibbs free energy and other operational losses. During an electrochemical reaction, the obtained Gibbs free energy can be expressed from Equation (24) as (Bockris, J.O.M. et al., 2000):

$$\Delta G = \Delta H - T\Delta S \qquad \text{Equation (24)}$$

Where:

ΔG= Gibbs free energy, J;

ΔH =the enthalpy difference obtainable from a thermodynamic reaction system, J;

ΔS=the entropy difference of a thermodynamic reaction system's energy, J/K; and

T= the temperature of a thermodynamic reaction, K.

Equation (25) expresses the maximal efficiency of an electrochemical energy converting to electric energy:

$$\eta=\Delta G/\Delta H \times 100\% \qquad \text{Equation (25)}$$

Where:

η= energy efficiency, %;

ΔG= Gibbs free energy, J; and

ΔH=the enthalpy difference between reagents and reaction products, J.

For most fuel cell system, the maximum energy conversion efficiency from electrochemical energy to electric energy is about 90% since ΔG is normally 10% lower than ΔH (Bockris, J.O.M. et al., 2000). This is vastly effective than traditional mechanical conversion using thermal combustion since the process is not limited by the efficiency of Carnot cycle. Equation (26) shows the conversion efficiency expression for the Carnot cycle, where the energy conversion efficiency for heat conversion is 30-50% (Bockris, J.O.M. et al., 2000).

$$\eta= (T_1- T_2)/T_1 \times 100\% \qquad \text{Equation (26)}$$

Where:

η= energy efficiency, %;

T_1= the temperature of the heat source, K; and

T_2= the temperature of the heat transferred reservoir, K.

So theoretically, the energy conversion efficiency from electrochemical reaction process around 90% is dramatically higher than that of thermal combustion reaction of 30-50%. This indicates that the MFCs process of electrochemical conversion can be much more efficient than traditional heat conversion. Figure 2.13 compares these two types of conversions and their losses. For the ideal

situation, there are around 10% of intrinsic losses in electrochemical process due to TΔS. However, during operation, extrinsic losses through overpotential can be as high as 20% to 30%. It is mainly due to the series of losses during the reaction and for MFCs these can be substantial. The effect of these losses causes a drop in the fuel cell potential as well as the energy conversion efficiency.

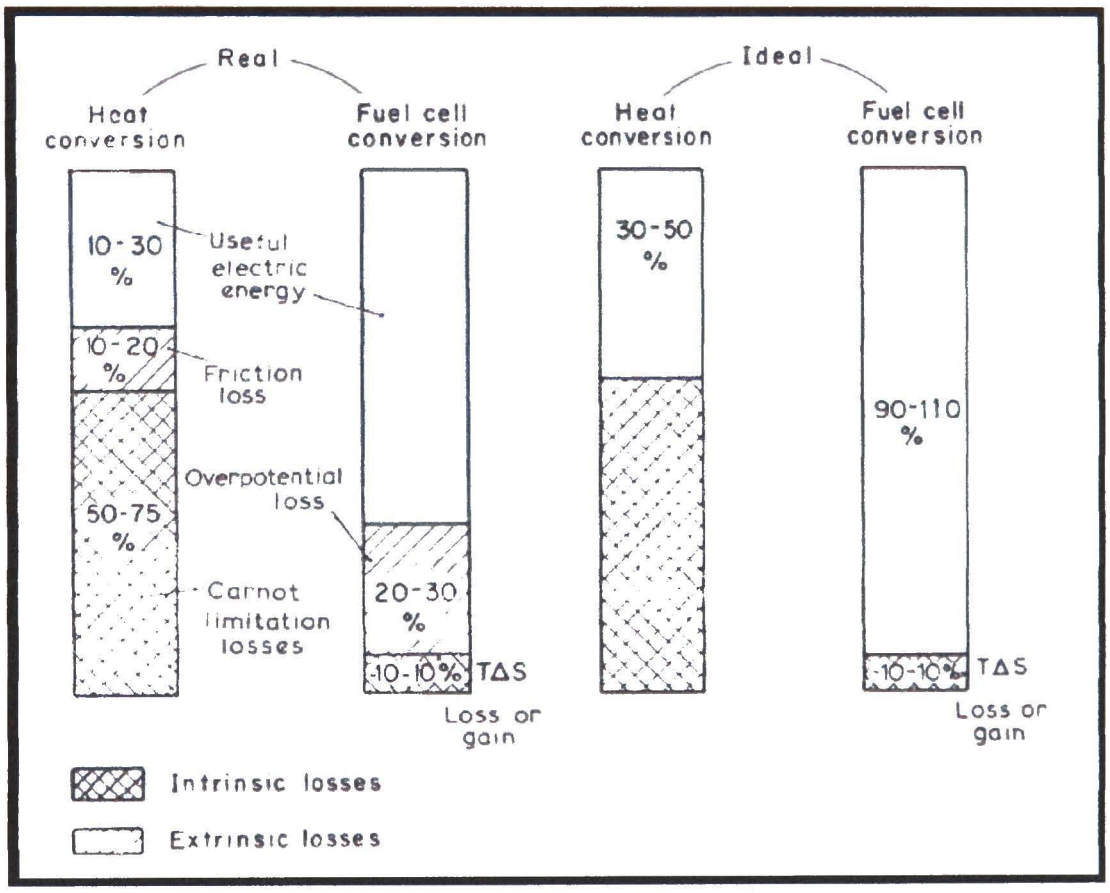

Figure 2.13 Comparison of the ideal and actual conversion losses for combustion systems versus electrochemical system (Bockris, J.O.M. et al., 2000)

2.4.2.2 Energy losses

2.4.2.2.1 Activation losses

The reduction of a compound at the bacterial surface during the bacteria metabolism, see Section 2.4.1.2, requires a certain activation energy to proceed. When the mediators transfer electrons to the anode surface, further activation energy is also required. These energy usages incur overpotential losses which is called activation losses. In order to reduce these losses, extra mediators can be

added into the system to help electron transfer. A catalyst can also be added to the anode to decrease the activation energy requirement and the potential for losses.

2.4.2.2.2 Ohmic losses

Ohmic losses result from electrode material limitations and the connection points of the circuit as the electrons travel through the anode and then transfer through the external electric route to the cathode. If there is a proton exchange membrane separating the anode and cathode chambers, the proton transfer also incurs ohmic losses due to membrane resistance. These losses follow Ohm's Law, which is linearly dependent on the current flowing through the MFC. Ohmic losses can be decreased by improving the electrode materials conductivity and the connection points. Also, optimizing any proton exchange membrane used is important to decrease the ohmic losses.

2.4.2.2.3 Concentration diffusion losses

If diffusion of substrate is limiting the redox reactions on the anode surface and this can cause potential losses. This is particular important for the process of electrons transfer by mediators, where the influx of reduced mediators towards the anode can be hindered due to the diffusion limitation through the anodic medium. The diffusion of protons out from bacteria and towards the membrane or cathode can also be hindered by the anodic medium. The final reactions on the cathode surface are limited by the diffusion factor of protons in the cathode chamber as well. All of these limitations incur potential losses which are classified as concentration diffusion losses. The choice of the electrode medium and the design of MFCs are crucial for reducing the concentration diffusion losses.

2.4.2.2.4 Identifying energy losses

The different energy losses can be identified and functionalised from the voltage the cell voltage polarization curve shown in Figure 2.6 in Section 2.3.1.1. At low currents, electron transfer efficiency is determined by the activation potential losses. At increasing currents, the ohmic losses are the main factor to decrease the cell voltage. Finally, at high current, the electrons and protons diffusion losses play the most important roles to induce the loss of cell voltage.

2.4.3 Limitations related to materials

2.4.3.1 Anode

The anode material can affect the bacteria behavior, their attachment on the anode surface, the formation of biofilm and the bacteria metabolism process, including the electron transferring to anode. The most common used anode is plain carbon materials that have very high conductivity and low electric resistance to reduce the total ohmic losses of the MFC system. However, without the electrocatalytic properties, there will be a large gap in the activation potential during the delivery of electrons from bacteria to anode surface as mentioned in Section 2.4.2.2.1.

2.4.3.2 Cathode

The cathode materials need to have good electrocatalytic properties to help the reaction between electrons and electron acceptors. Good conductivity also helps to reduce the ohmic losses in the system. However, catalyst materials account for a major cost issue that currently prevent the implementation of MFC technology (Logan, B.E. et al., 2006; Logan, B.E. and Regan, J.M., 2006). The most common used catalyst at the moment is Pt, that is very expensive and also is easily poisoned by other chemicals that reduce its electrocatalytic function. Research efforts have

been focused on alternative catalyst, but a low cost and long lasting candidate with good electrocatalytic properties have yet to be identified.

2.4.3.3 Membrane

MFCs can be operated with or without membranes. Both have their pros and cons. When the two chambers are separated using a PEM membrane, the coulombic efficiency is high due to good protons transfer. However, it also has the disadvantages of increasing the ohmic losses of the MFC and decreasing the power production. Furthermore, PEM membrane, such as Nafion (Dupont), is very expensive product that significantly increase the capital cost of MFCs.

Without the application of PEM, large amount of oxygen can diffuse into the anode chamber, upsetting the anaerobic condition in the anode chamber and consume electrons. Totally anaerobic conditions of MFCs could ease this condition. However, Liu and Logan proposed that the bacteria growing on the cathode side are likely to consume the oxygen and then regulate the oxygen diffusion towards the anode. A power density of 494 mW/m^2 for a non-PEM MFC was doubled that of 262 mW/m^2 for the same MFC with PEM under the same conditions (Liu, H. and Logan, B.E., 2004). Continuous flow of influent can also ease the issue of oxygen diffusing from the cathode chamber without using membranes.

2.4.3.4 Medium

Most of the phosphate buffer solutions and other culture medium includes phosphorus chemicals. They are utilized as a non-renewable medium and attempts have been made to recycle the phosphorus (Wiesmann, U. et al., 2007). Some of these chemicals, such as Cl^-, phosphorus and NH_4^+ are considered to be problematic since they interact with MFC materials and may form scaling. They

increase the complication of the MFC process since they need to be removed later on with the help of chemical precipitation, or using a specific element storing bacteria or activated carbon adsorption (Wiesmann, U. et al., 2007). Although a good medium composition may help to decrease the concentration diffusion losses, an incorrect concentration might lead to high reduction potentials which would result in loss of electrons and decrease the MFCs power production.

2.4.4 Limitations related to construction conditions and costs

Currently, one of main reasons for the MFC technology not yet well developed for practical industrial or household application is that the power produced at quite low levels. For future large scale applications of MFC technology, there are major issues concerning built environment requirements. Over the past 40 years, it has been suggested that MFCs might be developed for a wide range of applications (Lovley, D.R., 2006a). A large potential application is towards wastewater treatment to recover electricity energy and biogas, and simultaneously reduce the COD content. This option might be favourable for companies where water disposal costs and energy costs are significant issues.

It has also been suggested that MFC can be applied towards domestic households to act as an electric generator for the house, as well as collecting biogas to replace natural gas. The anticipated operational issues are even greater here than for the large scale application. Different MFC designs need to be considered for different house structure and total energy requirements, and a reservoir reactor needs to be built for long term treatment process. The biogas also needs to be purified, pressurised and kept in storage before being consumed. Similar to biogas digester technology, which has been tried in remote areas, major safety issues still exist. Another MFC application suggested is powering small scale items such as portable

electronic devices on vehicles and boats. However, the large amount of organic substrates required makes it difficult to apply on portable devices where vehicle and the maintenance costs would be a major barrier.

To become an economical attractive option for energy production, the MFC process must reduce the material costs to increase its capability to price ratio. This is especially important since power output from MFC is significantly lower than other technologies for power generation. The materials costs of current MFCs are considerable. Cathode material containing 0.5 g/m^2 of platinum costs roughly 1000 euro/m^2 and plain carbon cloth materials for anode costs around 70 euro/m^2. Based on the series of material costs presented and estimated by some groups, the estimated costs are around 4000 euro/m^3 of the electrode compartment. If 1 kW of power output can be produced per m^3 anode, it is still about 10 times that of the equivalent invest costs for conventional wastewater treatment processes (Tsuchiya, H. and Kobayashi, O., 2004; Rabaey, K. and Verstraete, W., 2005).

2.5 Related technologies

2.5.1 Traditional water treatment approaches

Traditional wastewater treatment is a process used to remove solid, organic and microbiological contaminates from wastewater to an acceptable levels for discharge to a receiving water body. Particular consideration is needed towards certain chemicals contained in wastewater like ammonia, nitrate, phosphorus, metals and specific organic pollutants (White, S. et al., 2007). The most common processes encountered in the treatment are screens, coarse solids reduction, grit removal, sedimentation, biological treatment and filtration (White, S. et al., 2007). The majority of the processes are collectively known as physical treatment. Figure 2.14 shows the schematic flow sheet of the traditional wastewater treatment

process (AWAG, 2008).

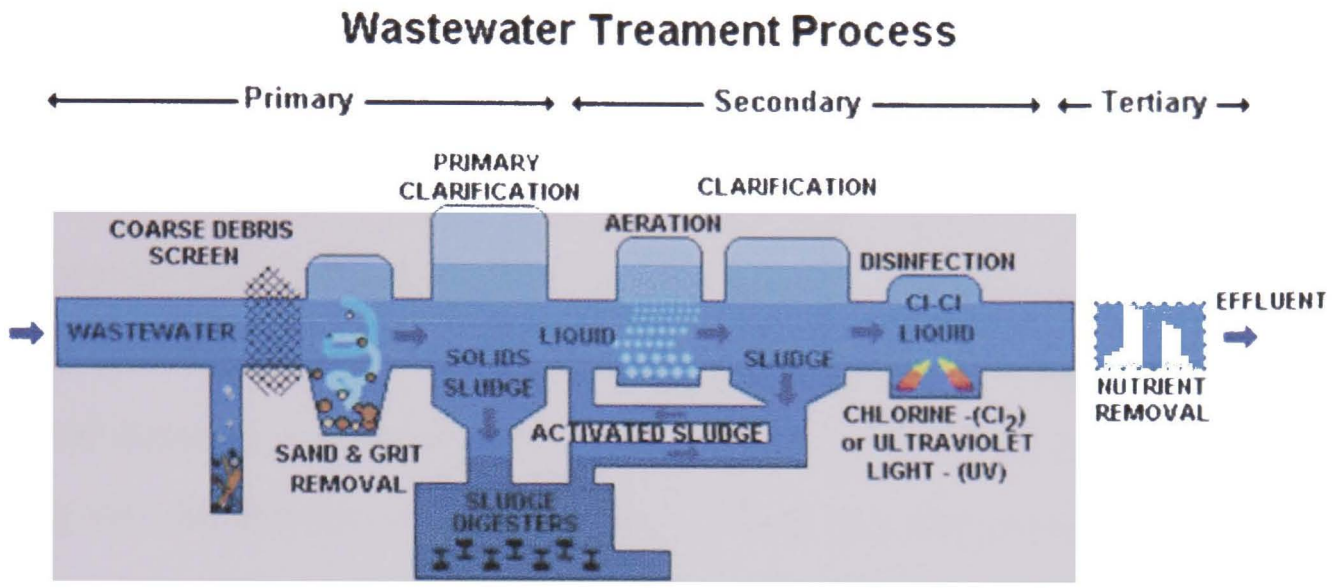

Figure 2.14 Wastewater treatment process diagram (AWAG, 2008)

The first three processes act as the basic physical treatments to remove larger scale particles and impurities contained in the wastewater. Sedimentation is normally achieved by the use of chemicals to precipitate some dissolved organic and inorganic components before filtration. After the physical treatment, a biological treatment is used where microorganisms remove dissolved organics as part of their growth cycle and convert some of the dissolved organic components to solids for filtration in downstream processes. Filtration is normally achieved using a granular bed, mainly sand, at relatively slow velocities. The removal is based on particles colliding and sticking to filter grains as the water flows past. The process is used to remove particulate material in water, including clays and silts, microorganisms and precipitates of organics and metal ions, from upstream water. The particles that are removed in this process are typically around 0.1-50 mm (White, S. et al., 2007). Normally the water treatment cost is based on the COD level received and processes that can remove COD prior to treatment, such as MFC or Anaerobic Digestion, are sough after.

2.5.2 Anaerobic digestion

Anaerobic digestion (AD) technology can be used as an alternative treatment process for the organic contaminants. Anaerobic digestion is a natural, biological process that similar to composting, breaks down liquid manure, sewage, or other organic wastes into gases and a thick sludge. Organic wastes are gradually fed and mixed at regular intervals into an anaerobic digester unit. The amount of biogas generated depends on the feedstock type, frequency of sludge collection, waste handling method and climate (USDA, 2007). The biogas produced contains about 60-70% methane and 30-40% carbon dioxide (EPA, 2002). This biogas makes an excellent energy source to produce heat or power. It reduces utility costs for the water treatment industry as well. The major disadvantage of this technology is the heavy thick sludge that needed to be settled and disposed off. The practical application of this technology still has many barriers such as the strict requirements of operational conditions and large amount of labour needed.

2.5.3 Sludge removal and MFC

Two major concerns within the wastewater treatment process are energy and sludge disposal. Energy comprises around 28 % of the operating cost of treating wastewater (White, S. et al., 2007). Energy savings are possible through better management practice and also innovation of the process. Around two thirds of the total costs of wastewater treatment are related to sludge removal (White, S. et al., 2007). Current options for sludge removal are limited and this is a critical barrier to improve the effectiveness of water treatment.

In terms of wastewater treatment, MFCs can extract energy in the form of valuable gases and electric energy, and at the same time, the MFC might reduce sludge formation during the process as well due to significant removal of COD. The

valuable gases, mainly produce from the wastewater fermentation during MFC process, is due to a process that uses anaerobic bacteria contained in the wastewater to metabolically breakdown the nutrient molecules, such as starch. Fermentation yields lactate, acetic acid, ethanol, or other secondary products, and this process reduces the production of sludge that contains rich nutrient components for bacteria fermentation and electricity extraction (Logan, B.E. et al., 2002). The application of MFCs into the water treatment process is a promising route towards reducing the costly aeration practice.

2.6 Summary

The global demand for sustainable energy and water will continue to grow and one of the possible solutions is MFC. Compared with traditional wastewater treatment technology, it is clear that MFCs technology has an outstanding potential to make the water treatment industry a key player in proving sustainable energy and water. Although MFCs have been studied extensively including their differ classifications, their materials requirements, the bacteria available for use, the electrochemical aspect of MFCs and the H_2 production in MFCs, the performances and efficiencies reported for MFCs are promising but scattered from different research groups. Besides the merits of MFCs, the limitation and drawbacks of MFCs needs to be addressed, including limitation in the aspect of microbiology, electrochemical losses and materials and construction limitations and costs.

This study has been focused on advancing the MFC technology as a potential and worthwhile technology for sustainable development. Key questions of this work have been aimed to address what kind of MFC design has the advanced power performance and benefit for the future industrial application? How can the power performance be improved while simplifying the treatment procedures and lowering costs? What are the major limitations that need to be addressed to achieve this

goal? For next several chapters, different types of MFC reactors developed and their performances will be compared. Materials improvements through simplified treatment methods to boost the power production performance are presented. Major MFC barriers have been identified and experiments were carried out to further understand the MFC principles and limitations.

The combination of design, material modification and understanding of barriers has enabled this study to identify a potential route towards industrial implementation of MFCs.

Chapter 3 Experimental

3.1 Microbes and feed

3.1.1 Procurement

Municipal wastewater samples and active sludge were collected from Severn Trent water Stoke Bardolph sewage treatment works located southeast of Nottingham city. All the samples were collected after primary treatment. The properties of wastewater and active sludge samples for each collection such as COD levels could vary slightly.

3.1.2 Incubation

For each MFC experiment, based on different MFC reactor designs, bacteria present in active sludge and wastewater were used to inoculate the MFCs anode to favor the formation of a mixed culture of microorganisms. There were no extra modifications, such as pH adjustments, addition of nutrients or trace metals, during inoculation. Around one third of the total effective volume was filled with active sludge, and the remaining two third was filled with municipal wastewater. If the system ran as an anaerobic MFC, N_2 gas was purged into the system at 0.1 L/min for 1 h to ensure that no oxygen was in the system. It took roughly 3 days for incubation to reach stable power generation conditions.

3.1.3 Substrates

Three substrates were introduced in different MFC reactors, namely (i) full-strength municipal wastewater with COD level around 200 mg/l; (ii)

wastewater with 1 g/L sodium acetate; (iii) wastewater with 1 g/L sucrose. For each experiment, the substrate was added into the wastewater sample to establish a COD level of around 1000 mg/L.

3.1.4 Artificial wastewater

In the stacked MFCs experiments, described later in Section 4.2.2, artificial wastewater was used as influent after the bacteria inoculation period. The artificial wastewater also acted as a pH buffer solution and the culture medium for bacteria growing. It consisted of 5.52mM K_2HPO_4, 4.49mM KH_2PO_4, 0.03M KCl, 0.07mM $CaCl_2.2H_2O$, 5.23mM NH_4Cl, 4.1mM $MgSO_4{\cdot}7H_2O$ and 1 ml/l trace elements. The composition of trace elements included 1.8 μM $FeSO_4{\cdot}7H_2O$, 0.26 μM $ZnCl_2$, 0.25 μM $MnCl_2{\cdot}4H_2O$, 0.05 μM H_3BO_3, 5.9 nM $CuCl_2{\cdot}2H_2O$, 0.05 μM $NiCl_2{\cdot}6H_2O$, 0.07 μM $Na_2MoO_4{\cdot}2H_2O$ and 0.5 μM $CoCl_2{\cdot}6H_2O$. The cathodic electrolyte acted as pH buffer medium and it included 5.52m M K_2HPO_4, 4.49m M KH_2PO_4 and 0.03M KCl without addition of trace elements.

3.2 Reactor manufacture and running conditions

3.2.1 Reactor factors

3.2.1.1 Operating conditions

All the experiments were operated at room temperature at around 25 °C and atmosphere pressure. For continuous mode, a peristaltic pump was used to control the influent flow rate at constant rate varying with different MFC reactor. The effluent of the MFCs was circulated back to the system in a closed loop to simulate a chain of MFCs.

3.2.1.2 Reactor setup

Several designs of MFC reactors are discussed in Chapter 4. The Micro-channel MFC and hexagonal tube MFC were designed to combine anode and cathode in a single chamber. The Micro-channel MFC was used to observe the feasibility for MFC using a relatively small effective volume of 13.3 ml. The hexagonal tube has an effective volume of 2.7 L which is a relatively higher treatment volume. The stacked MFC was designed as a two-chamber MFC separated with a cation exchange membrane with a total exchange capacity of 1.0±0.1 meq/g. The effective anode volume was 73 ml. One stacked MFC was set with an external resistor with air bubbling into the cathode chamber as a conventional MFC. Another stacked MFC was set act as a bioreactor with a power supply to provide additional voltages from 0.3 V to 0.95 V to boosts the hydrogen production. For the testing of barriers, and material treatment, simplified MFC setup similar to Figure 2.11 plot A was used. The construction details of each reactor were introduced in Chapter 4.

3.2.1.3 Cation exchange membrane (CEM)

The CEM used in stacked MFCs was type CMI-7000 and was supplied from membrane international INC., NJ, USA.

3.2.1.4 Polydimethylsiloxane material fabrication

The polydimethylsiloxane (PDMS) material was used as the channel sheet materials in Micro-channel MFC. The PDMS channel sheet can be assembled with other reactor materials afterwards. The fabrication steps were:

(i) Mask design for the channel shapes using Adobe Illustrator CS, Adobe Inc,

(ii) Channel model fabrication with machine tools,

(iii) PDMS micromoulding (Xia, Y. and Whitesides, M.G., 1998) where a mixture of

PDMS with curing agent was poured over the channel mode and placed on a level holder in a convection oven at 60°C for 2h. After curing, the PDMS sheet with channel structure was concreted and was gently removed from the model,

(iv) Channel inlet and outlet fabrication on the PDMS material. Two plastic tubes with 1mm diameter were inserted into the PDMS frame material and reach to the channel areas at the start and the end points, respectively. Peristaltic pump was connected with these tubes as inlet and outlet.

3.2.2 Electrode materials and connections

3.2.2.1 Anode materials

In the Micro-Channel MFC and Hexagonal Tube MFC, plain carbon cloth without wet proofing was used as anode materials. Two types of this material were used referred to as cloth B and D, and they differed in weaving method, material thickness and density. B was plain weaved and D was knitted weaved and Figure 3.1 shows the material structure difference. Higher magnification SEM photos of these materials are shown in Section 5.1. The overall thickness of B was 0.65mm and D was 1.0 mm. The density of B was 221 g/m^2 and D was 255 g/m^2.The carbon cloth was supplied by BASF Fuel Cell Inc., E-TEK Division, NJ, U S A.

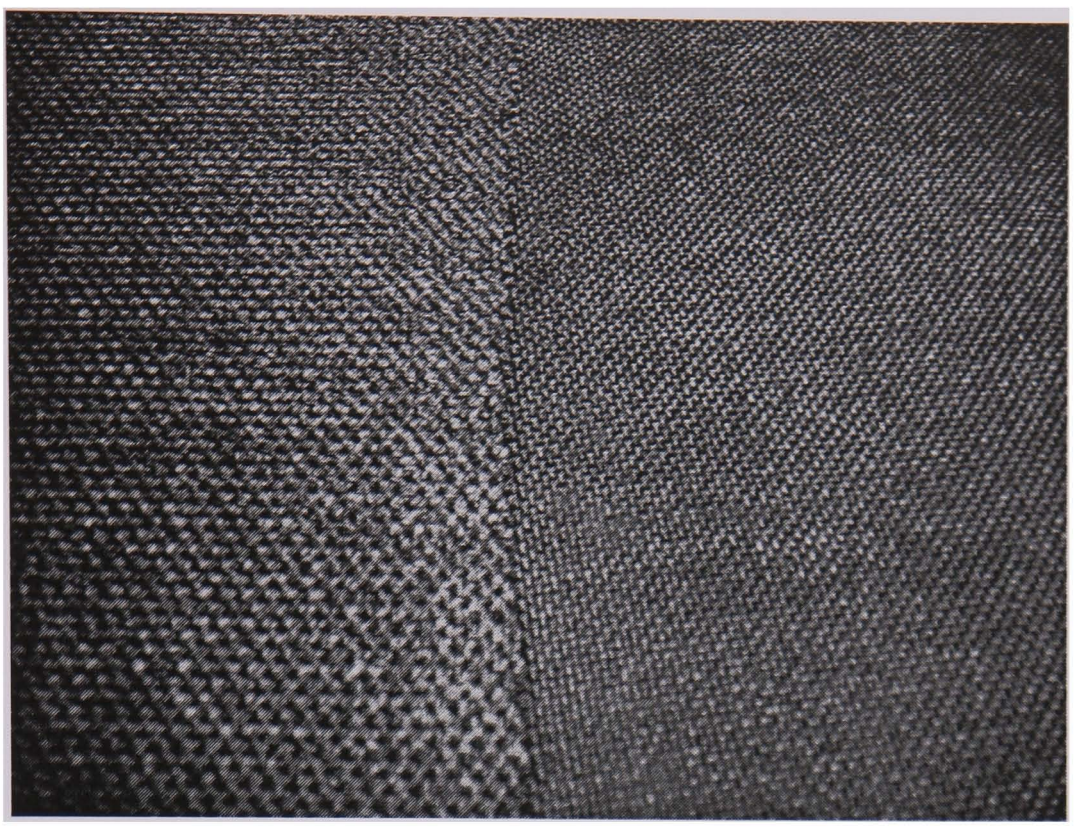

Figure 3.1 Carbon cloth materials designation B (right) and D (left)

Graphite granules were used in the stacked MFC to act as both anode material and electrode contact materials in cathode chamber as well. This material had a porosity of 0.53, an average granular diameter between 1.5-5 mm, and a bulk density around 1 kg/L. It was purchased from Le Carbone, Belgium. Prior to use, the granules were washed at least three times each with 1M of HCl and NaOH and distilled water. Carbon rods from Morgan, Belgium, with a diameter of 5mm were used as the connectors for anode and cathode materials. The power density data in this work was related to the outer surface of the granules. It was estimated that the granules with 3 mm in diameter and the surface area of a single granule was 0.28 cm^2, with a volume of 0.014 cm^3. For a single anode compartment, the total volume was 138 ml where the effective liquid volume was 73 ml and the actual granules volume was 65ml. The number of granules was calculated as 65 ml/ 0.014 ml = 4643 with a total surface area of 4643 * 0.28 cm^2 = 0.13 m^2 per anode chamber.

3.2.2.2 Cathode materials

A low Temperature ELAT® microporous Gas Diffusion Electrode supplied by BASF

Fuel Cell Inc., E-TEK Division, NJ, U S A was used as cathode materials in all three designs of MFCs. Two Pt loadings on a woven carbon cloth, LT 140E-W with 5 g/m^2 and LT 120E-W with 2.5 g/m^2 Pt were compared.

3.2.2.3 Flow and wiring connections

Recirculation between the anodic and cathodic chambers was maintained using peristaltic pumps from Watson Marlow, UK. With different reactors, the controlled influent flow rates were different. For the Micro-channel MFC, the flow rate was 0.12 L/h (2 ml/min). For the stacked MFC, a 1.4 L/h flow rate was used. For the hexagonal tube MFC, the flow rate ranged from 2.7 L/h to 10 L/h. The detailed flow rates data are specified for each reactor or experiment later. PVC plastic tubing was used to connect the influents, pumps and effluents.

A voltage data logger, described in Section 3.3.3.3, was connected to the graphite rods serving as electrode connection points or directly connected to the carbon cloth using copper wires and metal crocodile clips.

3.2.2.4 Gas sampling

For the Micro-channel MFC, a gas sampling bag with needle was connected to the anaerobic feedstock bottle and filled using the pressure from the biogas produced. The sample gas was then examined using a Micro GC later described in Section 3.3.3.1. For the hexagonal tube MFC, metal sampling tubing was directly insert into the headspace of the reactor to collect gas samples online using the Micro GC. For the stacked MFC, a gas collection setup was used to collect all the gases produced from the system, and a hydrogen sensor (Zellweger Analytics Ltd., Poole, Dorset UK) was used to measure the hydrogen concentration with the purge of gas mixture samples collected from the system.

3.3 Testing procedures and instruments

3.3.1 Tests related to wastewater

3.3.1.1 COD

The COD test was analyzed using a Hach Lange COD reactor and colorimetric determination analyzer. The range of digestion solution for COD was chosen between 0-150 ppm or 0-1500 ppm depending on the COD content of the wastewater. Only 2 ml of wastewater sample was required for the test. For original wastewater, the concentration of samples was diluted to 50% using distilled water due to the probability of the COD being over range. The treated wastewater, was directly tested where the estimated COD was less than 150 ppm. A blank sample of 2 ml distilled water was used as reference sample to compare with each wastewater sample in the colorimetric determination analyzer. The difference in water properties made the color of the reagent and water sample mixture different. With the blank sample as reference, different COD levels can be accurately measured. The steps of the COD test were followed using the Hach Lange manual for the COD reactor and colorimetric determination analyzer.

3.3.1.2 BOD

For the 5-day BOD test, the expected BOD of the sample which was calculated from the COD analysis as BOD=0.6*COD (Forster, C.F., 2003). According to this, the sample was diluted into a 300ml bottle according to a reference table (Hammer, M.J. and Hammer, M.J.J., 2008).The Dissolved Oxygen (DO) of the 300ml sample, D_1, was measured. The 300ml bottle was covered with a quick-fit top to keep oxygen from entering or leaving the bottle. After 5 days, the DO of the water sample, D_2, was measured. The BOD_5 (mg/L) was calculated as $(D_1-D_2)/ P$, where P is the dilution factor of the BOD bottle that is represented by the original water sample.

3.3.2 Scanning Electron Microscopy

A scanning Electron Microscopy (SEM) Quanta 600 by FEI was used to examine the bacteria species attached to the anode and cathode materials after MFC, in terms of their shapes, structures and association with the carbon materials. The SEM was also used to analyses the anode and cathode materials prior to MFC application and investigate the effects of physical and chemical material treatments.

For the bacterial studies, around 0.5 cm^2 of carbon cloth after MFC with the bacteria attached was cut from the MFCs anode or cathode. The sample was dried in a desiccator over night before the SEM test. The dry sample was adhered to a small aluminum pellet and then transferred through an airtight door to the SEM vacuum chamber. The chamber was evacuated to about 2 mbar to pressure the bacteria structure. A beam of high-energy electrons was vertically sent down through a series of magnetic lenses of the SEM which is in order to focus the electron to a very fine spot on the sample. At the bottom section of the chamber there was a set of scanning coils moving the focused electron beam back and forth across the carbon cloth. After hitting the sample, the electron reflected from the samples was detected by a sensor which generated the SEM image (Goldstein, J. et al., 2003). Samples with possible bacteria attachment were coated with Au prior the SEM observation in order to improve the picture definition by enhancing the electron conductivity of the bacteria (Goldstein, J. et al., 2003). Energy dispersive analysis by X-rays (EDAX) was performed on some SEM images to analyse the chemical compositions of a part or the whole observed image.

3.3.3 Performance of MFC

3.3.3.1 Micro GC for gas composition

An Agilent Micro GC 3000 was used to test the gas composition and concentrations

produced by the MFCs. Gas chromatography (GC) utilizes a column to separate different gases in a mixture so that they can be individually identified and quantified. The basic components of a GC are a carrier gas cylinder with a pressure regulator, a pump for drawing sample gas, a port for sucking sample gas in, a chromatographic column to separate different components of gas samples, a detector filament, an exit line and a chart data recorder. The schematic diagram of the components of the Micro GC used in this study is shown in Figure 3.2.

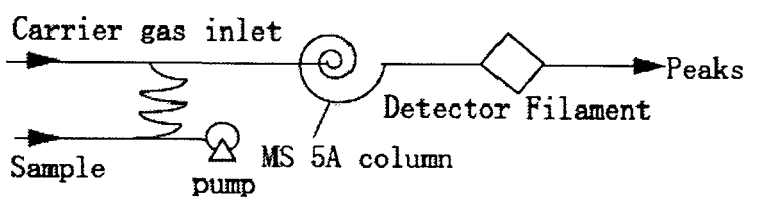

Figure 3.2 Schematic diagram of a GC (Agilent, 2006)

The gas to be analysed is heated to a certain temperature suitable for the chromatographic column and the detector, normal around 30 oC to 180 oC. Then the carrier gas carries the sample gas using a constant flow through the chromatographic column. Due to different physics and chemical characteristic, gases travel through the chromatographic column at different rates, and emerge out from the column at different retention times. Their presence in the emerging carrier gas is detected, e.g. by thermal conductivity method using a detector filament. The response of the detector filament is fed into an electronic integrated recorder and showed as different peaks in a spectrum. Each peak in the spectrum represents a specific gas or a mixture of gases with very similar retention through the column. The time for each gas sample to emerge from a given column is a characteristic of the gas and is known as its retention time. The area under the peak is proportional to the concentration of the gases in the sample. To accurately measure the quantity of sample gas, the calibration gases with known quantity and composition were used. The calibration gases normally contain the gases which are expected, may contain or would be measured in sample gases. In the MFC measurements, the calibration gas mixture (BOC, UK) contained H_2 (5 %), O_2 (5 %)

and CH_4 (1 %) in volume fraction with nitrogen balance. Comparing the peak areas at the same retention time between calibration gas and the sample gas, the quantity of specific gas component can be studied.

The column used in this study was a 10 meter long Molecular Sieve column 5 A, and the carrier gas used was N_2. The reason to choose N_2 as the carrier gas is that the target gas H_2 and N_2 have a relatively large difference in retention time with Molecular Sieve column 5A rather than other carrier gas, such as helium.

3.3.3.2 GC for organic in wastewater

A GC8000 Carlo Erba Instruments from Wigan, UK was used to analysis of the organic compounds isolated from the wastewater before and after MFC experiments. Diethyl ether was used to extract organic components from the water samples using 2 ml of wastewater sample and adding 0.5 ml 9.2M H_2SO_4, 0.4 g NaCl and 2 ml diethyl ether. The organic and water phase was separated using a rotary equipment and then centrifugation at 3000 rpm for 2 min and 3 min, respectively. The diethyl ether layer over the water layer was transferred into a 5 ml vial for GC injection. The column used was an Alltech Deerfield, USA EC-1000 (30 m, I.D.: 0.32 mm, df: 0.25 μ m) linked with a capillary Flame Ionization Detector (FID). The temperature was held at 135 °C for the isotherm oven and 200 °C for the detector filament and the injector and N_2 was used as the carrier gas at 3 ml/min.

3.3.3.3 Cell voltage data logger

A Keithley 2700 Multimeter /Data Acquisition System (Keithley Instruments Inc., UK) was used as the multimeter data logger for the hexagonal tube MFC. The cell voltage data for the Micro-channel MFC was collected by linking the MFC with the

serial communications port to a desktop PC via an sixteen-channel USB interface connected to a ADC-20 AD converter from Pico Technology Ltd., Cambridge, UK. Real time data was recorded using PicoLog® version 5.09.4 recorder software and retrieval of the data was performed using the PicoLog® version 5.16.2 Player software from Pico Technology.

For the simplified two-chamber MFCs, later described in Chapter 5 and 6, the cell voltage data for the eight set of MFCs with different anode or cathode materials were collected at the same time using the ADC-20 AD converter. The parallel data collection was achieved by recording all anode points together to the Ground point in the data logger, and all individual cathode points from different MFCs were connected with different channel points in the front channel panel of the data logger. A maximum of eight separated channels could be recorded. Thus, the voltage data was recorded online at the same time for easy comparison.

3.3.3.4 External resistance system

A self developed resistor box which had a range of resistance from 1 to 5 kΩ was used to measure the different power densities at different resistance for the hexagonal tube MFC to establish its polarization curves. From these measurements, the optimal external resistance was found that gave the maximum power density as described in Section 2.3.1.1.2. The electro circuit diagram of the resistance system designed to achieve the polarization curve tests is shown in Figure 3.3 when the cell current and voltage data can be tested and recorded.

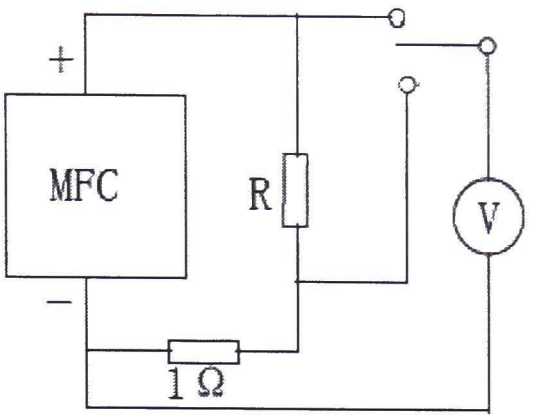

Figure 3.3 Circuit diagram of the external resistor system

3.3.3.5 Potentiostat

A Bi-Stat potentiostat from Princeton Applied Research, Claix, France, was used to measure the polarization curves of the stacked MFC. The polarization curve is expressed by imposing a linear voltage decrease followed by a linear voltage increase while measuring the current produced. The scan rate was set to 1mV/sec. The anode and cathode potentials were measured by coupling with a Ag/AgCl reference electrode of 197mV vs. a Standard Hydrogen Electrode from BASi, Warwick, UK, together with the potentiostat data logger system.

For the simplified two-Chamber MFC described in Chapter 5, an Autolab potentiostat PGSTAT30 from Eco Chemie, Netherlands was used. A linear voltage sweep was used to measure the polarization curves with a scan rate of 1mV/sec. Anode and cathode potentials was measured using the same Ag/AgCl reference electrode as described above, and the Potentiometry method was used to measure the open circuit potential of the MFCs.

3.3.3.6 Surface properties tests

A Micromeritics ASAP 2010 sorptometer was used to obtain nitrogen sorption isotherms of the anode materials before and after treatment at 77 K (condensation point of N_2) using N_2 in a conventional volumetric technique. BET-BJH calculations

were used to determination the surface area, pore volume and pore size distributions. The BET-BJH nitrogen sorption is a physical method to study sample surface properties by controlled condensation or adsorption of gas molecules with known sizes, generally N_2, Ar or CO_2, on an unknown material surface. The quantity of gas adsorbed and corresponding sample pressures are measured at a constant temperature (here is 77K as condensation point of N_2), to produce an adsorption-desorption isotherm and subsequently perform porosity calculations, with a certain amount of material sample (here is around 0.1-0.2 g). Before the measurement, processes of sample drying and degas at certain temperature were required. Due to the carbon sample were fairly dry, only degas process was carried to empty the air adsorbed on the sample material surface (Here is at 110℃ for about 4h). The Brunauer-Emmett-Teller (BET) model (Brunauer, S. et al., 1938) was used to determine the specific surface area of the samples, while the Barrett-Joyner-Halenda (BJH) theorem (Barrett, E.P. et al., 1951) was used to calculate the pore size distributions. In this work, it was used to compare the surface area of the plain and treated carbon materials as well as their distribution of micropore, mesopore and macropores sizes in the materials for compare. The surface area was calculated using the BET method based on adsorption data in the partial pressure (P/P_o) range of 0.05-0.35. The total pore volume was determined from the amount of N_2 adsorbed at P/P_o from 0.4 to 0.995. The average pore size was obtained from the adsorption data following the BJH method. The detailed analysis of the adsorption-desorption plots are introduced in Chapter 5.

3.3.3.7 Calorific value test

The calorific value in terms of the higher heating value (HHV) was analysed using an IKA 5000 Series bomb calorimeter. The ASTM E711 procedure, "Standard Test Method for Gross Calorific Value of Refuse-derived Fuel by the Bomb Calorimeter" was used to determine the higher heating value.

3.3.3.8 Anode treatment procedures

The physical treatment of the plain anode materials B and D was carried out using CO_2 gas at a flow rate of 0.1 L/min in a tube furnace at 5 different temperatures of 400 ^oC, 500 ^oC, 600 ^oC, 700 ^oC and 800 ^oC for 2 h. The chemical treatment procedure of the plain anode materials B and D involved 24 h treatment in 3M of HNO_3, H_2SO_4, HCl and KOH, respectively. The materials were then washed with distilled water for at least three times. The treated materials were examined using several tests before and after the MFCs process to evaluate the effects of the treatment on the power production performances of the MFC in Chapter 5.

Chapter 4 Development of continuous MFC reactor setup

4.1 Main reactor setup parameters

Several MFC reactors are investigated in this chapter to focus on continuous high flow rate applications, using a simplified non-membrane MFCs design with no-buffer medium solution applied. These setups were applied to address the issues mentioned in Chapter 2. The reactors included two miniature MFCs reactor, a micro channel MFC and a stacked MFC, and a larger scale hexagonal tube MFC design. A comparative study was carried out to compare how the MFC designs developed in this work addressed the main challenges and barriers preventing MFCs from large scale applications. The main barriers addressed were, firstly, obtaining a high flow throughput to treat large amount of wastewater, secondly, a simplified design was aimed for low maintenance, such as reactor cleaning and, thirdly, low capital costs.

4.2 Miniature MFC

The miniature MFCs have the advantages that they are easy to assemble and disassemble and require low maintenance. Due to the small size of the miniature MFCs, the anode and cathode can be located very close which is good for proton transport. They are straightforward to be controlled and managed as a whole set. The data collection system and other instruments can easily be connected to these MFCs. Two miniature MFCs, a Micro-Channel MFC and a stacked MFC are discussed in this section, and the advantages and disadvantages of miniature MFCs are compared.

4.2.1 Micro-channel MFC

4.2.1.1 Geometry

The Micro-channel MFC was designed with one inner channel as the reaction chamber. The design was based on the principle of micro-reactors, where decreasing the size of the reactor might increase the reaction efficiency and productivity in chemical reactions due to possible mass transfer improvement (Chiao, M. et al., 2003). High mass transfer rates are possible in microfluidic systems that allow reactions to be performed under more aggressive conditions with higher yields compared to conventional reactors (Jensen, K.F., 2001). Basically the Micro-channel MFC consists of two plates of Perspex clamped together using screws as shown in Figure 4.1 and 4.2. The channel was made with PDMS materials and placed in the centre of these two plates. The effective volume of the single chamber was 13.3 ml and the effective volume of the whole compartment was 32 ml. A carbon cloth anode and cathode of carbon cloth with 5 g/m^2 Pt were placed on either each side of the PDMS channel. The effective side of these electrode materials were faced towards the channel. Two sheets of rubber were applied between the Perspex and electrode materials to seal the reactor tightly. The effective surface area of both anode and cathode electrode was $2.65*10^{-3}$ m^2. The distance between anode and cathode was about 5 mm. No extra external connections were applied since both electrode materials were directly attached with data logging system to avoid any metal pollutant into the wastewater. Booki Min et al. designed a MFC reactor with a similar appearance (Min, B. and Logan, B.E., 2004). The key difference between these two designs is that, the two channel chambers were separated by a PEM membrane which might increase the internal resistance of MFC, while in this design, there is no membranes located between the anode and cathode materials. The influent substrate can freely be transport through the channel touching both electrodes. The design, flow sheet and the actual configuration of this reactor are shown in Figures 4.1 to 4.3.

A: Top view

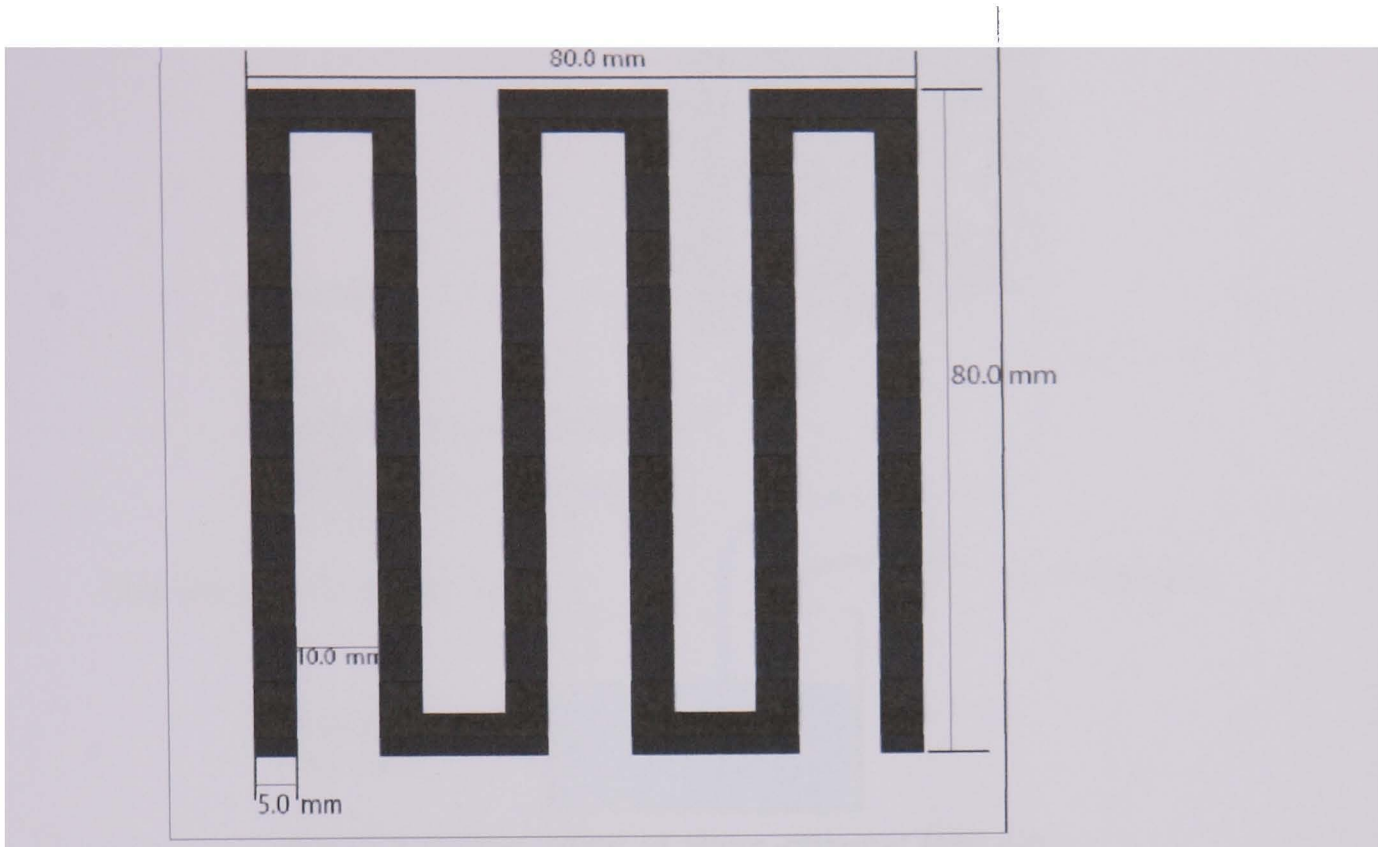

B: Side view

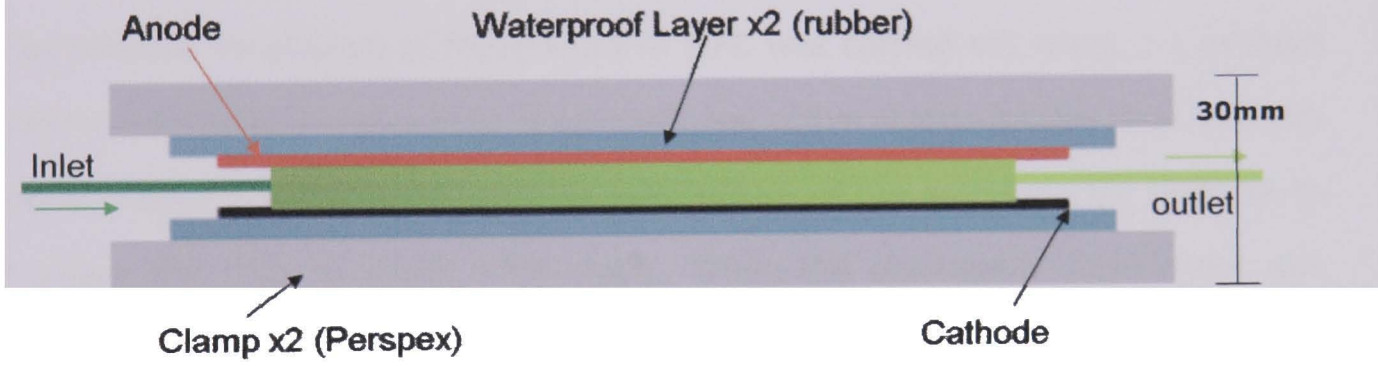

Figure 4.1 Schematic of Micro-channel MFC, (A) Top view and (B) side view

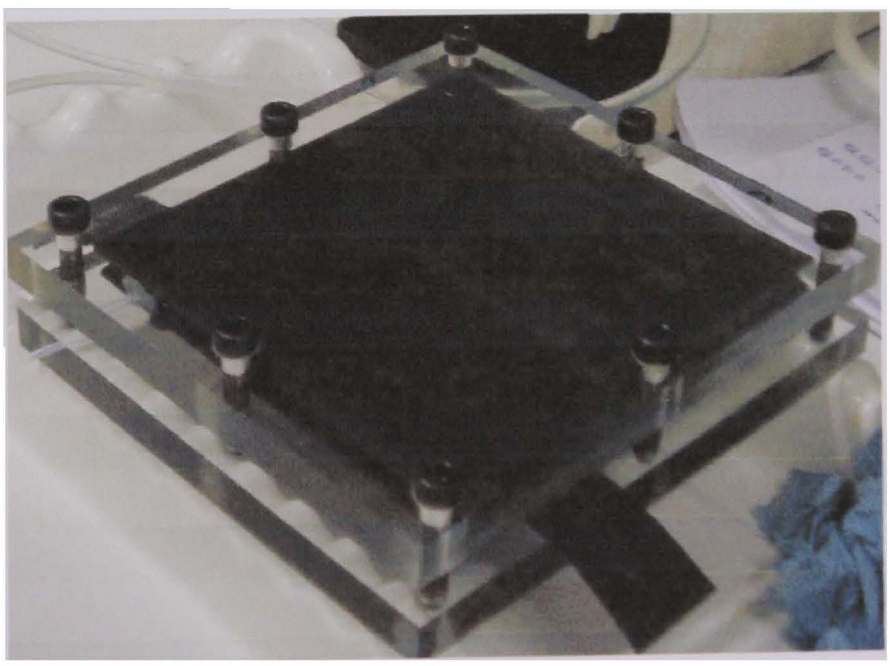

Figure 4.2 Actual Micro-channel MFC

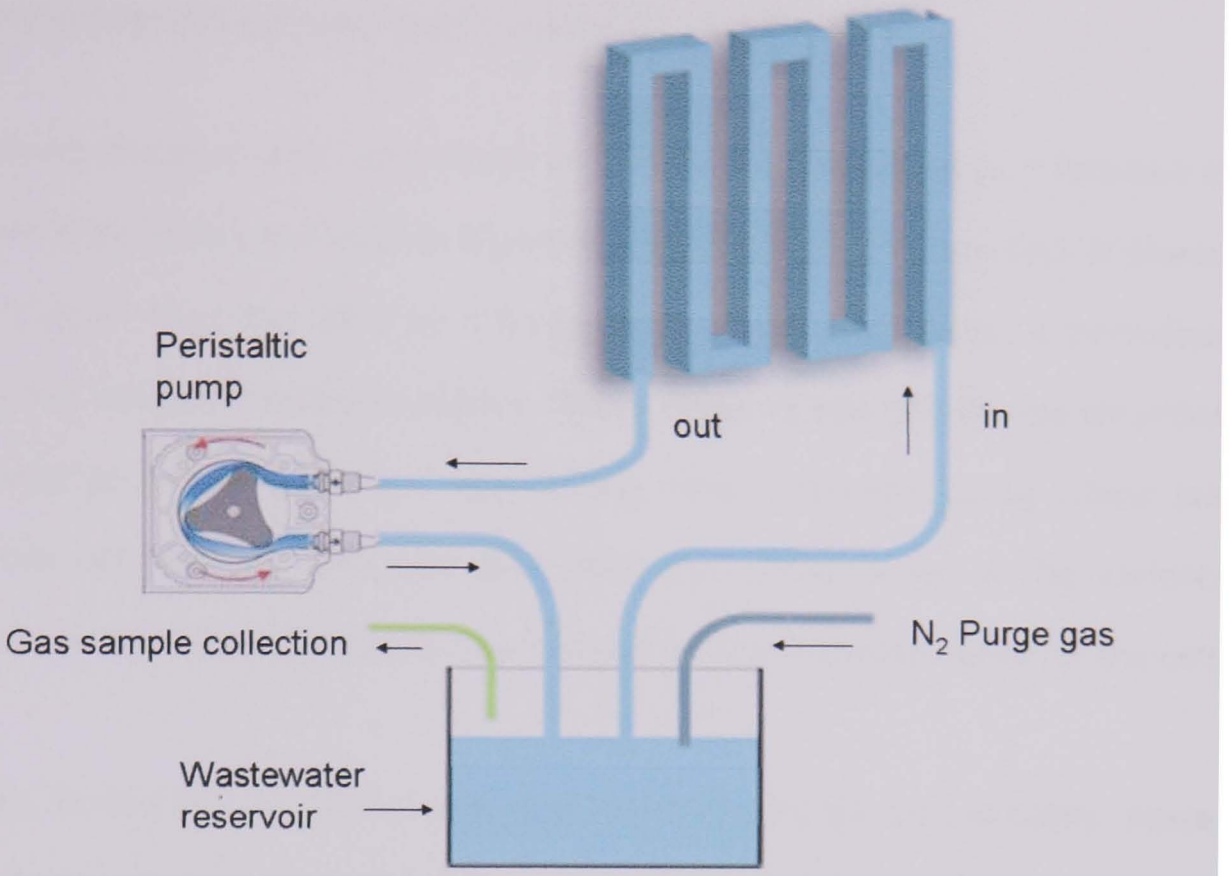

Figure 4.3 Flow sheet of Micro-channel MFC set

The bacteria incubation of Micro-channel MFC was carried out using 1 L primary treated wastewater with a COD of 62 mg/L and active sludge for two days at batch mode. About 1 g of sodium acetate was added as the substrate for bacteria to increase the COD to about 1800 mg/L. When the continuous experiment was started, a peristaltic pump was used to circulate the influent at a flow rate of 2 ml/min. The influent container was purged with N_2 gas for 1 h to drive out oxygen before pumping into the cell. The wastewater reservoir bottle was sealed to ensure no gas leakage or air exchange with the wastewater sample of 1 L and a headspace of 200 ml. A syringe needle connected to a gas bag was used to collect the gases produced from the reactor. An external variable resistor ranging from 4 Ω to 5000 Ω was used as the load for the cell. The voltage data of the cell was recorded using the data logger and the COD level was checked on a daily basis. The reactor was operated by continuously recycling the substrated wastewater at least three hydraulic retention times prior to further experiments.

4.2.1.2 Polarization curves and power output

The relationship between the cell voltage and the power densities as a function of the cell current densities is shown in Figure 4.4 after hours of incubation. It shows the power output from the MFC as a function of circuit load, using a periodical increase in the external variable resistor. The voltage of the circuit was recorded and converted to power densities. The current was calculated using Ohms law based on the cell voltage. The first test used the whole range of the variable resistors from 4 Ω to 5000 Ω to check the trend of the polarization curve for the cell.

As expected, during the incubation period of the bacteria, the cell voltages, power densities as well as the current densities are relatively low. From Figure 4.4, a maximum power density of 0.9 mW/m^2 was produce during incubation. Correspondingly, the optimal external resistance was found to be around 2000 Ω, which was used for further tests. When the cell voltage was decreased below 4 mV, Figure 4.4 showed abnormal curve behaviour. This might be because of mass transfer losses or COD concentration loss surrounding the anode, which is limited at high current density. Mass transfer losses occur due to the transmission limitation of substrates and degraded products near electrodes, since it might be difficult to increase the rate of supply of organic matters to quickly respond to demand. Concentration loss might occur due to the rapid consumption of organic matters surrounding the anode surface resulting in lower concentration compared with the bulk solution. This trend of power densities was in agreement with work by other MFC groups (Liu, H. et al., 2004; Rabaey, K. et al., 2004).

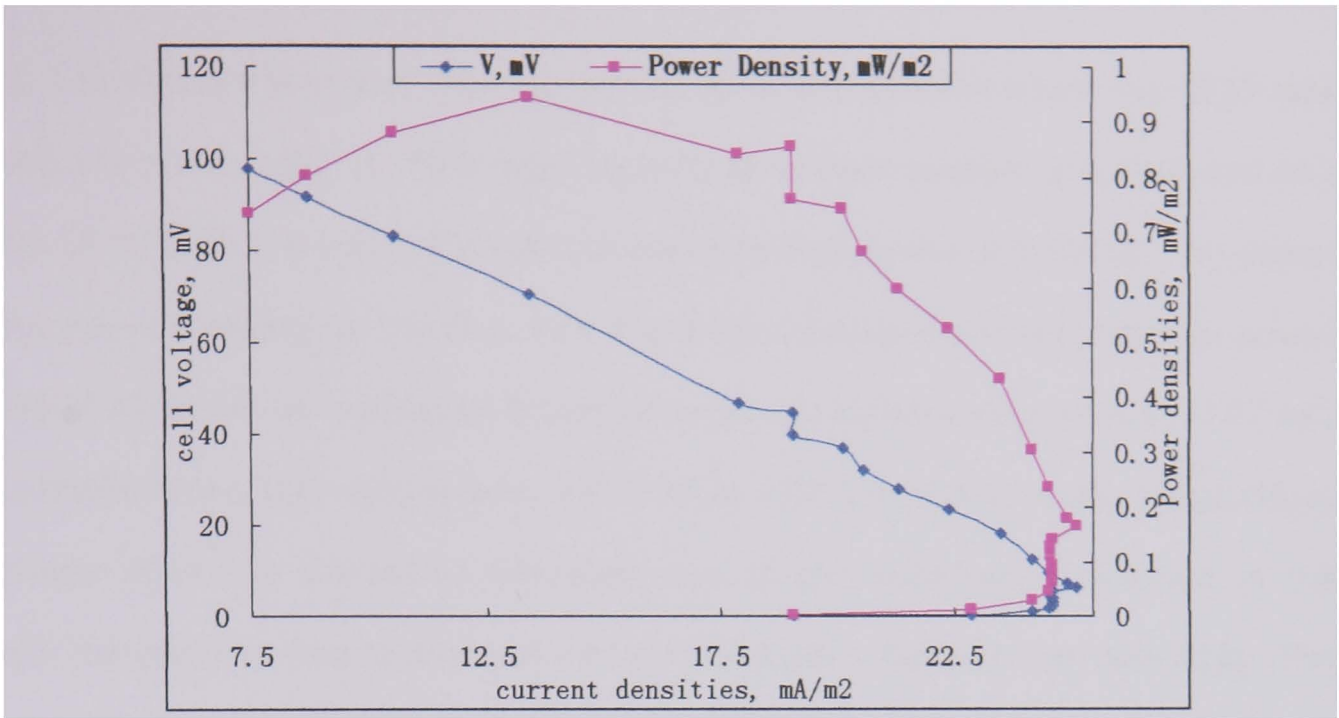

Figure 4.4 Brief polarization curve of the Micro-channel MFC during early incubation

A second test was carried out for the accurate optimal resistance at the end of incubation after two days by narrowing the external resistance between 900 Ω to 3100 Ω, and the optimal external resistance to reach the maximum power density was 2050 Ω. The internal resistance of 1805 Ω for the MFC was calculated from the slope of the cell voltage polarization curve in Figure 4.5. The maximum power density was 3.4 mW/m^2 in this experiment when the current density was 24.7 mA/m^2, corresponding to a cell voltage of 0.14 V.

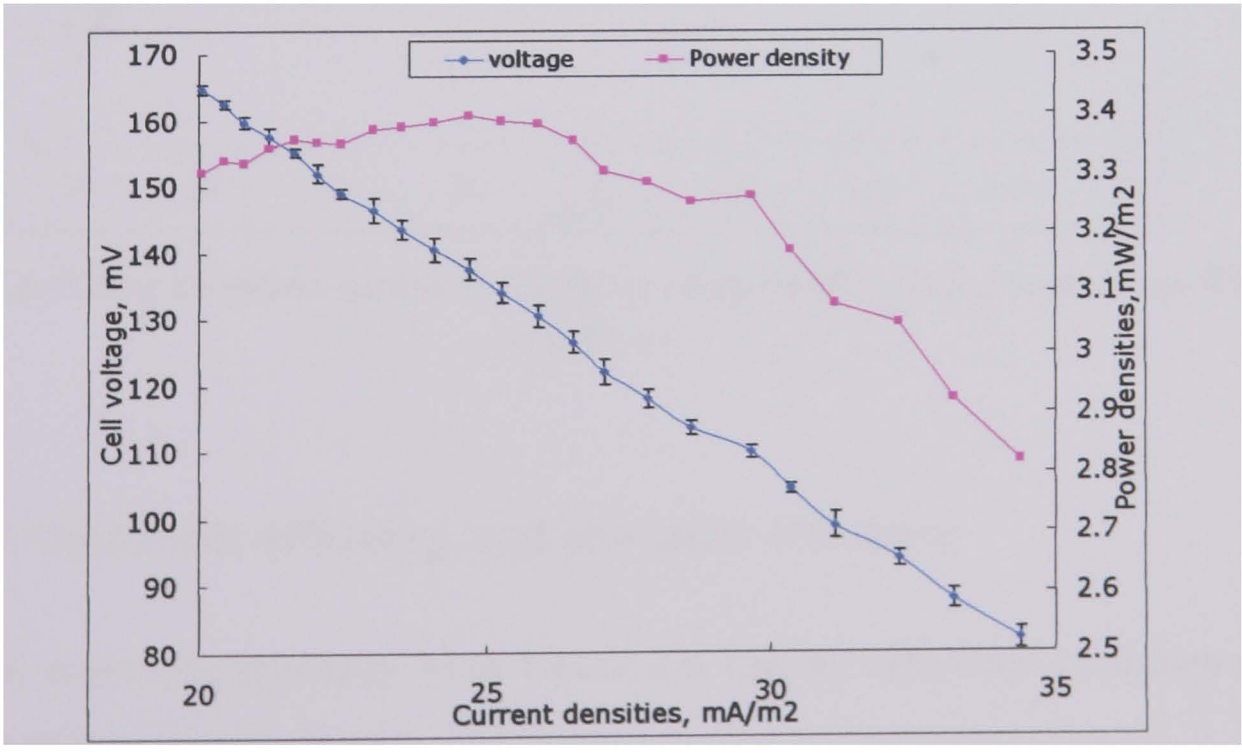

Figure 4.5 Partial polarization curve of Micro-channel MFC during late incubation

Figure 4.6 shows the power density produced in the system when the COD was increased from 62 mg/L to 1800 mg/L by adding sodium acetate at a flow rate of 2 ml/min (0.12 L/h) and using the optimal external resistance of 2050 Ω. The power density was increasing for the first 40 h and then stabilised with a maximum power density of 29.5 mW/m^2 produced based on an anode surface area of $2.65*10^{-3}$ m^2. The corresponding cell voltage was 0.4 V. After 150 h of stable power production, the power densities started to decrease due to the substrate contained in the influent wastewater was consumed and not enough substrate was available. The experiment was stopped after 160h and the COD was 600 mg/L.

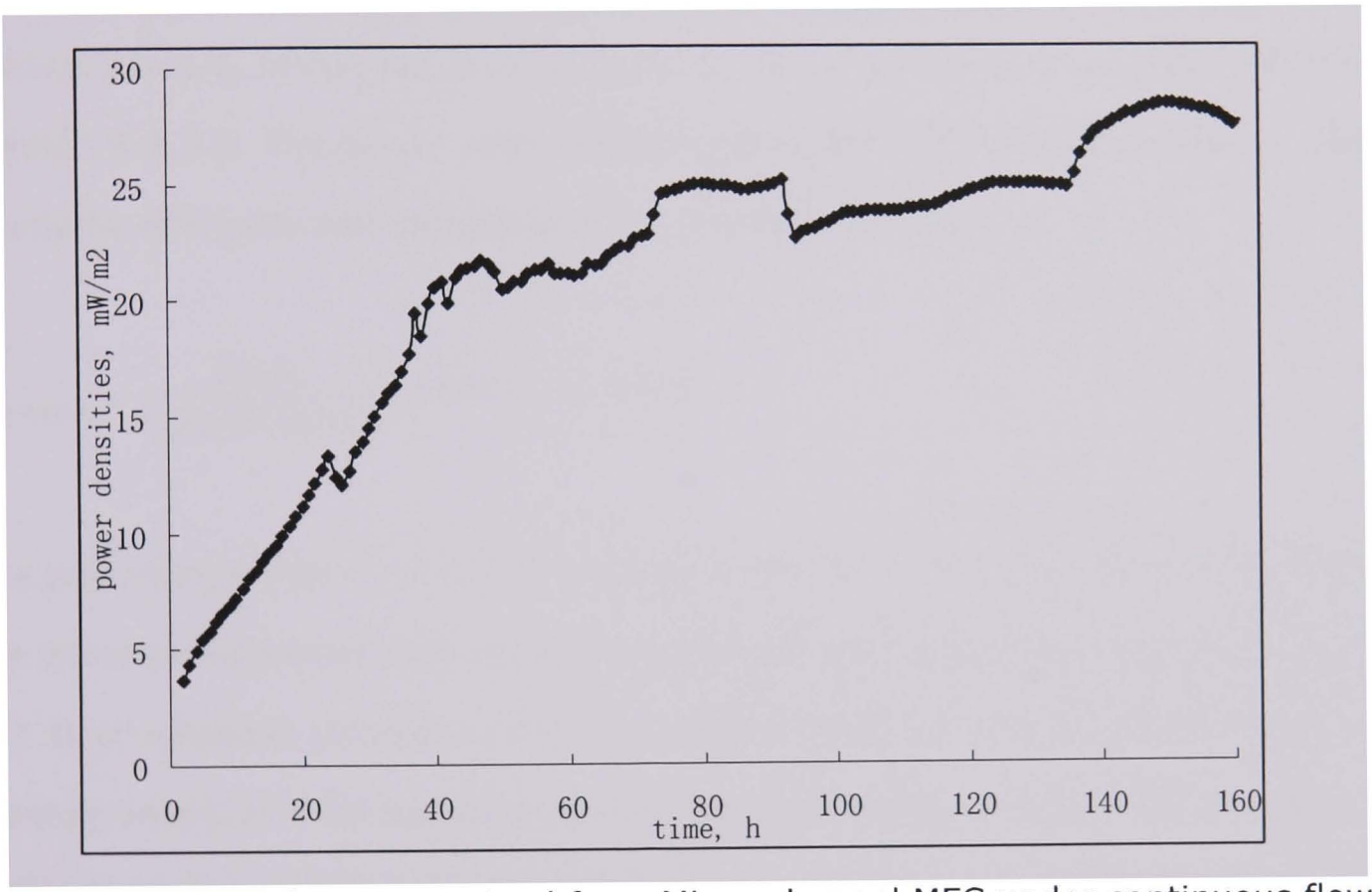

Figure 4.6 Power densities gained from Micro-channel MFC under continuous flow condition

4.2.1.2 Coulombic efficiency and energetic efficiency

The total coulombic efficiency from Figure 4.6 can be calculated according to Equation (18) in Section 2.3.1.2.1:

$$\eta_{coulombic} = \frac{97.15C \times 32g/mol}{F \times 4 \times 1.2g/L_{COD} \times 1L} \times 100\% = 0.7\%$$

Where 97.15 C is the total accumulated electron charges in the form of electricity during the total period of the experiment around 160 h, F is the Faraday's constant which is 96485 C/mol, 4 is the number of electrons exchanged per mol of O_2, which is 4 mol e^- per mol, 1.2 g/L is the COD difference between the beginning of the experiment and the end of the experiment, 1 L is the total effective volume of the influent entangled in this experiment and 32 g/mol is the molecule weight of substrates, which was converted to the COD, which is 32 g/mol O_2.

The energetic efficiency can be also calculated based on the sodium acetate as substrate using Equation (20). The energy contained in the removed COD was around 9.5 kJ/g, which was derived from the MFC experiments mentioned later on Section 4.3.3.2. The power accumulated during the 160 h run was 33.4 J. The energetic efficiency was calculated using Equation (20) as:

$$\eta_{energetic} = \frac{33.4J}{1.2g \times 9.5kJ/g} \times 100\% = 0.29\ \%$$

The coulombic efficiency of 0.7 % in this Micro-channel MFC was low indicates that the interaction between both wastewater and two electrodes was poor. Only around 0.7 % of available substrate electrons were transferred onto the anode surface. Further, only 0.29 % of available energy contained in the consumed substrate was utilized in terms of switching from chemical energy to electric energy. The probable reason is the bacteria was not well grown on the electrode surface and the electrons transfer from bacteria to electrode was not well built up or may have been blocked by biofilm insulator. Coulombic efficiency is the key factor to deal with in order to increase the electricity production performance.

4.2.1.3 COD removal rate

The average COD removal rates for five different runs using the Micro-channel MFC

are listed in Table 4.1. The COD reduction conversion in a single pass of wastewater ranged from 0.07 % to 0.25 % and the average value was 0.14 %. The calculation of the COD removal rate of single pass is based on the Equation (23). The average COD removal rate per day is 25.1 %.The COD removal rate mainly depends on the bacteria metabolism process. Low COD reduction rate indicates that the bacteria activities are low or the bacteria concentration is poor. It is interesting to note that for the experiments 1 to 5, the power densities kept increasing, probably due to better biofilm building, but the COD removal rate for each run slightly decreased. As the time passed, the biofilm layer was formed on the electrode surface, which helped the electron transfer to produce electricity but reduced bulk COD removal.

Table 4.1 COD removal in 5 repeated experiments in Micro-channel MFC

Items	Exp.1	Exp.2	Exp.3	Exp.4	Exp.5
Running period, h	22	24	49	90	94
Total passes	199	217	444	815	851
Inlet COD, mg/L	840	1272	818	1688	1712
Outlet COD, mg/L	512	1012	484	933	511
COD removal %	39	20.4	40.8	44.7	70.2
COD removal conversion /pass	0.25	0.11	0.12	0.07	0.14
COD removal %/day	41.9	20.4	22.9	14.1	26.2
Max power density,mW/m^2	0.95± 1.1	13.3± 2.3	25.7± 1.5	29± 2.1	30.1± 2.0

4.2.1.5 H_2 production

After 49 h circulation for experiment 3 in Table 4.1, the H_2 content in the 200 ml of gas was confirmed to be 21 ppm measured by a Micro GC, corresponding to molecule of 1.9 μmol. The total COD removal based on the MFC running period was 334 mg/L * 1 L = 0.33 g. Since the energy contained in the COD removal (9.5 kJ/g COD) was the same as the energy contained in the consumed substrate (10.6 kJ/g sodium acetate), 1 g COD is equivalents to 0.9 g acetate for energy content. Thus 0.33 g COD removal is equivalents to 0.297 g acetate, corresponding to 3.6 mmol acetate. The theoretical H_2 production of 12.7 mmol can be calculated based on

Equation (11). Thus H_2 recovery rate from substrate is 1.9 μmol / 12.7 mmol = 0.02 %. Thus the energy based on hydrogen production was also a small partial of the energy recovered from the total COD removal. The H_2 yield Y_{H2} (g H_2/g-COD) can be calculated as mol (1.9 μmol *2 mol/g) / 0.33g=0.0115 mg H_2/g-COD. Since N_2 gas was purged into the container during several period of experiment, and also some leakages, the tested value of H_2 was less than the actual value. But this is the evidence that this MFC system produced some amount of H_2.

4.2.1.6 Design evaluation

The Micro MFC showed good operational properties in terms of flow and connections, but the power generation was only 30 mW/m^2, and the hydrogen production was particularly low. The coulombic efficiency of the MFC was calculated to be 0.7 % indicating that the amount of bacteria with electron transfer ability was small or the electron transfer was limited by other factors such as lack of electron mediators and electrons may be consumed by other bacteria. Moderate biofilm formed on the electrode surface that helped electron transfer at longer residence times but if too thick it will block the electron transfer. Also, the COD removal rate of the MFC in 1 to 3 days was slow, which was due to the small amount of available bacteria resulting in low bacterial activities. The design of this MFC dramatically decreased the distance between the anode and cathode, which could improve the protons transport from anode to cathode. But the structure needs to associate the electrons transfer and the formation of biofilm. Thicker biofilm also could block the fine flow channel. For the large scale MFCs application concern, this type of MFC has small throughput and low effective volume to the whole compartment volume rate of 41.6 %, which is 13.3 ml versus 32 ml. In the next section, another miniature MFC was introduced with higher coulombic efficiency and COD removal rate.

4.2.2 Stacked MFC

4.2.2.1 Geometry

A stacked MFC using a CEM membrane was used during an eight weeks research stay between August and October 2006 at the Laboratory of Microbial Ecology and Technology at Ghent University, Belgium. This group has been active in the area of stacked MFC reactors (Aelterman, P. et al., 2006; Clauwaert, P. et al., 2008). The main aims were (i) Compare conventional PEM MFCs to that of non-membrane MFCs; and (ii) Compare bioelectrocemically assisted microbial reactor to boost the hydrogen production, see Section 6.2.7, with that of fermentation driven hydrogen production. As Figure 4.7 shows, the rig comprised of two MFCs clamped together, and separated by a rubber ring. For each of the two-chamber MFCs, the anode and the cathode were allocated in two chambers separated by a cation exchange membrane (CEM) CMI-7000. All of the chambers were filled with graphite granules (diameter between 1.5 and 5 mm) as anode materials and also as electrode contact materials in cathode chamber as shown in Figure 4.7. A woven carbon cloth, loaded with 5 g/m^2 Pt was used as cathode materials with 60 cm^2 surface area between the CEM and graphite granules in cathode chamber. The external contact was provided through graphite rods (5 mm diameter, Morgan, Belgium). The anode was inoculated with mixed bacteria culture obtained from a high performing MFC. The anodic effective liquid volume was 73 ml and the total MFC anode compartment volume was 276 ml. Figure 4.8 shows the schematic diagram of the stacked MFC setup.

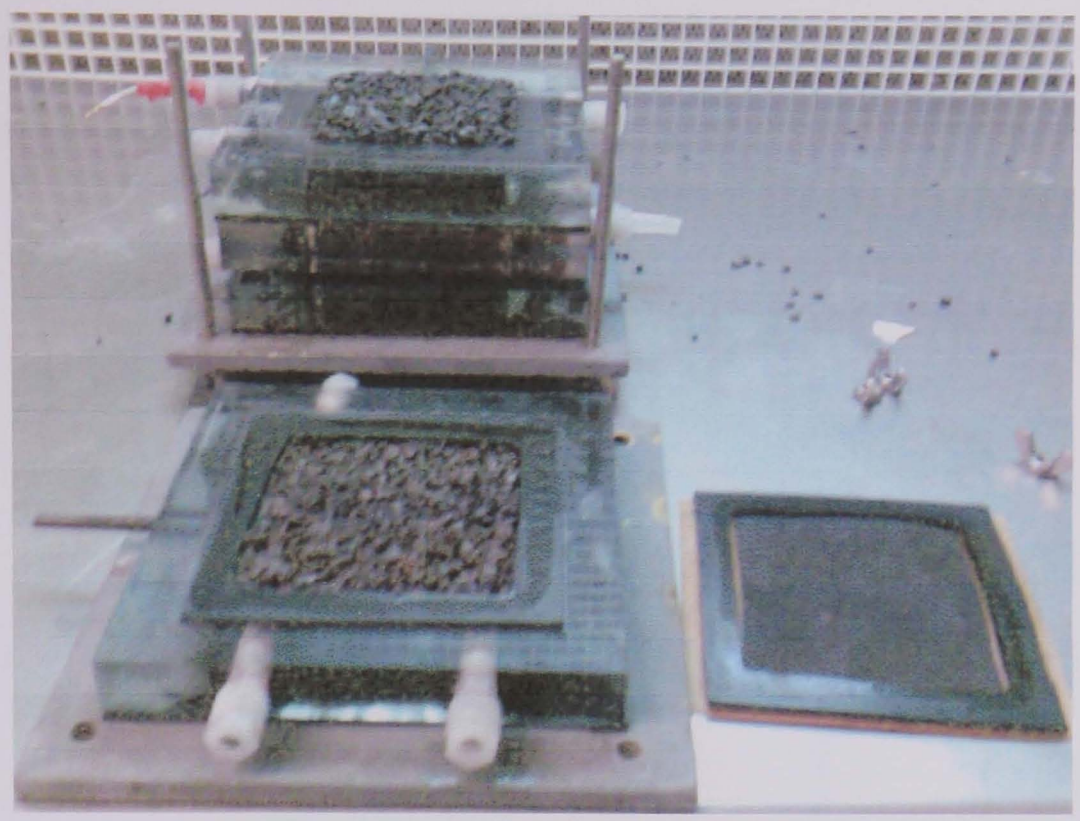

Figure 4.7 Actual assembly of stacked MFC

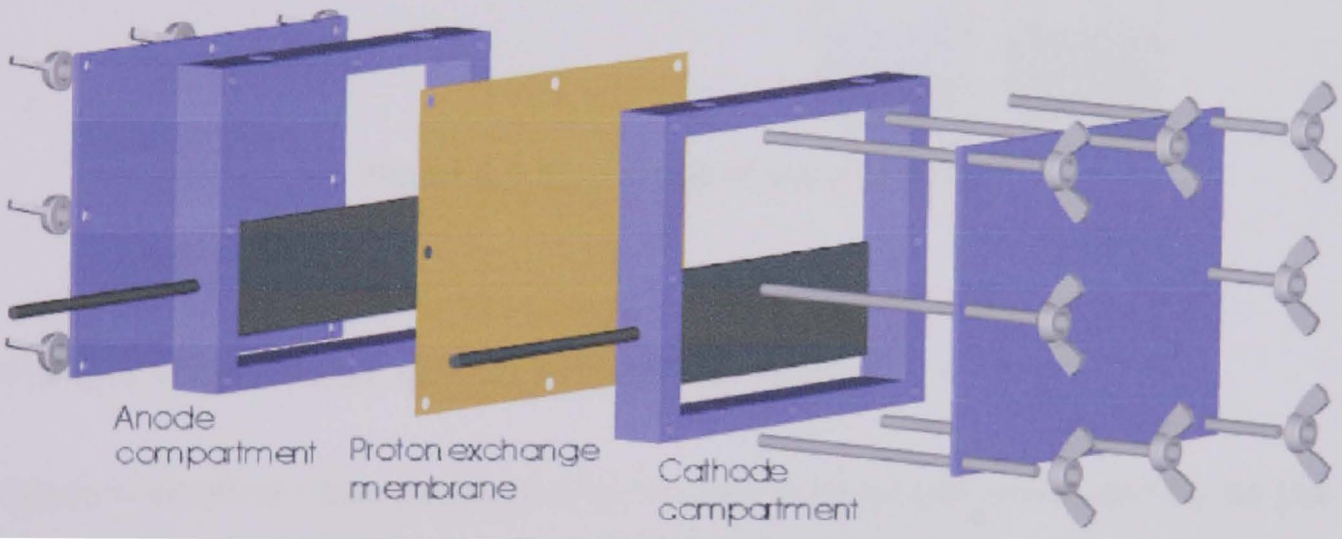

Figure 4.8 Schematic diagram of the stacked MFC setup (Rabaey, K. et al., 2004)

A potassium phosphate buffer solution 0.5 L with sodium acetate substrate was circulated in the anode chamber. The details of this buffer solution were reported in Section 3.1.4. The anodic recirculation was open to air in order to keep the gas pressures in and out of the anode chamber the same. The potassium phosphate buffer solution was circulated in the cathode chamber. Air was bubbled with a fish pump into the cathodic recirculation to system supply enough oxygen as the electron acceptor. Anodic and cathodic recirculation were set at 1.4 L/h and was supplied by a peristaltic pump (Watson Marlow, Belgium). A potentiostat was used

to test the polarization curve, control the cell voltages and recorded the power production data. The whole flow sheet of the stacked MFC set is shown in Figure 4.9.

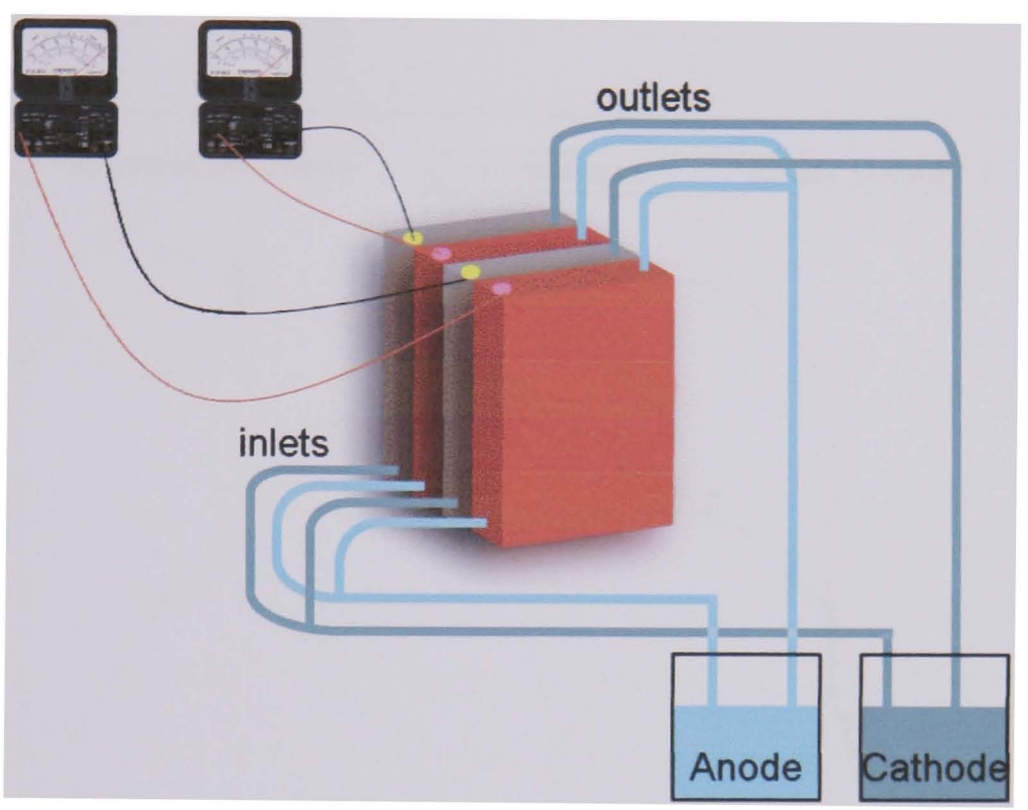

Figure 4.9 Flow sheet of stacked MFC

4.2.2.2 Polarization curves and power output

Figure 4.10 shows the polarization curve, cell voltage and power density as the function of current density produced in the stacked MFC. The polarization curve was measured with a scan rate of 1 mV/s. The highest power density produced from the stacked MFC was 11.6 W/m^3 MFC, corresponding to an optimal voltage of 0.32 V. The current density at this point was 35.6 mA/m^3, corresponding to current 10.7 mA. Thus the optimal external resistance was calculated as 0.32 V/10.65 mA = 30 Ω. The internal resistance was calculated from the slope of the voltage polarization curve as 22.8 Ω. The maximum power density of the stacked MFC based on the polarization curve test in Figure 4.10 was 11.6 W/m^3. It was MFC 43.7 W/m^3 based on the volume of anodic chamber, 532.2 W/m^2 based on the cathode material surface area, with the current 10.7 mA and current density 38.3 A/m^3 MFC.

In order to clearly compare with other MFC setups with power density unit expressed as mW/m^2, the maximum power density of the stacked MFC was calculated to 24.6 mW/m^2 and 81.3 mA/m^2 based on the anode surface area of 0.13 m^2 in the anode chamber (see Section 3.2.2.1).

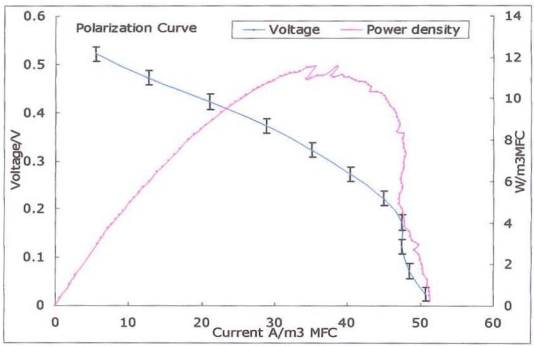

Figure 4.10 Polarization curve of stacked MFC

4.2.2.3 Coulombic efficiency and energetic efficiency

The stacked MFC was run using an external resistance 100 Ω for a total of 10 days. The coulombic efficiency was calculated using Equation (19) from the current produced over the total substrate concentration consumed.

$$\eta_{coulombic} = \frac{828.4C \times 82}{8 \times F \times 1.285} \times 100\% = 6.9\%$$

Where a total of 828.4 C of current was accumulated during the period, 1.285 g of sodium acetate (CH_3COONa) was consumed, F is the Faraday's constant which is 96485 C/mol, 8 is the number of electrons exchanged per mol of sodium acetate,

and 82 is the molecule weight of CH_3COONa.

The energetic efficiency of the MFC process during the 10 days' run was calculated according to Equation (20). The power produced during these 10 days was 141.4 J. From the calorific value of 10554 J/g for sodium acetate the energetic efficiency was calculated as:

$$\eta_{energetic} = \frac{141.4J}{1.285g \times 10554J/g} \times 100\% = 1.0\ \%$$

Both efficiencies indicate that only 6.9 % of the available electrons and 1.0 % of total energy contained in the substrate were converted into electricity in the stacked MFC. The reason was mainly due to poor electrons transfer from bacteria to electrode, limitation for substrate usage of bacteria that may have been blocked by biofilm as an insulator. In order to increase the electricity production, improvements in the electron transfer process is key.

4.2.2.4 Fixed voltage control

Figure 4.11 shows the changes in current densities and power densities of the stacked MFC as the fixed cell voltage was gradually increased from 0.05 V to 0.55 V with an interval of 0.05 V/h using a potentiostat. No extra electrons are added into the system during the experiment and the only difference with the conventional MFC mode was that the potentiostat was used to fix the cell voltage at a certain value lasting for one hour for each voltage value.

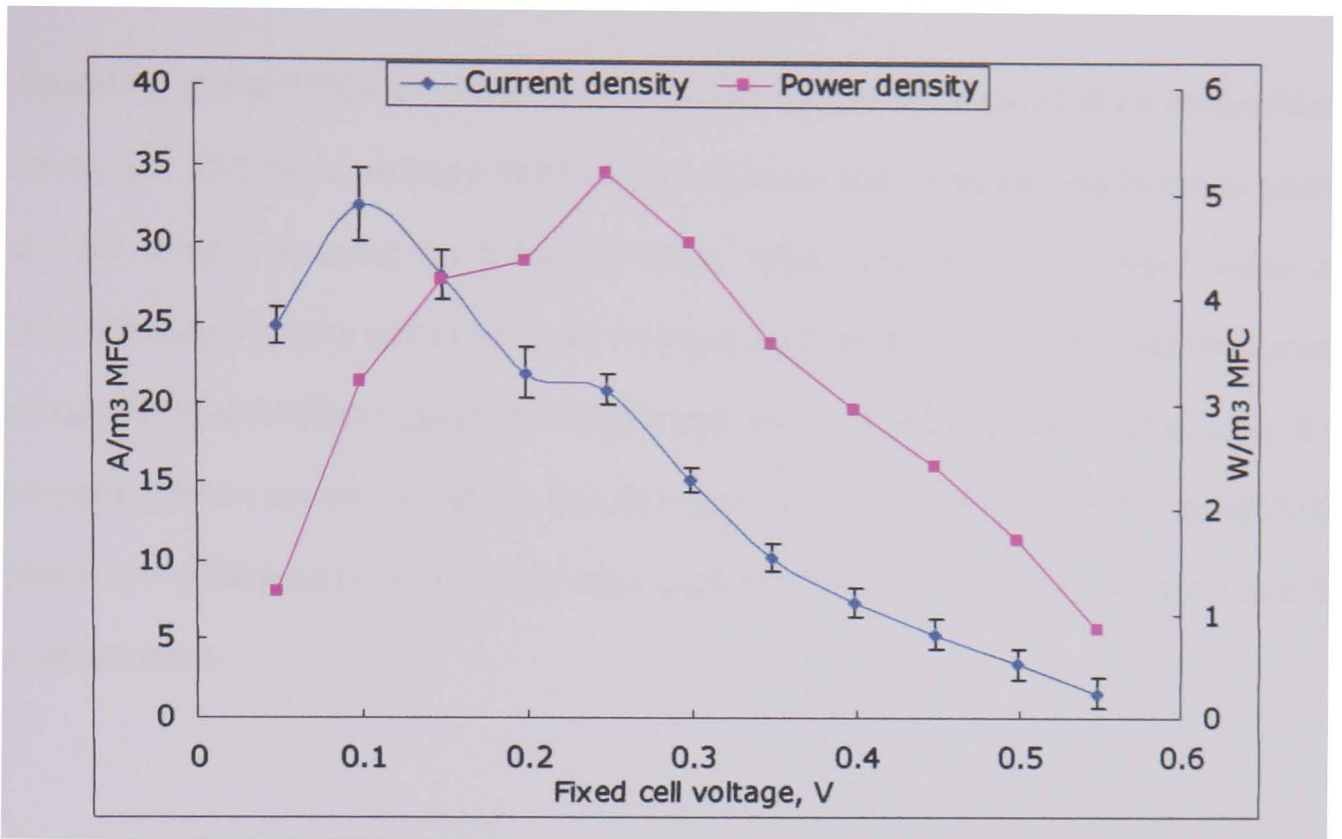

Figure 4.11 Current and power densities as the functions of fixed cell voltages for stacked MFC

Figure 4.11 shows that when the fixed cell voltage is gradually increasing, both power densities and current densities experienced peaks and then decreasing to very low values. A maximum power density of 5.2 W/m^3 was observed at a fixed voltage of 0.25 V. A maximum current density of 32.5 A/m^3 MFC was obtained when a fixed cell voltage of 0.1 V was applied, corresponding to a current of 9 mA. This shows that when the cell voltage is fixed at 0.1 V, the bacteria at the anode can transfer the largest amount of electrons from the substrates and produce the maximum rate of electron flow towards the cathode. When combining both the current and the voltage in the cell, a maximum power density of 5.2 W/m^3 was achieved when the fixed voltage was 0.25 V.

The results slightly differed from the polarization curve measurements where the power density was 11.6 W/m^3 with a cell voltage of 0.3 V. The main difference between these two techniques is that for the polarization curve test the cell voltage from the OCP to 0 V was increased during an interval times of only 5 s per voltage data, while for the fixed voltage control technique the fixed voltage interval was 1 h per data. The polarization curve test is generally used as a standard test to find

the capability of the MFCs or other fuel cells due to the very short data acquisition time involved. The fixed voltage control test is more time consuming but it is more realistic for a MFC running for a longer time. With regards to the lower value of maximum power density with the fixed voltage control technique, the bacteria may have experienced limited substrate supply during the 1 hour compared to only 5 s for the polarization curve. However, the corresponding optimal cell voltages of 0.32 V found from polarization curve test and 0.25 V from fixed voltage control are in good agreement.

4.2.2.5 Substrate consumption

During the stacked MFC runs, the substrate concentration of sodium acetate was measured by a GCMS. Table 4.2 shows the substrate consumptions in the MFC for various runs. The variation in the consumption of acetate was mainly due to the different test conditions. During the conventional run using an external resistance of 100 Ω, the cell voltage was around 0.3 V and the acetate consumption in one day was 78 %. The COD removal conversion in a single pass was 0.33 % since the anodic chamber was filled 460 times each day according to the Equation (23) in Section 2.3.1.3. For the fixed voltage controlled run, see Section 4.2.2.4 for detail, the average COD removal conversion per pass dropped to 0.06 % compared to 0.33 % for the conventional stacked MFC conditions. During the polarization curve tests, see Section 4.2.2.2, the average acetate consumption in the cell was 0.01 % - 0.09 % per pass. The substrate consumption results show that when the conventional MFC running mode was applied, it had the highest substrate consumption rate. For the fixed voltage control application and polarization curves applications, where fixed cell voltages were applied to the cell with different interval time, the substrate consumption was lower than the normal MFC application. With the applications of fixed control of cell voltages, bacteria were forced to transfer electrons to generate suitable current to response the fixed

voltage, this may affect the available bacteria and their activities to remove the COD.

Table 4.2 Substrate consumptions during the stacked MFC runs

Tests	1	2	3	4	5
Activities	Conventional MFC	Fixed voltage control	Polarization curve	Polarization curve	Polarization curve
Periods, day	1	4	5	3	7
Total passes	460	1840	2300	1380	3320
COD Removal rate, %	78.1	63.8	17.9	15.1	70.6
Average COD removal conversion/pass, %	0.33	0.06	0.09	0.01	0.04
Removal rate/ day, %	78.1	16.0	3.6	5.0	10.1

4.2.2.6 Design evaluation

In summary, the stacked MFC design does have the power generation of maximum 11.6 W/m^3 MFC compartment, corresponding to 24.6 mW/m^2 based on the anode surface area of 0.13 m^2 in the anode chamber (see Section 3.2.2.1). Hydrogen production was not observed in this setup since the anodic influent was open to air in order to avoid gas pressures. The coulombic efficiency was 6.9 % that it was higher than the Micro-channel MFC of 0.7 %. The substrate consumption conversion per pass in the stacked MFC was 0.33 % which was higher than the Micro-channel MFC of 0.14 %. The effective volume of 73 ml throughput is low compared to the whole anode compartment volume of 276 ml resulting in only 26.4 % of the space being available, which is lower than that of Micro-channel MFC 41.6 % (Section 4.2.1.6). With regards to large scale MFCs application, the performance of these two MFCs still needs to be improved. The use of buffer solution using potassium phosphate chemicals in stacked MFC is both costly and logistically challenging, since it needs to be refill or recycled before discharged. The CEM in stacked MFC was applied to separate the two electrodes, which increased the capital cost and also the internal resistance of protons transfer from anode to

cathode. In order to cater for the large scale industrial application, a new hexagonal tube concept design of MFC was set up.

4.3 Hexagonal tube MFC

In this section, a novel hexagonal tube MFC is introduced to address industrial requirements of high throughput, low cost, small space footprint and simple design for wastewater treatment and renewable energy production. The hexagonal tube MFC cater for applications with high continuous flow rate, non-buffer medium contained no membrane separation and simplified design using existing footprint for wastewater pipes. The performance of this hexagonal tube MFC in terms of electricity production, hydrogen generation and COD removal rate is presented below.

4.3.1 Geometry

The geometric design of the hexagonal tube MFC built on two recently published designs of single chamber MFC. Firstly, the horizontal design by H. Liu et al. in Figure 2.8 had good properties, such as short distance for proton transmission from anode to cathode, reduced footprint of MFC reactor, and cathode directly in contact with air (Liu, H. et al., 2004). Secondly, the upflow MFC by Z. He et al. in Figure 2.9 had large anode surface area, but the proton transport distance was very long (He, Z. et al., 2005). From these designs, the hexagonal tube MFC has optimized the distance between anode and cathode which having a large effective surface area and further simplified design.

The schematic configuration of the hexagonal tube MFC and the flow sheet of the whole reaction system are shown in Figures 4.12 and 4.13, respectively. The external tube was designed as a hexagonal prism. The main reasons for this were

(i) to facilitate stacking of large quantities of tubing MFCs reactor for further industrial scale application; and (ii) to make the water flow turbulent that allows substrate to contact to the anode and prolong the wastewater retention time. The anode material was plain carbon cloth B that was attached on the inner surface of the hexagonal prism. The inner tube was located in the center of the external tube and cathode material microporous layer including 5g/m^2 Pt electrode on woven web was wrapped over the surface of the inner tube. Wastewater flow was passed between the anode and cathode materials.

The effective volume of this single chamber MFC was 2.7 L with a length of 1m. The effective anode surface area was 0.14 m^2 and the effective cathode surface area was 0.12 m^2. The effective cathode volume for biogas collection was 4.4 L. The continuous experiments were carried out at room temperature. Electricity was observed in this tube MFC using domestic wastewater. An external variable resistor, which could be adjusted from 1 Ω to 5000 Ω, was used to connect a load between the anode and the cathode. The cell voltage across the external load was measured and recorded by a multimeter data logger. Two modes of aerobic MFC and anaerobic MFC hexagonal tube MFC were run and reported in Sections 4.3.2 and 4.3.3, respectively. During the aerobic MFC, the two lids on both side of the tubing were open and a fish pump with 0.9 L/min was used to supply air to the cathode. When running at anaerobic conditions, the two lids were sealed and N_2 was used to purge the cathode chamber prior to each test to vent out oxygen. During the anaerobic MFC, the biogas production was collected through a sampling tube inserted into the cathode tube.

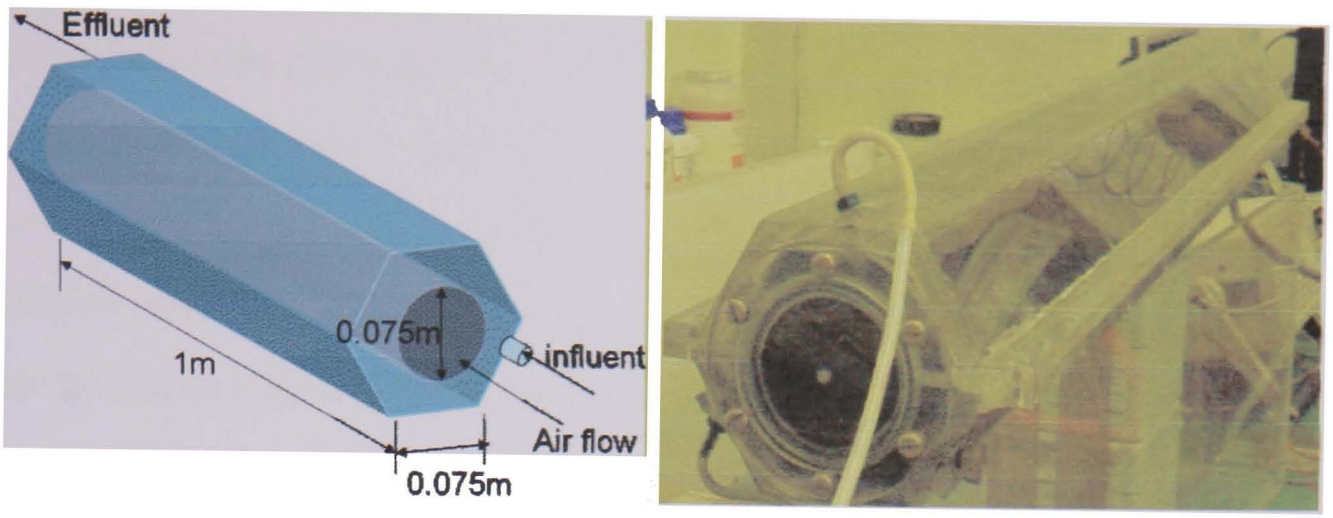

Figure 4.12 Configuration of the Hexagonal tube MFC

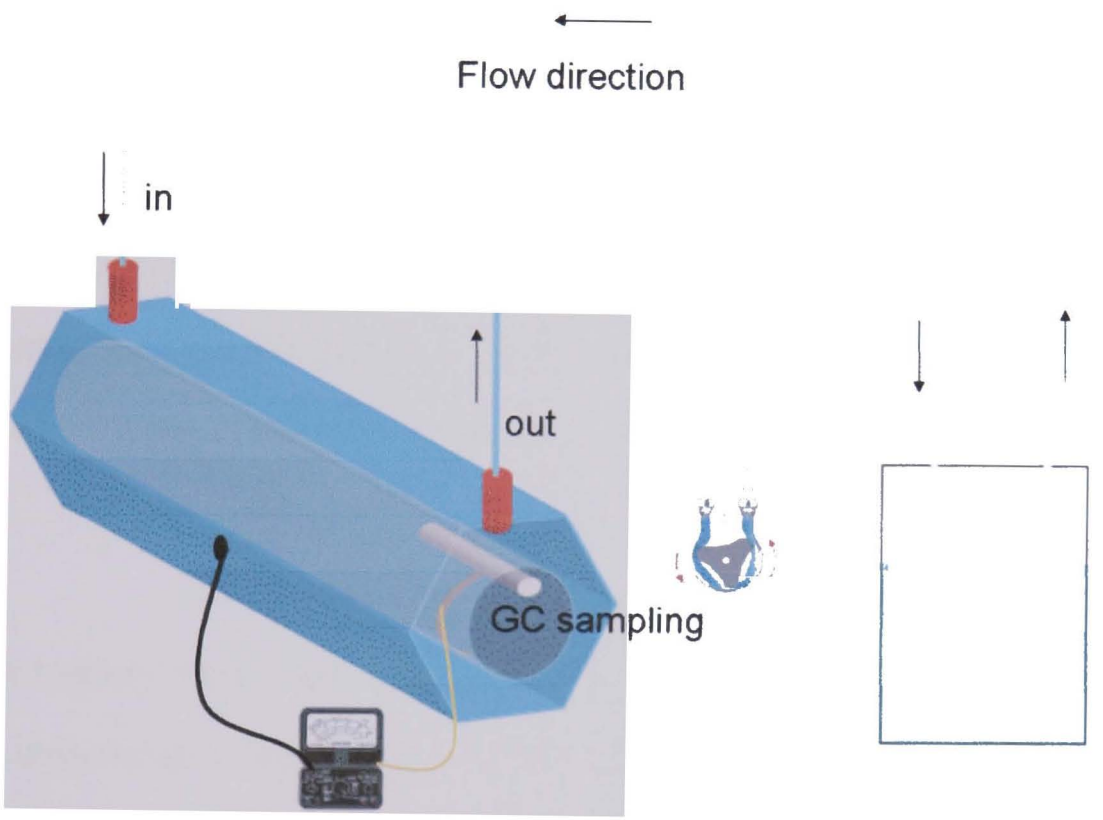

Figure 4.13 Flow sheet of the hexagonal tube MFC

4.3.2 Aerobic hexagonal tube MFC application

During the aerobic MFC application, the air supplied through the cathode tube could penetrate through the cathode material to the anode chamber due to the air permeable properties of the cathode material. The use of oxygen brings some disadvantages to the MFCs application. Oxygen has a high reduction potential and acts as electron acceptor competing with the anode electrode. The protons released to the medium can also be used for the formation of water together with

oxygen in the anode chamber. Thus, less electrons and protons can be used for the power generation in MFCs. Both batch aerobic MFC and continuous aerobic MFC were examined in this section. In continuous mode, the effluent was sent back to the influent reservoir as a recycle loop. All measurements were taken after the reactor had been operating for at least three hydraulic retention times to maintain a stable power output.

4.3.2.1 Polarization curves and power output

After around a week of incubation with primary treated wastewater, a polarization curve test was executed before all other tests in order to find out the the optimal external resistance. Figure 4.14 shows the polarization curve for the batch system and Figure 4.15 for the continuous system. The tests were run from 30 Ω to 5000 Ω.

For the polarization curve test under batch aerobic conditions in Figure 4.14, wastewater containing 116 mg/L of COD was used and the cathode air flow rate was kept at 0.9 L/min. The cell voltage decreased with increasing current density and the power density reach a peak of 2.1 mW/m^2 when the current density was at 12.1 mA/m^2 corresponding to a cell voltage of 0.17 V. The optimal external resistance was calculated as 100 Ω. The internal resistance of this MFC was calculated as 78 Ω from the slope of the cell voltage polarization curve.

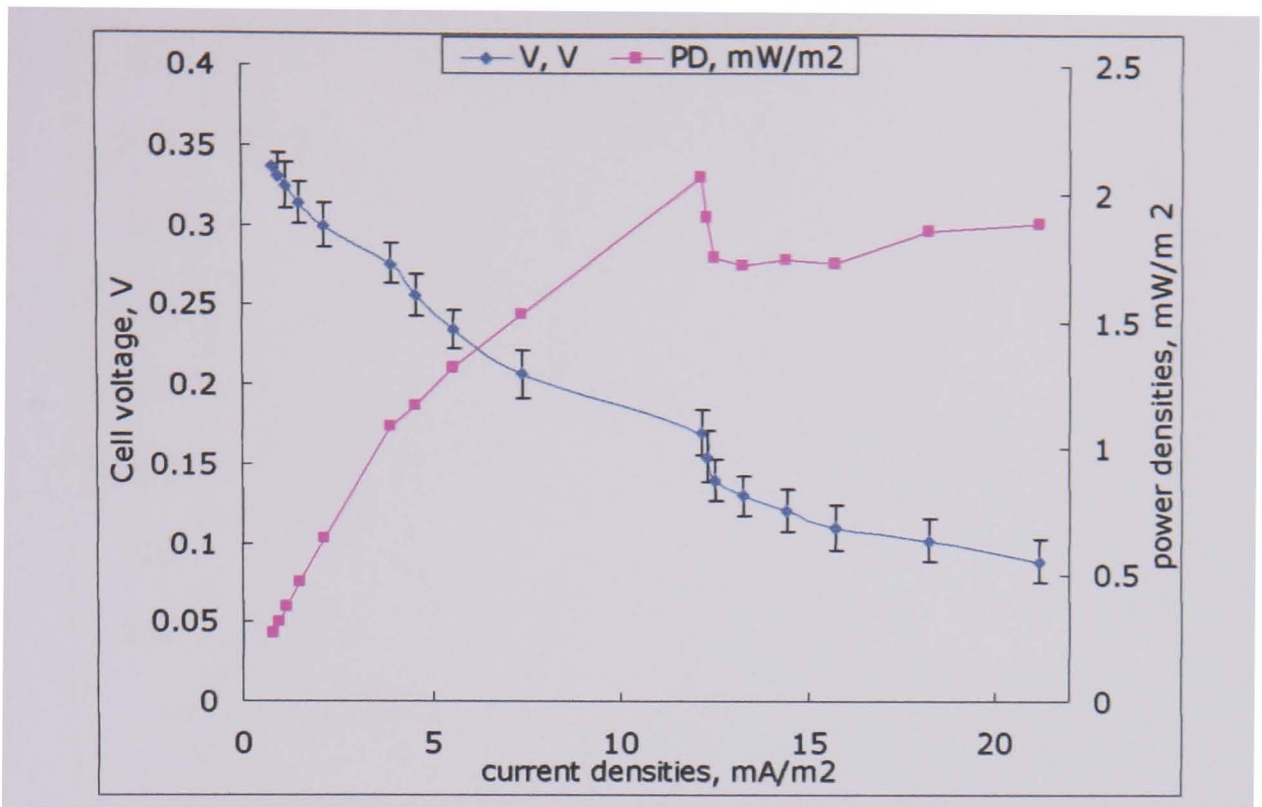

Figure 4.14 Polarization curve for batched aerobic hexagonal tube MFC

The polarization curve test found under continuous aerobic tube MFC in Figure 4.15 used wastewater containing 116 mg/L of COD at a flow rate of 2.7 L/h with a hydraulic retention time of 1 h. The cathode air flow rate was 0.9 L/min. The cell voltages decreased similar to the batch mode MFC with increasing current density. The power density peaked at 2.4 mW/m^2 when the current density was at 13.2 mA/m^2 and the cell voltage was 0.19 V. The optimal external resistance was calculated from these data as around 100 Ω as well. The internal resistance calculated based on this polarization curve was 77 Ω, which is similar to batch conditions.

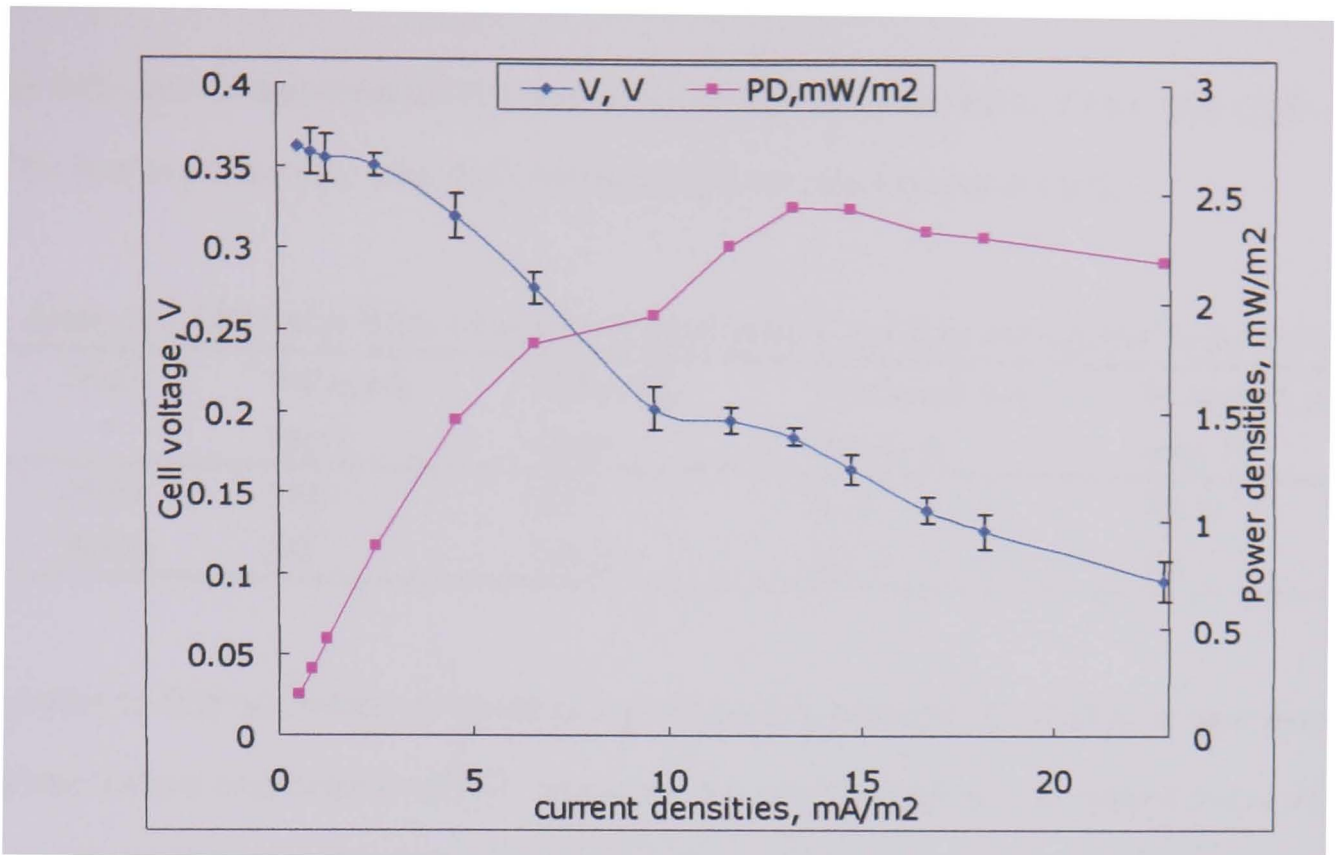

Figure 4.15 Polarization curve for continuous aerobic hexagonal tube MFC

As seen from the polarization curves in Figures 4.14 and 4.15, the maximum power density of 2.1 mW/m^2 under batch mode was lower than the 2.4 mW/m^2 observed under continuous mode. This indicates that continuous flow might help electron, substrate and proton transfer to increase the power density. However, both power densities were very low, which indicates that oxygen contained in the anode chamber decreases the power production of this MFC. Since the same optimal external resistance was established, an external resistance of 100 Ω was applied to all the experiments under continuous flow conditions unless specified otherwise.

4.3.2.2 COD Removal

Table 4.3 shows the COD and BOD results under continuous aerobic conditions for the hexagonal tube MFC. The initial inlet COD level was 160 mg/L and BOD_5 was 59 mg/L. The flow rate was 5.4 L/h (HRT=0.5 h). After the continuous aerobic MFC had run for 1h, the outlet COD was 156 mg/L and the BOD was decreased to 26.9 mg/L. The corresponding removal rates of COD and BOD_5 were calculated as shown in Table 4.3. The COD removal rate was much lower than the BOD_5 removal rate

that indicates that some BOD compounds were transferred to COD. The COD and BOD_5 removal per day was calculated based on the Equation (23).

Table 4.3 COD and BOD removal in continuous aerobic hexagonal tube MFC

Tests	Influent, mg/L	Effluent, mg/L	Removal per pass, %	Removal per day, %
COD	160	156	1.3	46.6
BOD_5	59	26.9	27.2	99

In order to find out whether there is a relationship between the influent wastewater concentration and both the COD removal rate and the power generated in the MFC, a series of MFC experiments was run with four different inlet COD values under the same HRT of 1h. Running flow rate is 5.4 L/h. The influent COD level was gradually decreased by diluting with inlet water. The COD of the effluent water samples were measured and the COD removal rates of run 2 to 4 were calculated. The COD removal conversions per pass were calculated according to Equation (23) in Section 2.3.1.3. Table 4.4 shows that the COD removal conversion per run increased from 1.3 % to 20.2 % from run 1 to run 4 indicting that transport issues are main barriers in the MFC.

Table 4.4 COD removal rate as a function of inlet COD

COD	Influent, mg/L	Effluent, mg/L	otal passes	Removal conversion / pass, %
Run1	160	156	2	1.3
Run 2	68	46	6.6	5.8
Run 3	30	25	2.8	6.3
Run 4	9	5	2.6	20.2

Figure 4.16 shows the maximum power density produced during the runs as a function of the inlet COD values. The threshold in this figure is probably due to the biological measurement error to a certain extent, but more data measurement are needed. However, Figure 4.16 indicates that by increasing the inlet COD the power densities can also be increased. Liu et al. also concluded that the voltage across the

circuit enhanced when the wastewater COD increased (Liu, H. et al., 2004).

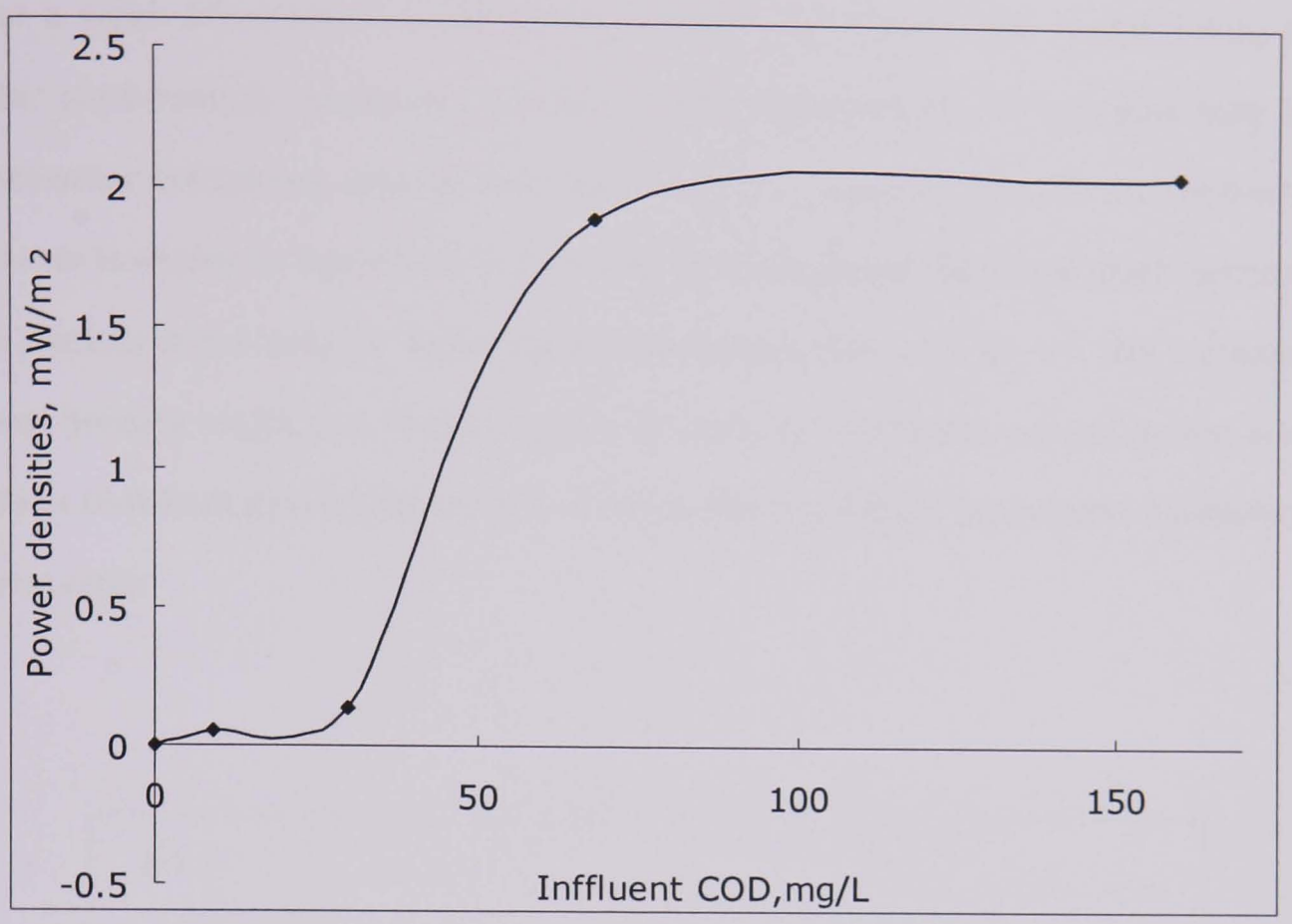

Figure 4.16 power densities of aerobic tube MFC versus influent COD

4.3.3 Anaerobic MFC application

During the continuous anaerobic MFC, there was no air supplied through the cathode chamber as the cathode chamber was tightly sealed by two lids at both sides and N_2 gas was used to purge the system before each experiment. No oxygen in the cathode chamber meant no oxygen would permeate into the anode chamber ensuring an anaerobic environment with no oxygen electron acceptor. The external resistance in all the experiments under anaerobic continuous condition was fixed at 100 Ω unless specified otherwise. All measurements were taken after the reactor has been operated for at least three hydraulic retention times to maintain a stable power output.

4.3.3.1 Power output, coulombic and energetic efficiency

After a week of incubation period under batch conditions, the power production under continuously anaerobic conditions was observed at 5.4 L/h flow rate with wastewater containing around 118 mg/L of COD. The power density during the first 260 min is shown in Figure 4.17. It shows that the power densities kept increasing to a plateau of 5.4 mW/m^2 based on anode surface area of 0.14 m^2. The increase of power density might due to the activity of anaerobic bacteria growth on the anode surface that kept producing more and more electrons from substrates contained in wastewater.

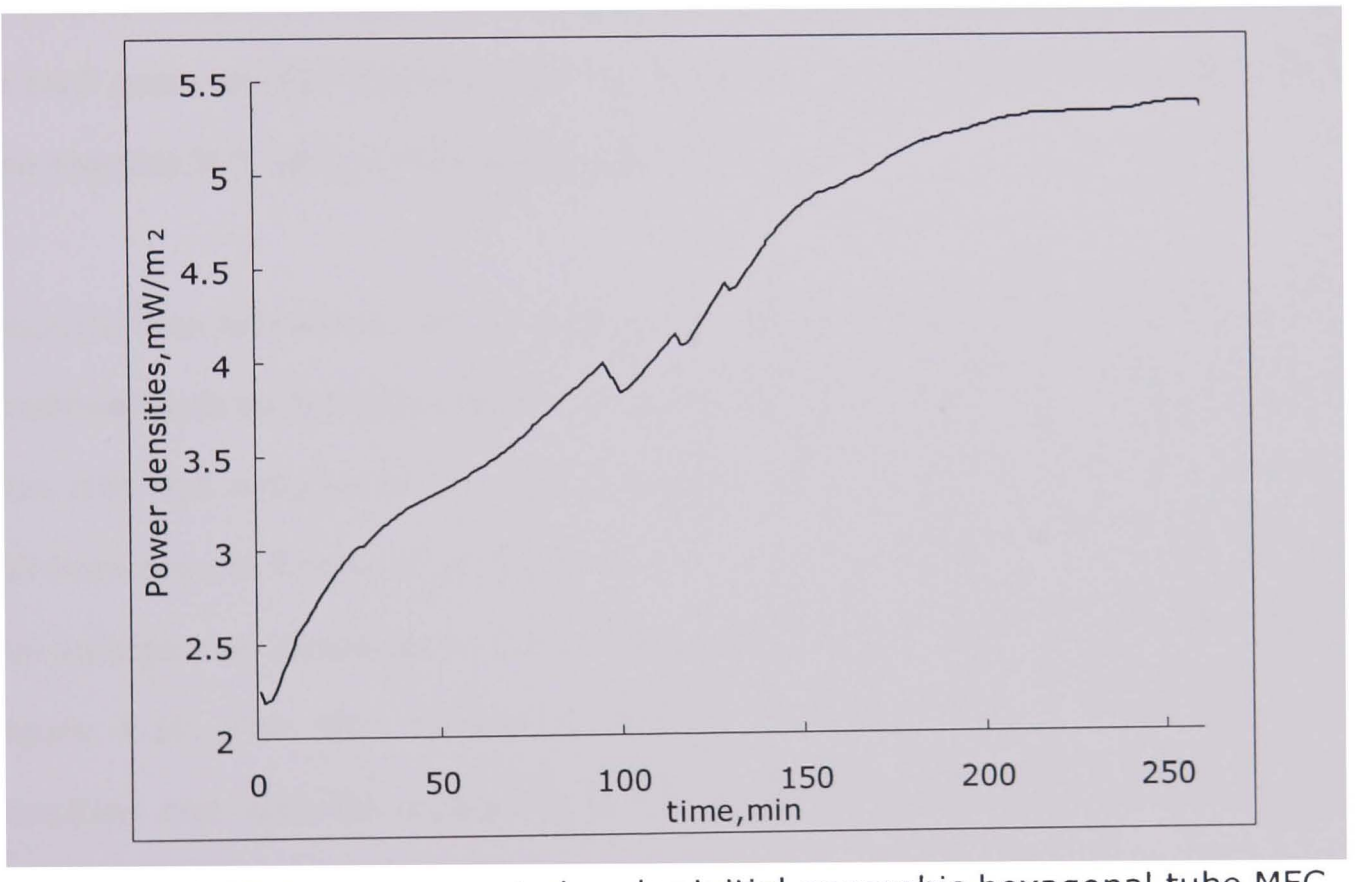

Figure 4.17 Power generated under initial anaerobic hexagonal tube MFC

The COD decreased from 118 mg/L to 56 mg/L, which is a 53 % removal rate in 260 min. The coulombic efficiency were calculated from Equation (18) as:

$$\eta_{coulombic} = 38.1\ C \times 32 / (4F \times 0.062\ g/L \times 2.7L) \times 100\% = 1.9\ \%$$

where 38.1 C was the total charges converted from produced electricity, F is the

Faraday constant which is 96485 C/mol, 0.062 g/L is the total COD removal in this period, 2.7 L is the total bulk volume of wastewater.

The coulombic efficiency indicates that only 1.9 % of the available electrons contained in the substrate was utilised in the system in the form of electricity production. This was lower than the coulombic efficiency for the stacked MFC of 6.9 % in Section 4.2.2.3. The energy efficiency was further calculated from Equation (20) as:

$$\eta_{energetic} = 9.4\ J/\ (9.5\ kJ/g \times 0.062\ g/L \times 2.7\ L) \times 100\% = 0.6\ \%$$

Where 9.4 J was the total energy produced, 9.5 kJ/g was the total energy contained in each gram of COD (Section 4.3.3.2). This was similar to the energy efficiency for the stacked MFC of 1.0 % in Section 4.2.2.3.

Sucrose was introduced as an extra substrate to increase the COD level of the wastewater to an the influent COD around 2000 mg/L following incubation and the flow rate was reduced to 2.7 L/h. Due to lowering the flow rate the power density fell from around 5 mW/m^2 in Figure 4.17 to 2 mW/m^2 in Figure 4.18. The maximum cell voltage was increased to 0.38 V and a maximum of 12.2 mW/m^2 was shown in Figure 4.18. This also confirmed that by increasing the inlet COD, the power densities can also be increased as found under aerobic conditions in Section 4.3.2.2.

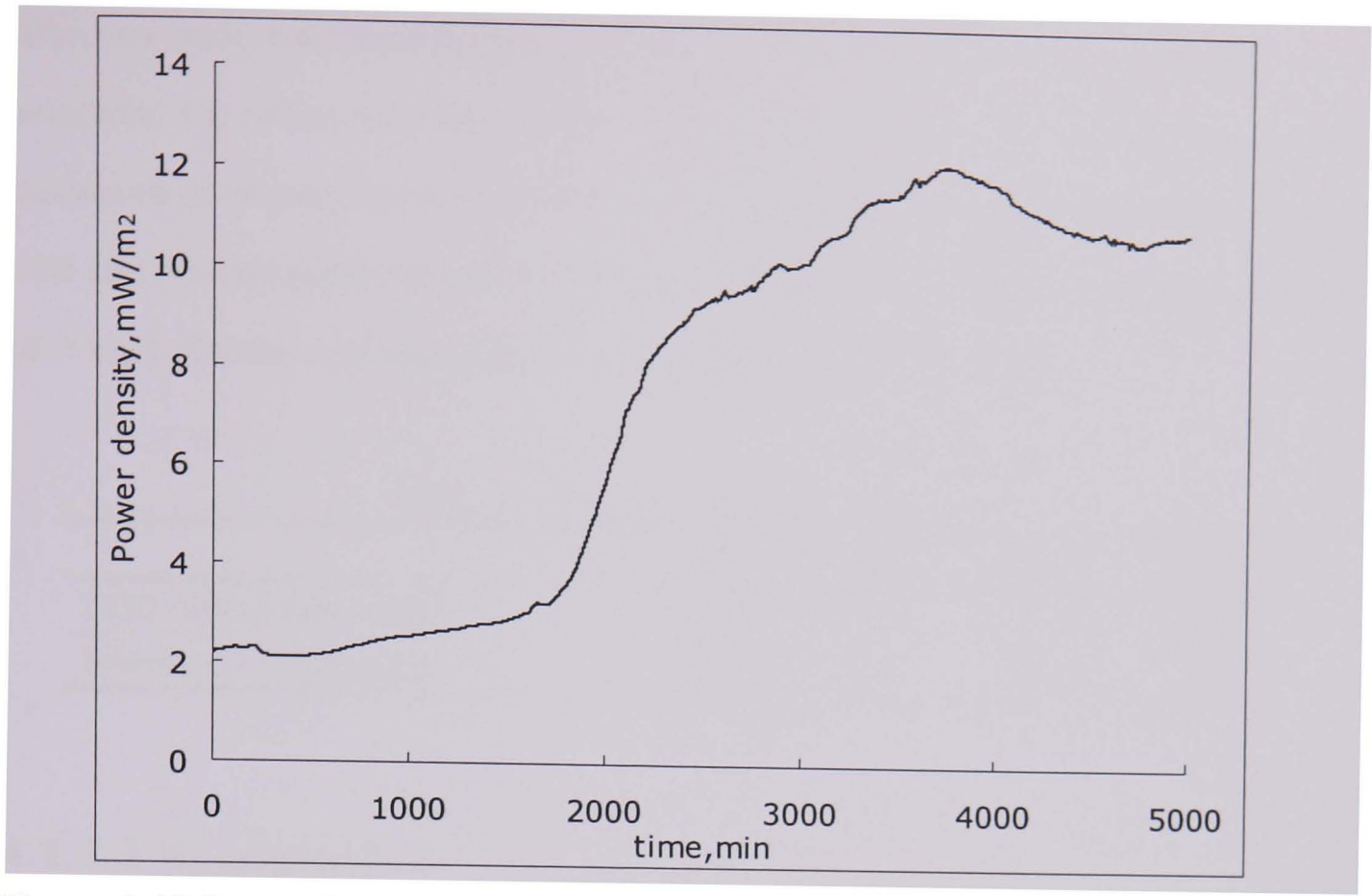

Figure 4.18 Power densities produced under high COD anaerobic hexagonal tube MFC conditions

4.3.3.2 COD removal and substrate supply

To test repeatability, COD samples were measured at the beginning and the end for 5 consequent runs experiments with the same flow rate of 2.7 L/h. The run times differed from 48 h to 190 h and the results are listed in Table 4.5. The COD removal rates per pass were calculated according to Equation (23) in Section 2.3.1.3. The COD removal conversion per pass ranged for 2.13 % to 4.41 % with an average value around 2.90 %. This indicates that the COD removal is fairly predictable using MFCs.

Table 4.5 COD removal rates under in anaerobic hexagonal tube MFC

Items	Run 1	Run 2	Run 3	Run 4	Run 5
Inlet COD	1865	1864	1826	1962	2100
Outlet COD	10	420	20	96	100
Total passes	190	48	100	140	140
COD removal	99.5%	77.5%	98.9%	95.1%	95.2%
COD removal conversion / pass	2.71%	3.06%	4.41%	2.13%	2.15%
COD removal/day	48.3	52.6	66.1	40.4	40.6

Based on Table 4.5, the energy contained in COD content can be calculated. Since the 1 g of sucrose was added for each run, the energy added can also be expressed as energy contained in COD, the average value of energy contained in COD can be calculated shown in Table 4.6. The calorific value of sucrose is about 16.7 kJ/g. So the average energy contained in COD is 9.5 kJ/g.

Table 4.6 Energy contained in COD

	Run2	Run3	Run4	Run5
COD consumed, mg/L	1854	1406	1942	2004
Energy in COD, kJ/g	9.0	11.9	8.6	8.3

4.3.3.3 H_2 production

4.3.3.3.1 Anaerobic MFC and fermentation process

During an anaerobic MFC run, H_2 can also be produced together with the power generated. The produced H_2 gas may come from the MFC process itself or from the competing fermentation process in the bulk wastewater. A series of tests was run to find the relationship between fermentation and the MFC process. Under MFC conditions, the anode and the cathode were connected to the external resistor box and the data logger. During fermentation only, no external load was applied and the voltage recording of the system was disconnected. A micro GC test was conducted every hour using the online gas sampling test from the reactor in Section 3.3.3.1. For each experiment, 1 g/L of sucrose was added into the system to increase the COD level to act as substrate for the bacteria. 20 L of bulk wastewater was applied. The order of the experiments is list consecutive in Table 4.7 below where one experiment was following the other. First, four MFC tests were carried out, followed by four fermentation only tests, then switched to another MFC test, and finally the experiment was switched back to two fermentation tests. Only some of these runs produced H_2. For the first two MFC runs, no H_2 was produced, probably due to the build up of biofilm on anode during MFC operation as indicated by increasing power

density. A small amount of H_2 was observed during MFC-3 and 4. Then for the next four fermentation processes, only Ferm-1 and 4 produced H_2 but for Ferm-2 and 3 no H_2 was observed. Afterwards, both the MFC process and the fermentation process generated relatively large amount of H_2. The produced amounts of H_2 indicate that the H_2 production may be attributed and affected by a combination of the fermentation process and that of MFCs process. The hydrogen production started during the MFC runs 1 to 4 and first peaked as 0.07 mmol/min during Ferm-1. It then fall off and was kicked back by MFC-5 to 1.31 mmol/min, peaking at 2.44 mmol/min for the next Ferm-5 and then falling off again. The power density for the MFC tests generally increasing from start till the end of the series of experiments due to good build up of biofilm. The power production during the MFCs process might impact on the H_2 production. The flow rate of the influent was changed in some tests to elucidate the function of flow rate for the two processes. The results suggested that increasing the flow rate will increase the hydrogen production, power production performances for the MFC process confirming from entire findings, and also impact the hydrogen production during fermentation.

Table 4.7 Comparison of the anaerobic MFC and the fermentation processes

Run Period	MFC	Fermentation	Flow rate, L/h	Produce H_2	Max mmol H_2/min	COD removal conversion/ pass	Power densities, mW/m^2
190h	MFC-1	/	8.2	N	/	0.4	0.23
92h	MFC-2	/	8.2	N	/	0.7	0.74
42h	MFC-3	/	8.2	Y	0.020	1.5	1.42
18h	MFC-4	/	8.2	Y	0.023	1.8	2.25
118h	/	Ferm-1	8.2	Y	0.070	0.7	/
137h	/	Ferm-2	8.2	N	/	0.4	/
42h	/	Ferm-3	13	N	/	0.6	/
19h	/	Ferm-4	10.9	Y	0.023	0.8	/
71h	MFC-5	/	10.9	Y	1.307	0.5	3.42
48h	/	Ferm-5	10.9	Y	2.441	0.5	/
24h	/	Ferm-6	16.3	Y	1.311	0.6	/

Since the COD removal rate was 2.9 % at 2.7 L/h in Section 4.3.3.2, 1.5% at 5.4 L/h in Section 4.3.3.3.3 and average 1.1% at 8.2 L/h, it is clear that the COD removal rate is a function of flow rate that higher flow rates reduced the COD removal rate in MFC process. The COD removal rates were similar at different flow rates in fermentation process. This indicates that COD removal rate in fermentation process independent to the flow rates.

4.3.3.3.2 H_2 production profiles

Figures 4.19 and 4.20 compare the H_2 production with time for the MFC and fermentation tests where H_2 was observed in Table 4.6. All the hydrogen production profiles start from zero, reaches a peak and then decreases again. Figure 4.19 compares the H_2 productions during MFC-3 and MFC-4 versus Ferm-1 and Ferm-4. The overall hydrogen production was low (Table 4. 6). The hydrogen production during the MFC-5 process was 776 mmol. The flow rate in MFC-5 was increased to 10.9 L/h, and a H_2 peak of 1.5 mmol/min was observed, shown in Figure 4.20. After that the H_2 production in Ferm-5 doubled with a peak of 3 mmol/min with a total of 876 mmol was produced. This shows that both the MFC process and fermentation only process have the ability to produce H_2. According to Figures 4.19 and 4.20 the fermentation only process produced more H_2 than MFCs process. This indicates that the use of electrons to produce electricity in MFCs may affect H_2 production from fermentation where some of the electrons from bacteria are transferred to the anode to form current rather than being used to reduce the substrate to form H_2 and secondary substrates.

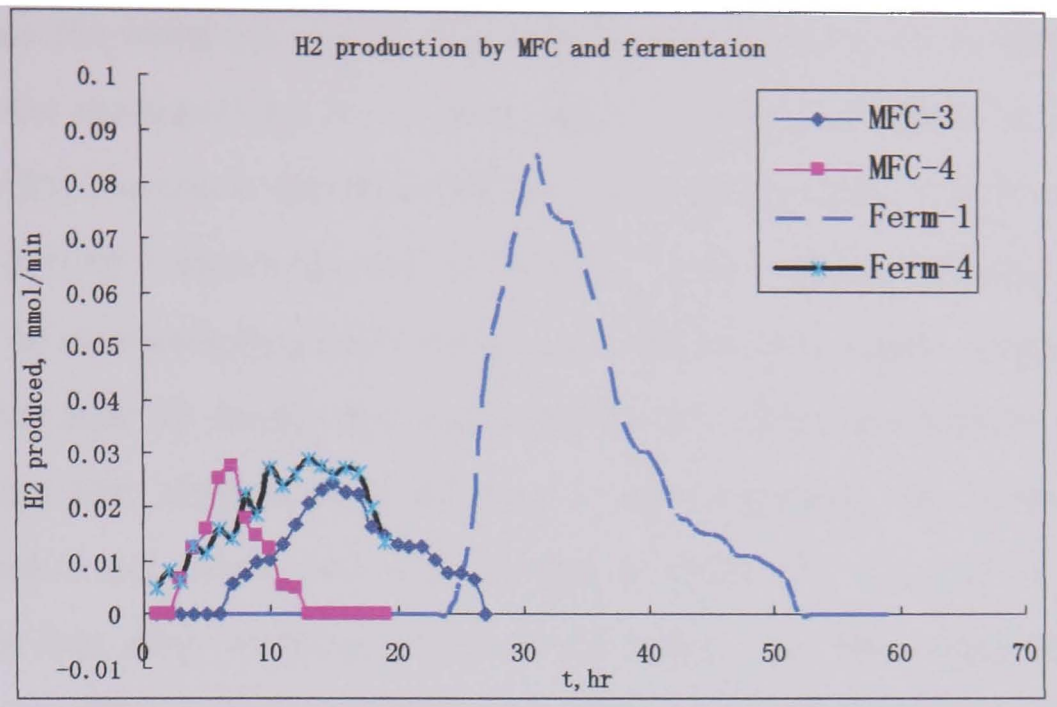

Figure 4.19 H_2 productions by MFC and Fermentation processes

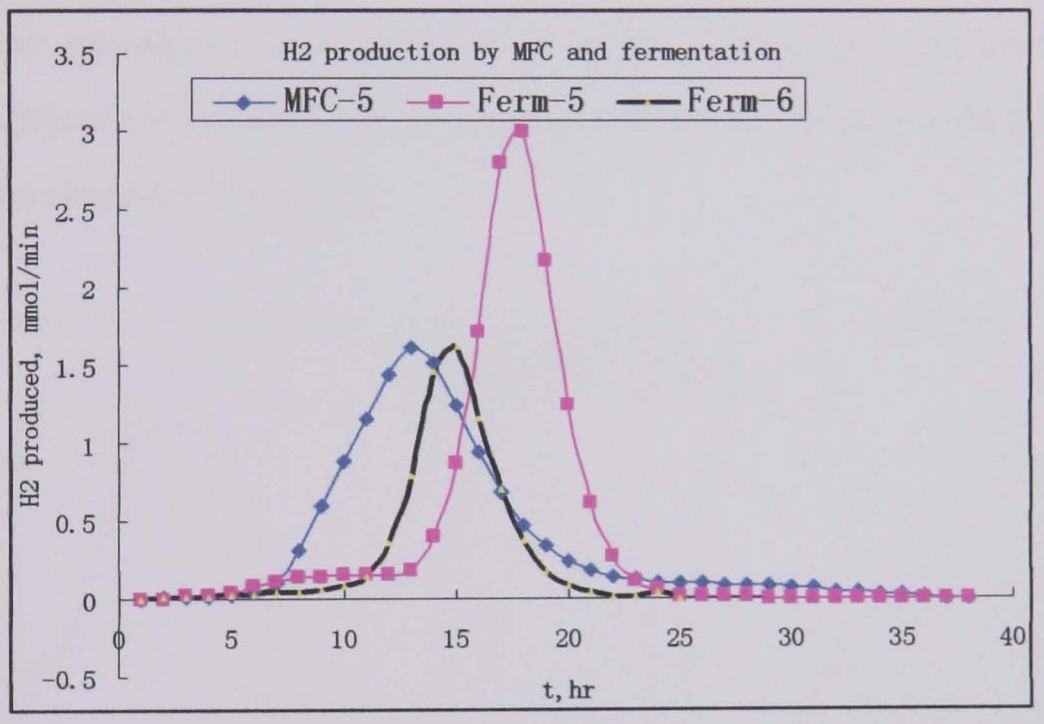

Figure 4.20 H_2 productions by MFC and Fermentation processes 2

4.3.3.3.3 H_2 production versus power generation

Another experiment was carried out to compare the changes in power densities with hydrogen production over time under anaerobic condition. A flow rate of 5.4 L/h was used and the initial COD was 1900 mg/L obtained adding 1 g/L of sucrose. The COD was reduced to 440 mg/l after 48 h run and about 96 passes were conducted with an average COD reduction of 1.5 %. After incubation at batch

conditions the initial cell voltage was 0.29 V when starting the continuous MFC experiment corresponding to an initial power density of 7 mW/m^2 as shown in Figure 4.21. The power density increased rapidly when adding sucrose with a cell voltage of 0.40 V after 8 hours to 13.3 mW/m^2. After reaching this peak in power density, an increasing H_2 production was observed and rose rapidly to a peak of 0.6 mmol/min after 23 hours. This was followed by a sharp decrease in hydrogen production that stopped after 40 hours. Correspondingly, the power density decreased to 4-5 mW/m^2 with a cell voltage of about 0.17 V to 0.23 V. The data indicated that after reaching a certain cell voltage the MFC might support H_2 production under anaerobic conditions. It shows that electrons were transferred to substrate in anode as the process of fermentation instead of transferred to anode for current generation after the peak of power production. This indicates the bacteria degrade very soon after the peak of electron transportation which may due to the mass transfer limitations.

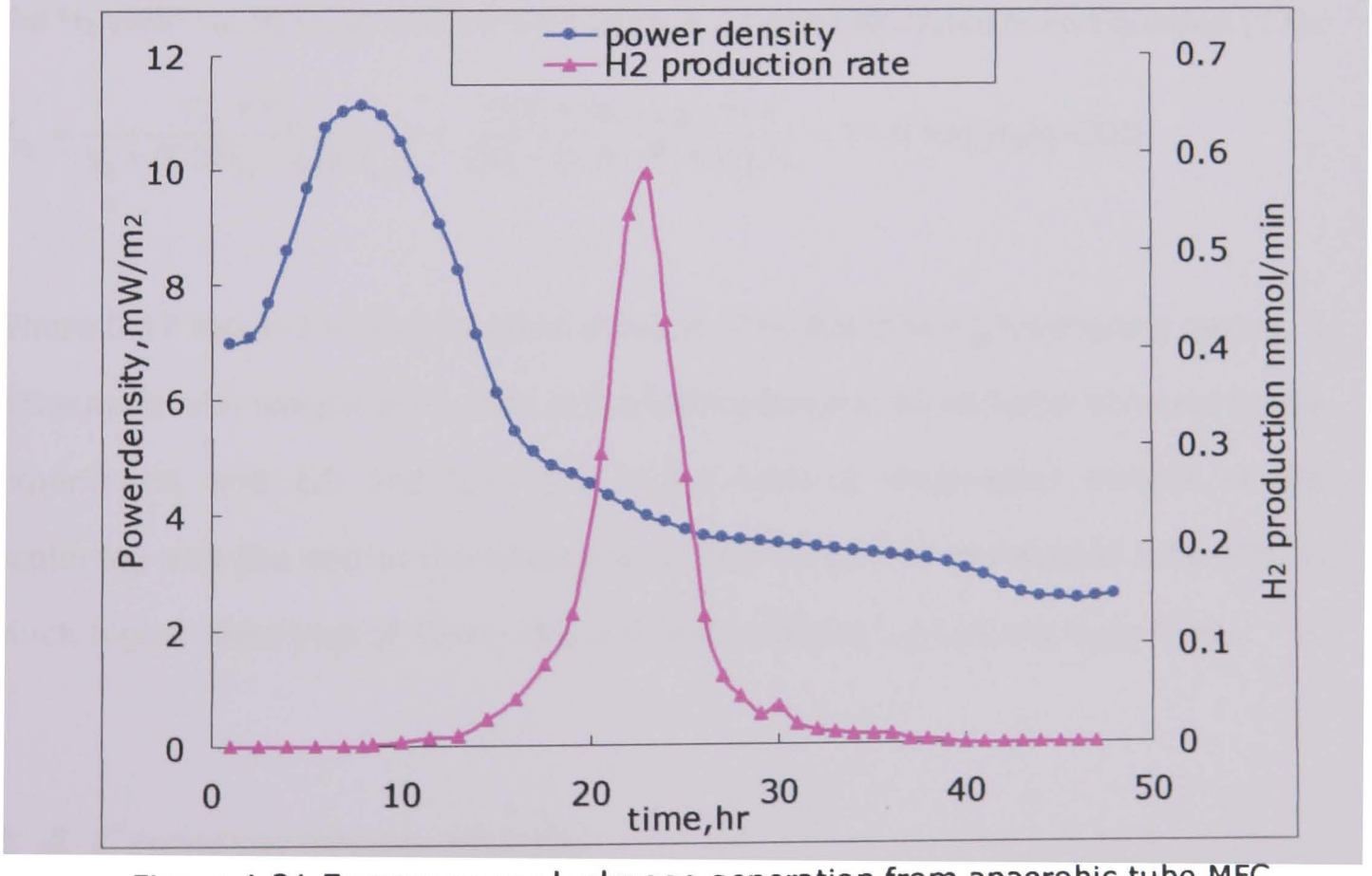

Figure 4.21 Energy versus hydrogen generation from anaerobic tube MFC

4.3.3.3.4 H_2 recovery rate from substrate and H_2 yield

Figure 4.21 from Section 4.3.3.3.3 shows that the H_2 production peaked at 0.6 mmol/min after 8 h. For the 32 h of H_2 actual production, the accumulated H_2 production from 7h to 39 h sample points per hour can be calculated from the integral of the hydrogen curve in Figure 4.21 which is 0.17 mol. The total COD removal based on the MFC running period was 1460 mg/L * 20 L = 29.2 g. Since the energy contained in the COD removal (9.5 kJ/g COD) was the same as the energy contained in the consumed substrate (16.7 kJ/g sucrose), 1 g COD is equivalents to 0.6 g sucrose. Thus 29.2 g COD removal is equivalents to 17.5 g sucrose, corresponding to 0.051 mol sucrose. The theoretical H_2 production of 1.23 mol can be calculated based on Equation (13). So the overall H_2 recovery rate from substrate is 0.17 mol/ 1.23 mol = 13.8 %

The H_2 yield Y_{H2} (g H_2/g-COD) from Figure 4.22 was calculated from Equation (17):

$$Y_{H_2} = \frac{n_{H_2} \times M_{H_2}}{V_e \times (COD_{in} - COD_{out})} = \frac{0.17mol \times 2g/mol}{20L \times (1.9 - 0.44)g/L} = 11.6 \text{ mg } H_2\text{/g-COD}$$

Where 0.17 mol is the accumulated amount of H_2 over the 32 h sampling period, 2 is the molecular weight of H_2, 20 L is the total volume of wastewater involved in this experiment, and 1.9 and 0.44 g/L is the COD of wastewater sample at the beginning and the end of the experiment. The H_2 yield in Hexagonal tube MFC is much higher than that of Micro-channel MFC which is 0.0115 mg H_2/g-COD.

4.4 Comparative study

Based on the performance and experiment data for the Micro channel MFC, the stacked MFC and the hexagonal tube MFC, it has been shown that all three MFC designs are capable of generating electricity, produce hydrogen and remove organic matter. However, their MFC performances are quite different, and can be

related to differences in their structure, electrode material and other environmental and experimental conditions. It is necessary to compare their performances in these areas to find the advantages and disadvantages of each design and identify an optimum structure for further MFC designs.

4.4.1 Power production

Table 4.8 compares the three individual polarization curves were obtained for each MFC design from Figure 4.5, 4.10 and 4.15 in this chapter. The polarization curves for the Micro MFC and the hexagonal Tube MFC were found from a partial voltage range with an external variable resistor box changing the resistance from 30 Ω to 5000 Ω. The polarization curve of the stacked MFC was established using a potentiostat, which can observe the integrated plot from OCP to the maximum current density of the system. In these three MFCs, the power and current densities units were unified to present based on the anode surface areas. The maximum power density produced in each MFC with their corresponding cell voltages and current densities are compared in Table 4.8 as well.

Table 4.8 Power densities performance for the three MFCs

MFCs	Max PD, mW/m^2	CD, mA/m^2	Cell voltage, V	Optimal R, Ω	Internal R, Ω
Micro-	29.5	73.6	0.4	2050	1805
Stacked-	24.6	81.3	0.32	30	22.8
Tube-	13.3	33.3	0.4	100	77

During the polarization curve tests, the MFCs systems might undergo the bacteria incubation period such as the data of Micro MFC. But later on the actual experiment running, the maximum power density of Micro MFC can arrived to 29.5 mW/m^2. For the anaerobic tube MFC test, the actual experiment produced the maximum power density of 13.3 mW/m^2.

4.4.2 Coulombic efficiency

The coulombic efficiency is related to the rate at which substrate is consumed by bacteria and the transfer of electrons and protons in the MFC to produce electricity. With increasing coulombic efficiency, a higher portion of consumed substrates can be used for electricity production. Lower coulombic efficiency means little consumed substrate is used for electricity production and most of it is used for bacteria metabolism. This indicates that the amount of wastewater in relation to the available anode may be a crucial factor governing MFC. Table 4.9 compares several designs of MFCs with their coulombic efficiency data on an anode versus volume basis. An interesting relationship was found between the coulombic efficiency and the MFC anode surface area per volume unit of wastewater in the anode chamber.

Table 4.9 The relationship of anode (cm^2/ml) and the coulombic efficiency

MFCs	Anode surface, cm^2	Anode volume, mL	cm^2/ml	X axis: Log_{10} (cm^2/ml)	Coulombic Efficiency%	Y axis: Log_{10}(CE)
Two-chamber*	14	500	0.03	-1.553	0.001	-3
Micro	26.5	13.3	1.99	0.299	0.7	-0.16
Tube	1400	2700	0.52	-0.285	1.9	0.28
Stacked	1300	73	17.81	1.251	6.9	0.84
Optimized**	/	/	109.3	2.04	100	2

*: the coulombic efficiency data was collected from two-chamber MFC designation for anode and cathode treatment in Chapter 5

**: theoretical maximum calculation not experimental

Figure 4.22 shows the log-log relationship of anode surface area over the volume of anode chamber and their coulombic efficiencies. From the trend line, the point of optimal anode surface and anode volume ratio can be calculated as 109.3 when the assumed coulombic efficiency was 100%. This means if the anode surface area and anode volume ratio can be achieved at 109.3 cm^2/ml, the probably coulombic efficiency might be achieved at a very high percentage. Since MFC is a complicated

reactor with the assistant of bacteria as catalyst, the anode design ratio can not be seem as the only the definitive reason to improve coulombic efficiency, but structure, conditions and bacteria species, also play a role. However, Figure 4.22 indicates that the anode configuration probably is the key to advance the MFC design configuration to help with the crucial performance factors in MFCs.

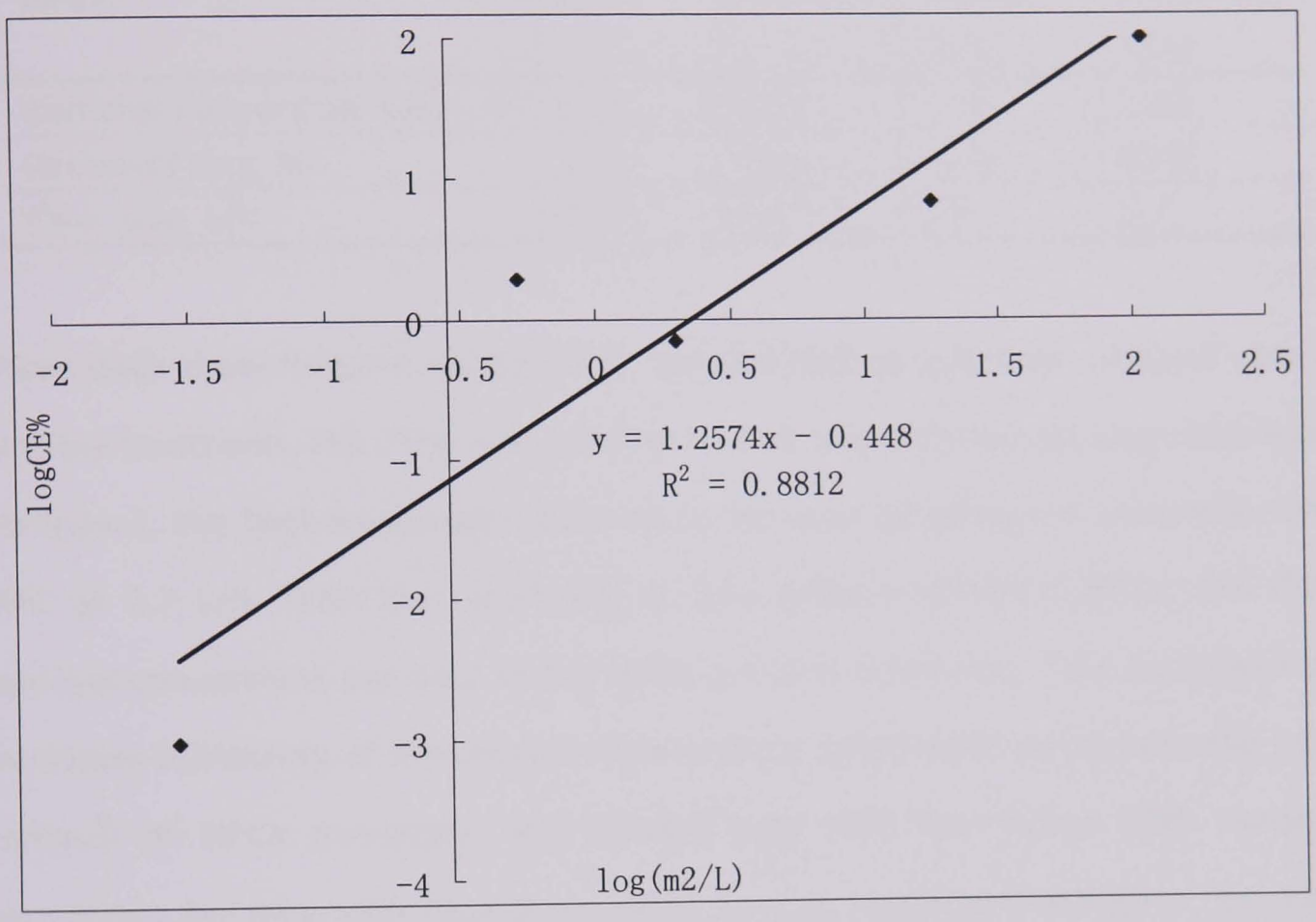

Figure 4.22 Log CE% as a function of the log (m^2/l)

4.4.3 COD or substrate removal

Table 4.10 shows the wastewater removal in each types of MFC from Sections 4.2 and 4.3. The flow rate for each continuous MFC were cited from their best results during experiments and showed in table 4.10 as well. The average COD removal rate in the Micro-channel MFC in a single day can be calculated as around 25.1 % and the average removal conversion per run was 0.14 %. For the stacked MFC, the removal conversion in a single pass of wastewater in the anodic chamber can be calculated as 0.33% in the anodic chamber per day. Similar calculations were obtained for the tube MFC under aerobic condition and anaerobic condition. The

removal conversion for aerobic MFC in a single pass was 1.3 %, so around 46.6 % in a single day of removal. In anaerobic MFC, the average COD removal conversion in a single pass was 2.9 % for a single run, and the average COD reduced in a single day was around 49.6 %.

Table 4.10 COD or substrate removal in three continuous MFCs and their flow rates

MFCs	Micro-	Stacked-	Aerobic Tube-	Anaerobic Tube-
Removal conversion/ pass, %	0.14	0.33	1.30	2.90
Removal/ day, %	25.1	78.1	46.6	49.6
Flow rate, L/h	0.12	1.4	5.4	2.7

These data show that the stacked MFC had the highest substrate removal rate in one day treatment. But if the removal rate in each run of the anodic chambers were compared, the best wastewater treatment rate was by using the anaerobic tube MFC at 2.7 L/h. With the increasing of flow rates in different MFCs, the COD removal conversions per pass of the MFCs are also increasing. This indicates that moderate increasing of the influent flow rates at small scale might help the COD removal of MFCs processes. But aerobic tube MFC had lower COD removal conversion per pass with high flow rate of 5.4 L/h indicates that higher flow rate prevent the sufficient MFC process to remove COD contents in substrate.

4.4.4 H_2 production

In micro channel MFC, it was proved that some hydrogen was produced from the system. The observed H_2 concentration was 21 ppm by Micro GC with an average H_2 production rate of 0.02 % and a H_2 yield of 0.0115 mg/g COD.

In the anaerobic Tube MFC, a production peak of H_2 can be observed in the Figure 4.21 presented the peak of H_2 in related to the electricity generation. Around 0.17 mol of H_2 were produced during the accumulated 40 h. The maximum production

rate of H_2 can arrive to 0.6 mmol/min (36mmol /h) at the peak point which is much higher than that of the micro channel MFC. This indicates that hexagonal tube MFC has higher hydrogen production rate with higher running flow rate and higher COD removal rate. The H_2 recovery rate at this maximum value can be calculated was 13.8 % and the H_2 yield was 11.6 mg/g COD. Power production during MFC process might impact on the H_2 production. Compared with fermentation process in Table 4.7, MFC process producing smaller amount of H_2 demonstrated a competition between power production and H_2 production. H_2 peaked after power in Figure 4.21 showed that power production was dominated at first and H_2 production take over to reach another peak. Then both decreased to low level due to mass transfer limitation.

4.5 Design configuration

The comparison of MFCs performance in Section 4.4 can be used to assess the different design configuration, in terms of electrode performance, external conditions and design factors.

4.5.1 Electrode performance

Table 4.11 Electrode materials used in three MFCs

MFCs	Micro MFC		Stacked MFC		Tube MFC	
PD, mW/m^2	29.5		24.6		13.3	
Electrodes	Anode	Cathode	Anode	Cathode	Anode	Cathode
Materials	Cloth	woven web	granules	woven web	Cloth	woven web
Composition	Carbon	Pt, Carbon	Graphite	Pt, Carbon	Carbon	Pt, Carbon
Surface area, cm^2	26.5	26.5	1300	60	1400	1000
A&C Distance	0.5 cm		0.05 - 1.5 cm		2.7-6.5 cm	

Table 4.11 shows the different electrode materials used in three types of MFCs. Both anode materials used in Micro MFC and Tube MFC were the same carbon cloth while graphite granules were used in the stacked MFC. From the power densities produced, it appears that the carbon cloth and graphite had similar properties in terms of electrons transfer and facilitating bacteria growth on their surfaces.

For cathode materials, all three MFCs were used the same carbon cloth containing 5 g/m^2 of Pt. In the stacked MFC, the graphite granules were also used in cathode chamber to act as conducting material which might have assisted the MFC performance. Pt is a good catalyst to help the electrons, protons and oxygen to form water or even to form hydrogen gas.

The effective surface areas for anode and cathode in Micro MFC and Tube MFC were similar, but in stacked MFC, due to the high surface area of the granules, the cathode surface area were much smaller than the anode surface area. It seems from stacked MFC that the cathode surface area may not necessary be of similar size to the anode surface area. Smaller cathode area can reduce capital costs of the whole MFC construction, while the power production can be comparable to that of MFCs that have similar anode and cathode surface areas.

Table 4.11 shows the power density of MFCs was increased with the decreasing of anode and cathode distance. This indicates that minimising the anode and cathode distance will help the protons transfer from anode to cathode and then improving the power density. The stacked MFC that has the application of CEM membrane to separate the anode and cathode chamber did not help the power density of MFCs. This shows that the application of CEM membrane is not necessary and effective.

4.5.2 External conditions

The external conditions of MFCs include flow rates, buffer medium, inoculums of bacteria and substrates used as the "food" for bacteria. Table 4.12 lists these parameters for the different MFCs studied.

Table 4.12 External conditions for three MFCs

MFCs conditions	Micro MFC	Stacked MFC	Tube MFC
PD, mW/m2	29.5	24.6	13.3
Flow rate, L/h	0.12	1.4	5.4
Buffer Medium	Wastewater(Ww.)	Phosphates *	Ww.
Inoculum	Ww. & active sludge(AS)	Anaerobic Sludge	Ww. & AS.
Bacteria	Mixed	Mixed	Mixed
Substrate	Acetate	Acetate	Sucrose

* The detailed buffer solution composition was described in Chapter 3.

The flow rates of these three MFCs ranged from 0.12 L/h to 5.4 L/h. For the medium solution, both micro channel MFC and Tube MFC were using actual wastewater which means no buffer solution was used in the system. Stacked MFC used potassium phosphates and some other trace elements to support the metabolism of bacteria as buffer and culture medium. This indicates that buffer solution might not be best way forward for MFCs.

The inoculum sources for MFCs were from active sludge and wastewater collected from the water treatment company when the channel and tube MFCs were using the same inoculum. For the stacked MFC, the bacteria had experienced a very long incubation period and the MFC was run for weeks to obtain very consistent and stable power production as the substrate was continuously fed. All bacteria used were mixed species which is more advantages than the applications of single species. This indicates that active sludge is a flexible inoculum to be used for MFCs.

The substrate used in Micro MFC and Stacked MFC were acetate that had no

secondary organic matters for further oxidation showed in Equation (11). Sucrose was used in Tube MFC that degradable for secondary or further products and can be oxidized and used as substrate for bacteria as well. The high substrate removal for both acetate and sucrose in Table 4.12 indicates that active sludge inoculum can work actively with a range of substrates and secondary substrates.

4.5.3 Design factors

In Table 4.13, the power densities and COD removal rate per pass were calculated based on the effective anode compartment volume of the MFCs. The Tube MFC had the highest COD removal rate based on the effective volume. The stacked MFC had the highest power density of 11.6 W/m^3 while the tube MFC had power density of 0.6 W/m^3. However, it needed 9 times as much anode material to produce 19 times the amount of power density. For the cathode surface and volume ratio, the stacked MFC had the lowest value which means it had the smallest amount of cathode materials among three MFCs. Based on these factors, stacked MFC seems to be the optimal option for MFC construction in a compact mode with lowest cost.

Table 4.13 Effective factors in three MFCs

MFCs	Micro-channel	Stacked	Hexagonal-tube
Effective volume(EV),m^3	$13.3*10^{-6}$	$2.8*10^{-4}$	$2.7*10^{-3}$
COD reduction per pass,%	0.14	0.33	2.9
PD/EV, W/m^3	5.9	11.6	0.59
Anode/EV, m^2/m^3	199.3	471.0	51.9
Cathode/EV, m^2/m^3	199.3	21.7	37.0
Chambers	Single	Double	Singe
Membrane	N/A	CEM*	N/A

*: Cation exchange membranes

4.6 Summary of major findings

In summary, three different designs of MFCs were introduced in Chapter 4. The

power productions, coulombic efficiencies, COD removal rates and H_2 productions were found for each MFC design and a comparative study was carried out. A summary of the major findings in this chapter is given below.

The combined polarization curves and power density based on the data logger show that, micro-channel MFC has the maximum power density of 29.5 mW/m^2, stacked MFC has the maximum power density of 24.6 mW/m^2 while the anaerobic hexagonal tube MFC has the maximum power density of 13.3 mW/m^2. Based on the coulombic efficiency data of these MFCs, a log-log relationship of anode surface area over the volume of anode chamber and their coulombic efficiencies can be summarized. A derived data 109.3 cm^2/ml of anode surface area and anode volume ratio can be achieved from Figure 4.24, which indicates the probably very high value of coulombic efficiency might be obtained. It shows that the anode configuration probably is the key to advance the MFC design configuration to help with the crucial performance factors in MFCs. The COD removal rates per pass in these MFCs were typically between 0.14 to 2.9 % with high COD loadings. The H_2 produced was derived from both fermentation and from the MFC process and MFC process do affect the H_2 produciton.

For the electrode configuration, it is concluded that by decreasing the cathode/anode ratio can still yield power density comparable to that of MFC with similar anode and cathode surface areas. This can clearly reduce the capital costs. It was also found that minimising the distance between the anode and the cathode will improve power production. Since the three MFCs differed in structural design, inoculum used, medium applied and flow rates are very different, it is difficult to individually compare these factors with the final power production from them. However, for further industrial application, the Tube MFC showed the best promise due to its high treatment flow rate, high throughput, relatively high electricity and hydrogen production and low capital and operating costs though more efforts are needed to the designs especially for the effective factors.

Chapter 5 Electrode materials

Anode and cathode materials treatments are of great concern towards improving the power production of MFCs. Treatments suggested in the literature in Section 2.3.3 involve increased surface charge on the anode surface, incorporated mediator components onto anode or cathode electrodes, or applied electrocatalytic active catalysts on the electrode materials. In this chapter, several simplified anode and cathode materials treatment procedures are introduced and the applied experimental results are discussed.

5.1 Characteristics of materials

5.1.1 SEM

Two types of plain carbon cloth with designation B and designation D without wet proofing were used as anode materials and an LT 120E-W Low Temperature ELAT® Gas Diffusion Electrodes microporous layer including 2.5 g/m^2 Pt electrode on woven web was used as cathode material on most MFCs (Section 3.2.2). Figure 5.1 shows the SEM images with 100 times magnification of the two anode materials. It is clear that both anode materials were composed of carbon fibres where the weaving method differs. B shows a traditional textile crossing pattern while D has a plaited pattern.

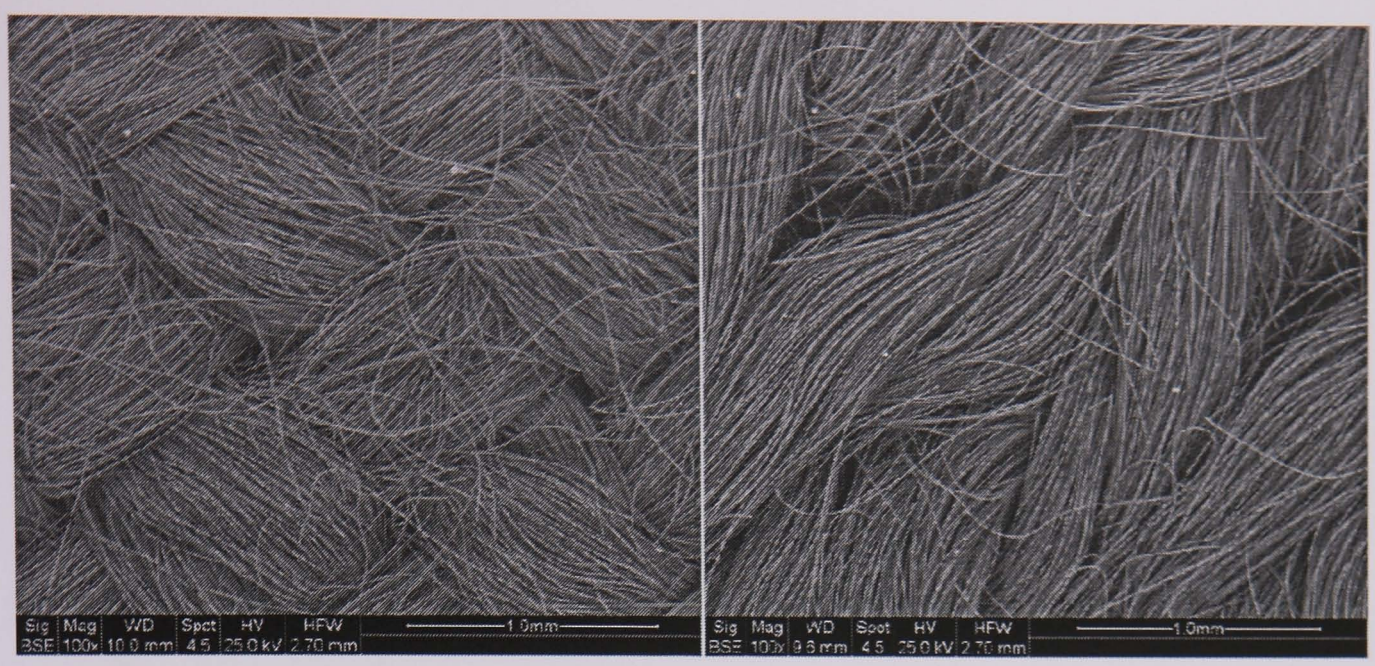

Figure 5.1 SEM images of plain carbon cloth B (left) & D (right)

Figures 5.2 and 5.3 show the SEM EDAX spectra of these two anode materials. Both materials have a main carbon peak, which indicates that both materials have very high carbon contents. The shoulder to the right of the main peak has not been resolved but might be that of terminal carbon as the carbon. The large hump from 1-7 keV has not been resolved either but might be due to EDAX background noise.

Figure 5.2 SEM EDAX spectrum of plain carbon cloth B

Figure 5.3 SEM EDAX spectrum of plain carbon cloth D

Figure 5.4 shows the SEM image of the cathode material at 3000 times magnification (left) and 31000 times magnification (right). The image shows materials deposited on the carbon fibres and the structure is not as simple as the plain anode material in Figure 5.1. The material safety data sheet from the supplier indicated that the material comprised of (Ⅰ) carbon cloth, (Ⅱ) carbon black, (Ⅲ) polytetrafluoroethylene (PTFE) and (Ⅳ) Pt. Figure 5.4 indicates that the Pt has been deposited on the carbon black and PTFE has been used to attach the carbon black on the fibre surface. The EDAX spectrum in Figure 5.5 shows the surface composition of the cathode material. It is clear that the composition of the cathode material is much more complex than that of the anode material.

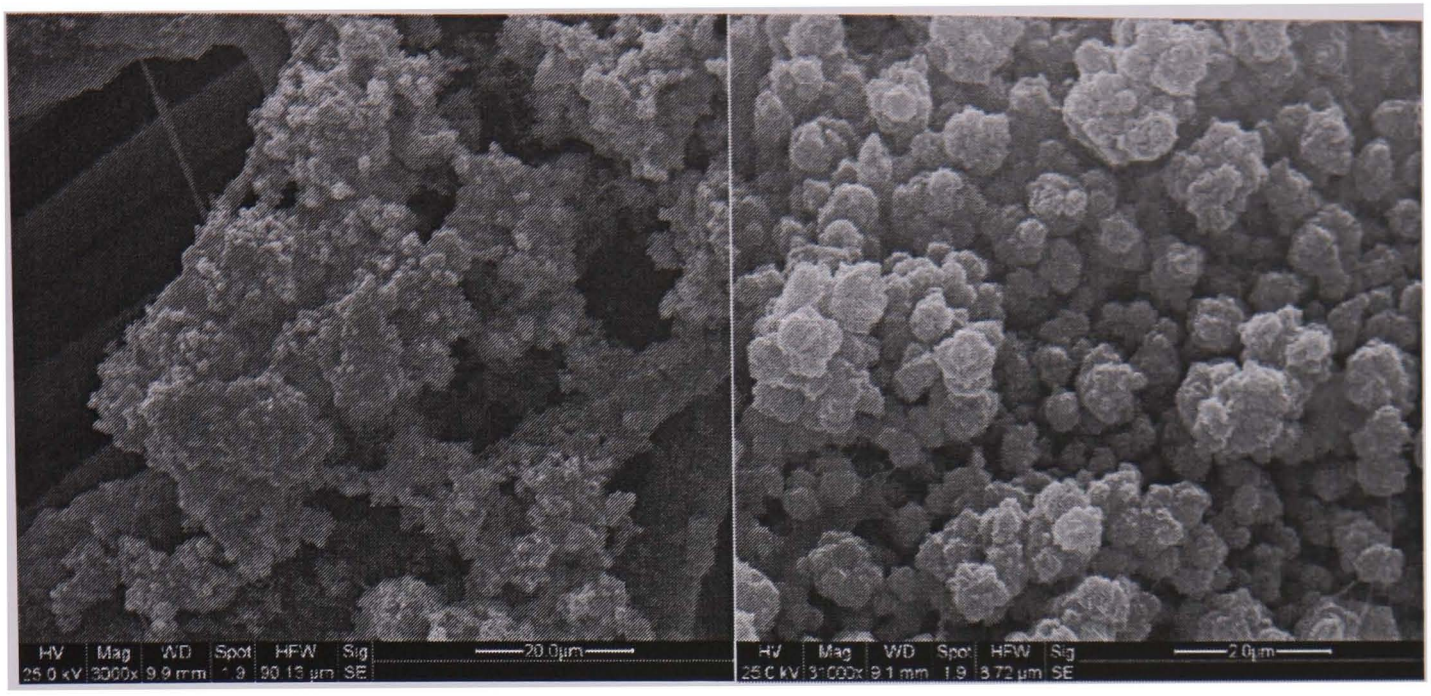

Figure 5.4 SEM images of woven web with 2.5 g/m^2 Pt at magnifications 3000 times meg. (left) and 31000 times meg. (right)

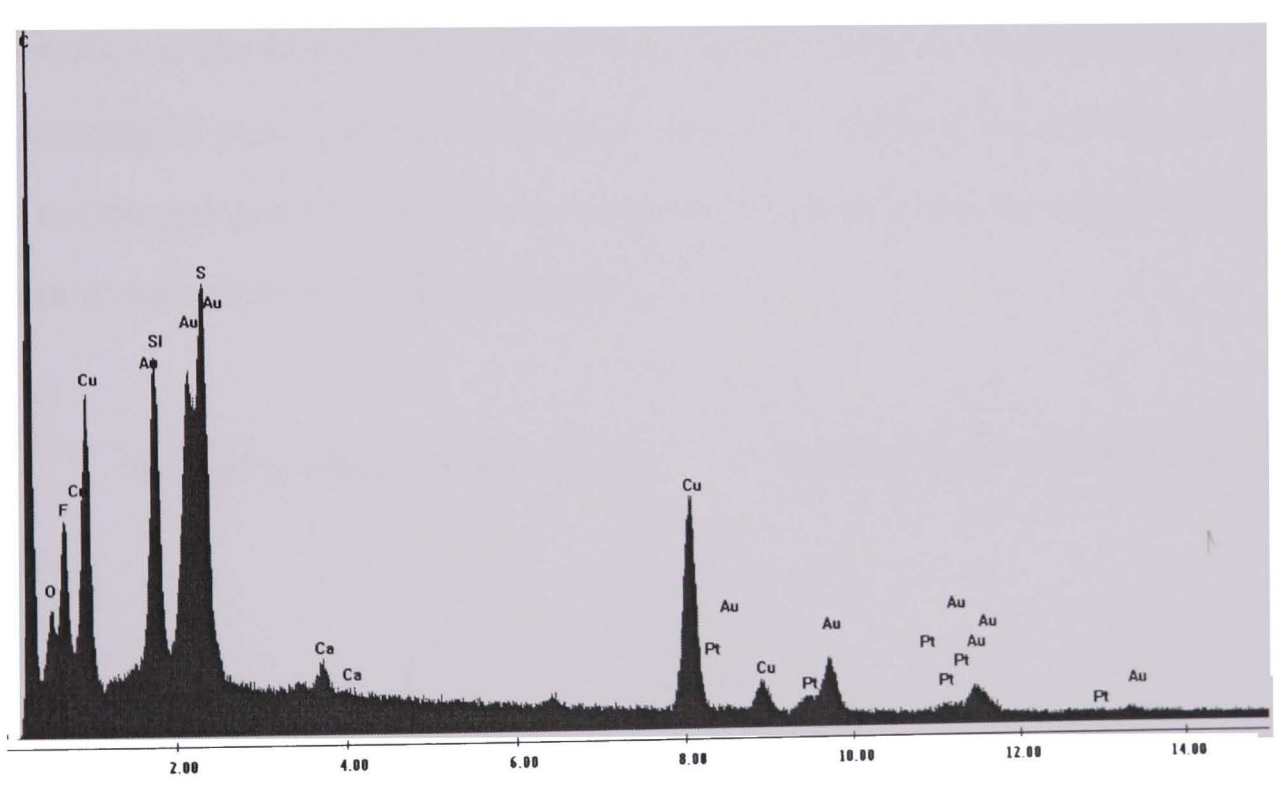

Figure 5.5 SEM EDAX spectrum of woven web with 5g/m^2 Pt

5.1.2 Textural property measurements

The textural property measurements based on Brunauer Emmett Teller (BET) theory were used to determine the surface area, pore volume and pore size

distributions of the anode materials. The surface area of the plain B and D materials were 2.67 m^2/g and 2.47 m^2/g, respectively. Figure 5.6 shows the nitrogen adsorption curve for the B and D anode materials. Both materials had very little uptake at relative pressure less than 0.1 indicating low volume of micropores. At relative pressure between 0.1 to 0.9, there is evidence of some mesopore volume with pore size between 2 nm-50 nm. There is a great increase at relative pressure from 0.9 to 0.995 indicating that macropores larger than 50 nm are measured. Since the bacteria sizes are around 1000-5000 nm in size, the macropore volume highlights the possible area for bacteria to stay and grow within. From Figure 5.6, the macropore volume of plain B material was roughly calculated as 0.66 cm^3/g, while the macropore volume of plain D material was 2.27 cm^3/g. The larger macropore volume of plain D material indicates that when it is used as anode material it might allow greater bacteria growth which could help the power performance of the MFC. Regarding to the shapes of sorption-desorption curve are open instead of overlapping, it indicated that the shape of the mesopore shape might not be straight forward, i.e. during the desorption process, some N_2 gas was trapped in mesopore without desorption.

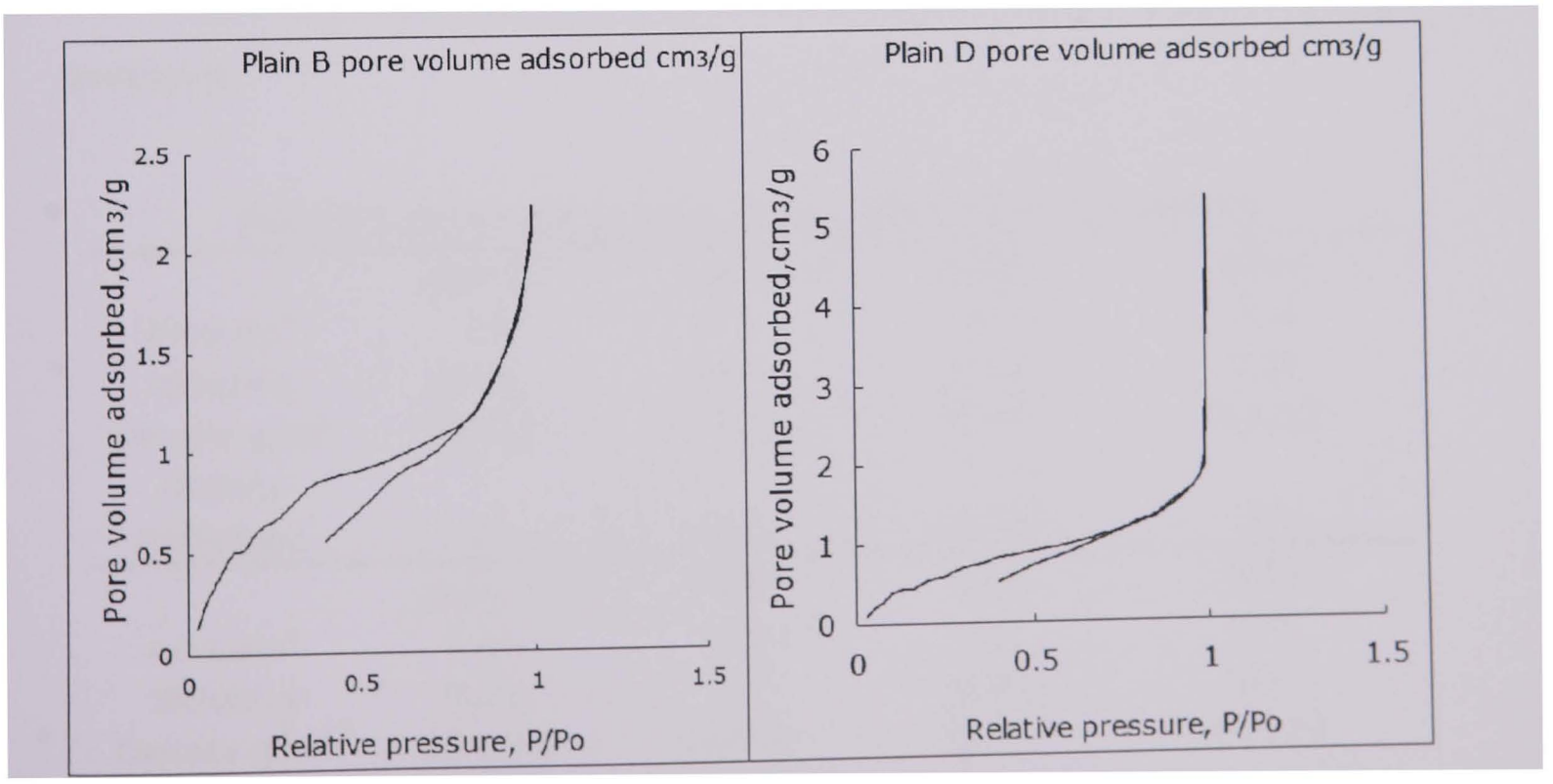

Figure 5.6 Nitrogen adsorption curve of plain B and D anode materials

5.2 Physical treatment of anode materials

This section compares the effect of physical treatment of the anode material towards the MFCs power production. The main driving force for this investigation is outlined in Chapter 4.4.2, where the amount of influent in relation to the effective anode material was shown to be a crucial factor towards improving the performance of MFCs.

5.2.1 Experimental methods

Two plain anode materials B and D were treated with CO_2 gas at flow rate 0.1 L/min in a tube furnace at 5 different temperatures 400°C, 500°C, 600°C, 700°C, 800°C for 2 h each generating a series of 10 samples. The reason of using CO_2 is that at high furnace temperature, CO_2 works as a mild oxidant that may modify some part of the carbon surface. Uneven carbon surface might help bacteria to stay and adhere to the surface. Addition of oxygen functionalities may also help to increase the power production during MFC application. Table 5.1 shows the burn off data for the materials where most of the material densities decreased after the physical treatment.

Table 5.1 Material density decreases after physical treatment

	plain B	600B	700B	800B
Area cm^2	7.9	7.7	8.6	10.5
Weight g	0.19	0.17	0.17	0.22
Density g/m^2	236.49	225.58	199.42	208.19
Density decreased	/	4.6%	15.7%	12%
	plain D	600D	700D	800D
Area cm^2	7.15	9.75	8.4	7.8
Weight g	0.21	0.29	0.24	0.25
Density g/m^2	297.34	293.54	283.69	318.33
Density decreased	/	1.3%	4.6%	7.1%(increased)

Several MFC designs were described in detail in Chapter 4. All of their applied anode materials were plain carbon or graphite materials. The power generation performance and corresponding anode materials in the three MFCs were shown in Table 4.12. Due to the amount of anode material used in these designs, it was not feasible to test the treated anode material in these MFCs. In order to focus on the anode treatment and the competitive results before and after treatments, a simplified MFC reactor was built. It was a two-chamber MFC consisting of a anode chamber and a cathode chamber with 500 ml space before MFC fittings, respectively. A "n" shape tube was connected between two chambers for proton transfer. Two series of experiments, using (i) a multiple and (ii) a single anode system were set up to check the data validity.

In the multiple anodes MFC, a little star-rack was assembled to fix eight separated small pieces of different treated anode materials with surface areas in the range of 6-13 cm*1.1cm. A single piece of cathode material (9 cm*1.2 cm) containing 2.5 g/m^2 Pt was fixed in the centre of the cathode chamber. Actual domestic wastewater was used in the system at a flow rate of 30 ml/min. The COD level of wastewater was initially around 1000 ppm for each experiment. In the single anode setting, instead of eight separated anodes in one MFC, single piece of anode and cathode material were allocated in each anode and cathode chamber, respectively. The individual cathode material contained 2.5 g/m^2 Pt with a dimension of 7.2 cm*1.2 cm. Eight separated MFCs were observed. These systems were tested at recycle loop and the COD level of the wastewater was maintained at around 1000 ppm. A Pico data logger with 8 channels was connected to record the individual cell voltage data. A potentiostat was used to test the polarization curves of each MFC at a scan rate of 1 mV/s. The OCP of the systems, the anode and cathode potentials were tested as well.

5.2.2 MFC performance

5.2.2.1 Performance based on the star rack anode setting

The experiments were run continuously for 7 days where the cell voltage data was recorded and the level of produced cell voltages of each treated materials were compared. The external resistors were all fixed at 10 kΩ. The average cell voltages were calculated during these 7 days and the power densities based on average cell voltages was used to compare the materials. The impact of the treatments on the MFC performances are shown in Figures 5.7 and 5.8 comparing cell voltage data of the treated B materials and D materials in a certain period, respectively. The trends of cell voltages based on different treated anode materials are similar with their power densities due to the same external resistance and the similar effective surface areas of these materials.

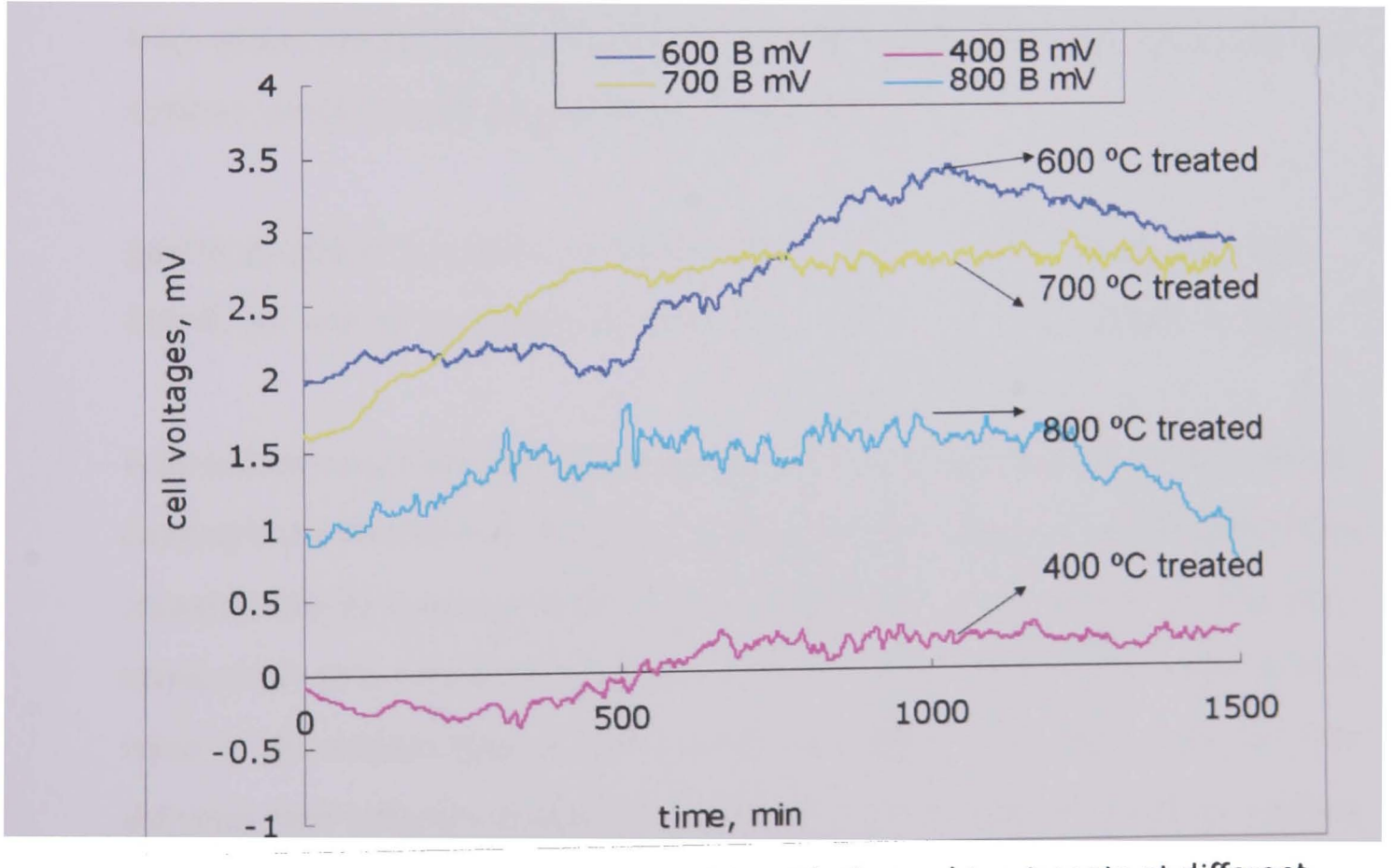

Figure 5.7 Cell voltages of B materials with thermal treatments at different temperatures with star rack anode setting

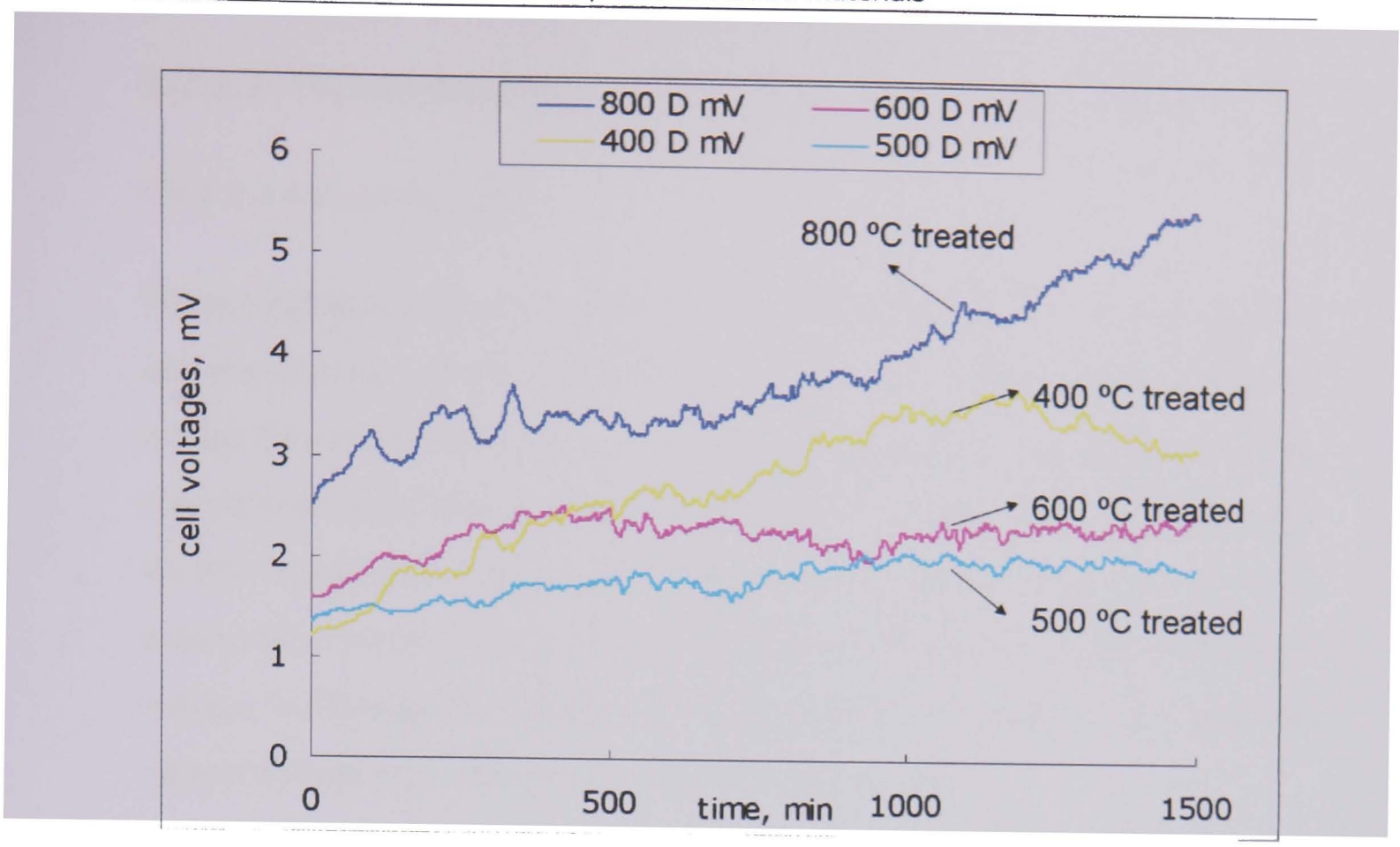

Figure 5.8 Cell voltages of D materials with thermal treatments at different temperatures with star rack anode setting

From these continuous experiments, an average order based on the output PD with different treated anode materials was established as:

600 °C B>700 °C B> 800 °C B >400 °C B Equation (27)

800 °C D> 400 °C D> 600 °C D>500 °C D Equation (28)

Both orders show that treatment under CO_2 gas changed the power output results. Generally the treated material D had a better power generation performance than treated material B according to the cell voltage data in Figures 5.7 and 5.8. Also, some of the data periods indicated the chaos of the electron acceptors and donors issue in the system due to some anode cell voltage data were negative. This indicates that different anodes may play the role of electron acceptors to gain electrons released from other anodes in a multiple anode setting. A separated anode setting in 5.2.2.2 provided a comparison to further evaluate physical treatments of anode materials.

5.2.2.2. Performance based on the separated anodes setting

5.2.2.2.1 Cell voltage data

The cell voltage data were collected from the data logger for 1 data/min for 90 h and the external resistors were all 10 kΩ. Figures 5.9 and 5.10 show the cell voltage data of treated B and D materials using separated anode chambers. Due to only eight available channels was available on the data logger, only the 600 °C, 700 °C, 800 °C treated and plain B and D materials were observed. From the trends of each curve in Figure 5.9, the B material treated at 600°C displayed the highest cell voltage, confirming the similar order established from Equation (24) and the highest voltage was with 600 °C treated B material.

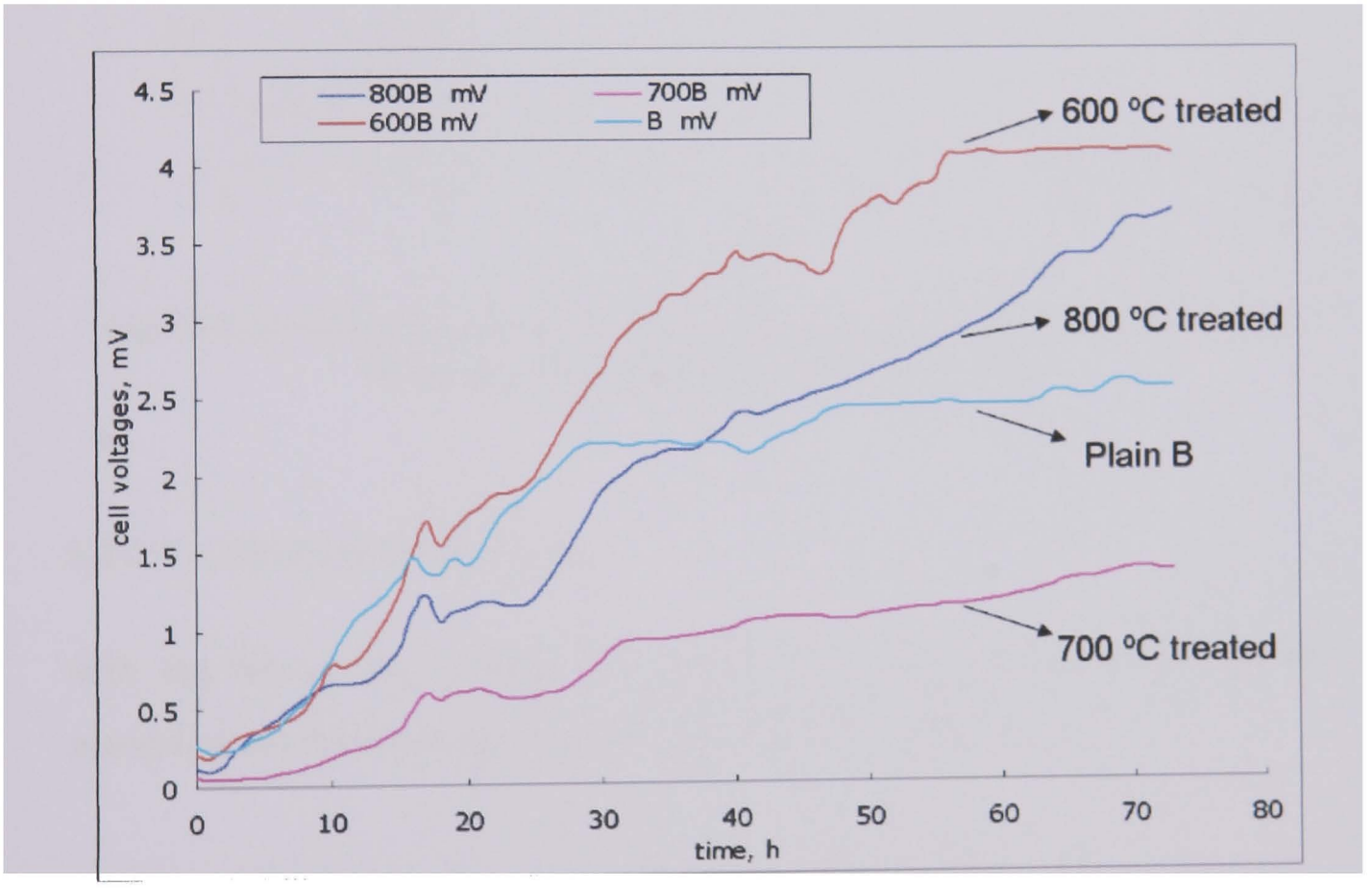

Figure 5.9 Cell voltages of B materials with thermal treatments at different temperatures with separated anode setting

Based on the trends of the curves of the treated D materials in Figure 5.10, the 800°C treated D materials displayed the highest power densities, confirming the observations from Figure 5.8. The plain D showed the lowest cell voltage. The data

confirms the similar order shown in Equation (25). The material treated at 400°C shows similar behaviour to 700°C indicating that there is some degree of surface modification has advantages for MFC process.

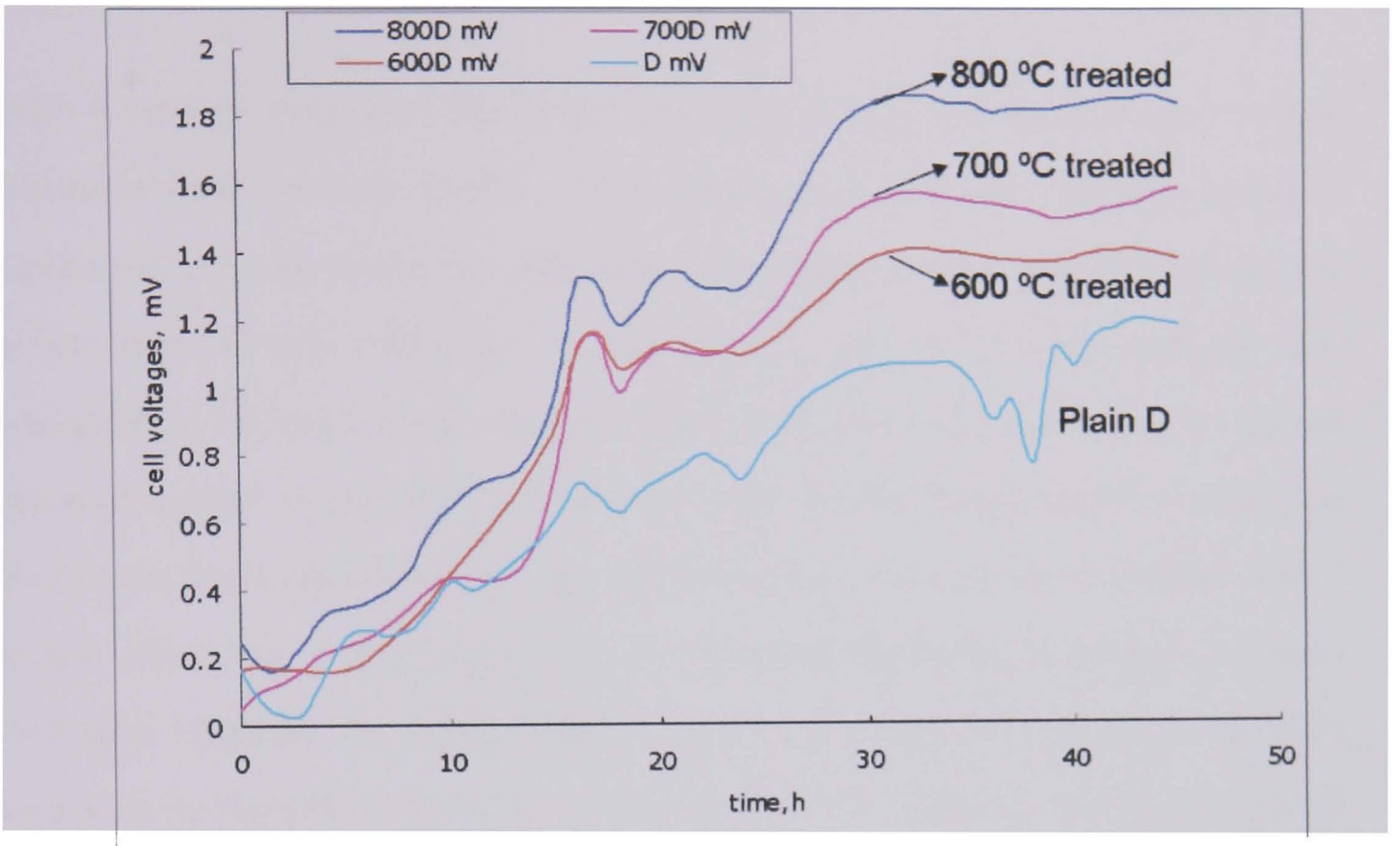

Figure 5.10 Cell voltages of D materials with thermal treatments at different temperatures with separated anode setting

5.2.2.2.2 Electrochemical analysis

With the help of the Autolab potentiostat equipment, several electrochemical aspects of the materials were tested before and after treatment.

5.2.2.2.2.1 OCPs

The OCP tests were carried out using the cyclic voltammetry chrono method by applying a potentiometry and the results are shown in Table 5.2. The approximate OCP for each treated material was recorded for around 100s to maintain a cell voltage of MFC system stable.

Table 5.2 OCPs of B and D materials before and after physical treatment

B materials	Plain B	600B	700B	800B
OCP, V	0.272	0.414	0.401	0.357
D materials	Plain D	600D	700D	800D
OCP, V	0.225	0.312	0.308	0.298

Both B and D materials after 600°C treatment had the highest OCP in their individual MFC systems. Higher OCP means higher potential difference between anode and cathode electrodes with higher possibility for electron transfer between anode and cathode chambers at open circuit. The OCP results indicate that oxidation at relatively lower temperatures might activate the material surface to promote power production in MFCs, but with higher temperature of oxidation processes, more carbon fibre on the material surface is likely to be oxidised, which might affect the ability of the fibre to transfer electrons. However, increased oxidation compare to plain material might generate an increase in suitable locations for bacteria on the fibre and the overall power generation process appears to be a compromise between these two processes.

5.2.2.2.2.2 Electrode potentials

The electrode potential data for plain and treated carbon B and D are shown in Tables 5.3 and 5.4. The highest potential difference was observed for the 600°C treated B and D materials similar to the OCP data in Section 5.2.2.2.2.1. The difference is that, for the OCP test a working electrode and reference electrode were connected for both the cathode and anode electrodes. For electrode potential test, a reference electrode was introduced to accurate record the single electrode potential relative to a standard reference. The electrode potential difference indicates the actual potential differences between anode and cathode during the close circuit test. The results showed that the potential differences were very similar to the OCP data ranging from 0.22 V to 0.42 V. The cathode potential was stable around 0.10 V to 0.17 V, while the anode potential varied from -0.05 to -0.25 V. Thus the anode potential is the dominant factor that affects the power production

from MFCs. By increasing the potential differences between the electrodes, the electrons from the bacteria donor are increasingly promoted to enter the MFC circuit. Hence, greater amount of energy will be gained by bacteria through the processing of more organic matter. As the bacteria contribute more electrons, the higher anode potential facilitates higher electrons transfer that induces higher power production in MFCs.

Table 5.3 Electrode potentials of B materials with physical treatment

Treated anodes	Plain B	600 B	700 B	800 B
Anode potential, V	-0.13	-0.25	-0.25	-0.2
Cathode Potential, V	0.13	0.17	0.15	0.16
Electrode potential difference, V	0.26	0.42	0.4	0.36

Table 5.4 Electrode potentials of D materials with physical treatment

treated anodes	plain D	600 D	700 D	800 D
Anode potential, V	-0.05	-0.17	-0.13	-0.12
Cathode Potential, V	0.17	0.17	0.18	0.17
Electrode potential difference, V	0.22	0.34	0.31	0.29

5.2.2.2.2.3 Polarization curves

Polarization curve tests were carried out to assess the current response of MFCs when applying a gradually increased external control potential to the system. The maximum power density of each material can be found from the polarization curves as shown in Figure 5.11 for plain and treated B anode material. It is clear that the 600°C treated B materials had the highest maximum power density of 0.60 mW/m^2. The corresponding optimal external resistance was around 61.2 kΩ. The power density for the 700°C treated B material was 0.35 mW/m^2 which was only slightly higher than that of the 800°C treatment. The plain B material had the lowest maximum power density around of 0.2 mW/m^2. The ranking of the power generation ability from the polarization curves corresponds very well with that of the electrode potential difference from Tables 5.3, the OCP in Table 5.2 and is similar with that of the actual cell voltage data in Figure 5.9.

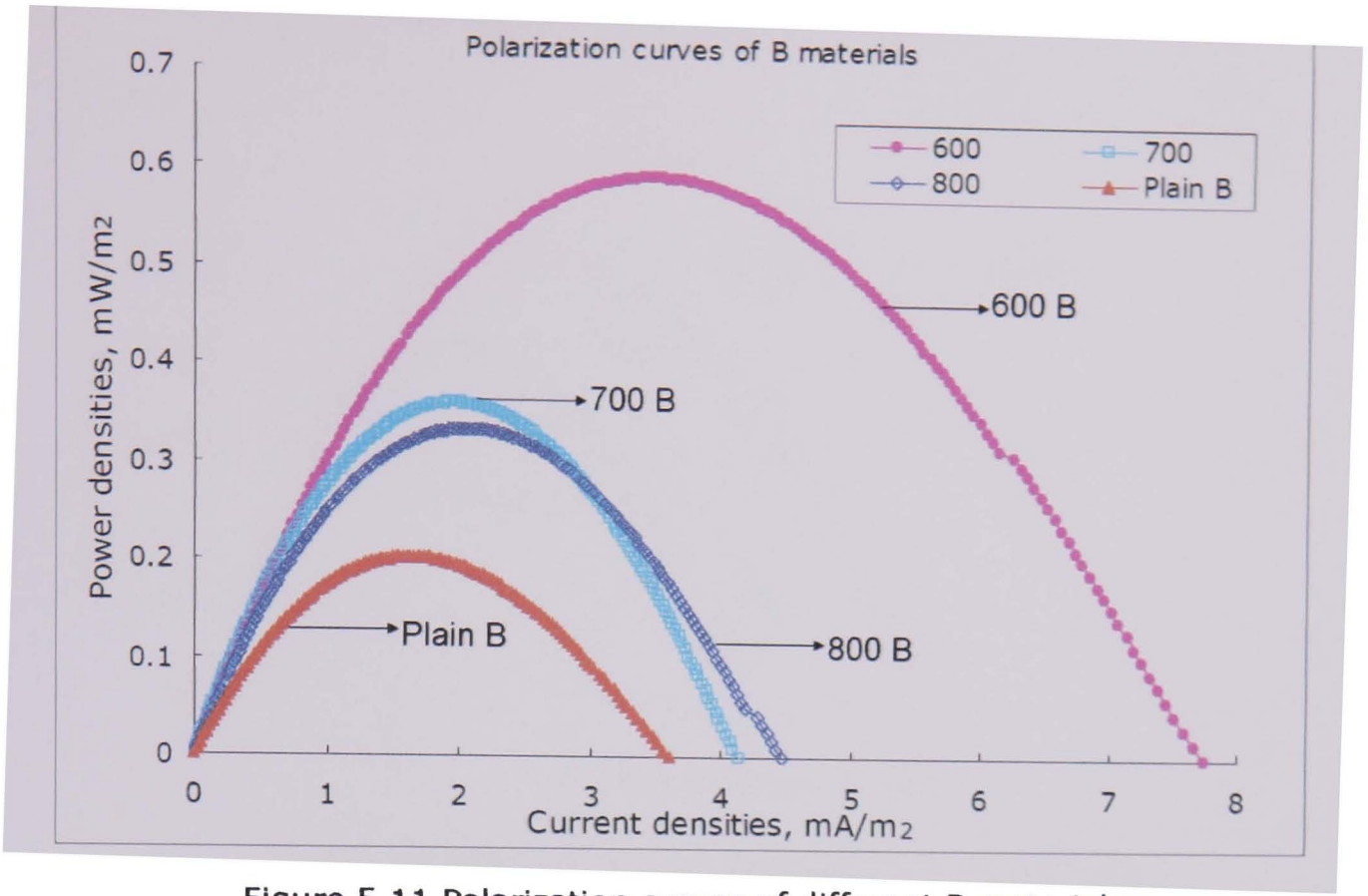

Figure 5.11 Polarization curves of different B materials

The polarization curves for the plain and treated D materials are shown in Figure 5.12. The 800°C treated D materials had the highest maximum power density of 0.33 mW/m^2 with a corresponding optimal external resistance of 111.5 kΩ. The power density for the 700°C treated D material was higher than that of the 600°C treatment, which were 0.25 mW/m^2 and 0.21 mW/m^2, respectively. The plain D material had the lowest maximum power density of around 0.18 mW/m^2. The polarization curve results of the D materials compares very well with the OCP results in Figure 5.10. However, there are some discrpancies with the data from the electrode potential difference in Tables 5.4 and OCP results in Table 5.2. OCP and electrode potential tests were carried out first and then polarization curve. With experiment time passed, bacteria and material interaction may vary, This may explain the power performance were different with different tests.

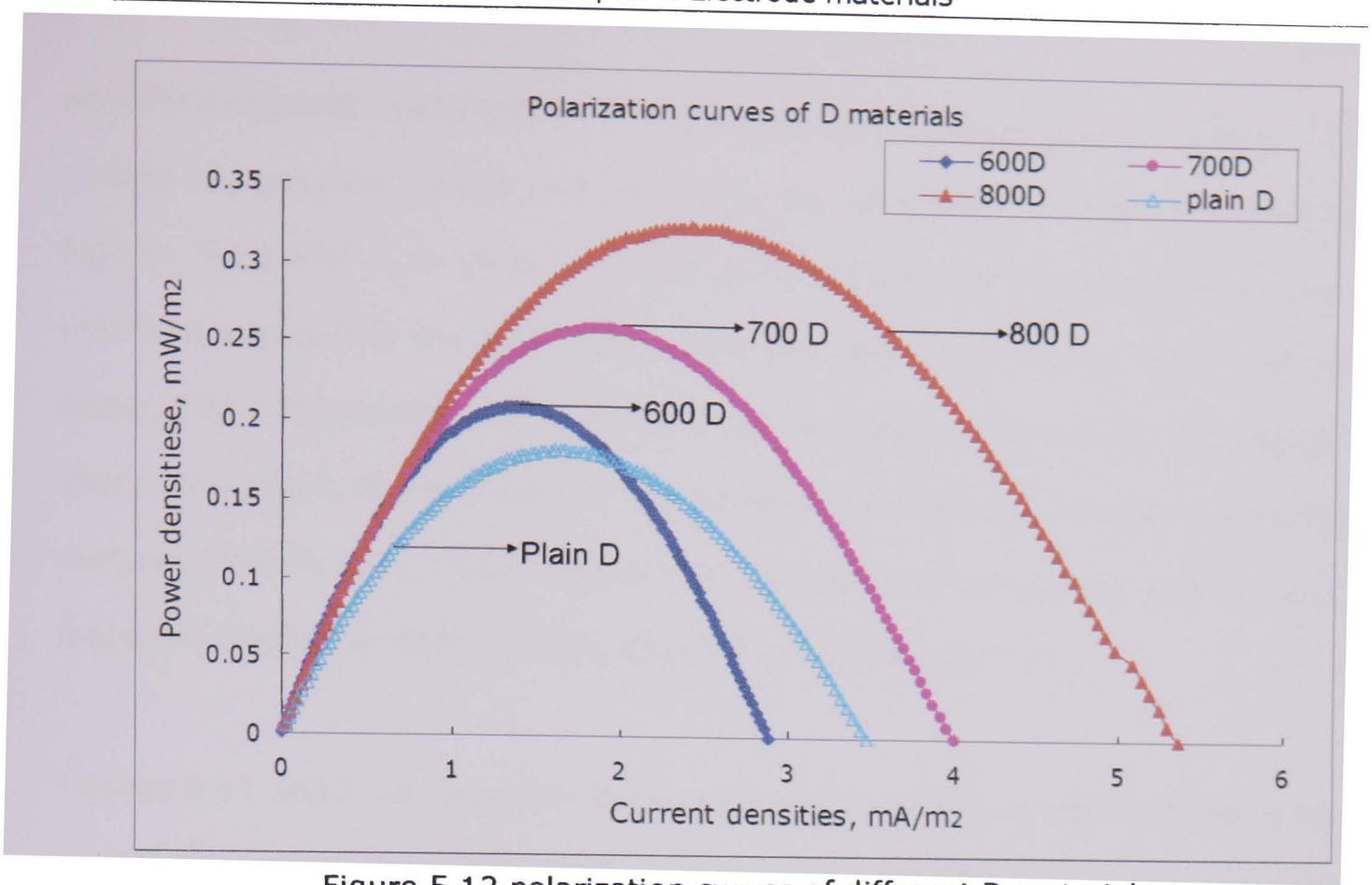

Figure 5.12 polarization curves of different D materials

It appears that the B material had the optimum treatment at 600°C while the D material showed better treatment at 800°C. The reason for this may be due to the difference in thickness. The cloth thickness of the D material was 1 mm that was about 50 % thicker than the 0.65 mm thick B material. In addition, the fibre thickness of the D material was about 9 μm compared to 8 μm for the fibres in the B material which can be estimated from Figure 5.13 and figure 5.14. In the B materials series only 600°C was needed to reach the optimal burn off to gain the highest maximum power density. But for the D material, the data suggest that 800°C or more was needed for the D material to reached optimal burn off to gained the highest maximum power density. For 700ºC and 600ºC treatment of the D material, they had not arrived to the optimal burn off amount yet to enhance the power densities.

5.2.3 SEM results of materials

In order to find out the reasons for the improved MFC power production using this

simplified physical treatment, SEM analysis was used to examine the change of the surface morphology before and after CO_2 gas treatment at high temperatures. Figures 5.13 and 5.14 show a series of fibres from the cloth of the B and D materials comparing the materials before and after treatment at 800°C in CO_2, respectively. The anode material was examined after using them in the MFCs to assess the effect of treatment on the bacteria cultures attached on the material surfaces. Figure 5.15 shows bacteria on the material surfaces of both B and D materials treated at 800ºC in CO_2 after using them in the MFC.

Figures 5.13 and 5.14 show that both the B and D materials after treatment have experienced some exfoliation on the surface of the fibres. This means that during the CO_2 gas oxidation at higher temperatures, the carbon on the surface has been rearranged from an aligned structure typical for a carbon fibre to that of a random structure typical for a char. This exfoliation created on the carbon fibre surface might help bacteria to attach themselves to the fibre and form cultures in this area for power production improvement.

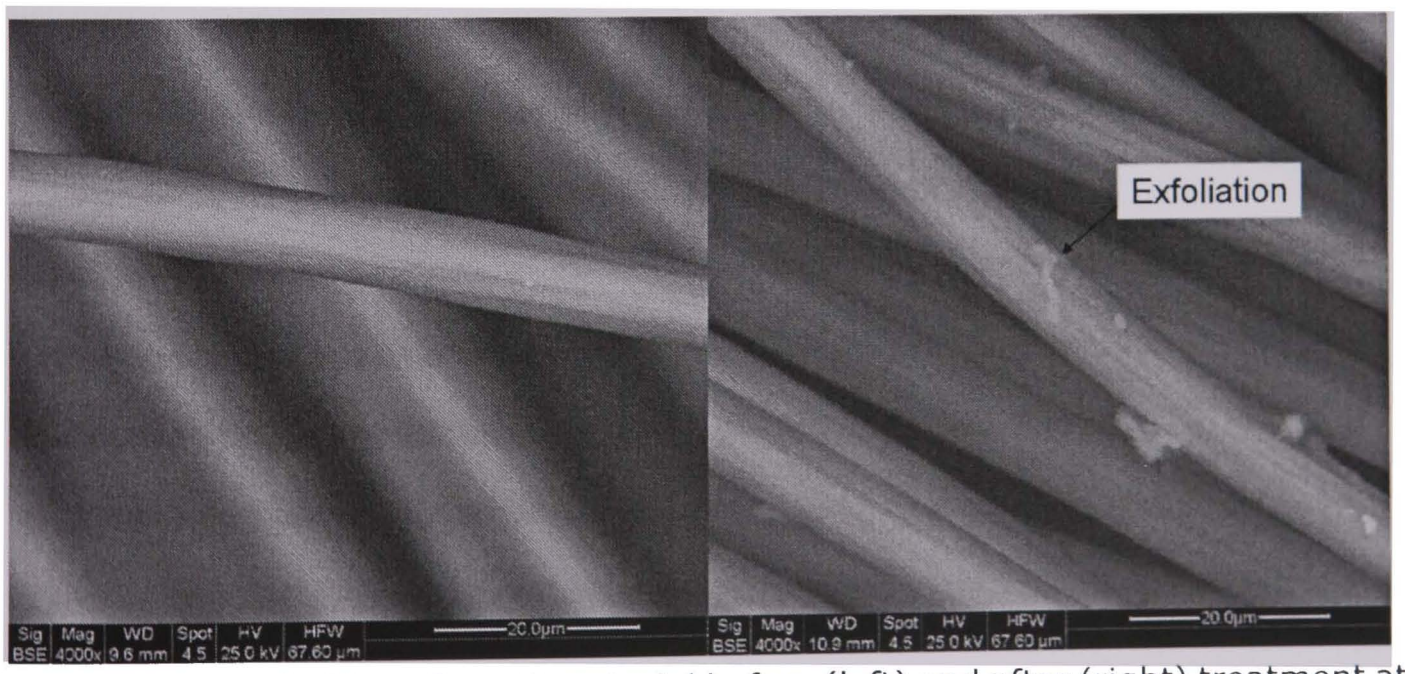

Figure 5.13 Single fibres from B material before (left) and after (right) treatment at 800ºC in CO_2

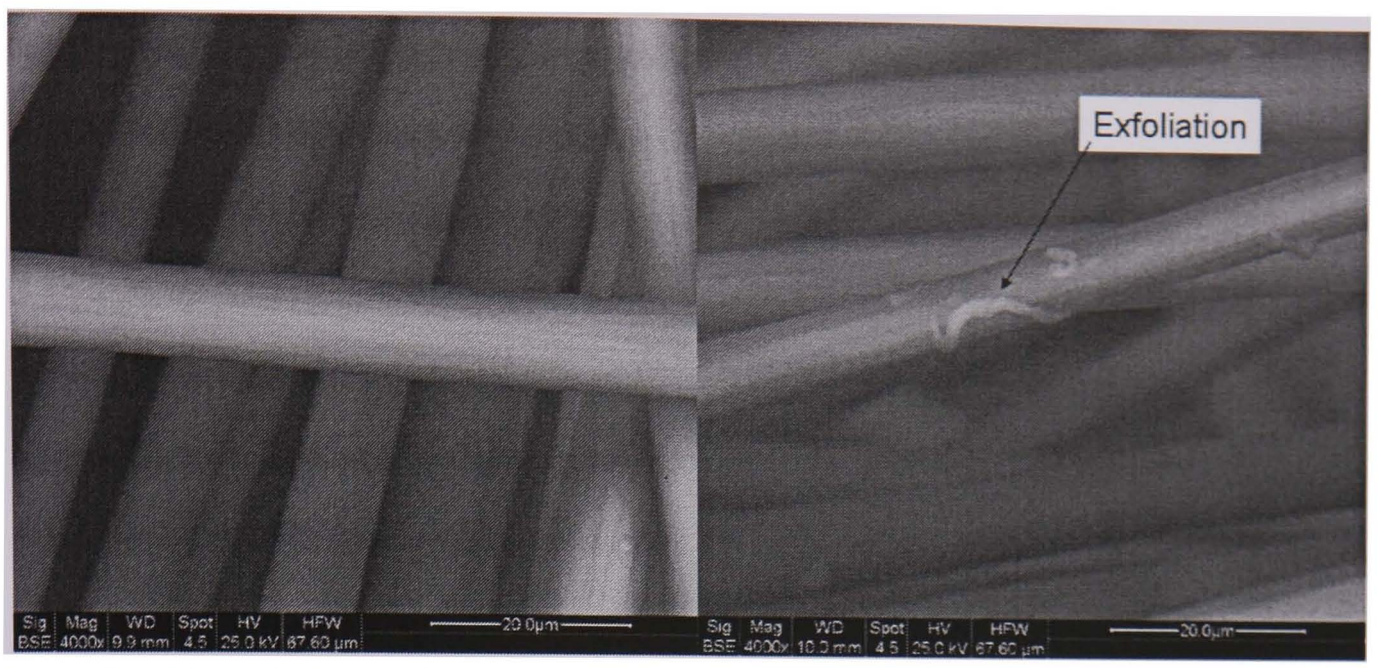

Figure 5.14 Single fibres from D material before (left) and after (right) treatment at 800ºC in CO_2

Figure 5.15 shows SEM images of microbes attached to the 800ºC CO_2 treated B and D materials after MFC process. Due to the properties of anaerobic bacteria, after removing them from the MFC anode chambers, most of them will die and dehydrate. Also due to the technique of SEM, where a high vacuum environment is required, the bacteria may shrink to various shapes and forms that might. The SEM images in Figure 5.15 are fairly representative of the observed microbial growth on the fibre surface after MFC application. It can be seen that for the bacteria to grow on the fibre surface some sort of anchoring point needs to be provided. In the top SEM image of Figure 5.15 the bacteria has utilised an area where surface roughness has been created by CO_2 treatment and organic deposition from wastewater has occurred. In the bottom image of Figure 5.15 it can clearly be seen that the exfoliation of the D material has provided a sites for several bacteria to fix themselves to the fibre surface.

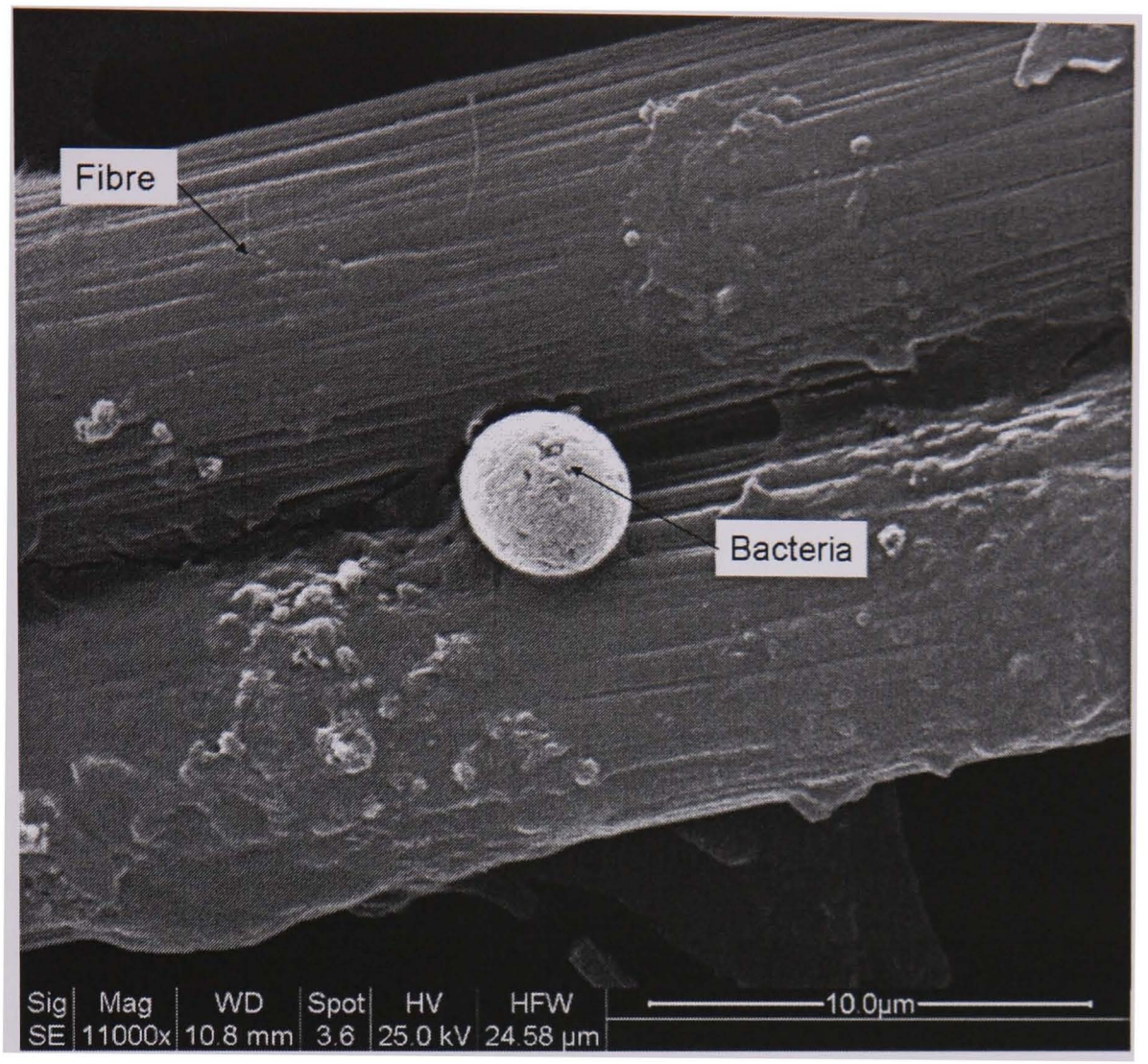

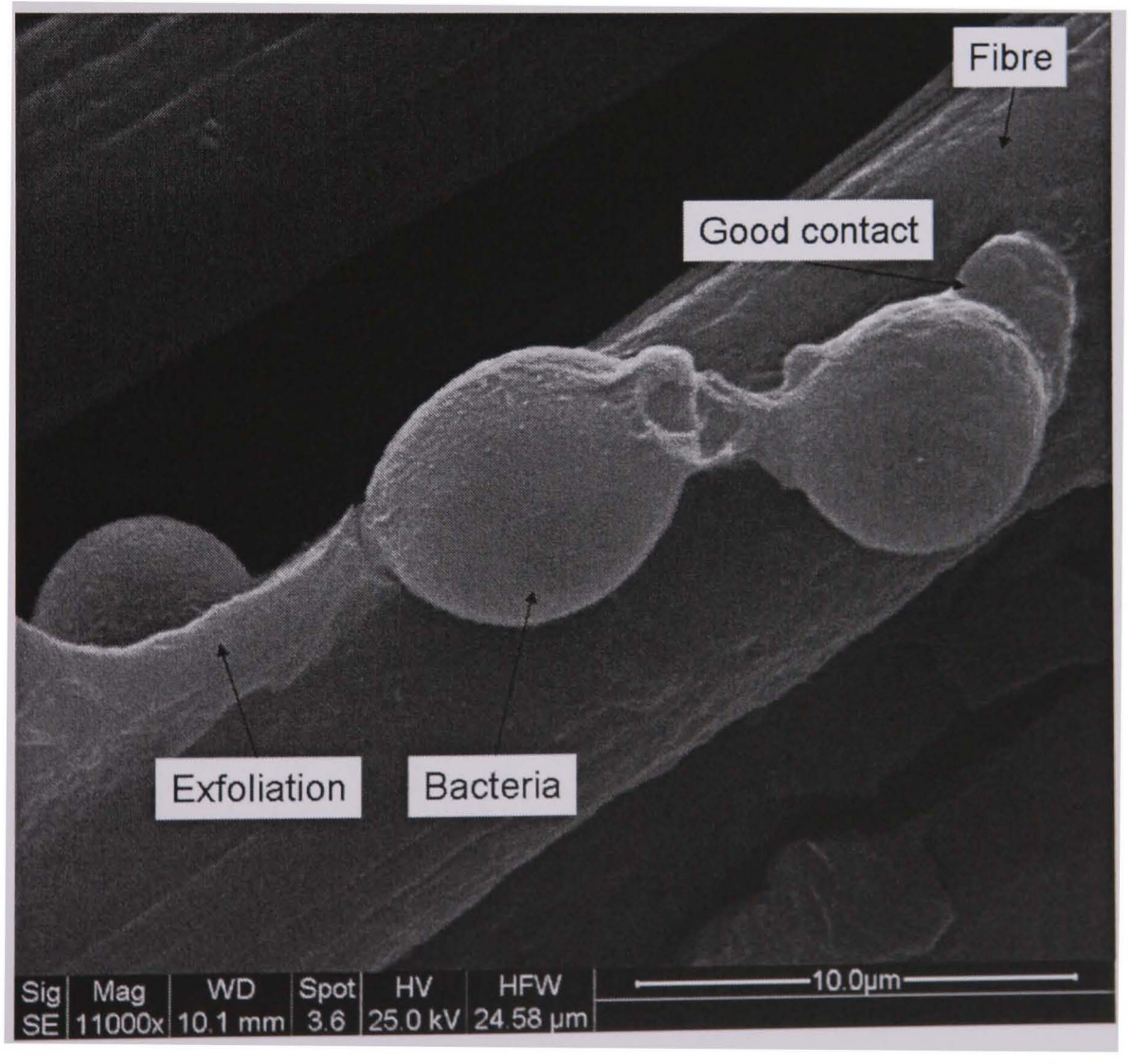

Figure 5.15 SEM images of microbes attached to the 800°C CO_2 treated B material (above) and D material (below) after using them in MFC

5.2.4 BET results of materials

In order to find out whether the high temperature gas oxidation treatment helps towards the enlargement of the pore size distribution, BET tests were carried out to test the surface area and pore size distributions of these materials. Especially the macropore size distribution was of interest since this was assumed to be strongly related to an increase in the power performance during MFCs application of the treated anode materials. Figures 5.16 and 5.17 compare the nitrogen adsorption isotherm profile of the 600 ^{o}C treated B material and the 800 ^{o}C treated D materials with their untreated materials, respectively. Figure 5.16 shows that at relative pressure from 0.9 to 0.995, the 600 ^{o}C treated B materials dramatically increased the macropore volume of 2.79 cm^3/g compared to 0.66 cm^3/g for that of plain B material. This indicates a significant increase in macropore adsorption. Similarly, in Figure 5.17, the 800 ^{o}C treated D has increased its macropore volume to 5.33 cm^3/g compared to 2.27 cm^3/g for the plain D material. The results are consistent with the total adsorbed volume trends in Table 5.5.

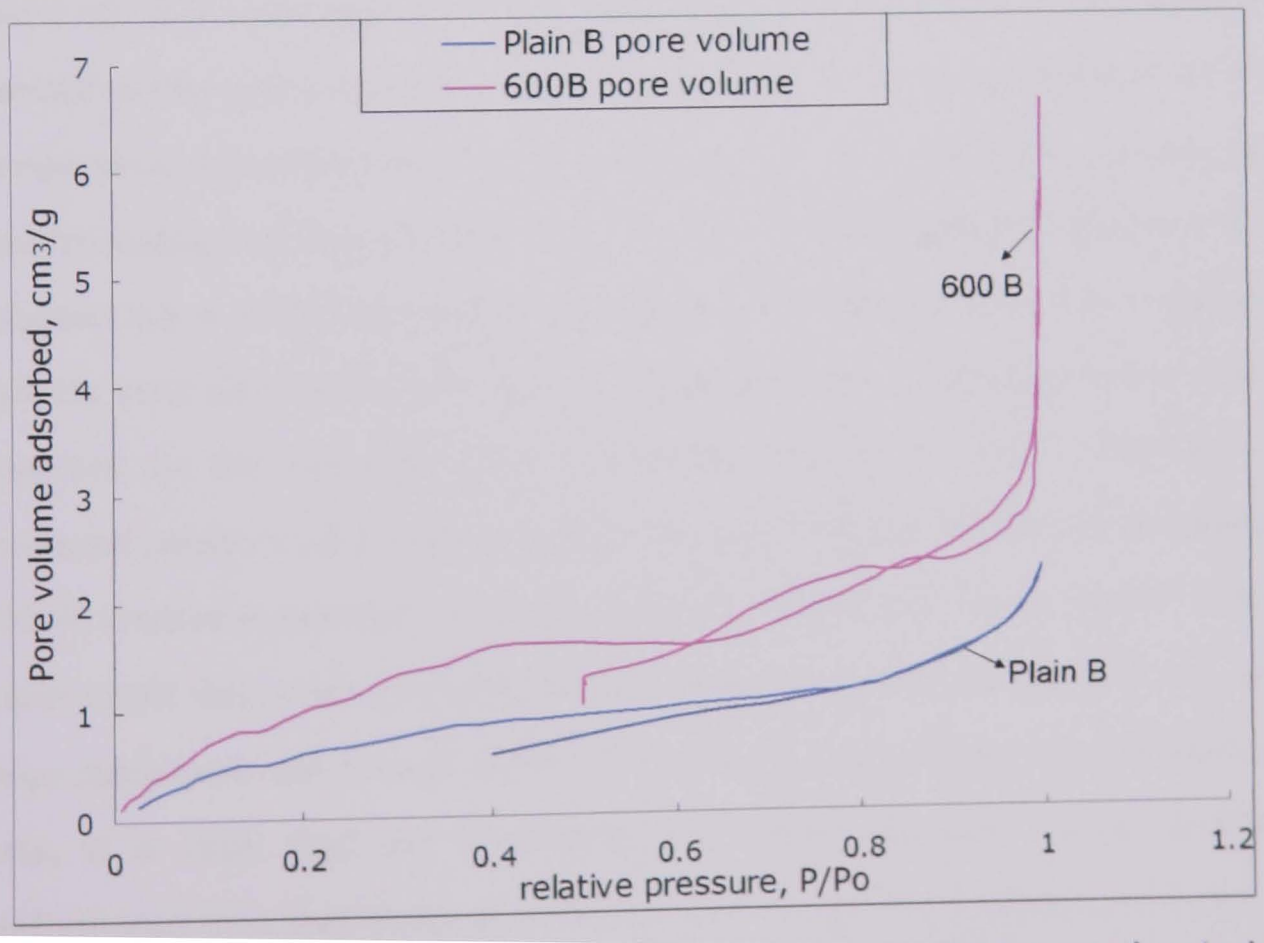

Figure 5.16 Nitrogen adsorption isotherm of plain B and 600 ^{o}C B treated materials

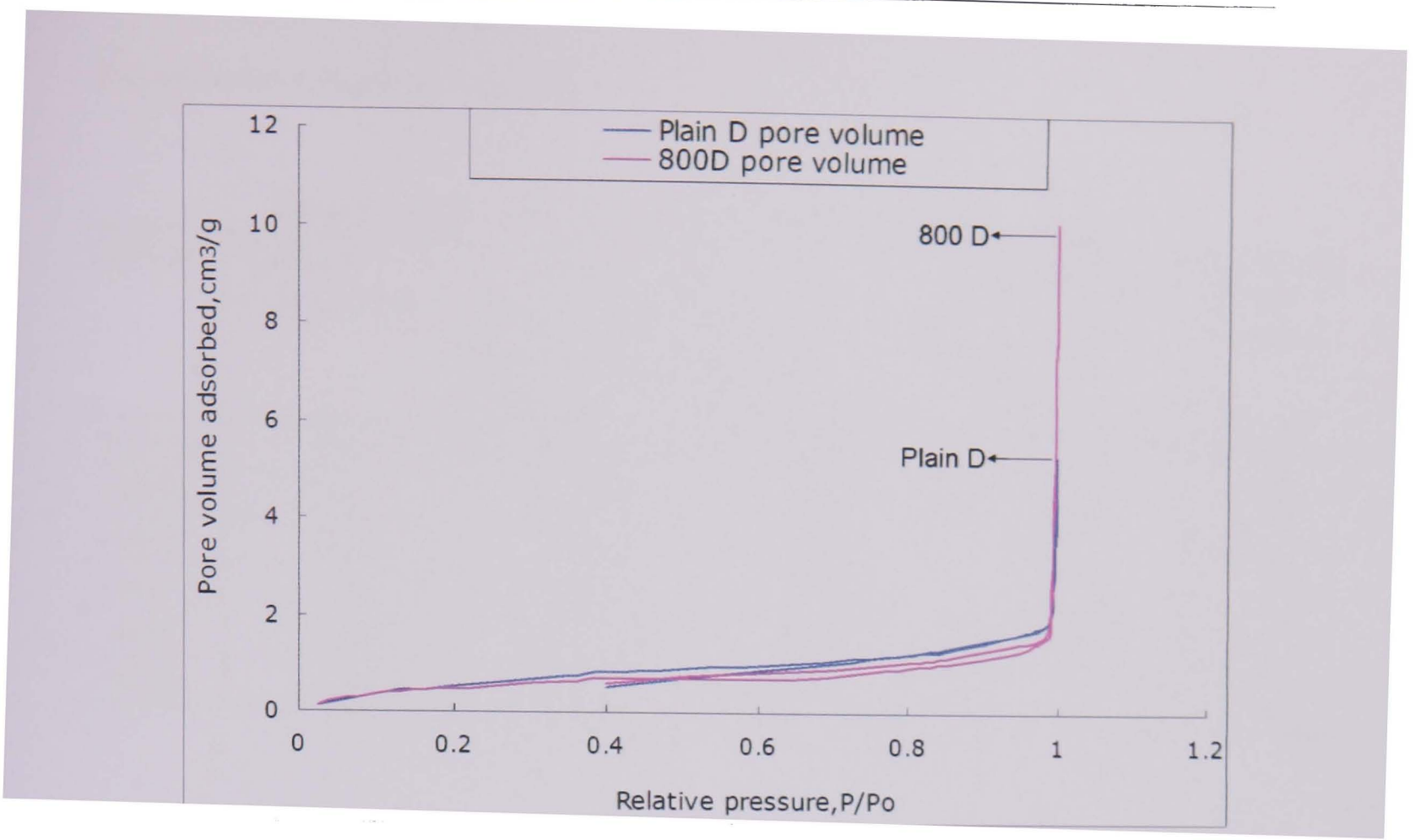

Figure 5.17 Nitrogen adsorption isotherm of plain D and 800 °C D treated materials

Table 5.5 lists the BET results as well as the corresponding maximum power densities of each materials based on the polarization tests found from Figures 5.11 and 5.12. It is clear that the surface area data of these materials are increased parallel to the power densities except for the 800 °C treated B material. At high temperature oxidation treatment, the material pore sizes less than 40nm are kept relative stable, but the pore sizes up to 300 nm and the macropore volumes at P/Po between 0.9 to 0.995 are both increasing. From the data in Table 5.5, it indicates that the pore sizes larger than 300 nm dominates most of the macropore volume adsorbed in the materials. The macropore volumes of these materials are increased parallel to the power densities except for the 800 °C treated B material. 800 °C treated B material has larger macropore volume but lower power density which might due to the shortage of valid pore size for bacteria growing, i.e. very large macropore size around 1000 nm. From the corresponding power densities data, it is clear that the B material has better improved power densities performance than that of the D materials after treatment, again probably due to

the material differences between the cloths as reported in Section 5.2.2.2.2.2.

Table 5.5 BET results and their maximum power densities

Material	Surface Areas, m^2/g	Pore volume, cm^3 /g, diameter <40nm	Pore volume, cm^3/g, diameter 1.7-300nm	Macropore volume at P/Po 0.9-0.995, cm^3/g	Power densities, mW/m^2
Plain B	2.67	0.003	0.003	0.66	0.2
600B	4.8	0.004	0.009	2.79	0.59
800B	2.84	0.003	0.002	10.68	0.33
Plain D	2.47	0.003	0.008	2.27	0.18
600D	3.89	0.003	0.008	3.19	0.21
800D	2.04	0.002	0.015	5.33	0.32

5.2.5 Summary of physical treatment

The physical treatment results showed that under CO_2 oxidation environment with high temperature an improvement in the power densities performance based on MFCs was observed. Comparing the B material with thinner carbon fibre layer to that of the thicker D material, the B material displayed a better treatment performance with regards to power density in the temperature range from 400 to 800°C. For different treatment conditions within the same materials, the B and D material results showed consistent results based on data logger and electrochemical tests. The best results were obtained for the 600°C CO_2 treatment for the B material and 800 °C CO_2 treatment for the D material. The 600°C B material has an improvement of around 195 % in power density compare to plain B materials and the 800 °C D material has an improvement of around 78 % in power density compare to the plain D material based on the polarization curves data. Further examination, including SEM, demonstrates that the increased performance of the high temperature treated anode may be attributed to the exfoliation of the carbon firers after treatment that helps bacteria more easy fasten to and grow on the surface of the fibres. The BET analysis indicated that the macropore volumes of the 600 °C treated B and 800 °C treated D materials were

greatly increased compare to those of plain B and D materials. The macropore pore size range that was enhanced during treatment was larger than 300 nm while the normal size of bacteria is around 1000 nm to 5000 nm. As a function of macropore volume, the B material displayed a better improved power densities performance than that of D materials after treatment showed in Table 5.5. The data suggests that the enlarged macropore pore volumes after gas oxidation treatment might have the effect to attract more bacteria and thus increase the electron transfer as well as the power performance in MFCs.

5.3 Chemical treatment of anode materials

5.3.1 Experimental methods

Chemical treatment of the plain anode materials B and D were carried out using 3M of HNO_3, H_2SO_4, HCl and KOH, respectively, for 24h followed by washing with distilled water for at least three times. The reason for using these acid and alkaline solutions for chemical treatment was that, firstly, concentrated acids and alkaline may erode the material surfaces and make the surface coarse. The uneven surface and added functional groups might make bacteria more likely to attach to the anode. The second reason was that the chemicals might form some element-containing functional groups on the surface during the treatment, which may increase the positive or negative charge distribution on the anodes. The increase of the surface positive charge could attract more bacteria that have an abundance of negative charge, i.e. electrons. In this case, more electrons would like to be transfer onto the anode surface and higher power densities and higher coulombic efficiencies would be achieved. These hypothesises were tested using several experiments as outlined in this section. Table 5.6 compares the changes in material density after chemical treatment of both material B and D. The data shows that the B material densities are decreasing after chemical treatments while the D

material densities are slightly increased after chemical treatments which might due to some chemical deposition. This treatment trend confirms the overall reactivity observed under thermal treatment where material B was more reactive while material D was more difficult to thermally treat.

Table 5.6 Material density changes after chemical treatment

	plain B	HNO_3B	H_2SO_4B	KOHB
Area cm^2	7.92	7.7	7.59	8.52
Weight g	0.19	0.16	0.16	0.16
Density g/m^2	236.49	213.51	210.14	191.08
Density decreased	/	9.72%	11.14%	19.2%
	plain D	HNO_3D	H_2SO_4D	KOHD
Area cm^2	7.15	7.7	7.37	8.14
Weight g	0.21	0.24	0.23	0.25
Density g/m^2	297.34	308.31	308.14	309.21
Density increased	/	3.69%	3.63%	3.99%

For the examination of chemical treated materials, the simplified MFC was set up exactly the same as the experiments for the physical treatment with the multiple and single anode systems as outlined in Section 5.2.1 except for the anode materials being the materials after chemical treatment.

5.3.2 MFC performance

5.3.2.1 Performance based on the star rack anode setting

The experiments were run continuously for 13 days. The average cell voltages were calculated as an average of theses cycles and the power densities based on the average cell voltages were used to range the performance of the materials by the treatments as showed in Figures 5.18 and 5.19. Both figures compare the cell voltage for plain and treated B and D materials in one experimental cycle.

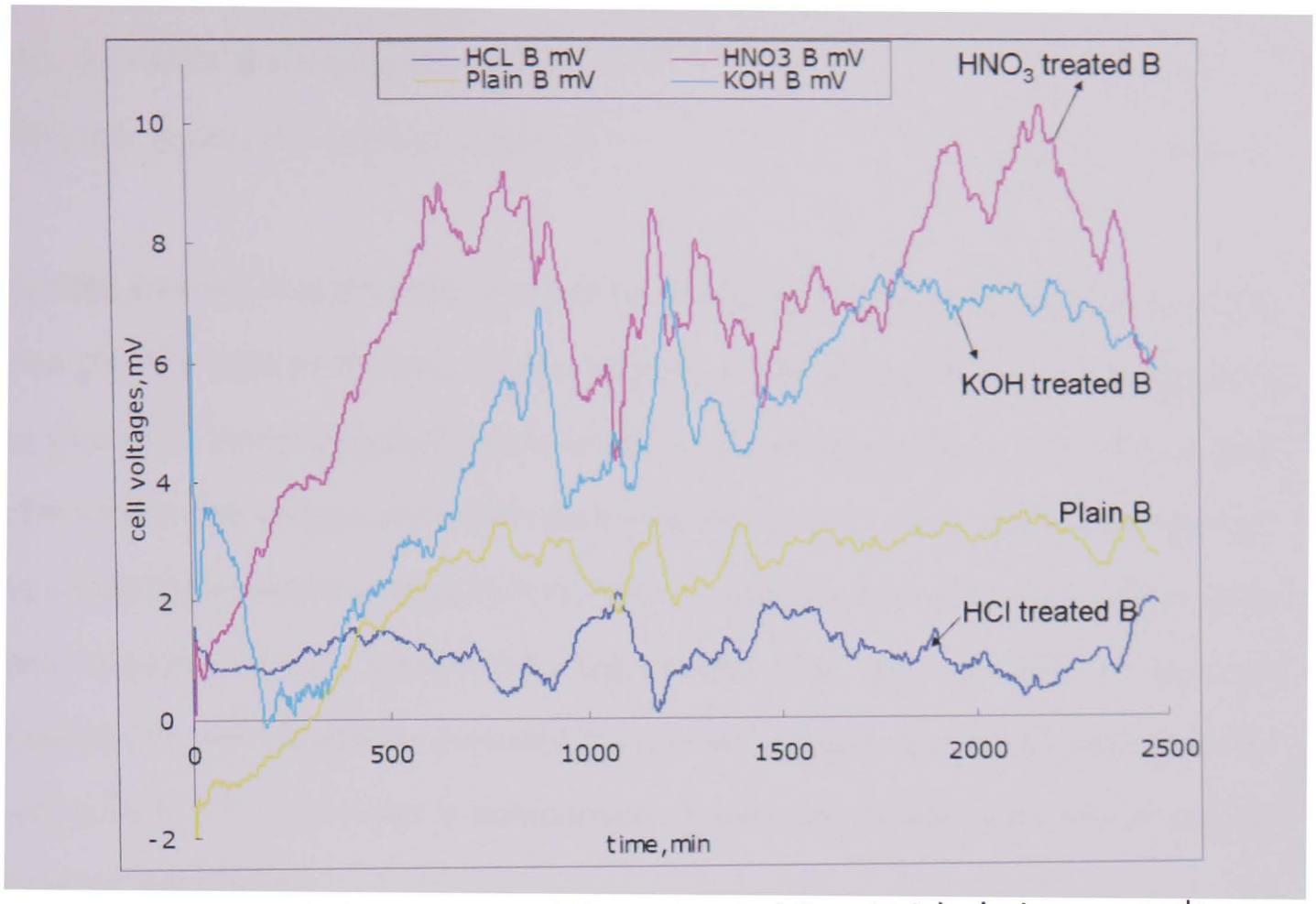

Figure 5.18 Cell voltages of different treated B materials during one cycle

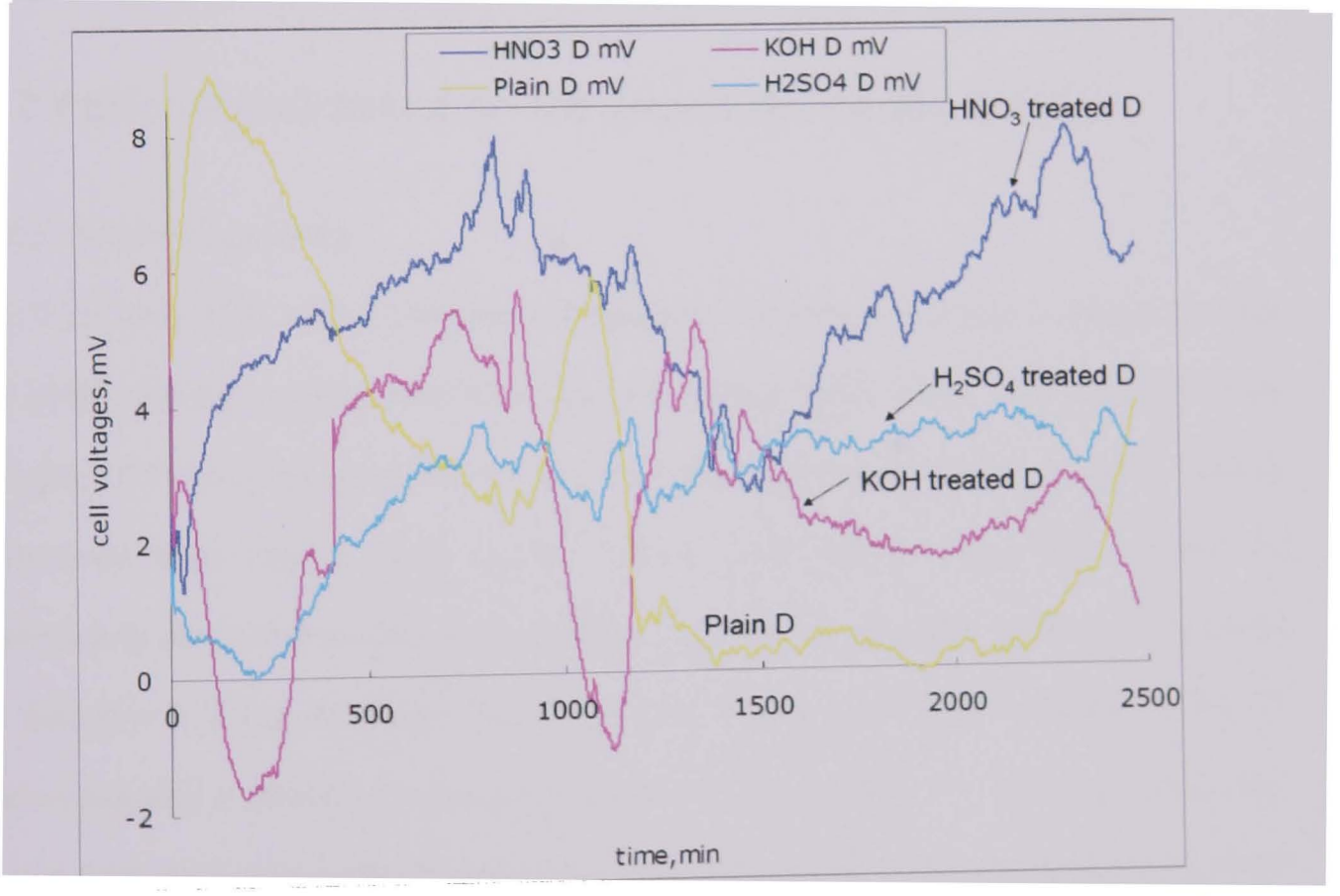

Figure 5.19 Cell voltages of different treated D materials during one cycle

From the repeated 13 periods of continuous experiment, the average order of output power densities (PD) with different treated anode slices was:

HNO_3 B > KOH B >> plain B> HCl B Equation (29)

HNO_3 D > H_2SO_4 D > KOH D >plain D Equation (30)

The data showed that the HNO_3 treated materials had the best power output results. Generally the treated B material had a better power generation performance than the treated D material based on the scale of cell voltage data in Figures 5.18 and 5.19. In the cell voltage data with data logging system, some of the data showed the chaos of the electron acceptors and donors due to some anode cell voltage data were negative, which means different anodes may play the role of electron acceptors to gain electrons released from other anodes. So the separated anode setting in 5.3.2.2 provided a comparison to evaluate anode materials based on chemical treatments.

5.3.2.2 Performance based on the separated anode setting

5.3.2.2.1 Cell voltage data

Figures 5.20 and 5.21 show the cell voltage data of treated B and D materials for around 100h of recording time where the cell voltage data were collected from the data logger at 1 data/min and the external resistors were all 10 kΩ. Limited by the eight channel data logger, only H_2SO_4, HNO_3, KOH treated and plain B and D materials were observed in these experiments, since these were found to perform best in Section 5.3.2.1 in Figure 5.18 and 5.19. In Figure 5.20, all four of the B materials showed a similar response under MFC conditions by a strong increase during the first 30 hours and then reaching a plateau. The HNO_3 treated B material displayed the highest cell voltage data, and the H_2SO_4 treatments showed the lowest cell voltage. The KOH treated B material had a slightly higher cell voltage than plain B material. These results have the same order as the results based on star rack MFC setting presented under Section 5.3.2.1.

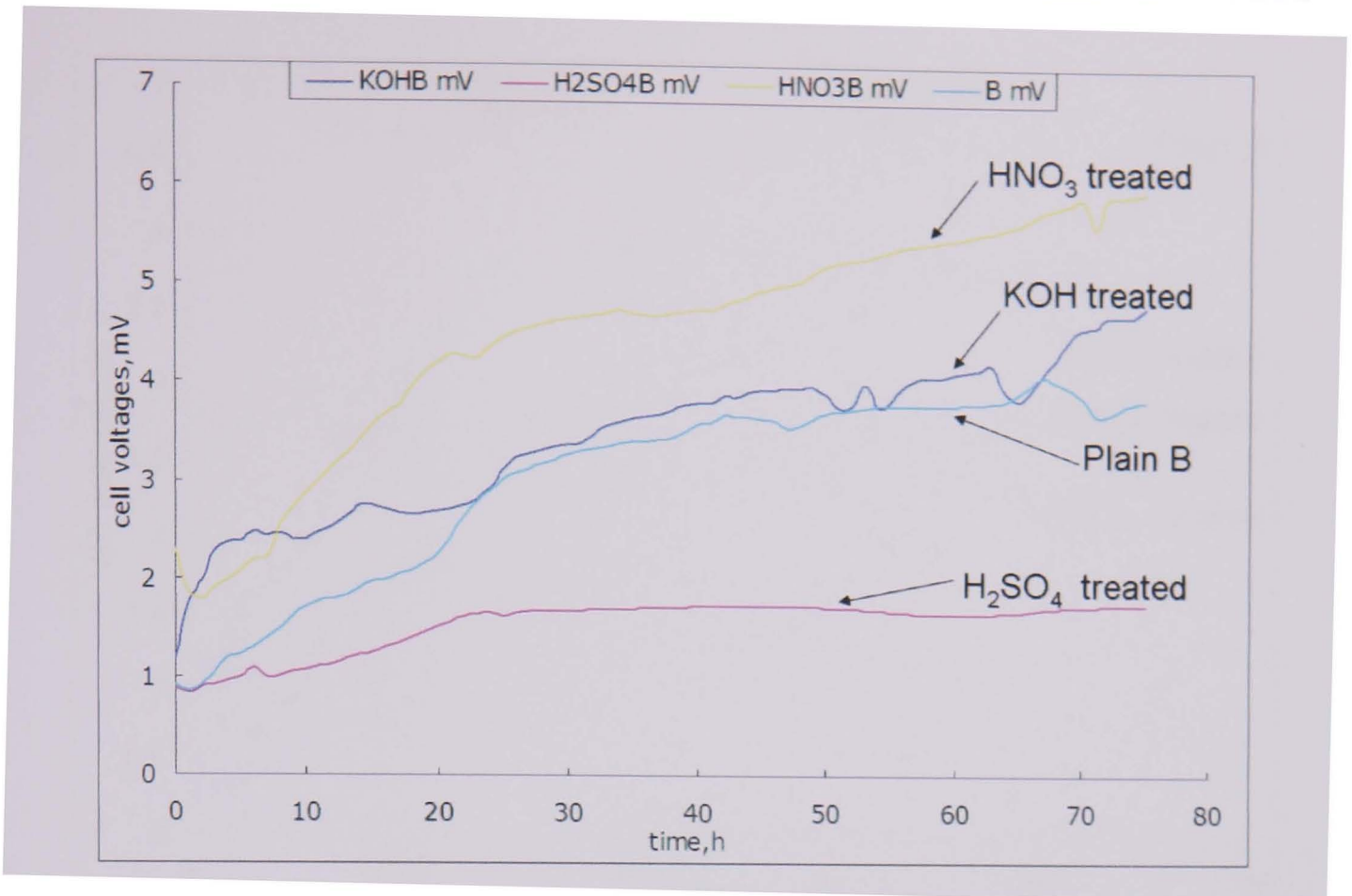

Figure 5.19 Cell voltages of B materials with different treatments

The voltage curves for the D materials in Figure 5.21 shows that during the first 60 hours the KOH treated D material displayed the highest power densities, but after 60 h, the plain D material started to increase to the highest value and not reaching a plateau. Both the H_2SO_4 and HNO_3 treated D showed lower cell voltages. These results are different from the results based on star rack MFC setting presented under Section 5.3.2.1. However, they support the observation of chemical treatment effect on carbon density in Table 5.6 where material B was found to be more reactive under chemical treatments and virtually no reactivity was observed for material D. Generally the treated B material had a better power generation performance than the treated D material based on the scale of the cell voltage data.

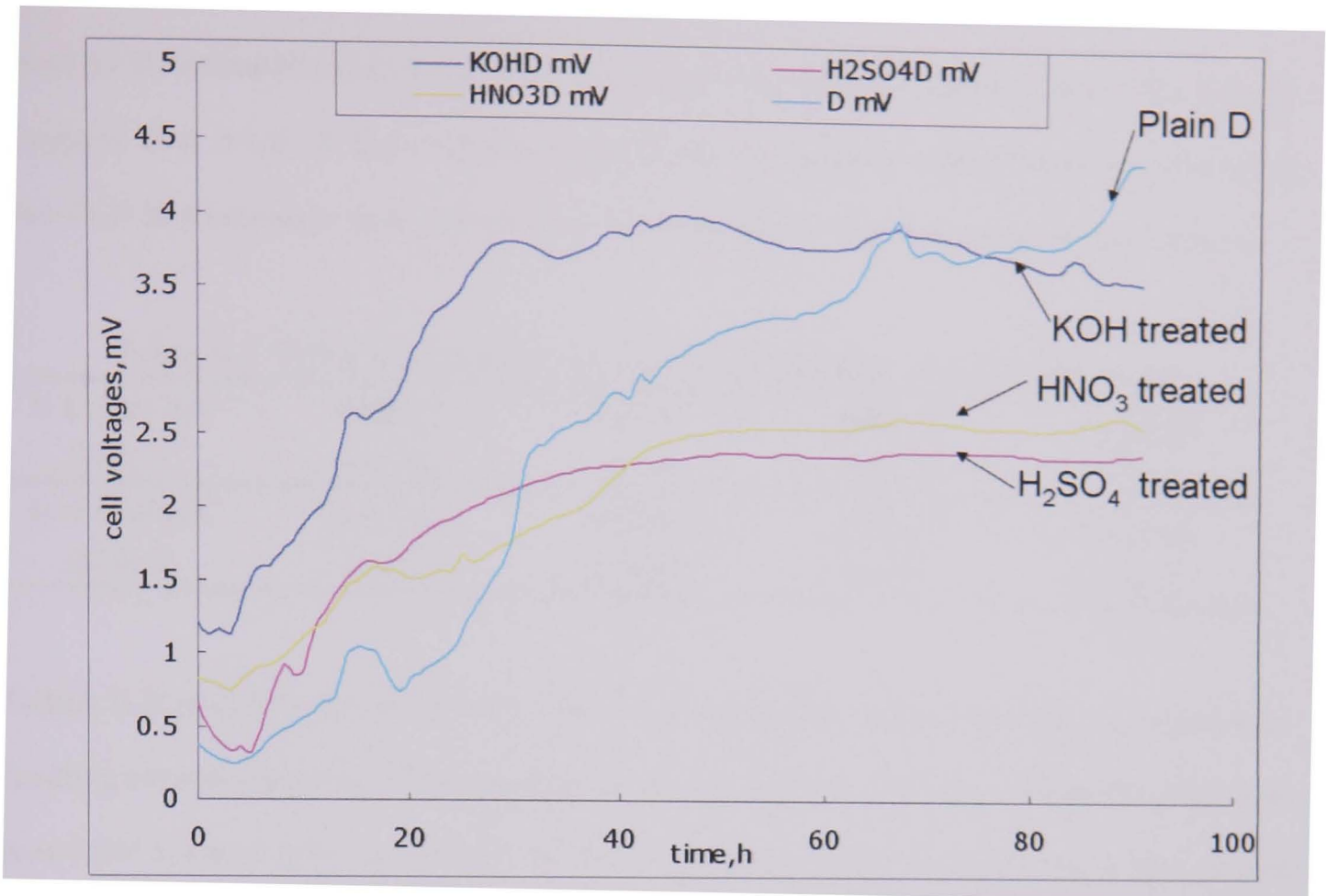

Figure 5.20 Cell voltages of D materials with different chemical treatment

5.3.2.2.2 Electrochemical analysis of MFCs

Further analysis was needed to find out the actual performance of these chemical treated material and electrochemical measurement, in terms of OCP, electrode potentials and polarization curves, were applied to demonstrate the electrochemical properties of the materials.

5.3.2.2.2.1 OCP and electrode potentials

Table 5.7 lists the OCPs of the plain and chemical treated B and D materials. Compared to the MFC performance, the most striking OCP values for both the B and D material was that of the alkaline KOH treatment, where the KOH treated B material had the highest OCP compare with other B materials, while the KOH treated D material had the lowest OCP. However, the OCP appears to be related to the material density changes under Table 5.6 where B material was found to be more reactive than the D material under chemical treatments. The OCP results are also consistent with the finding that the treated B materials were better than the

treated D material related to their power performance. However, the OCP results suggest that most of the chemical treatment had a poor effect towards improving the OCP of materials that potentially could increase the cell current production.

Table 5.7 OCPs of the plain and chemical treated B and D materials

B materials	Plain B	KOHB	HNO_3B	H_2SO_4B
OCP, V	0.543	0.547	0.523	0.512
D materials	plain D	KOHD	HNO_3D	H_2SO_4D
OCP, V	0.55	0.348	0.435	0.435

Tables 5.8 and 5.9 show the MFC electrode potential differences for the chemical treated anode materials. The treated material with the highest potential difference was KOH treated B material with 0.55 V. However, all the OCPs of chemical treated material were lower than their plain counterpart. As electrode potentials induce higher energy production, the order of materials in terms of better power production was determined, and the order of the electrode potentials was virtually the same as for the OCP data in Table 5.7. This indicates that chemical treatment generally does not improve the electrode potentials and the OCP of carbon cloth. This suggests that acids and alkaline treatment does not help to improve the power performance in MFCs.

Table 5.8 Electrode potentials of B materials

Treated anodes	Plain B	KOH B	HNO_3 B	H_2SO_4B
Anode potential, V	-0.39	-0.38	-0.29	-0.36
Cathode Potential, V	0.15	0.17	0.13	0.16
Electrode potential difference, V	0.54	0.55	0.42	0.52

Table 5.9 Electrode potentials of D materials

treated anodes	plain D	KOH D	HNO_3 D	H_2SO_4 D
Anode potential, V	-0.42	-0.21	-0.38	-0.26
Cathode Potential, V	0.16	0.16	0.14	0.18
Electrode potential difference, V	0.58	0.37	0.52	0.44

5.3.2.2.2.2 Polarization curves

Figures 5.22 and 5.23 show the maximum power density of each material obtained from their respective polarization curves. In Figure 5.22, the optimal maximum power densities were all around 0.9 to 0.95 mW/m^2, it is clear that all the B materials after different chemical treatment had very similar polarization curves to the original material. However, a slight difference was observed and the sequence of the best power densities of these materials was similar to the cell voltage data shown in Figure 5.20. These results illustrate that chemical treatment did not improve the power densities which is in corresponding with the actual MFC experimental results in Section 5.3.2.2.1. From the results of the polarization curves of the D materials in Figure 5.23, the sequence of the best power densities corresponded with the previous results for the cell voltage data in Figure 5.21 and that of the electrochemical tests. Plain D material without any treatment in both methods shows the best power density 0.61 mW/m^2. The KOH treated D had the lowest maximum power density 0.46 mW/m^2.

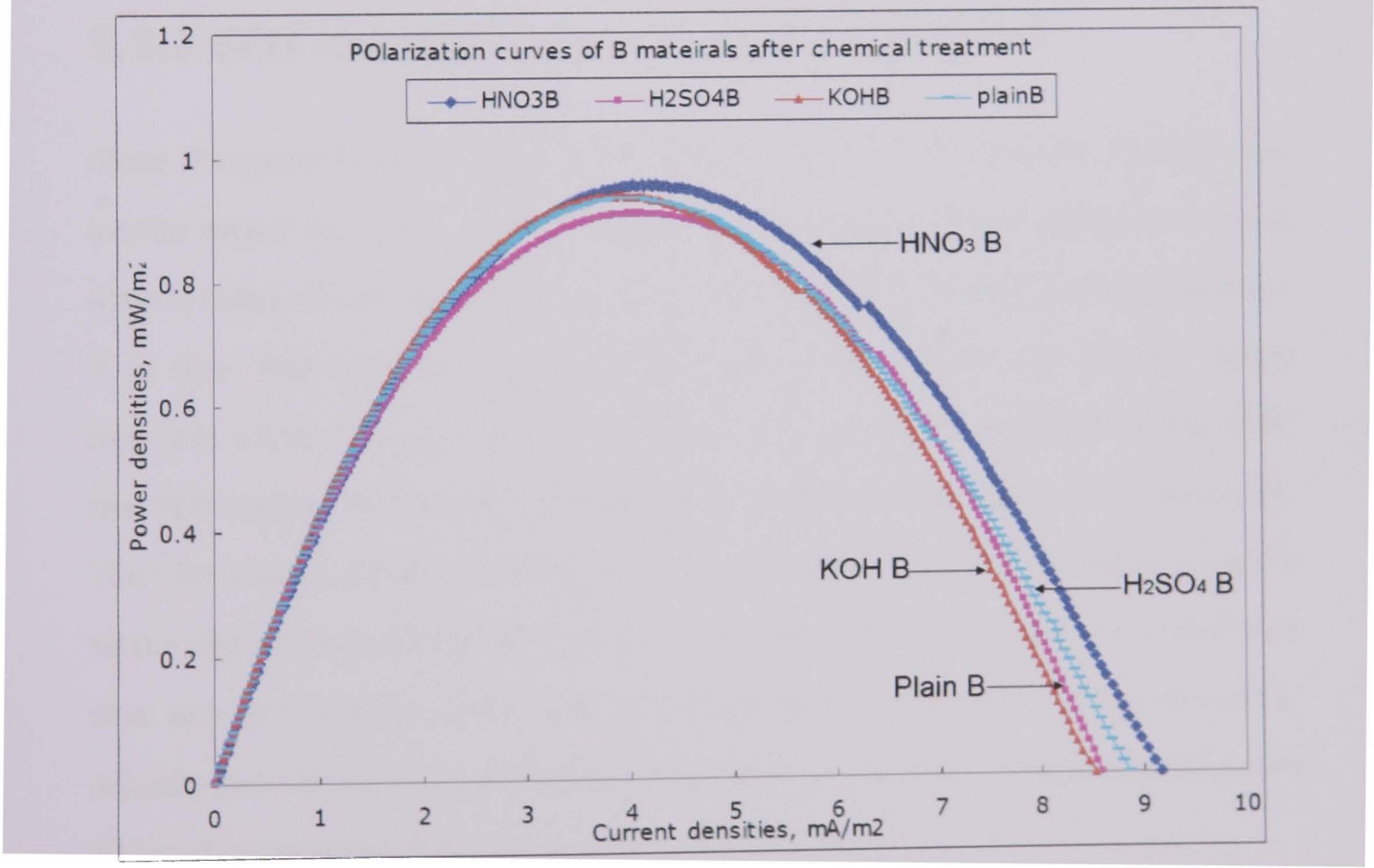

Figure 5.21 Comparison of the polarization curves of the B materials before and after chemical treatments

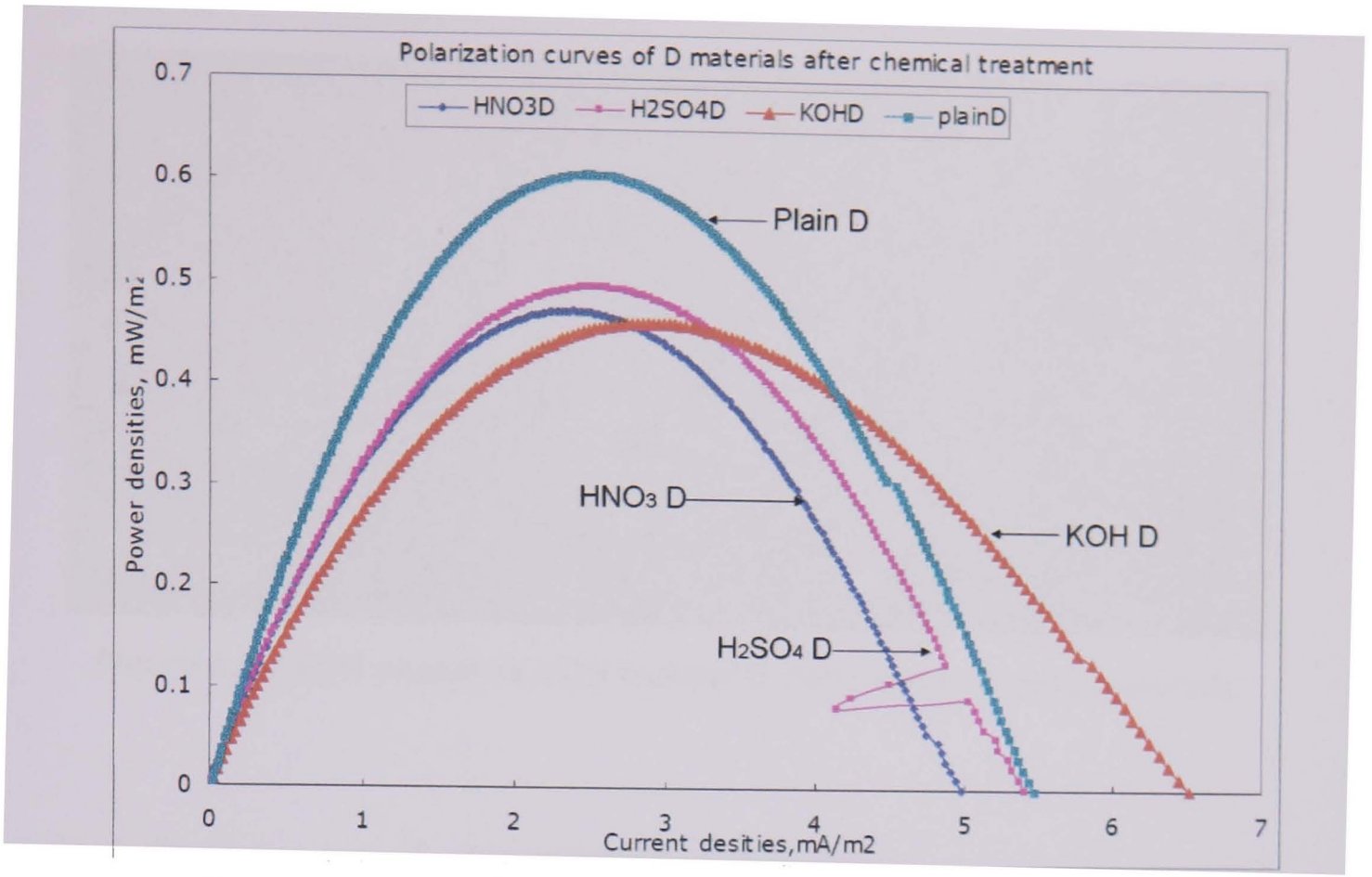

Figure 5.22 Comparison of the polarization curves of the D materials before and after chemical treatments

5.3.3 SEM investigation of chemical treatment

Since the polarization curves of the plain and treated B materials showed very similar power densities, while the polarization curves of the D materials showed plain D material had the higher power density than all the other treated materials, it is clear that chemical treatment had poor influence to improve the power densities under MFC conditions. The reason for this was investigated using SEM, the SEM images of the KOH treated B and D materials are shown in Figure 5.24. The SEM images show that there is almost no change to the fibre surfaces compare to the plain B and D materials (Figures 5.13 and 5.14). This observation indicates that acid and alkaline treatments may clean the surface of the carbon fibre that actually prevent bacteria growth on the surface rather than change their structure and surface functional groups for improved interaction.

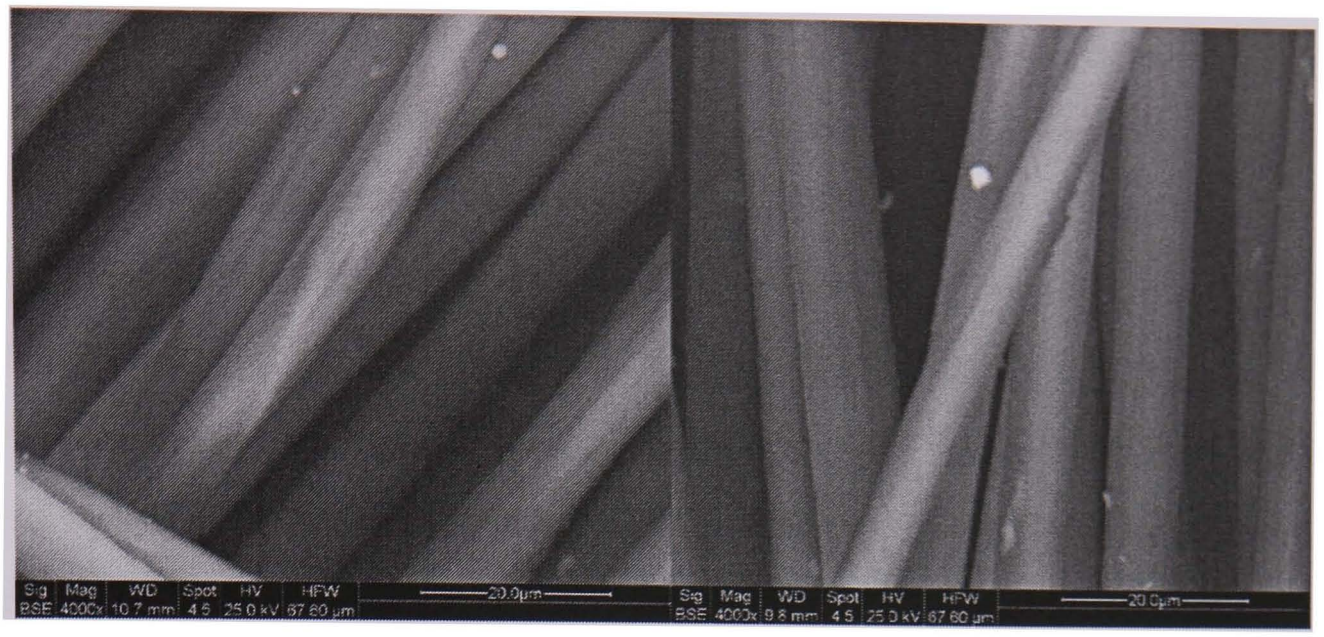

Figure 5.23 SEM photos of KOH treated B (left) and D (right) materials

5.3.4 Summary of chemical treatment

In summary, the OCP and electrode potentials electrochemical tests showed that KOH treated B and untreated plain D materials had the highest power densities potential. For the polarization curves tests, both the plain and treated B and D materials were ranked similar to both the OCP and the electrode potentials results, all indicating that the untreated materials had better performance than the chemical treated materials. This indicates that chemical treatment of the B and D carbon fibre cloth materials does not have positive influences for power performance during MFC.

5.4 Graphite granules as cathode materials

Two series of experiments were designed to test the performance of plain graphite granules used as cathode material compared to the more expensive Pt contained cathode material, using the stacked MFC described in Section 4.2.2. The reactor structures, anode bacteria inoculation procedure, buffer solutions concentrations used in anode and cathode, buffer solution recirculation flow rate were all the same as described in Section 4.2.2. The only difference with these two sets was that the

carbon cloth cathode loaded with 5 g/m^2 Pt was exchanged with plain graphite granules used as cathode material.

Figure 5.25 shows the polarization curve of the stacked MFC with plain graphite cathode versus that using a Pt contained cathode. The OCP was obtained using a voltage scan rate of 1mv/s down to 0 V. The polarization curve shows that the MFC performance was dramatically decreased due to the Pt cathode removal. The power densities curves indicate that there were mass transfer limitations near the electrodes for both types of cathodes, arguably slightly higher for the Pt cathode than the granular cathode.

Figure 5.25 indicated that the highest power density produced from the stacked MFC without the Pt contained cathode was 3.5 W/m^3 MFC, corresponding to an optimal Voltage of 0.24 V and current of 14.7 A/m^3 MFC. So the optimal external resistance was calculated to be 0.24 V/4.05 mA = 59 Ω compared to 30 Ω in the MFC with Pt in cathode. Compared with the MFC polarization curve performance with the Pt contained cathode, the maximum power density was 11.6 W/m^3MFC, the corresponding cell voltage was 0.32 V and the current density was 35.6 A/m^3MFC. Hence, even without the 5 g/m^2 of Pt to act as a catalyst, the stacked MFC still have a decent power generation. The maximum power density was decreased to 69.8 % compared to the Pt contained MFC and a corresponding decrease in current density of around 58.7 % in Section 4.2.1.1.

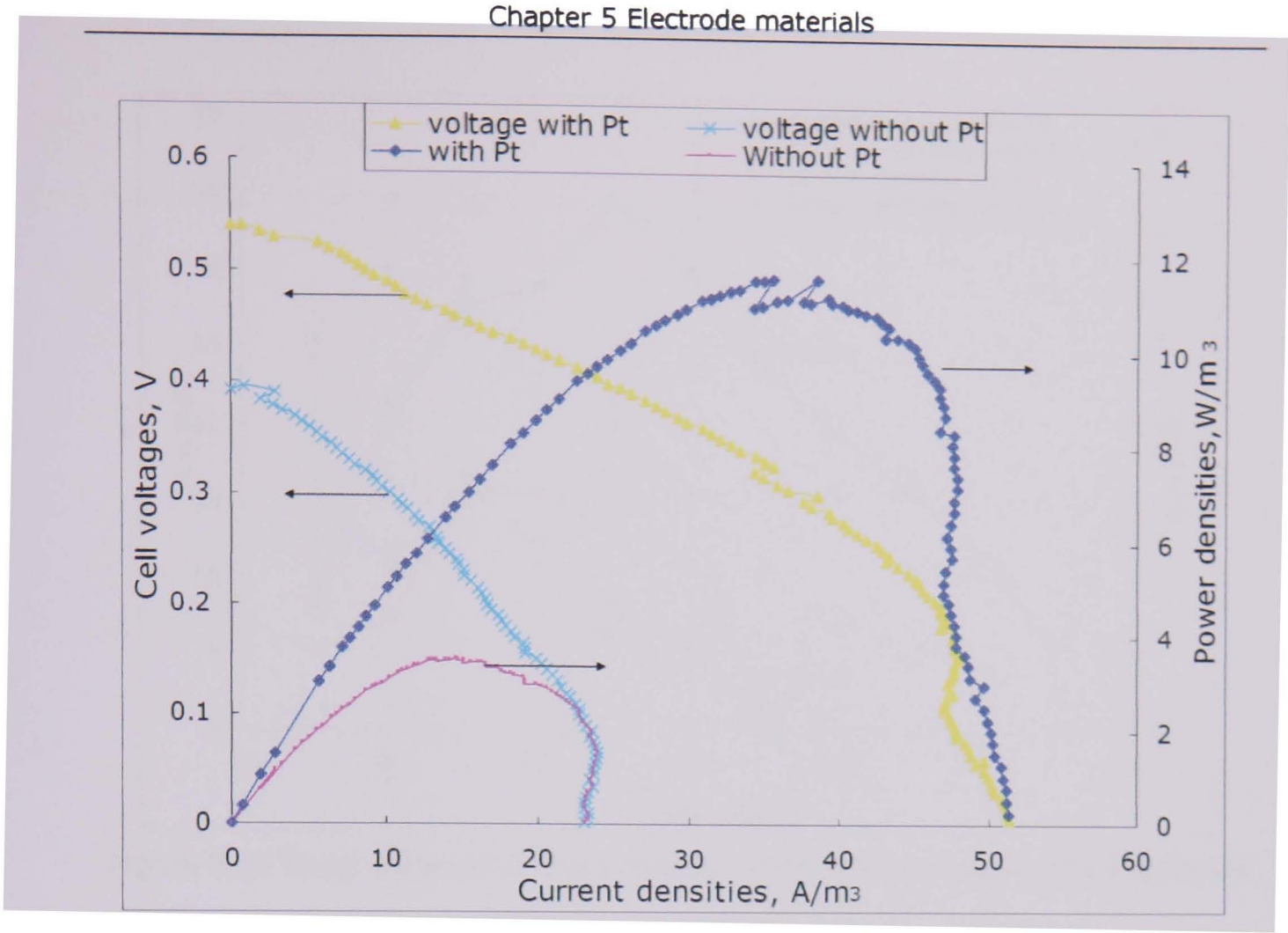

Figure 5.24 Polarization curves in stacked MFC with and without Pt in cathode

The fixed cell voltage method was used to check the response of the current and the power densities with applying a fixed cell voltage in several periods. It helps to evaluate the actual capability of the MFC while the longer period of observation at certain cell voltage. A series of fixed cell voltage were applied by the potentiostat to the cell from 0.05 V to 0.55 V with the interval of 1h per fixed voltage. Without extra electron flow into the system, the potentiostat system was used to control and fix the cell voltage at a certain value. Figure 5.26 shows the trend of current densities and power densities as the function of the gradually increasing fixed cell voltages in the stacked MFC with and without Pt catalyst. At a fixed cell voltage of 0.2 V, the maximum power density was 2.3 W/m^3 for the MFC containing non-Pt cathode compared to 5.2 W/m^3 MFC with Pt contained cathode. At a fixed voltage of 0.15 V, the maximum current density was 15.7 A/ m^3 without Pt compared to 32.5 A/ m^3 with Pt contained cathode. The maximum PD was decreased 55 % compared with the Pt contained cathode and the produced maximum current density was decreased with about 52 %.

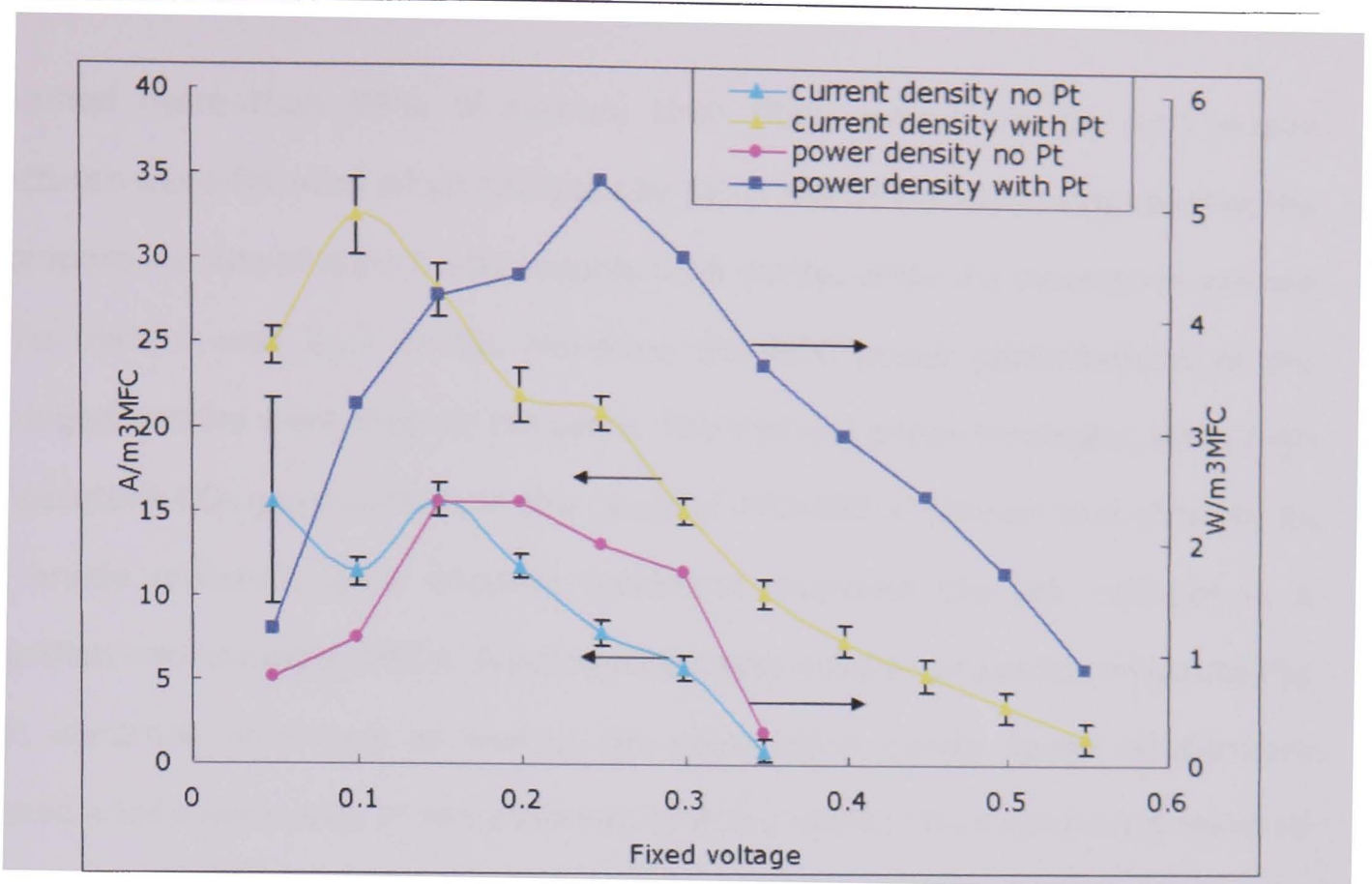

Figure 5.25 Fixed voltage control in stacked MFC with and without Pt in cathode

The results indicate that without Pt as a catalyst in the cathode materials, stacked MFC still can have some power generation. But the power densities and produced current densities were reduced with 52 % to 55 % compared with Pt as cathode catalyst during the actual running of the stacked MFC. However, moving away from a Pt based cathode can remove one of the major economic barriers for the further industrial applications of this technology. Thus, an alternative catalyst may be needed to maintain performance and reduce the investment costs.

5.5 Summary

In this chapter, thermal and chemical anode treatment methods were introduced and the performances of the treated anode materials were tested. An alternative cathode material using graphite granules in the stacked MFC was also tested and compared with cathode materials containing Pt.

Although the two plain carbon cloth anode materials tested, namely B and D, both

contained more than 99% of carbon, their fibre, overall density and weave structures were different when analysed by SEM. The BET analysis showed that the macropore volume of plain B was roughly 0.66 cm^3/g, while the macropore volume of the plain D was 2.27 cm^3/g. However, the MFC power performances of the untreated anodes were roughly the same. The thermal anode treatment using high temperature CO_2 gas oxidation in the range of 400-800°C showed that virtually all the anode materials after thermal treatment improved the cell voltages in a simplified two-chamber MFCs. A potentiostat was used to accurately measure the OCP, electrode potentials as well as the polarization curves based on different treated anode materials. It was observed that the 600°C CO_2 treatment B material and the 800 °C CO_2 treatment D material had the best power performance. The 600°C B material has an improvement of around 195% in power density compare to that of plain B materials and the 800 °C D material has an improvement of around 78% in power density compare to that of plain D material based on polarization curves data. Further examination using SEM demonstrates that the increased performance of the high temperature treated anode may be attributed to the exfoliation of the carbon fibres where the exfoliation might help bacteria to fasten and grow on the surface of fibre.

Chemical treatment of the anode material using common acids and alkaline was also carried out. The cell voltage data as well as the polarization curves data indicated that the MFCs with anode materials before and after treatment had very similar power densities, or that chemical treatment even resulted in decreased power densities. The data indicated that chemical treatment does not improve power performance for the fibre based anode materials. SEM suggested that there was almost no change of the fibre surfaces compare to the plain B and D materials. It was concluded that, rather than changing the anode materials structure and surface functional groups, acids and alkaline treatment may have the effect of cleaning the surface of anode fibre to prevent the bacteria growth on the surface.

For the cathode alternative materials, it was shown that pure graphite granules without catalyst can be used as cathode materials. The power density result based on stacked MFC shows that the maximum power density and current density were to 2.3 W/m^3 and 15.7 A/ m^3, respectively. Although the power density and current density are around 50% lower than that of the MFC with Pt as cathode catalyst, the market value of graphite granules compare to Pt catalyst contained cathode materials is still very attractive. The removal of Pt catalyst removes one of the major economic barriers for the further industrial applications of MFCs technology.

Chapter 6 Barriers

6.1 MFCs barriers

From the background study of MFCs in Chapter 2 and the MFC experiments data and analysis shown in Chapters 4 and 5, it is clear that the power generated from MFCs currently is not comparable to the normal energy requirements for most industries. The present industrial interest in MFCs is towards its potential to reduce COD without requiring aeration, i.e. as a low cost alternative to traditional water treatment technology. However, increasing the energy output of the MFCs can greatly enhance its wider uptake as a green technology. It is therefore urgent that the limitations and barriers that hinder the development and further applications of MFCs be defined and solved for its commercial use. The current MFC performance limitation will be introduced and the main rate limiting steps of MFCs are summarized in this chapter.

The main barriers identified during this work are related to the size of the reactor, the volume of its chambers, the distance between chambers, materials used and the way they are applied in the reactor as electrodes and medium for cell cultures used in the system and the connections of electrodes in the overall MFC. These are the main factors identified in this work that affect the performance of the MFCs and correlates well with other research groups' results where several internal aspects of MFCs have been found to restrict and impact MFC performance. On the macroscopic aspects, the design of MFCs plays a significant role in MFCs, including the structure of the MFCs, their effective volume of anodic and cathodic chambers, the distance between anode and cathode and the electrode connection points. The running mode of MFCs, either continuous or batch, the influent flow rates, environmental conditions such as temperature, pH value of medium solution and the reactor pressure are also factors that affect the MFCs performance. The

efficiency of the bacteria cultures in the MFCs is one of the most essential factors that affects MFCs performance, and a great deal of work is applied by biologists to identify high-performance bacteria. Also, the morphology and materials of electrodes, ion exchange membranes used to separate anode and cathode chambers, the influent medium as well as the substrates contained in the medium all can impact the MFCs performance. However, some barriers are of significant importance while others have minor parts to play. The main aim with this work is to identify which barriers are most important for the overall MFC setup of this work.

Figure 6.1 illustrates the main barriers of MFCs during the energy transformation process within the whole MFCs process. From introducing the organic content to converting it to electrical and chemical energy contained in produced gases, a substantial number of processes and transfer steps can be distinguished in relation to the organic matters contact with electrode materials, bacteria metabolism, electrons and protons generation, donation, transportation and reaction afterwards. The procedure can be roughly separated to seven transfer steps.

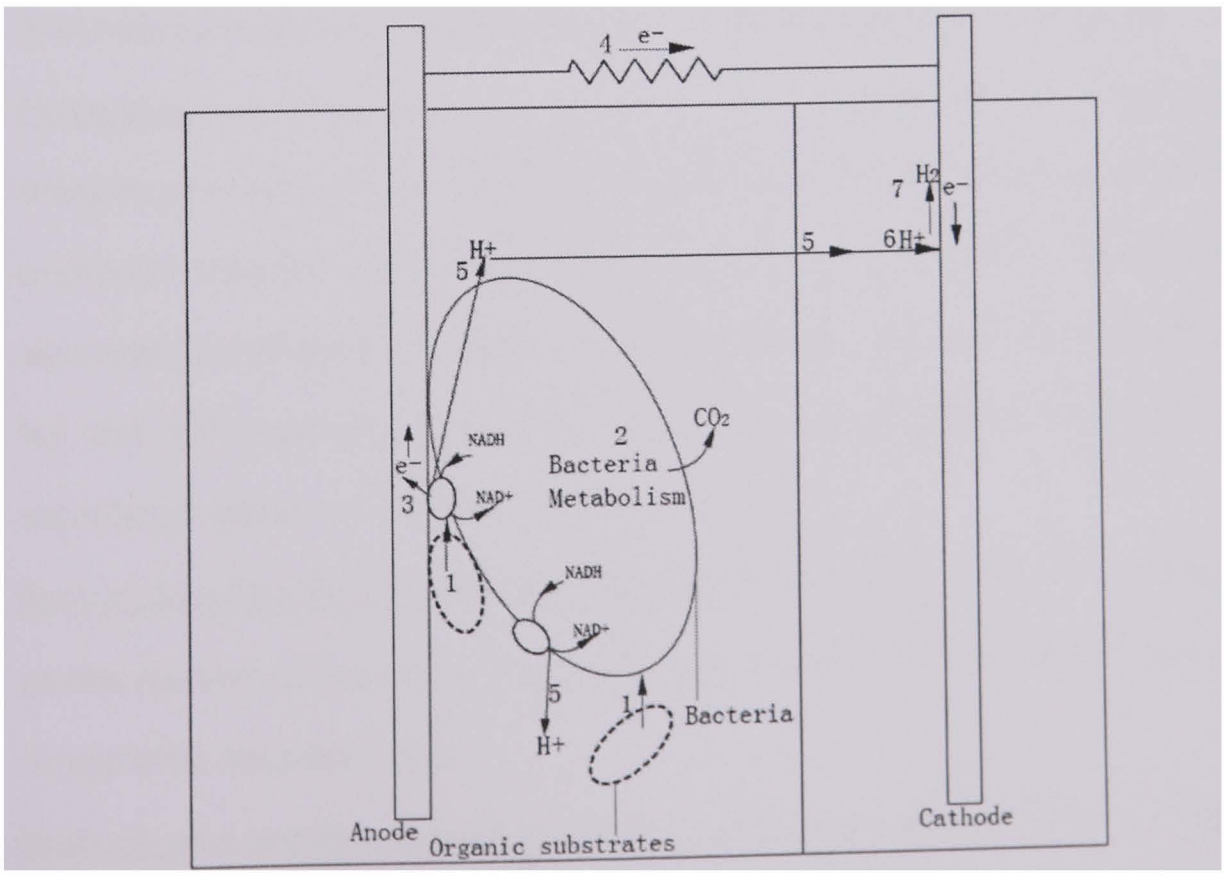

Figure 6.1 Overview of the seven transfer steps during the MFC process (adapted from Korneel Rabaey, W.V., 2005)

1. Organic substrate uptake by the bacteria. This initial process involves substrates and organic matters mixing into the liquid reactor phase and then diffusing to the bacteria surface where the bacteria start to collect attainable substrates;
2. Bacteria metabolism. The metabolism process is a complex biological process where the bacteria are consuming all or parts of the substrate as outlined in Section 2.2.5.2;
3. Electrons go out of bacteria and transfer to the anode. After the bacteria have satisfied their own needs such as self-living and energy for their other activities, extra electrons are transferred towards the extracellular environment as well as electrode at a certain transfer rate. The transfer rate of electrons to anode determines the coulombic efficiency. The transfer processes to anode, including several different routes such as directly transfer and transfer with mediators. It is a crucial process that determines the current densities of MFCs;
4. Electrons through external circuit to cathode electrode. This process mainly depends on the external resistance and also including the wire materials and connection materials which have resistance to electrons transfer as well. It determines potential losses between anode and cathode electrode;
5. Protons go out of bacteria and transport to the cathode. Similar to the electrons transfer process, protons are also released to the extracellular environment at a certain transfer rate. If the transportation of protons to cathode is rapid, abundantly and easily carried out without too much obstruction, it will be easier for the MFCs power generation. It is also a substantial process that has significant effect on the MFCs performance;
6. Proton transfer to the surface of cathode. The process of protons congregating on the surface of the cathode is also important to determine the redox reactions in cathode chamber; and
7. Protons and electrons produce H_2 at cathode electrode. This is probably the most difficult process within the MFC system. Some research suggests that the formation of H_2 need a potential difference of minimum -0.42 V. It is difficult for

protons and electrons to directly form H_2 in this circumstance. An external voltage applied over the cell might help achieve the H_2 production process.

With their crucial effect on MFCs' performance, several of these most difficult rate limiting steps and most intricate parts are briefly summarized to highlight their importance. Step 1 can be directly enhanced using engineering principles but might impact Step 2 that deals with the complicated bacteria metabolism process, which is difficult to influence and control. The bacteria metabolism routes are difficult to change except for some further techniques such as species cultivation or genetic engineering to find high-performance species which have higher potential to transfer more electrons and protons outside of the bacteria. The work here has used a readily available bacteria culture that the industry is used to working with and investigated the operational barriers concerning this culture. Step 3 is the crucial processes for electron transfer from the bacteria side to cathode and has been tested in this work, while Step 4 is governed mainly by the quality of the material available. Steps 5 and 6 are the processes of proton transfer from anode to the cathode, where the MFC reactor setup and the internal usage of any membranes will affect the proton transfer rate between chambers and onto the cathode surface. According to several research groups (Jang, J.K. et al., 2004; Oh, S.E. and Logan, B.E., 2006), the transfer resistance between anode and cathode chambers can be greatly reduced by operating without the proton exchange membrane that make proton more likely to travel to cathode chamber. Medium solution condition in cathode chamber is another crucial factor to control the transformation of protons onto cathode surface. On the other side, this could result in the bacteria growth on the cathode electrode as well, which might have further advantages for the MFCs system. Step 7 is the process of electrochemical reaction to produce H_2. The potential difference between anode and cathode are the essential factor. In order to illustrate the importance of these steps and also find out the chief factors of the whole MFCs processes, several experiments were designed and carried out.

6.2 Rate limiting steps

A range of experiments were carried out to establish the main rate limiting steps for the MFCs studied in this work. Detailed results and discussion are provided below.

6.2.1 Substrate uptake by bacteria

It is commonly accepted that with increasing concentration of biological organisms, such as bacteria concentration in a wastewater, the organic matters contained in wastewater is consumed quicker. To find the optimum range of bacteria concentration for MFC applications that address both the rate of organic removal and also the coulombic efficiencies from converting organic contents into electricity, experiments were carried out in both batch and continuous mode as outlined below:

(1) A total of 6 simplified two chamber MFCs containing 500 ml wastewater with 5 g, 10 g and 20 g of active sludge added in duplicate set up. After mixing, the wastewater mix was used as anode influent.

(2) For the batch MFCs the cathode medium used was plain wastewater with COD level as low as 18 mg/L. For continuous MFCs, the same medium as for the anode was used for the cathode in order to maintain the same level of COD in the system. The medium were circulated during experiments with a peristaltic pump at approximately 11.5 ml/min.

(3) About 1.0 g/L of acetate was added into anode influents as bacteria substrate as well as the cathode medium in continuous MFCs and the initial COD level in the anode chamber was tested.

(4) The experimental physical condition were kept the same, including identical anode and cathode electrode materials applied, the use of an "n" shaped tubing to connect anode and cathode chambers, running for 5 days as

anaerobic batch or continuous MFCs, and recording all cell voltage data through a data logger system.

(5) After the experiments stopped, the COD of the wastewater in the anode chamber was tested again.

For the process of substrate transportation to bacteria, the experimental COD removal results are shown in Table 6.1. For the three batch MFCs with increasing amount of active sludge MFC2 with moderate active sludge level had the highest overall COD removal rate. However, based on the COD removal per gram of activated sludge added, there was a sharp decreasing trend from 49 to 23 when increasing the activated sludge from 10g to 40 g, respectively. This indicates that for batch mode the transfer of organic components to the bacteria is the rate limiting step. In the three continuous MFCs, the COD removal rates were increased with increasing amount of active sludge. In addition, the COD removal per gram of activated sludge added was levelling out at a factor of about 29. This indicates that for continuous MFCs, higher concentration of active sludge induces higher COD removal rate, i.e. the substrate to bacteria step is not a significant barrier in the continuous MFCs process. Compared to batch conditions, higher concentration of active sludge is needed for continuous MFCs to obtain improved efficiencies. This suggests that the barrier of transport of organic to the bacteria is significantly reduced with continuous MFC if high concentration of bacteria is applied.

Table 6.1 MFCs with different substrate concentrations and COD removal rates

MFCs	Batch MFC 1	Batch MFC 2	Batch MFC 3	Conti. MFC 1	Conti. MFC 2	Conti. MFC3
Active sludge, g/L	10	20	40	10	20	40
BOD mg/L	48	71.7	150.6	48	71.7	150.6
COD with acetate, mg/L	792	850	1360	792	850	1360
COD after mg/L	304	104	440	400	288	192
COD Removal per g AS	49	37	23	39	28	29
COD Removal Rate, %	61.6	87.8	67.6	49.5	66.1	85.9

6.2.2 Bacteria metabolism

The process of organic matters consumed by the bacteria was reviewed in Section 2.3.6. The mechanisms and limitations of microbial activities in terms of the bacteria metabolism and the produced electrons and protons migration out of bacteria were introduced. The brief limitations of bacteria and related areas have been explained. Since the improvement of certain bacteria properties, such as electron and proton transfer out of bacteria, is within a biological research scope and not within the scope of this work, only a few experiments related to this area were performed in this work applied to the same bacteria culture. The role of electron and proton migration barriers were assessed by chemically changing their concentrations in anode and cathode chambers shown later in Section 6.2.4.

6.2.3 Electron transfer to the anode

6.2.3.1 Electron transfer efficiency

The MFCs setting outlined in Section 6.2.1 was used to do the further tests for electron transfer behaviours. The coulombic efficiency was calculated as shown in Table 6.2. The data indicate that the coulombic efficiency is reduced while increasing the active sludge concentrations under both batch and continuous mode and is hence a significant rate limiting step during the MFCs process. The limited sites on the anode surface for bacteria interaction could be a possible explanation for this decrease. The transfer and usage of extra electrons is forced to take place in free water instead of at the anode surface. Developments in Chapter 5 can mitigate for these factors. It is interesting to note that both batch and continuous decreases about 1/3 from 10 g to 40 g activated sludge added, indicating that the effect is independent of the mode used.

Table 6.2 Coulombic efficiencies of MFCs with different conditions

MFC	Activated Sludge, g/L	Coulombic Efficiency,%
Batch1	10	$4.5*10^{-4}$
Batch2	20	$3.6*10^{-4}$
Batch3	40	$3.1*10^{-4}$
Continuous 4	10	$2.4*10^{-4}$
Continuous 5	20	$1.9*10^{-4}$
Continuous 6	40	$1.6*10^{-4}$

The corresponding cell voltage data from power productions are shown in Figures 6.2 to 6.5, where Figure 6.2 and 6.4 shows the incubation period and Figure 6.3 and 6.5 shows the data at relatively stable conditions for both batch MFC and continuous MFC, respectively. The trends of the cell voltages based on different MFCs are similar with their power densities due to the same external resistance and the similar effective surface areas of anode material used in these MFCs.

Figure 6.2 indicates that during the bacterial growth period, the three batch MFCs experienced bacteria incubation and some of the bacteria developed on the surface of anode materials as indicated by increasing cell voltage. At the beginning of the MFCs experiments, the produced cell voltages were very low and all the batch MFCs had almost identical growing tracks based on the cell voltages data. After around 17 h of bacteria cultivation, the three batch MFCs appeared to differ in power performances. The MFC2 had the higher cell voltage of around 0.4 V, while MFC1, which contained little active sludge used as bacteria culture, had the lowest cell voltage of around 0.2 V. After 25 h, the cell voltage of MFC3, which contained the larger amount of active sludge, increased to the top at around 0.5 V as expected. As the description of the conditions of MFCs before experiments, the only difference of these three batch MFCs was the amount of active sludge as bacteria culture. Figure 6.2 shows that after the basic bacteria incubation period, the one with the most of active sludge had the highest cell voltage and corresponding power density.

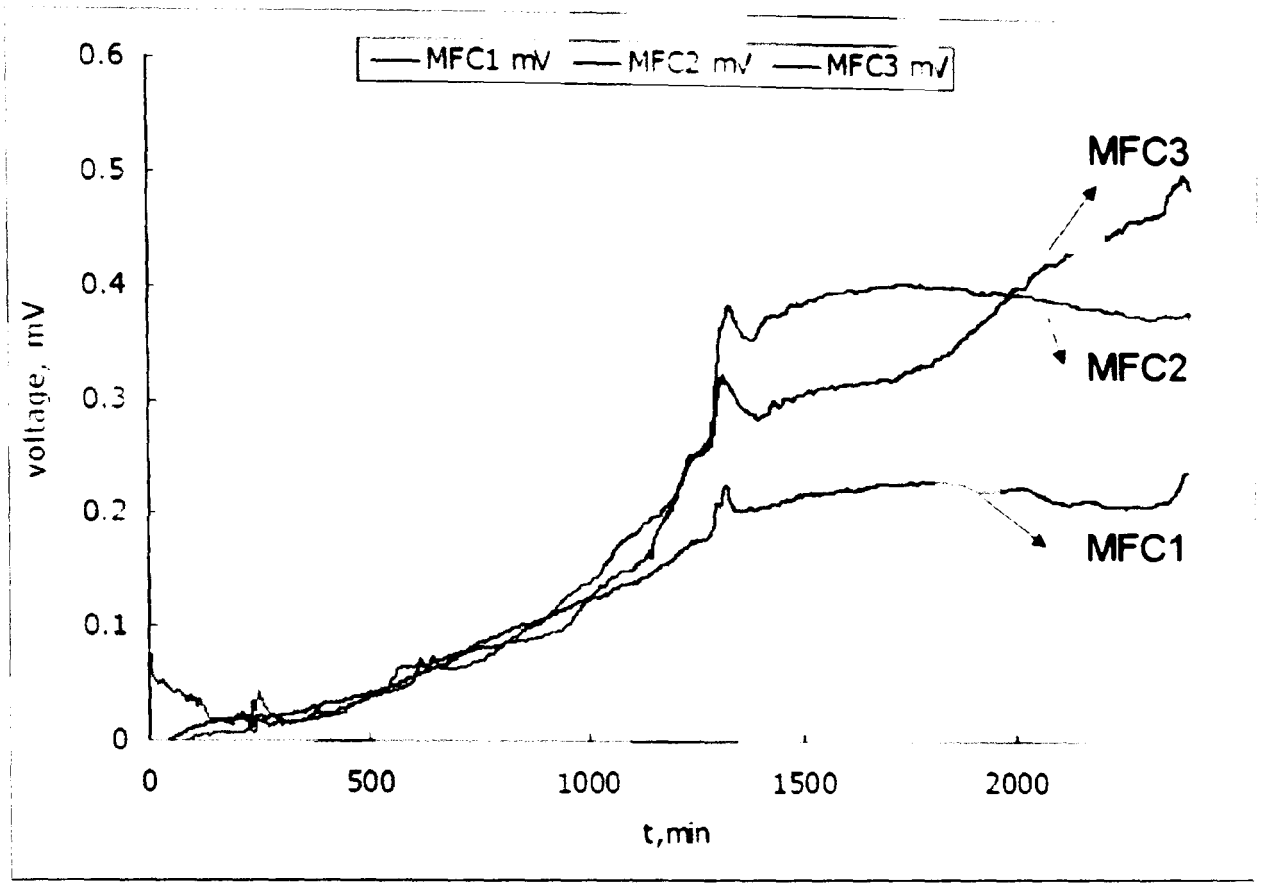

Figure 6.2 Cell voltages of three batch MFCs during incubation period

During the relatively stable period in Figure 6.3, the three batch MFCs were more or less at a steady state where the anode wastewater chamber medium supplied a firm support of substrates to bacteria. From Figure 6.3, it is clear that at the first 40 h to 85 h, MFC3 with most amount of active sludge had the highest power density, which was around 0.7 mV, while MFC2 and MFC1 had slightly lower levels of power densities, which were approximately 0.4 mV and 0.3 mV, respectively. But after 85 h from the beginning of experiments, the situation was altered initially. Both MFC1 and MFC2 increased, but MFC3 with more bacteria contents decreased to around 0.5 mV. This is probably due to excessive bacteria growth in MFC3 with 40 g active sludge added, while the bacteria growth in MFC1 and 2 are catching up with the initial concentration of MFC3. It demonstrates that cell voltages produced from these three MFCs were not proportionate to the initial amount of bacteria. Bacteria would occupy the anode surface to form the biofilm. But not all of these bacteria have the ability to directly transfer electrons onto the anode surface. It indicates that increasing the sites on the anode for electron transfer is essential for improved electricity generation.

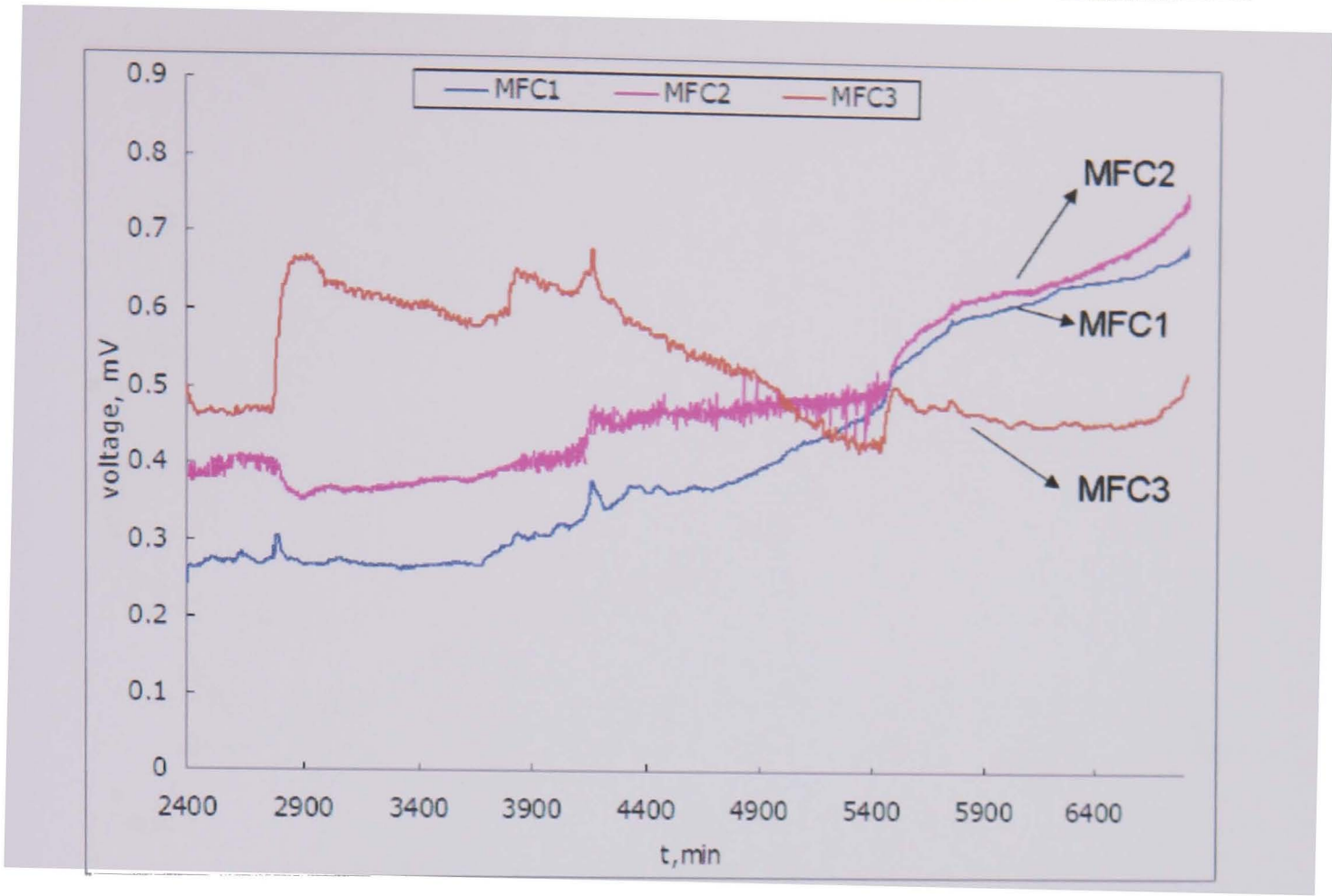

Figure 6.3 Cell voltages of three batch MFCs during stable period

Figure 6.4 shows the cell voltage data of the continuous MFCs during the incubation period. MFC6 with more extent of active sludge as bacteria incubation culture had a more rapid production of electricity at the beginning of MFC running. It is interesting to note that the voltage increase is faster than compared to the batch mode in Figure 6.2. After 1400 min, MFC5 improved compared with MFC6 to a slightly higher cell voltage of 0.8 mV with a difference around 0.1 mV. A bad connection made the voltage data of MFC4 not available. Figure 6.4 indicates that the increasing cell voltages of MFC5 and MFC6 were not proportionate to the initial amount of active sludge, again indicates that the amount of sites on the anode for electron transfer is a key factor. Compared with Figure 6.2, the role of mediators might not be large due to enough substrates being supplied to fulfil the bacteria metabolism that might produce self-mediators for electron transfer later on.

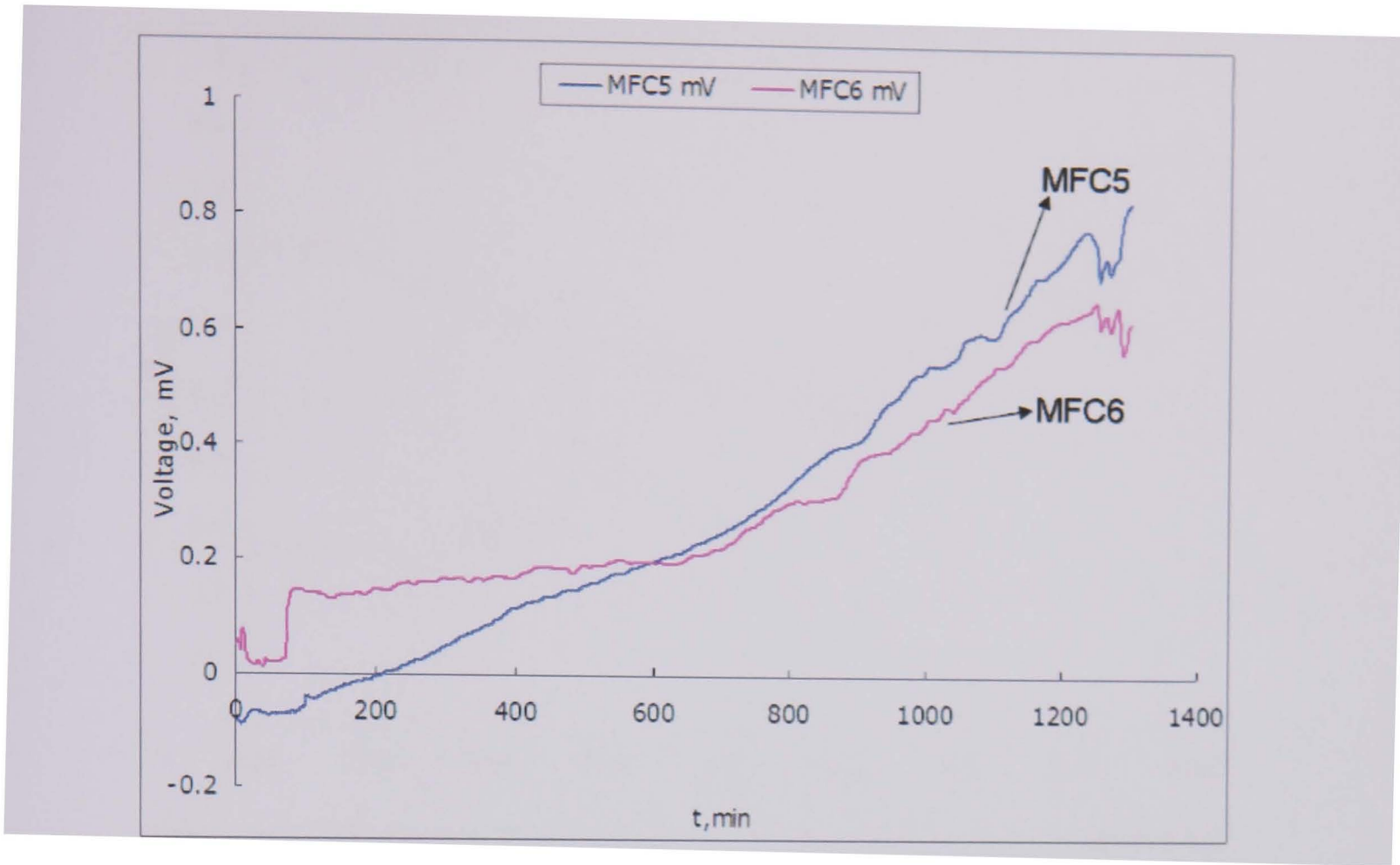

Figure 6.4 Cell voltages of continuous MFC5 & MFC6 during growing period

Figure 6.5 shows the cell voltages of continuous MFCs at a relatively stable state. The cell voltage of MFC5 was dramatically decreased due to failed connection of the data logger with the extended wires. However, MFC4 was re-established and shown. The data of MFC5 should be similar to MFC4. From Figure 6.5, between 47 h to 88h from the beginning of experiments, the MFC6 with higher extent of bacteria had higher cell voltage of 0.6 mV, while the MFC4 had the cell voltage of around 0.3 mV. After 88 h, it seemed the cell voltage of MFC4 started to increase to a level as high as 0.9 mV. MFC6 started to slow the increasing rate and kept around 0.7 mV similar to MFC3 under batch condition in Figure 6.3. This indicates that the increasing cell voltages of MFC4 and MFC6 were not proportionate to the initial amount of active sludge as well.

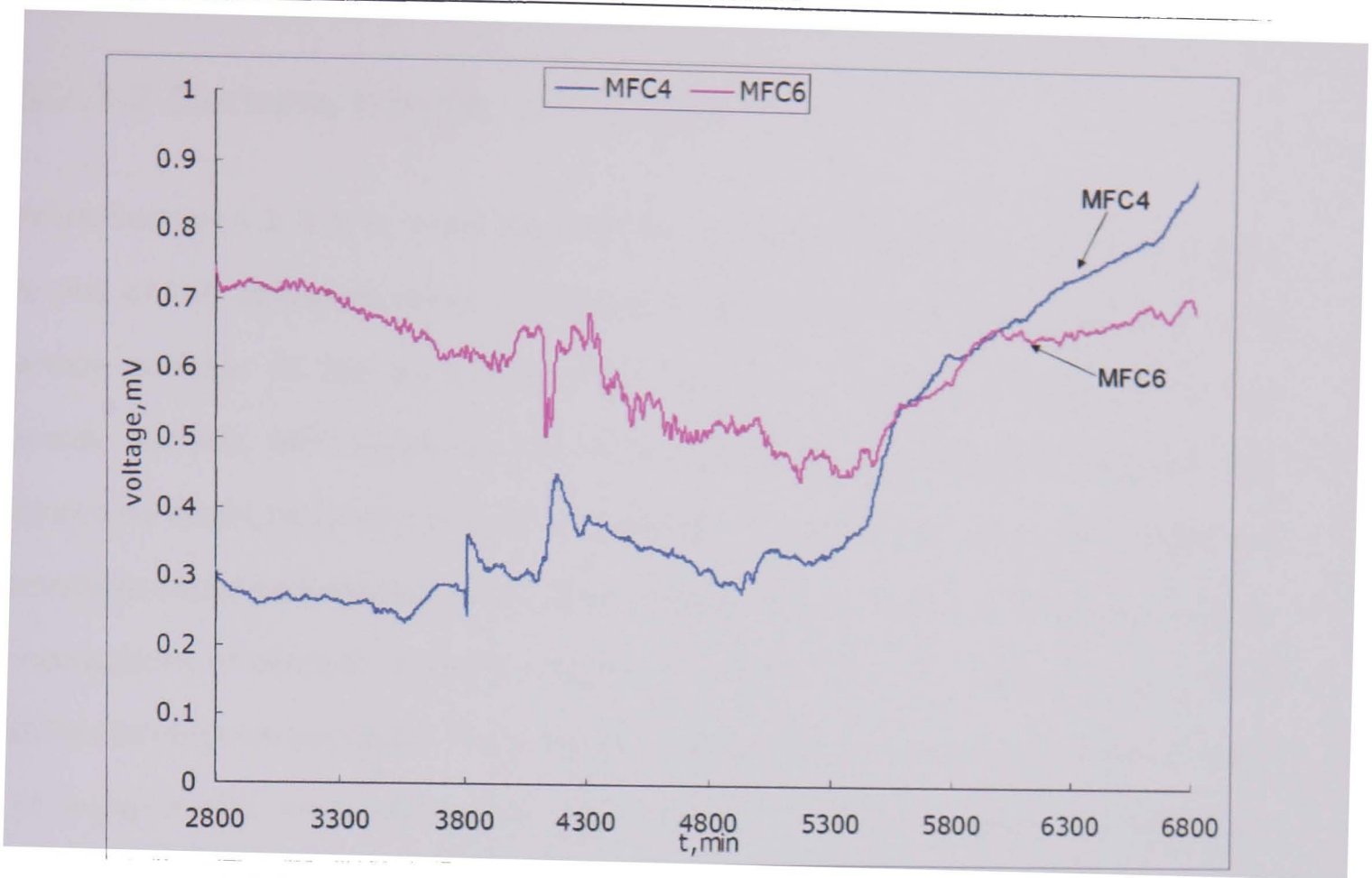

Figure 6.5 Cell voltages of two continuous MFC4 &MFC6 during stable period

In summary, by comparing the coulombic efficiency data with the COD removal rate data, the experiments suggest that larger amount of active sludge induces higher COD removal rate at continuous flow, which means the transfer process from substrates to bacteria is not limited, especially in the case for continuous MFC. Hence, the bacteria metabolism is not limited by the substrate transfer process. It shows that the role of bacteria external mediators produced from bacteria for electron transfer is not large. But with higher bacteria concentration in the influent wastewater, the overall coulombic efficiencies were lowered which means smaller amount of electrons converted from substrates by bacteria are transferred to the anode. This indicates that the increasing cell voltages of MFCs were not proportionate to the initial amount of active sludge added to the system. The feasible amount of sites on the anode surface for electron transfer is therefore pivotal for electrons to be successfully transferred to the anode. The sites available on the anode are the main limitation step in MFCs process compared to substrate transport.

6.2.3.2 Electrons transfer onto anode

From Section 6.2.3.1, it concludes that the amount of sites available on the anode is one of the limitation steps of the electron transfer processes from bacteria to anode surface. As the electron transfer chain of the bacteria terminates at the anode surface, MFC relies on the anode reducing the electrons. However, the electrons might be involved in other spontaneous reductions before they reach the anode to cause cell efficiency reduction. Therefore, it is important to investigate the interactions of electron acceptor in the wastewater. In order to find the effects of different electron accepters in the anode chambers under batch conditions, a range of experiments were conducted. Equations 1, 31 and 32 show the reductive reactions of these chemicals and their reduction potentials (Madigan, M.T. and Martinko, J., 2006).

$NO_3^- + 2H^+ + 2e^- \rightarrow NO_2^- + H_2O$ E_0': +0.43V vs. NHE Equation (31)

$SO_4^{2-} + 9H^+ + 8e^- \rightarrow HS^- + 4H_2O$ E_0': -0.22V vs. NHE Equation (32)

$4H^+ + 4e^- + O_2 \rightarrow 2H_2O$ E_0': +0.82V vs. NHE Equation (1)

(1) In total 4 parallel MFC experiments were carried out. The anaerobic anode chambers were all kept the same using wastewater with 4.5 g/L active sludge and 1 g/L acetate as substrate. The cathode chambers were wastewater with 2 g/L active sludge.

(2) The initial COD levels of the anode feed were tested.

(3) 10.0 ml of 1M Na_2SO_4 and KNO_3 were added into MFC1 and MFC2, respectively. The MFC3 was a normal batch MFC without additives. MFC4 was aerobic MFC with O_2 pumping into the anode chamber.

(4) The MFCs were run for 24 hours and the open circuit cell voltages were continuously monitored using a data logger. The end COD in the anode chamber was measured.

The change in cell voltage was calculated based on the conventional cell model where the OCP is determined by taking the difference between the cathode and anode. The cell voltages are proportional with OCP. In principle, $E_{cathode}$ remains constantly and E_{anode} will change when a variety of oxidative species are introduced into the anode chamber.

Anode: Organic substrate $+H_2O \xrightarrow{(bacteria)} CO_2+H^+ + e^-$ Equation (33)

Cathode: $4H^+ + 4e^- + O_2 \longrightarrow 2H_2O$ $E=0.82$ V (PH=7, NHE) Equation (1)

Ideal OCP difference= $E_{cathode}$- E_{anode} Equation (34)

Figure 6.6 shows the cell voltage changes of the MFC, in presence of KNO_3 and Na_2SO_4, respectively. The chemicals were added twice (i) initially, and (ii) after around 18 h. The cell voltage of MFC3 without addition is steadily increasing from about 0.1 mV initially to about 0.8 mV after 24 hours under batch conditions. When 10 ml Na_2SO_4 (1M) was introduced in the anode chamber of MFC1, it had virtually no effect. This indicates that electron can not be donated to Na_2SO_4 as a redox reactor because of its potential barrier in Equation (32). But the power density was generally higher than normal MFC, which might due to SO_4^{2-} acts as an extra e^- carrier to help e^- transfer onto anode. The cell voltages changes when adding the same amount of KNO_3 in MFC2 shows a rapid increase at the beginning and the cell voltage gradually dropped from 2.5 mV to 1 mV. This phenomenon can be explained that electrons produced from organic degradation were donated to KNO_3 in terms of a reduction reaction (Equation 31). A new complex equilibrium was established with lower anode electrode potential. e- would like to be transferred to matters with higher potential, i.e., more likely to transfer to NO_3^- (Eo=0.43V) instead of anode electrode (Eo=0V). However, as system continuous consumed KNO_3, the anode potential decrease towards the cell voltage of normal MFC3. The result of the second addition of KNO_3 proved that the OCP can be increased temporarily by adding KNO_3.

In summary, it is indicated that the use of external oxidative species (E>0) can enlarge the potential difference between the two chambers, which means higher current production. But the modified cell voltage reduced gradually to the value without addition when external oxidative species were consumed completely. Utilizing a small amount of oxygen might be an easy way to achieving this.

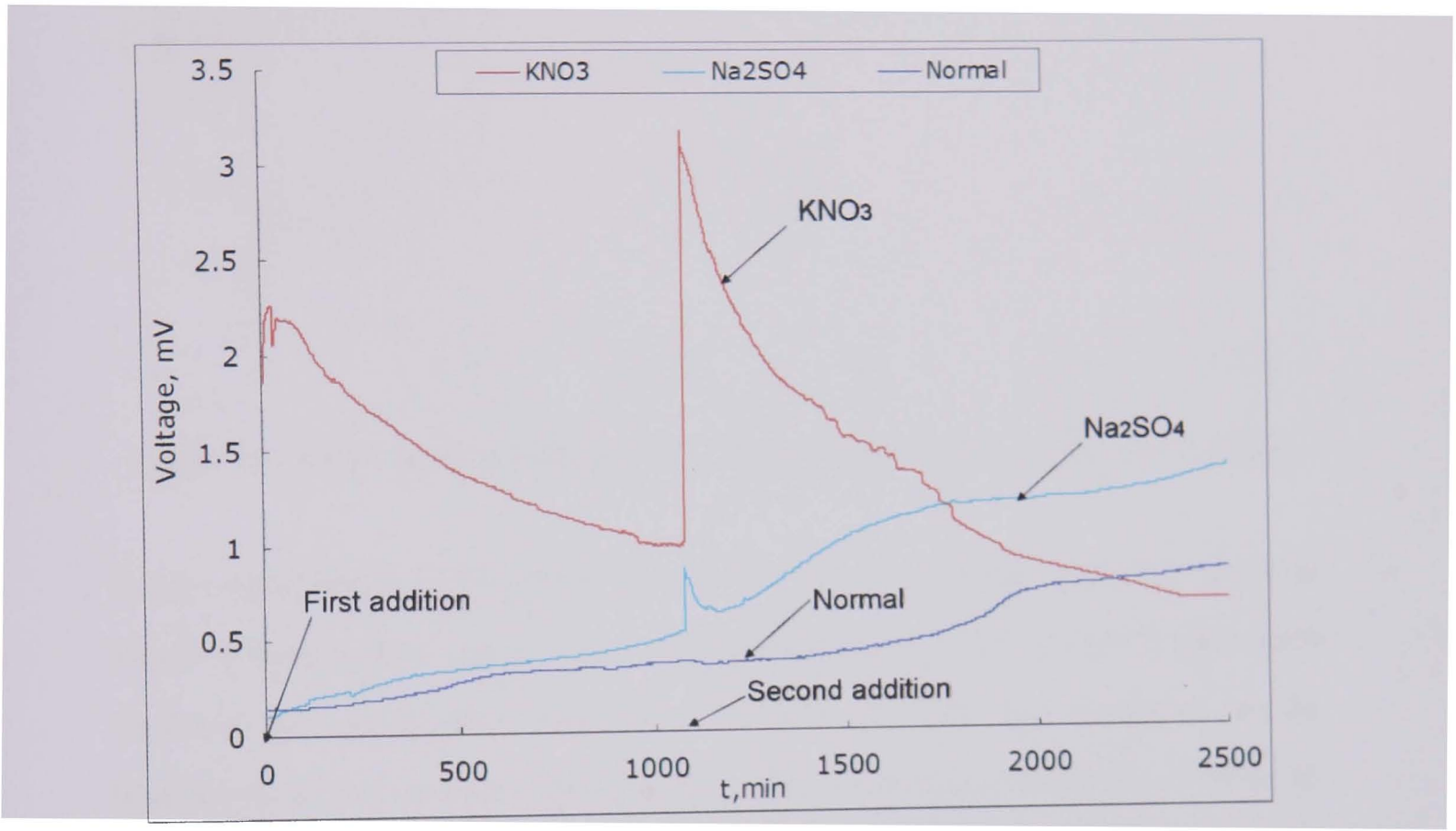

Figure 6.6 cell voltages of MFCs with 2 different electron acceptors added in anodes compare with normal batch MFC

Figure 6.7 compares the normal bath MFC3 with MFC4 where air was supplied in the anode chamber. For the first 25 h, MFC4 was run as the normal MFC which has similar cell voltage data as MFC3. After 25 h, the air was continuously bubbled into anode chamber of MFC4 which induced a sudden decrease in cell voltage. This is because the anaerobic bacteria in the system were killed by rich O_2 environment, organic matters were consumed by aerobic bacteria and the produced electrons were directly consumed by O_2 without transferring to the anode.

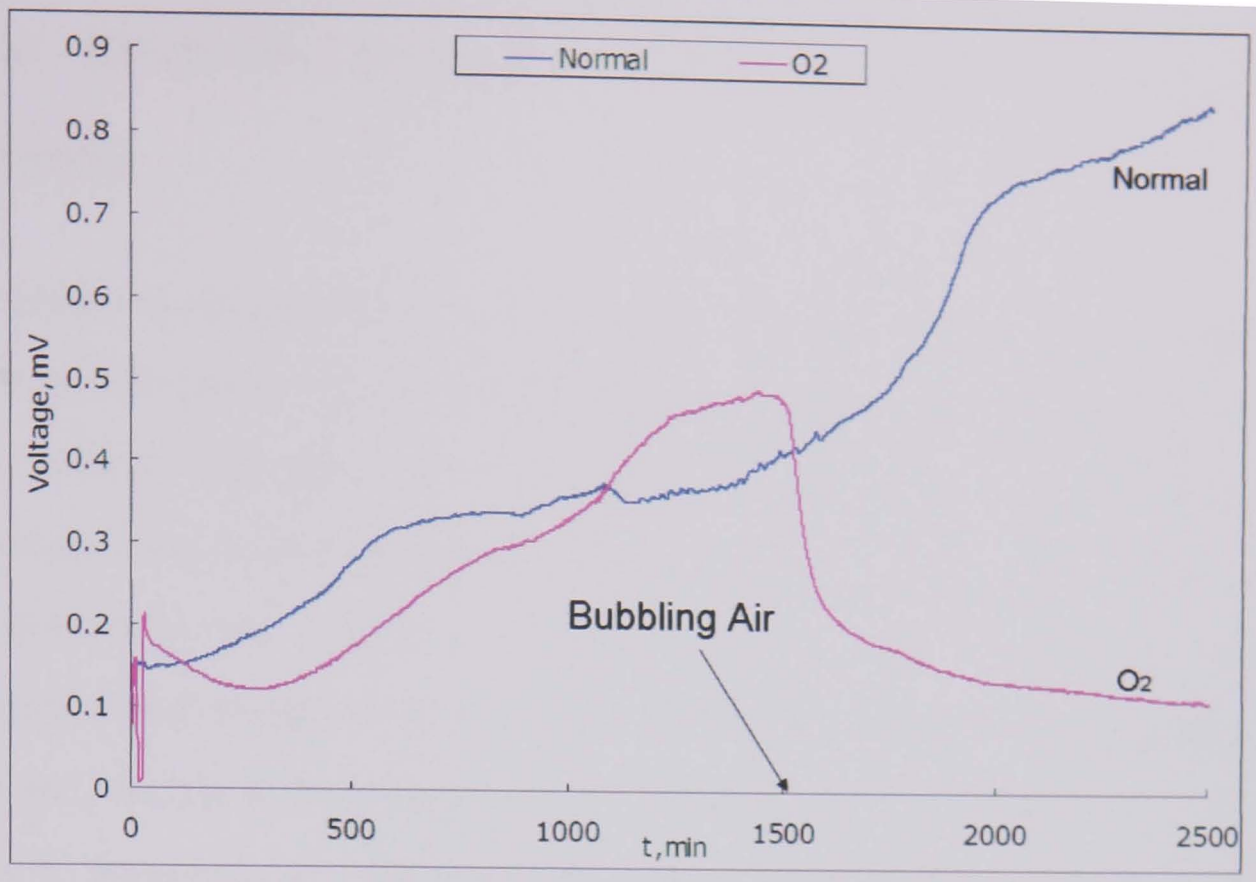

Figure 6.7 MFC4 with air bubbled in anode compared with normal batch MFC3

These experiments demonstrate that it is difficult to donate electrons to MFCs anode in presence of oxygen. The reduction reactions of KNO_3 and O_2 react with electrons are spontaneous reactions. Consequently, little free electrons can be transferred to the anode or electron mediators to generate electricity. In order to improve the power production in the MFCs, these chemicals are needed to be eliminated, thus the electrons transfer on anode can be maintained for electricity generation in MFCs. The dramatic decrease in cell voltages with the presence of other chemicals in the medium proves that an effective transfer of electrons from bacteria to anode is a very important factor for the power performance of MFCs. This could be achieved by attaching mediators to the anode surface or by a control of oxygen.

6.2.4 Electrons through external circuit to cathode electrode

When electrons are gained by the anode electrodes, it will be transferred from the electrode materials to the contact points and then through the external wire with resistor loading. The resistance of the external circuit produce losses. Meanwhile, the protons need to be transported from anode medium to cathode medium, and then arrived to the surface of cathode materials, integrated with electrons transported from the external circuit to form the reaction product. According to Ohm's law, the size of the voltage drop is simply proportional to the current, which is V=I*R (Larminie, J. and Dicks, A., 2003). Figure 6.8 shows the voltage polarization curve based on the stacked MFC. The zone of ohmic loss can be distinguished from Figure 6.8. For the zone between the current densities 5 to 40 A/m^3 of the MFC, the loss of cell voltage was almost linear dependent on the current flowing through the MFC, where the ohmic losses mainly occurred. The internal resistance was calculated from the slope of the voltage polarization curve as 22.8 Ω. The resistance of the anode contact points, the losses during the electron transfer through the metal wires, the medium resistance during proton transport from anode chamber to cathode chamber and the application of membrane in the case of the stacked MFC all affect on the value of the internal resistance in this MFC system that is translated into the power performance of the MFC. Since the factors that determine the internal resistance are fixed, this means that internal resistance is a factor that affects MFC performance but can be modified by changing the material used and is therefore generally a barrier towards cost.

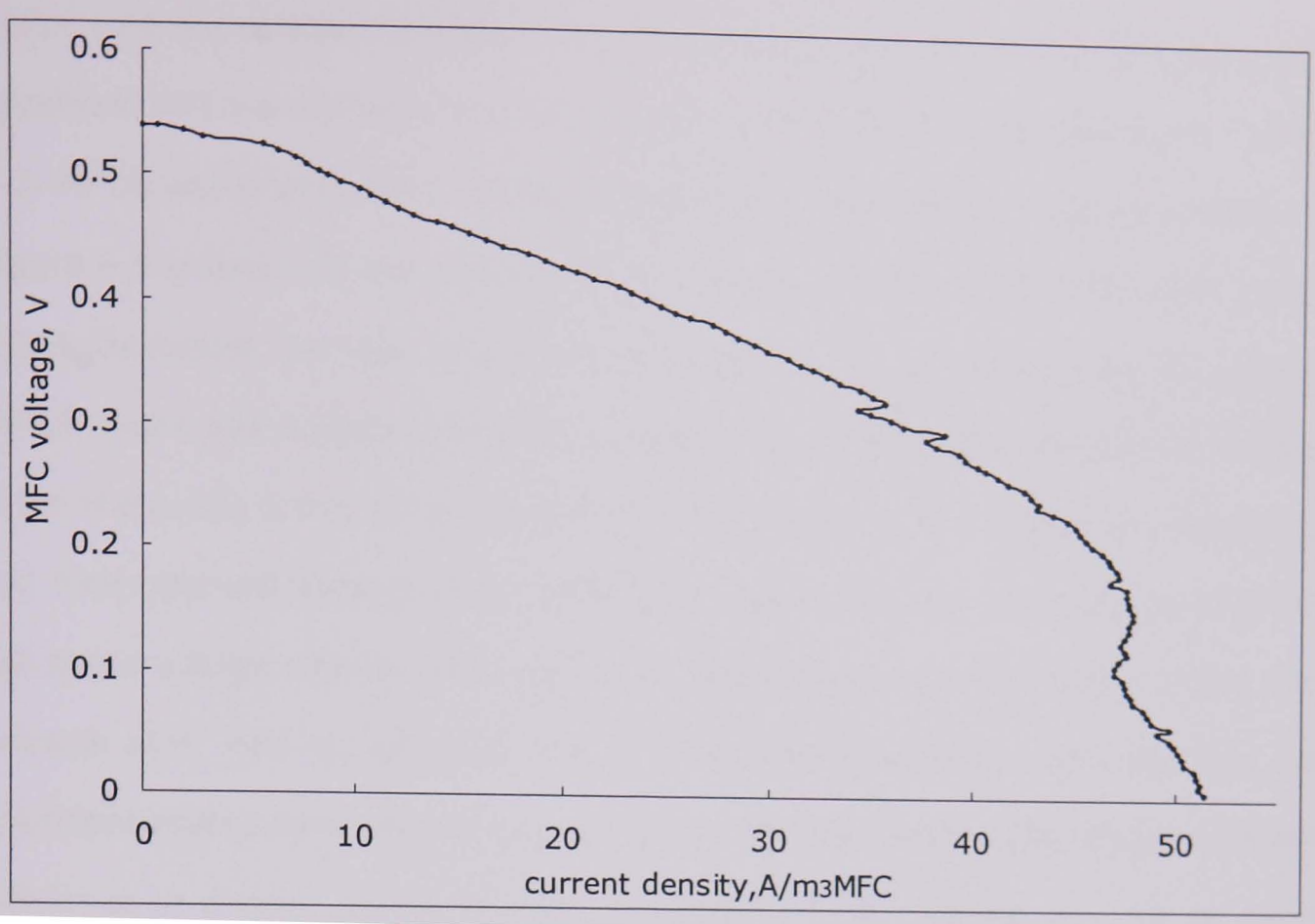

Figure 6.8 Cell voltage polarization curve of the stacked MFC

6.2.5 Proton concentration and transfer activities

It is quite important to see the dominate factors for protons transport from bacteria in anode chamber to cathode chamber as well as the effect of proton concentration towards the MFCs performance. In order to demonstrate the significance of proton transportation from anode to cathode and also test the protons concentration limitation, a series of experiments were designed.

6.2.5.1 Proton transfer in anode

The first range of experiments was designed to show the effect of proton concentration in MFCs anode and cathode, individually. Three simplified two-chamber batch MFCs were used in this experiment. In MFC1, about 0.35 and 2.00 mL of 0.50 M H_2SO_4 was added into the 500 mL cathode chamber at 0 and 35 minutes, respectively. For MFC2, the same procedure using 1.00 M NaOH was

added into the anode chamber. From the start of experiment, two additions were applied to MFC1 and MFC2. The addition times and amount are listed below in Table 6.3. MFC3 was a batch MFC without adding any chemicals to act as the reference. Figure 6.9 shows that the abundance of protons in cathode chamber after adding H_2SO_4 increased the cell voltage of MFC1 to 1.2 mV compared with the normal MFC3. There was a slight decrease in voltage to 1.0 mV before the second addition when there was a further increase to 2.0 mV followed by a steady increase to 2.3 mV. From the cell voltage curve of MFC1 in Figure 6.9, the first addition of H^+ did not make a large change of curve which might be due to the mixing of the small amount of H^+ was not efficient. But for the second addition, it is clear that with abundant proton concentrations in cathode, the cell improved the electron transfer efficiency in anode, which directly increased the cell voltage as well as power production in MFC1. This indicates that high proton concentration around the cathode is a significant factor for improving the power production in MFC. For MFC2 the cell voltage is initially very high, about 4.5 mV, and decreases quite rapidly by 1 mV to about 3.5 mV and stays stable until the second addition at 35 min where the voltage again is sinking by 1 mV to about 2.3 mV. The initial high potential probably is due to a rapid reaction with initial available protons to promote more electrons and protons transfer from bacteria. With the diffusion of large amount of OH^-, parts of the protons in the anode was neutralized and lack of protons transported to cathode dramatically decreased the cell voltage of MFC2. The proton concentration in the cathode was lower due to reduced the amount of electrons would transfer to cathode. Thus the total cell voltage was decreased. In summary, both an increased proton concentration in the cathode chamber and the rapid proton removal from the anode chamber improved the cell power performance compared with a normal system, indicating that rapid proton transport is essential for improved power performance for the MFC.

Table 6.3 The additions of H_2SO_4 and NaOH in MFCs

Addition time, min	0 min	35 min
MFC1 in Cathode	0.35 ml H_2SO_4	2 ml H_2SO_4
MFC2 in Anode	0.35 ml NaOH	2 ml NaOH
Batch MFC3	/	/

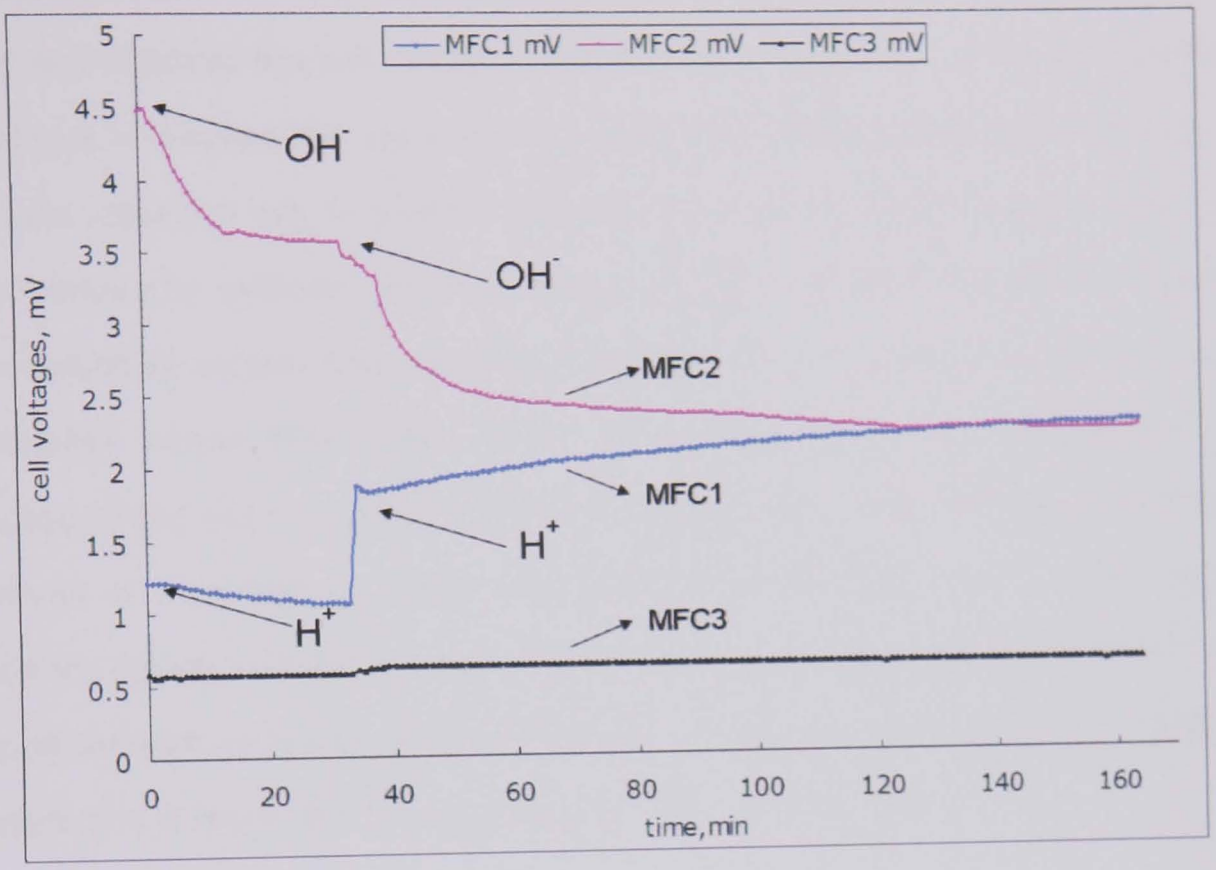

Figure 6.9 Adding acid in MFC1 cathode or alkaline in MFC2 anode

6.2.5.2 Proton transfer to cathode

The second experiment was designed to evaluate the H^+ transfer process from the anode to the cathode chamber. The same concentration of OH^- and H^+ were added into anode and cathode chambers in the same simplified two-chamber batch MFC in order to presume that the process of H^+ transfer was complete and not impacted by other factors. This should simulate a situation where all protons produced in the anode chamber were instantly transported to the cathode chamber to simulate very high flowrate. About 10 ml of 0.50 M H_2SO_4 was added in the cathode chamber and 1.0 M NaOH was added in the anode chamber at the beginning of the experiment and again after 22h. The amount of protons neutralized by OH^- in

anode was equal to the amount of protons manually added into the cathode chamber. Another batch MFC without adding any chemicals was used as the reference. Figure 6.10 shows that for the first addition of acid and alkaline, the cell voltage of the MFC with addition rapidly arrived to a maximum value 8 mV and then gradually decreased to a stable stage around 2.2 mV. For the second addition of acid and alkaline, the cell voltage increases was not as high as the first addition. However, it followed the same trend that gently decreased and then keep the cell voltage around 3 mV. In general, with the assumed complete transfer of protons from anode to cathode, the cell voltage of the MFC after two times of proton concentration control was raised from around 0.5 mV in batch mode to 3 mV in simulated instant flow mode. At the same time, the gently decreasing of cell voltage might due to e^- and H^+ produced in anode were directly consumed or large amount of electrons in anode directly transfer through the "n" shape tubing between anode and cathode rather than the transfer through external wire. This result supports that the proton transfer in MFCs from anode chamber to cathode chamber is a major barrier that affect the MFCs performance.

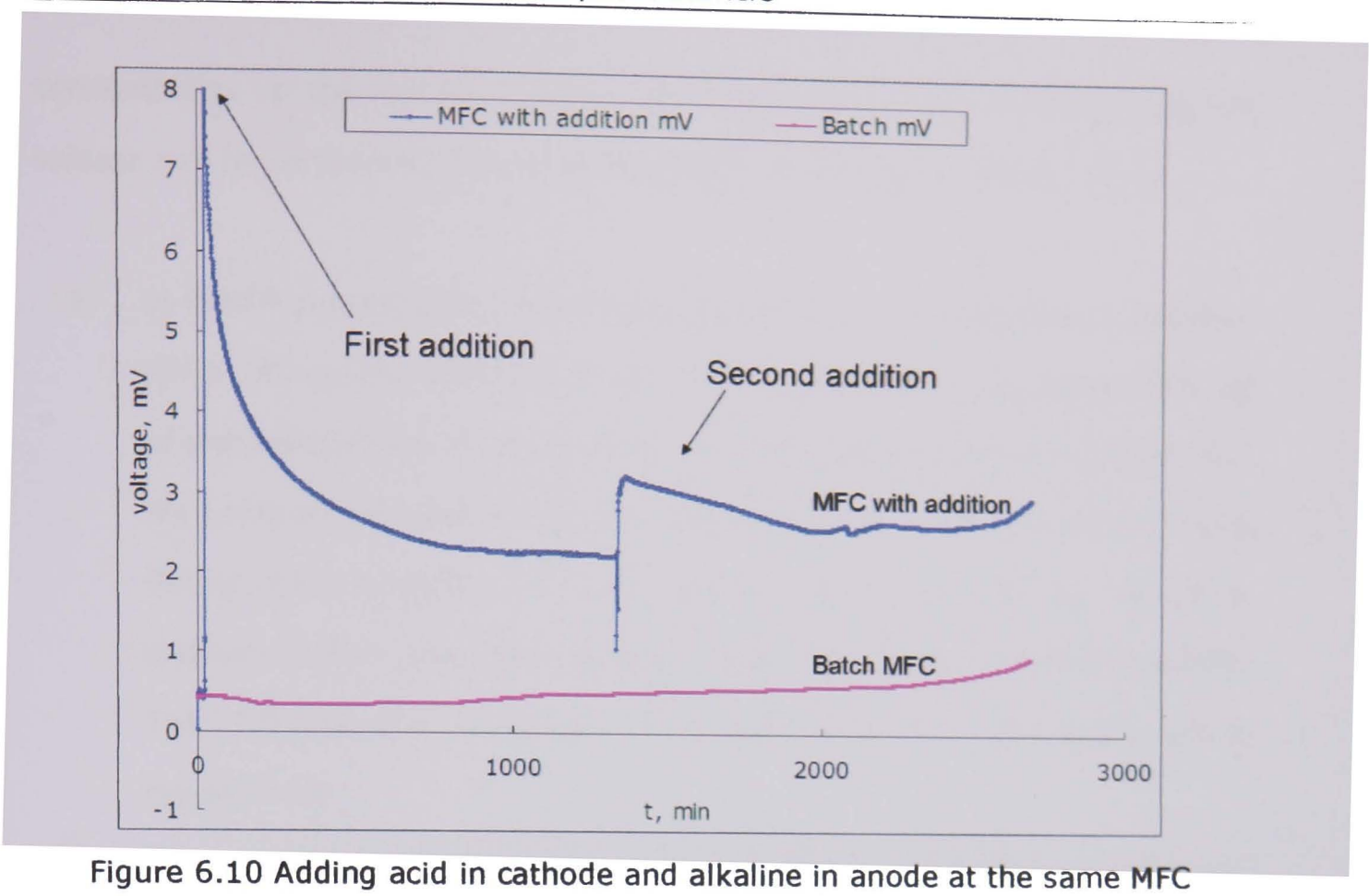

Figure 6.10 Adding acid in cathode and alkaline in anode at the same MFC

In summary, two sets of experiments were conducted to evaluate the significance for (i) proton concentration available close the cathode, (ii) protons transport away from bacteria in anode chamber, and (iii) instant transfer of protons from anode to cathode chamber. The results indicate that proton transfer from anode chamber to cathode chamber is a major barrier that affects the MFCs performance, where removal of the protons from the microbe might be the most significant factor based on increased power density. The data suggest that the flowrate in a continuous MFC can be utilized to help proton transfer to improve the power performance of MFCs.

6.2.6 Protons on the surface of cathode

6.2.6.1 Different proton concentrations in cathode

In order to find out to what extent the proton concentration on the cathode surface affects the MFC performance, an experiment was designed to observe the cell performance with different concentrations of inorganic acid contained in different cathode mediums. Different acid concentrations in cathode means the proton

concentration on the surface of the cathode differed and the corresponding cell voltage can be compared. The detailed experimental steps are listed below.

(1) In total 4 parallel experiments were carried out in 4 simplified two-chamber MFCs. The anode chamber condition was kept the same consisting of 500 ml of wastewater with 7 g/L active sludge and 1 g/L acetate as substrate. For the cathode chamber, the cathode medium of MFC1, MFC2 and MFC3 were 500ml of 0.5 M H_2SO_4, 1 M H_2SO_4 and 2 M H_2SO_4, respectively. The MFC4 cathode medium was plain wastewater with COD 18 mg/L as reference MFC. The COD and pH of the anode and cathode chambers were tested before experiment.

(2) The cell voltage was recoded continuously using a data logger for 23 h and at the end of the experiment the COD and pH in both the anode and cathode chambers were measured again.

Table 6.4 shows the changes in pH before and after the MFCs experiment for both cathode and anode chambers. The pH changed slightly from 7.3 to 7.5 in all the anode chamber which might be reducing of H^+. The protons contained in the cathode chamber were consumed significantly in all four MFCs, resulting in pH values being increased after 23 h of experiments. For the three MFCs with acid in the cathode medium, there was a correlation between higher concentrations of acid, i.e. proton concentration added to the cathode chamber, and the amount of protons in cathodes being consumed after the same period of experiments. This indicates that with more abundant amount of protons in cathode, more protons in the cathode chamber were consumed.

Table 6.4 Changes of pH values before and after MFCs experiment

PH values	MFC1	MFC2	MFC3	MFC4
Cathode	0.5 M H_2SO_4	1 M H_2SO_4	2 M H_2SO_4	Plain wastewater
Before Anode	7.3	7.3	7.3	7.3
23 h Anode	7.5	7.5	7.5	7.5
Before Cathode	0	-0.3	-0.6	7.3
23 h Cathode	1.1	0.9	0.7	7.4

Figure 6.11 shows the cell voltage data of the four MFCs. Compared to normal batch MFC4, all three MFC1, MFC2 and MFC3 had higher cell voltages, which indicates that with initial higher concentration contained in cathode, higher electron transfer occur resulting in higher cell voltages. MFC1 with 0.5 M H_2SO_4 had a stable cell voltage around 1.8 mV, while MFC2 with 1 M H_2SO_4 had a stable cell voltage around 1.3 mV and MFC3 with 2 M H_2SO_4 had a stable cell voltage around 0.8 mV. Batch MFC4 had a gradually increasing cell voltage to around 0.4 mV. The data indicates that with higher concentration of protons in cathode chamber, a lower cell voltage was observed. This can be explained that although with higher concentration of protons in cathode, more protons were consumed, indicating more electrons were consumed as well. Electrons were transported to cathode directly through the "n" shape tubing rather than external load. The loss of electrons through external wire induces lower cell voltages. The higher the proton concentration in the cathode, electrons were more likely to move in this manner.

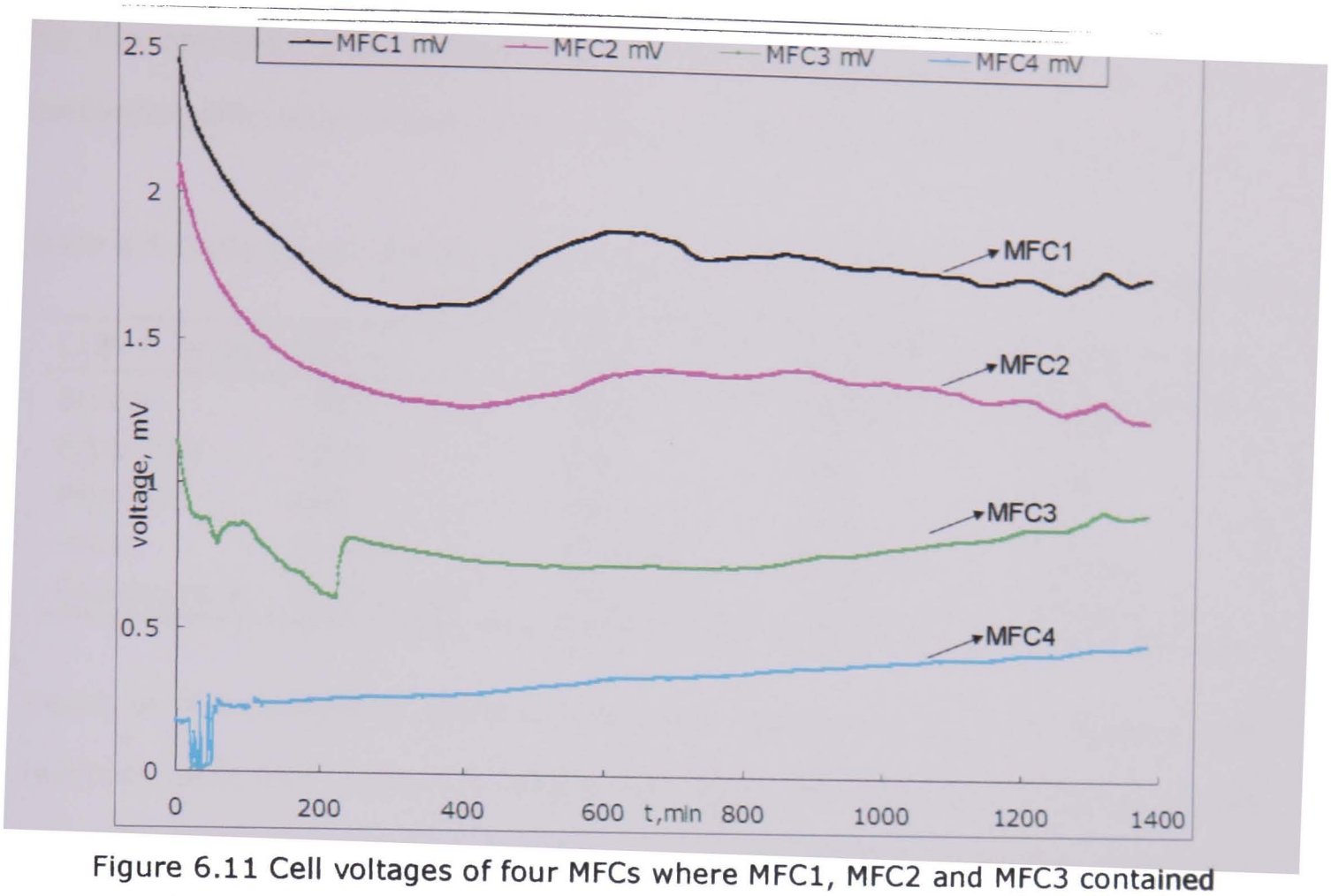

Figure 6.11 Cell voltages of four MFCs where MFC1, MFC2 and MFC3 contained 500ml of 0.5 M H_2SO_4, 1 M H_2SO_4 and 2 M H_2SO_4 in cathodes, respectively, and MFC4 contained plain wastewater in cathode

Table 6.5 shows the COD removal rates in the anode chamber and the corresponding coulombic efficiencies of the four MFCs. The COD removal rates indicate that for the three MFCs with acids in cathode chamber, a higher proton concentration resulted in higher COD removal rate, which means more organic matters were consumed in the anode chamber. However, since the cell voltages were decreasing as the proton concentration in the cathode chamber was increasing, the corresponding currents produced from the MFCs were decreasing as well. Due to the concept of coulombic efficiency based on current production versus the available electrons converted from COD removal, decreasing electrons converted from currents and increasing COD removal induce a decrease in coulombic efficiencies from MFC1 to MFC3 (Table 6.4). It can be deduced that only parts of the energy gained from COD removal was used for electricity production. For batch MFC4, it is clear that batch mode of normal MFC had a small COD removal rate and the smallest coulombic efficiency. The data indicate that there is a window

for the optimal proton concentration in the cathode chamber with an optimal coulombic efficiency as well as the highest cell voltage as shown in Figure 6.12.

Table 6.5 Comparison of the COD removal in anode chamber and coulombic efficiency of H_2SO_4 doped MFCs experiments

COD in anode	MFC 1	MFC 2	MFC 3	MFC 4
Before	1560	1560	1560	1560
After 23h	1070	970	850	1000
Removal	490	590	710	560
Rate	31.40%	37.80%	45.50%	35.90%
Coulombic E	$5.03\%*10^{-4}$	$3.24\%*10^{-4}$	$1.53\%*10^{-4}$	$0.83\%*10^{-4}$

Based on the changes of pH before and after experiment, the cell voltages, COD removal rates and coulombic efficiencies, it is clear that with a higher proton concentration in the cathode chamber, a higher amount of protons is consumed, a higher COD removal is obtained, however a lower cell voltage is observed and a lower coulombic efficiencies is obtained. It can be concluded, firstly, that compared to the batch MFC4 reference cell voltage, the initial higher proton concentration at the cathode in MFC1 induces higher electron transfer from the anode chamber, as shown by the cell voltage increasing from 0.1 to 2.5 mV in Figure 6.12. Secondly, with increasing proton concentrations at the cathode, more electrons are probably directly transfer through the "n" shape tubing from the anode to cathode chamber using mediators instead of transferring through the external wire for power generation. This leads to a lowering in cell voltage with increasing concentration of sulphuric acid. Figure 6.12 can be used to demonstrate the cell voltages as a function of proton concentrations in cathode comparing the H_2SO_4 data in Figures 6.9 and 6.11. It indicates that there is a window between 0.35 mmol to 0.5 mol of H^+ for an optimal proton concentration at the cathode. The dashed curve in Figure 6.12 shows this window. It also indicates that moderate proton concentration in the cathode helps the MFC performance, but excessive proton concentration decreases the cell voltage as well as coulombic efficiencies.

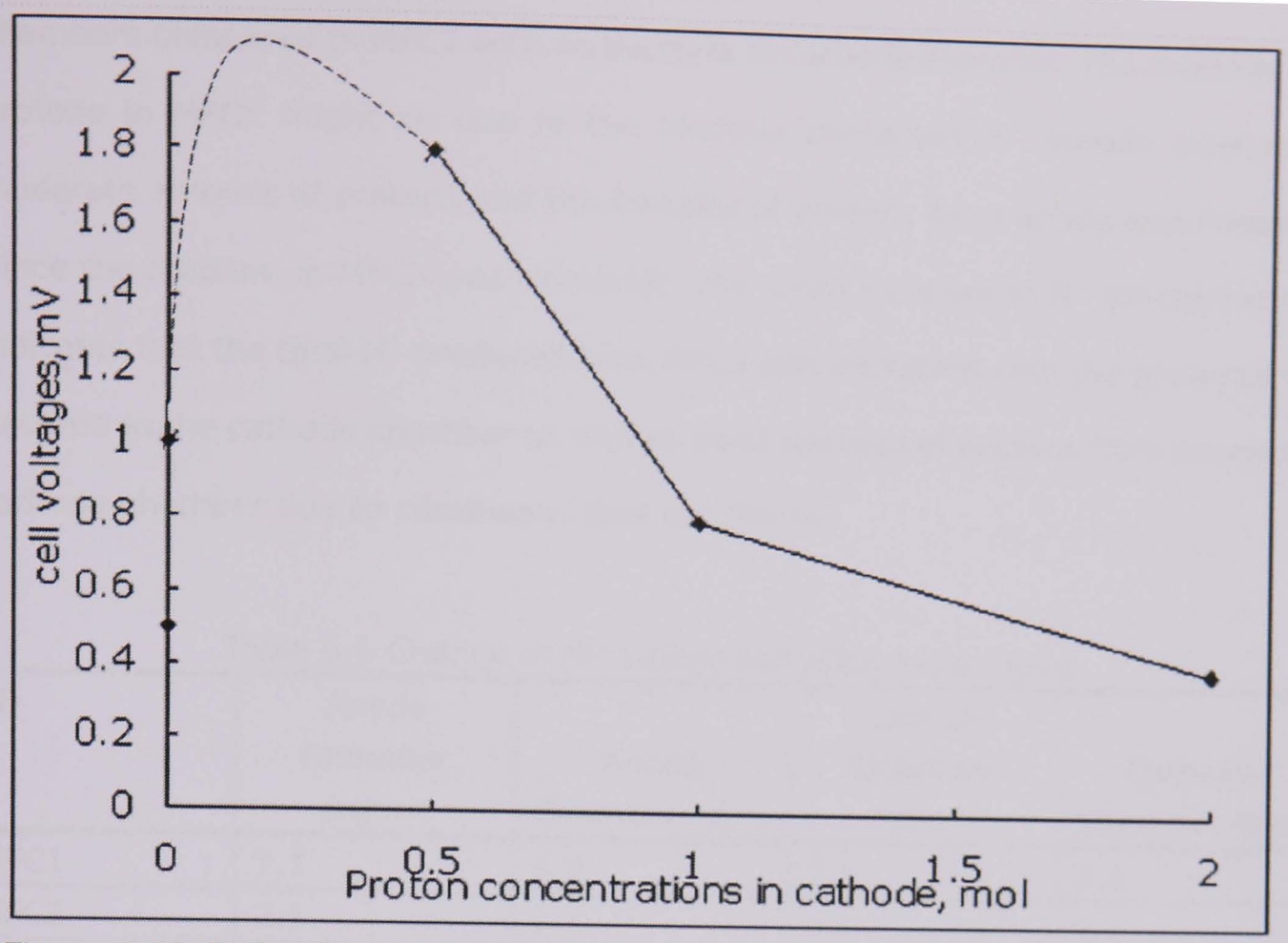

Figure 6.12 Cell voltages as a function of proton concentration at the cathode

6.2.6.2 Bacteria in cathode versus cell voltage

Some bacteria might aid the transport of proton surrounding the cathode surface and thus increase the electron transfer from the anode as well as the cell voltage. In order to validate this hypothesis, an experiment was designed with 3 parallel simplified two-chamber MFCs. The three MFCs included a batch MFC1 with large amount of active sludge contained in the cathode chamber for bacteria incubation, a batch MFC2 that had no bacteria at all in the cathode chamber and a continuous MFC3 that had similar bulk bacteria concentration in the cathode chamber as the anode chamber due to continuous pumping of the influent. The pH and COD values for both chambers before and after experiments are shown in Tables 6.6 and 6.7, respectively, and the cell voltages are shown in Figure 6.13.

From the changes in pH in Table 6.6 it is clear that both batch MFC1, that contained a high bacteria concentration in the cathode chamber, and the continuous MFC3 had a slightly increase in proton concentration both in anode and cathode

chambers compared to MFC2 with no bacteria in cathode chamber. The increase of protons in MFC1 might be due to the bacteria contained in cathode produced moderate amount of protons and the transfer of protons from anode was limited. Since the medium in MFC3 was circulated, the small increase in H^+ concentration indicates that the total H^+ produced from MFCs was increased with the presence of bacteria in the cathode chamber as well as good transfer of protons from anode to cathode chamber due to continuous flow conditions.

Table 6.6 Change in pH before and after experiment

PH	Anode Chamber Before	Anode Chamber After	Cathode Chamber Before	Cathode Chamber After
MFC1	7.1	6.9	7.1	7.0
MFC2	7.1	7.3	6.7	7.1
MFC3	7.1	7.0	7.1	7.0

Table 6.7 shows the COD removal rates as well as the coulombic efficiencies of the three MFC experiments. Although the batch MFC2 without bacteria culture in cathode chamber had the highest COD removal rate of 34.1%, it also had the lowest coulombic efficiency. The batch MFC1 with bacteria contained at the cathode had the lowest COD removal rate but the highest coulombic efficiency. For the continuous flow MFC3 the coulombic efficiency and COD removal rate were both in between the MFC1 and MFC2. The data indicates that bacteria contained in cathode might help the reaction between electrons and protons on the surface of cathode, thus making the system more likely to collect electrons at the anode.

Table 6.7 COD removal before and after and coulombic efficiency of MFCs

COD	Before anode, mg/L	after anode, mg/L	Removal, mg/L	Removal rate	CE %
MFC 1	1640	1197	443	27.0%	$9.6\%*10^{-4}$
MFC 2	1640	1080	560	34.1%	$5.6\%*10^{-4}$
MFC 3	1640	1152	488	29.8%	$8.3\%*10^{-4}$

Figure 6.13 shows the cell voltages for the three MFCs. It is clear that the

continuous flow MFC3 had the best cell voltage around 3.5 mV and kept increasing. The voltage produced from MFC1, with active sludge in cathode chamber as bacteria culture, was a bit higher than MFC2 where plain wastewater was used as cathode medium. However, the increased value of cell voltage between bacteria cathode to plain cathode was only around 0.4 mV. This indicates that when the bacteria generate both protons and electrons in cathode, the electrons are transfer by the mediators contained in the medium while the protons are probably in bulk water. Thus the diffusion of electrons is controlled by mediators while protons might self-diffuse in the bulk water. The produced protons in cathode can therefore in batch MFC readily react with electrons hold by mediators rather than the electrons transferred from the anode. So the reduced interaction with electron containing mediators in bulk phase in the anode chamber reduces the overall organic consuming thus reduced the COD removal rate. The data further indicates that continuous flow MFC can counteract this to a certain degree by transferring protons to the cathode.

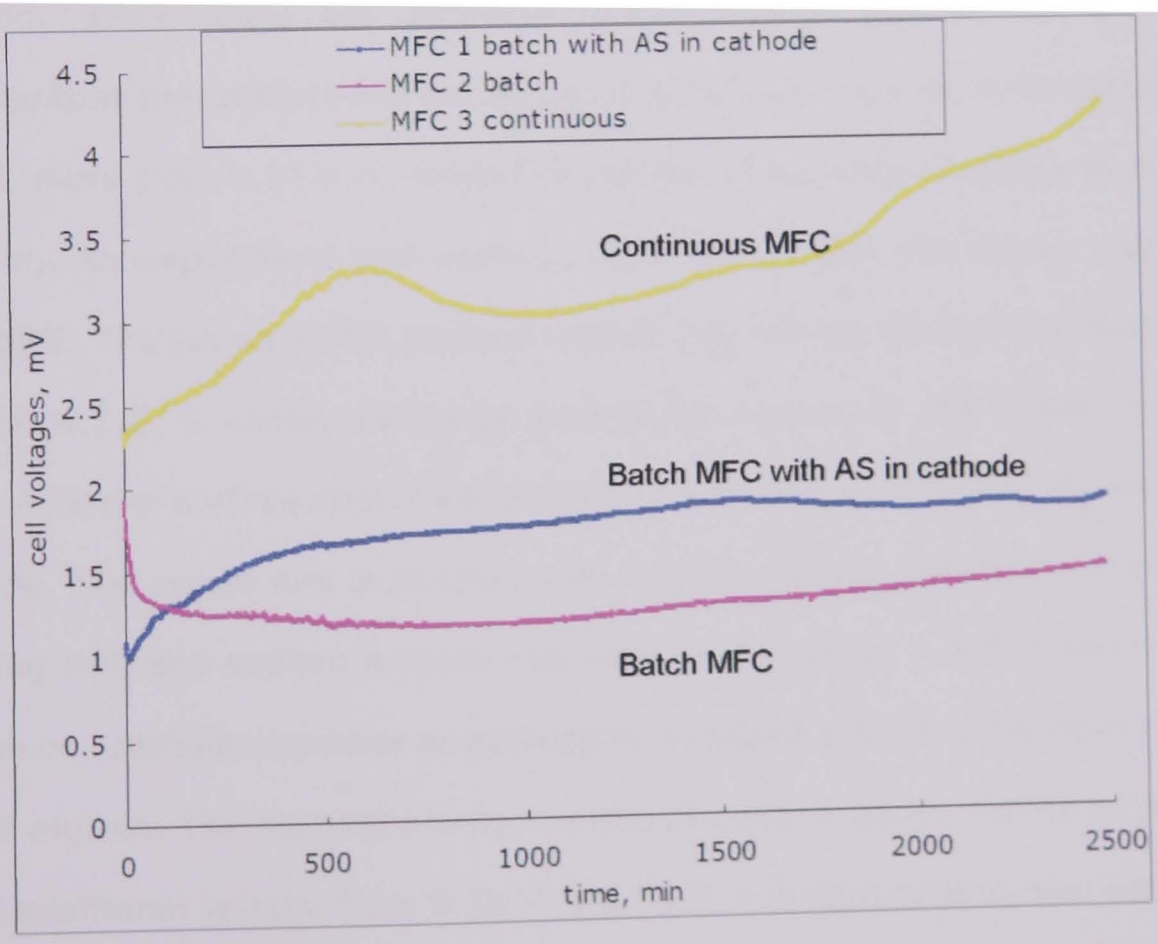

Figure 6.13 Cell voltages for three MFCs with different cathode medium

In summary, the effect of proton concentration and its limitations to the MFCs performance were investigated in this section. It is concluded that maintaining a proton concentration at the cathode between 0.35 mmol to 0.5 mol of H^+ could improve the overall cell power performance, but excessive proton concentration decreases the cell voltage. Introducing bacteria at the cathode increases the electrons and protons transfer in the MFCs but might lower the overall COD reduction.

6.2.7 H_2 production in cathode electrode

The detailed principle of the electrochemical process to produce hydrogen gas in cathode chamber was discussed in Section 2.2.7.2. Most studies suggest that a theoretical 0.1 V voltage potential is needed to be applied to decrease the cathodic potential lower than the normal potential to obtain bioelectrochemical hydrogen production. Since there are potential losses mainly due to the activation requirements at the cathode and the bacterial need for energy for their metabolism activities, more than 0.21 V is needed in practice to be added into the system to produce H_2. An experiment was carried out to further test this theory using the stacked MFC. The set up of this stacked reactor was exactly the same as described in Section 4.2.2. A cation exchange membrane separated the anode and the cathode. A 60 cm^2 surface area of woven carbon web, including 5 g/m^2 Pt, was used as cathode. The anode was inoculated with bacteria culture obtained from a high performing MFC and sodium acetate was used as substrate. A buffer was used in the anode and cathode chamber as outlined in Section 3.1.4.1 and the flowrate was set at 23 ml/min. The stacked bioreactor was set with a power supply to provide different additional voltage from 0.30 V to 0.95 V. A Bi-Stat potentiostat was used to record the cell voltage and related tests. Table 6.8 shows that significant amounts of H_2 were produced with the addition of different voltages. The variability of H_2 production during the same voltage application might be due to the bacteria

metabolism activity variation or the substrate supplying situation. The corresponding recovery rates were calculated as cathodic hydrogen efficiency converted from electrons based on observed current from Equation (22).

Table 6.8 Daily H_2 production and daily recovery rates from stacked MFC

Period, day	Added Voltage, V	H_2 observed mmol	Theoretical H_2 based on current mmol	Recovery rate%
1	0.34	0.07788	1.171	6.651
1	0.57	0.196	0.434	45.16
1	0.57	0.197	2.306	8.543
1	0.57	0.225	2.44	9.221
1	0.57	0.474	2.33	20.34
3	0.57	4.1	7.508	54.61
1	0.57	0.866	1.692	51.18
1	0.57	0.965	2.29	42.14
1	0.57	2.27	1.3	/
1	0.75	0.376	0.694	54.18
3	0.75	0.324	4.4	7.364
Total: 15	/	9.993	25.565	39.1

During the 14 days run, the coulombic efficiency was calculated to be $\eta_{coulombic}$ = 26.6 %. The overall H_2 efficiency based on Acetate→H_2 was based on the total charges contained in the actual H_2 production against the amount of total charges that contained in substrates, which can be calculated as coulombic efficitency multiply with H_2 recovery rate as: 39.1 %*26.6 %=10.4 %. This is somewhere low compared to other groups' work, where a coulombic efficiency higher than 98 % and a corresponding overall H_2 efficiency of 57 % at 0.5V of applied voltage was formed (Rozendal, R.A. et al., 2006). This group used a long term cultivated bacteria species and the cathode material used was a titanium mesh with 50 g/m^2 Pt coating. The amount of Platinum used as catalyst contained in the cathode is important for H_2 production but might render the MFC very costly.

After 14 days running with various applied voltages, a total of 9.993 mmol H_2 was produced from the cathode chamber. The H_2 yield can be calculated as 9.993 mmol/0.276*10^{-3} m^3 MFC/14 days =2.59 mol/m^3 MFC/day. The input energy of the

power supply can be calculated that 414 J of energy needed in totally 336 h. The energy needed for each mole of H_2 production in the stacked MFC can be calculated as 414 J / 9.993 mmol =0.0115 kWh/mol H_2. This is much more economic than the abiotic water electrolysis process that need 1.8 to 2.0 V external voltage applied (Cheng, H. et al., 2002) and normally 4.5-5 kWh/m^3 H_2 (about 0.1 kWh/mol H_2) of energy is needed (Stojic´, D.L. et al., 2003).

Figure 6.14 shows the plot of hydrogen recovery rate as a function of applied voltage. It shows that by increasing the applied voltage from 0.34 V to 0.75 V, the H_2 recovery rates increased from about 6 % at 0.34 V to more than 50 % at 0.75 V. Based on the concept of recovery rate, this indicates that with the increase in applied voltage, the extent of H_2 production improvement was higher than the same amount of consumed current. The data indicate that providing higher external voltage, i.e. lower the cathode potential, results in an increased H_2 recovery rates when the applied voltage was increased from 0.34 V to 0.75 V. The higher potential difference between anode and cathode push the flow direction of electrons and protons for the MFC system, and appears to promote proton transfer and more amount of H_2 is produced at the cathode. But further higher voltage applied may destroy the bacteria.

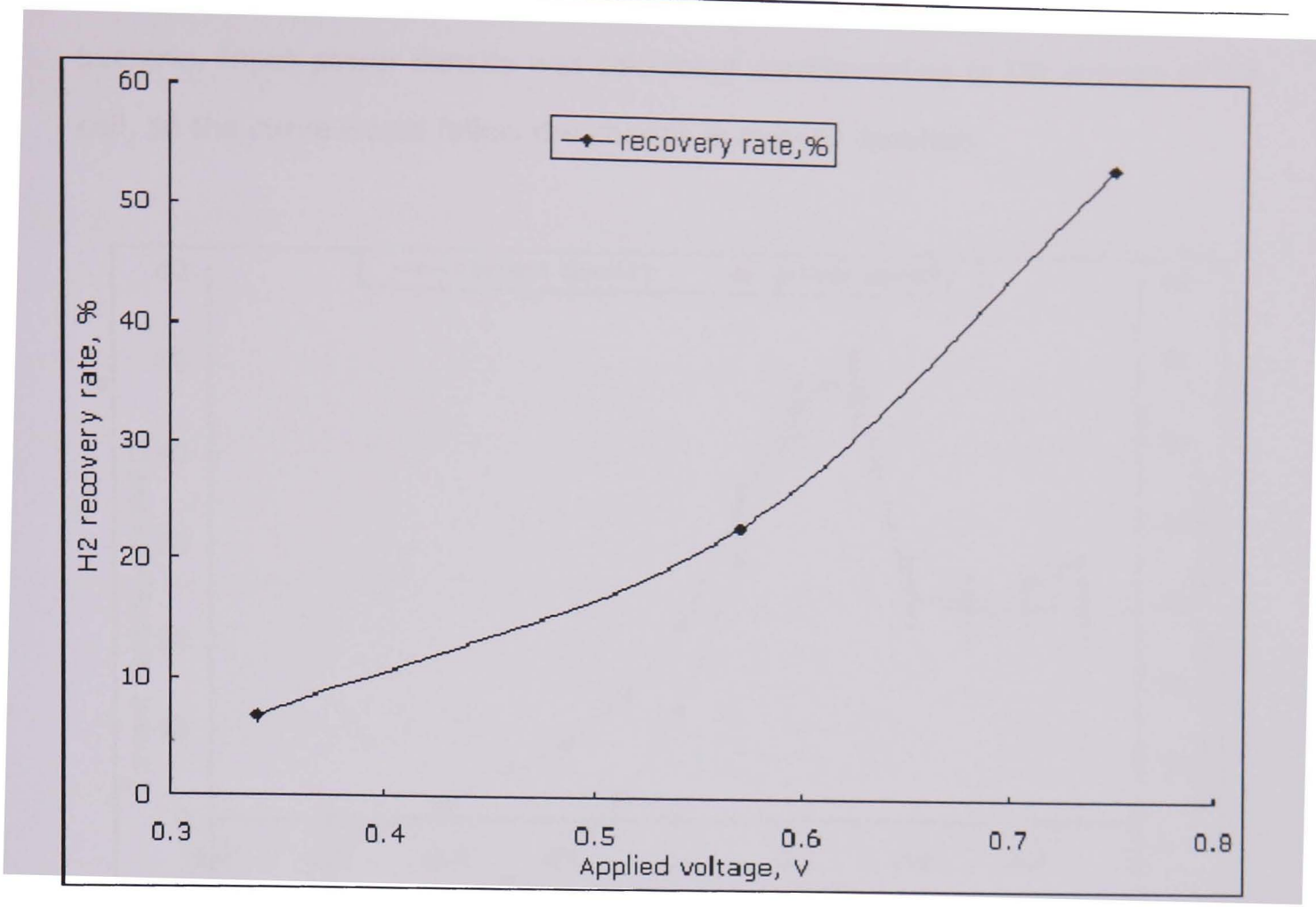

Figure 6.14 Hydrogen recovery and average power density as a function of applied voltage

By applying a series of fixed voltages over the stacked MFC for a set period, the maximum capacity of the reactor to produce hydrogen and the corresponding optimal applied voltage for this design of reactor can be found. Figure 6.15 shows the applied voltages over the stacked MFC as a function of current densities produced by anodic bacteria as well as the power densities applied over the cell externally. With increasing applied voltage from 0.30 V to 0.75 V, the current densities and input power densities are both increasing. As the voltages increased from 0.75 V to 0.95 V, current densities and power densities both decreased to around 24 A/m^3MFC and 21 W/m^3MFC, respectively. Afterwards, both current and power densities stabilised. Figure 6.15 indicates that when applying a voltage of 0.75 V, the MFC reached a maximum current density of 46.8 A/m^3MFC, or 2.2 A/m^2 cathode surface area, corresponding to a cell current of 12.9 mA. Meanwhile, with the applied 0.75 V, the input power density was 35 W/m^3 MFC or 1.61 kW/m^2 cathode surface area. The reason for the decrease in current densities after the optimal applied voltage 0.75 V is most likely due to the limitation of the anodic

bacteria. Input power density was calculated corresponding to the current of the cell, so the curve would follow the change in current densities.

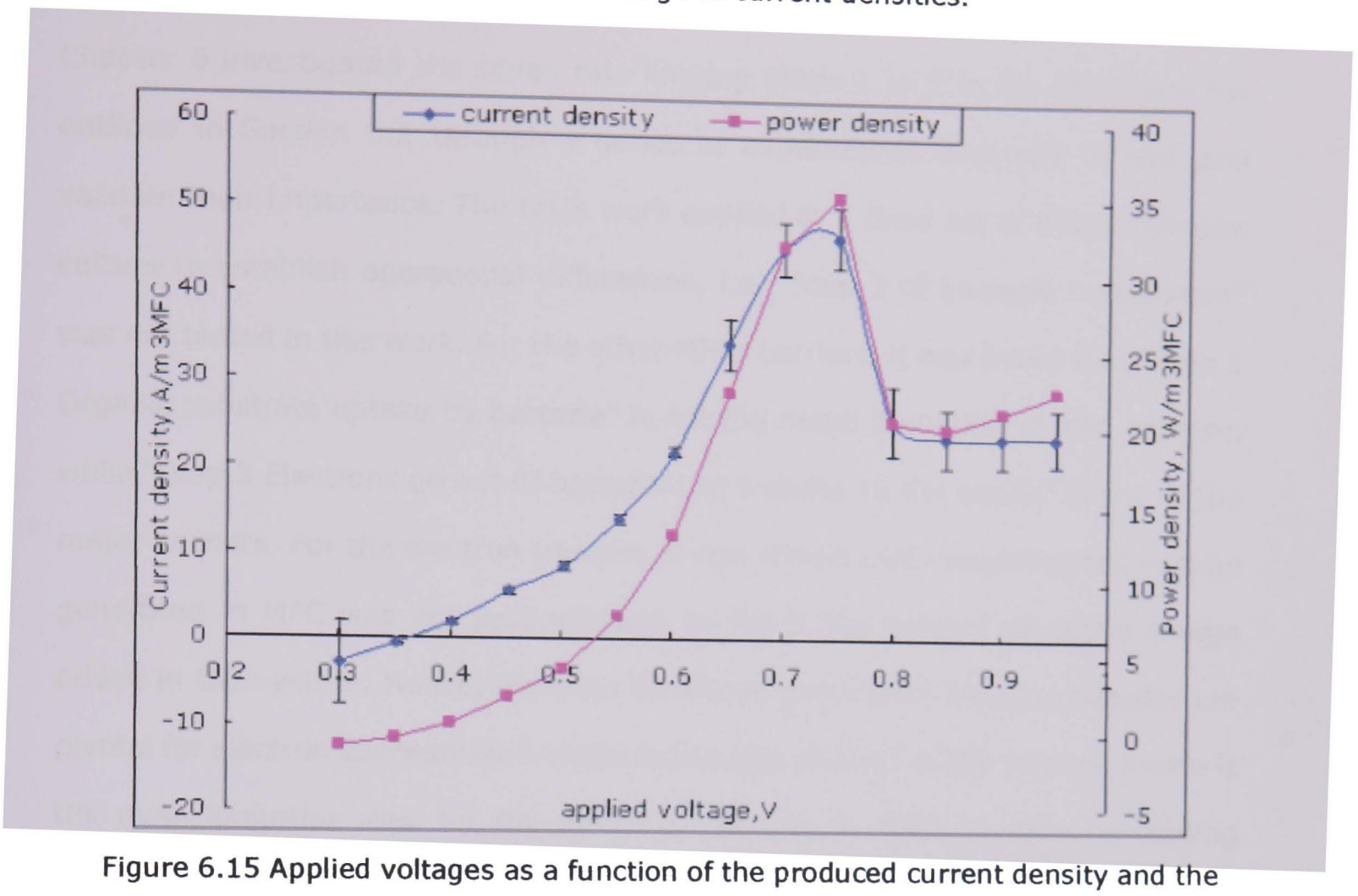

Figure 6.15 Applied voltages as a function of the produced current density and the input power density

In summary, for the electrochemical process to produce hydrogen gas in the cathode chamber, there is a limitation for the application of extra voltages in the system which is mainly due to the bacterial properties. The overall H_2 production as well as the H_2 recovery rates were increasing for the stacked MFC setup in the applied voltage range of 0.3 V to 0.75 V, with an optimal applied voltage to aid the H_2 production found to be 0.75 V yielding a current density of 46.8 A/m^3MFC. This indicates that for the cathodic H_2 production, the potential of the cathode is the key factor to control the yield and the recovery rate of H_2. The electrochemical active microorganisms could also be used to assist the H_2 production when an internal voltage difference large enough to drive the hydrogen production.

6.3 Summary of MFC internal barriers

Chapter 6 investigated the seven rate limiting Steps 1 to 7 in the MFCs process outlined in Section 6.1 through a series of experiments designed to test and validate their importance. The tests were applied to a fixed set of mixed bacteria culture to establish operational differences, i.e. "Step 2 of bacteria metabolism" was not tested in this work. For the other MFCs barriers, it was found that "Step 1 Organic substrate uptake by bacteria" is not the major limitation of MFC process, while "Step 3 Electrons go out of bacteria and transfer to the anode" is one of the major barriers. For the electron transfer, it was shown that increasing cell voltage generated in MFC was not proportionate to the initial amount of active sludge added in the system. Hence, the sites on anode surface for electron transfer are pivotal for electron successfully transferred on the anode, i.e. the sites on anode is the main limitation step for the electrons transfer in MFCs process confirming findings in Chapter 5. Several chemicals with high reduction potentials such as KNO_3 and O_2 were found to act as super electron acceptors to complement the anode electrode to produce current. The most sustainable system appears to be based on controlled trace amounts of oxygen. Further, it was found that "Step 4 Electrons through external circuit to cathode electrode" is important to affect the MFC performance but the barrier can be amended by improving materials to decrease the internal resistance. Another major barrier in the MFC process was "Step 5 Protons go out of bacteria and transport to the cathode". For this proton transfer step, proton transfer from anode chamber to cathode chamber is a major barrier that affects the MFCs performance, where the removal of the protons from the microbe might be the most significant factor. Continuous flow might aid in this process. It was found that "Step 6 Proton transfer to the surface of cathode" was not a key barrier and the results indicate that there is a range of proton concentration yielding better MFC performance. On the other hand, "Step 7 Protons and electrons produce H_2 at cathode electrode" was found to be an essential barrier. It was found that the MFC system requires a certain voltage difference for the

protons and electrons transferred to the cathode to form H_2 instead of H_2O. The potential of the cathode is the key factor to control the yield and the recovery rate of H_2. An optimal applied voltage can be established to aid the H_2 production in cathode.

Chapter 7 MFC solutions for industry applications

The interest of industry in Microbial Fuel Cell is three fold. First of all, it has a great potential to sustainably remove organic compounds from industrial process water. This could lead to carbon footprint reduction but more importantly to cost reductions. Secondly, the electricity produced could be used to offset electricity costs and requirements, and thirdly, the hydrogen gas produced could be harvested and sold as a commodity or simply burned in a boiler to offset natural gas requirements. So far, MFC has not been implemented by industry mostly due to great uncertainties about its operation. The increased understand of the internal barriers and bottlenecks of MFCs established in Chapter 4 to 6, including the limitations in the electrons and protons transfer related to power production and coulombic efficiencies, could help MFCs reach commercialisation. Of the three different types of MFCs compared in Chapter 4 the hexagonal tube MFC was considered the best option for further research for the industrial application. Chapter 5 identified low cost optimisation of anode and cathode materials for MFCs that currently is a major economic concern. Chapter 6 identified opportunities for efficient electron and proton transfer to enhance both the power performance and increase the organic removal rate. By summarising the knowledge and the research results gained in this work, this chapter outlines a possible implementation of the hexagonal tube MFC at an industrial site to demonstrate the potential applications towards industry and the economic benefit.

7.1 Sustainable organic removal

The main and most important direction for industry application is wastewater treatment. In contrast to the traditional wastewater treatment industry that

currently uses energy to physically degrade the organic matters contained in wastewater by aeration, the MFCs open a brand new technology to both remove the organic contents by using no energy for aeration and also produce hydrogen and electricity for other use at the same time. At present, most of the MFC research groups show high organic removal rate in their bench scale of MFCs devices but they are typically using very low volumes and flowrates (Liu, H. et al., 2004; He, Z. et al., 2005; Min, B. et al., 2005b; Catal, T. et al., 2008). In this work, the hexagonal tube MFC discussed in Section 4.3 operated with a large treatment volume of around 2.7 L and around 1 m long of the effective chamber, the COD removal rate can arrived to 2.9 % per pass at a flow rate of 2.7 L/h or an hourly retention time (HRT) of 1 hour, i.e. all the volume of the 1 m long MFC is exchanged each hour. This means that in a 100 m tube, the COD removal rate can be about 94.7 % after a single pass through the system with an HRT of 1 hour per meter which is a considerable amount for practical application. Since the COD removal is a function of flow rate that, higher flow rates reduce the COD removal rate and it could be treated by simply increasing the treatment route to longer or zigzag tube. The data show that doubling the flow rate to 5.4 L/h reduced the COD removal rate to 1.5 % (Section 4.3.3.3.1). The data therefore suggests that the hexagonal tube MFC could comfortably be achieving COD removal rates of about 1.5 % per pass with higher flow rate of 5.4 L/h. This would lead to a decrease in COD of 95.1 % after 200 m. For most companies this could directly save them disposal costs, since wastewater costs are based on the Mogden formula in the UK where as much as 70-90% of the cost can be associated with the COD content of the disposed water (OFWAT, 2007).

During MFC operation on industrial process water there are several considerations that are needed for its long term application. The formation of thick biofilms that might isolate the anode electrode from the liquid phase as well as the organic matters contained in the industrial process water can be expected, especially on the area of reactor turning route. Consequently the accumulation of some

recalcitrant substrates should be anticipated. Several possible solutions could be used to amend this, such as applying temporary much higher flow rate, at lease one order of magnitude larger than the normal influent flow rate to break down the thick biofilm or sparging some off gases of the reactor to removal extra biofilm formation.

7.2 Power redeem

The power densities of MFCs investigated were low compared to other studies mainly due to the poor coulombic efficiencies and other related factors as outlined in Chapter 4. The maximum power density currently achieved using the hexagonal tube MFC design was around 13.3 mW/m^2. Chapter 5 indicated that by thermal treatment of the anode material the power density was increased by a factor of around 2 (Table 5.5) as B material as the anode material. So the power density could be 26.6 mW/m^2. Although this level is not impressive, this work has identified opportunities towards changes in MFC configuration and design that can lead to power production from MFCs in wastewater treatment industries to be significantly increased. Indeed, Figure 4.24 suggests that packing more anode surface per volume of MFC anode can greatly increase the power densities in the form of coulombic efficiency improvement. Assuming that 10% of the volume of the hexagonal MFC can be filled with anode carbon cloth B material containing about 0.005 m^2/g anode surface and 1.75 g/cm^3 in carbon fibre density, then each litre of MFC can contain 0.875 m^2 of anode. In other words, 1 m^3 of hexagonal MFC should be able to produce around 23.3 W, which is comparable to the power production observed in the stacked MFC (Section 4.2.2.3).

7.3 H_2 production

The MFC treatment of industrial process water also produces H_2. Based on the H_2

production data of anaerobic hexagonal tube MFC, the overall H_2 recovery rate from substrate can be calculated as much as 13.8 %. This study showed that the H_2 yield Y_{H2} (g H_2/g-COD) can be as high as 11.6 mg H_2 /g-COD (Section 4.3.3.4). A company discarding 1,000 kg COD per day through its process water could achieve a daily H_2 production of 11.6 kg. Currently, the H_2 price is around £6/kg (or 15 p/kWh) so they are in effect flushing £25,000 of hydrogen down the drain each year.

7.4 Outline of industrial implementation of MFC

7.4.1 Industrial setting

A typical industrial setting for UK is a food production plant that produces 50 m^3/day of wastewater where the COD is around 5000 mg/L. Figure 7.1 outlines a typical site where the factory has a discharge pipe to a local wastewater connection point. In order to achieve the lower COD level to avoid heavy responsibility for the wastewater treatment cost for local water connection facilities, the outlet COD of process water has to be less than 351 mg/L based on the Mogden formula assuming the plant is connected with Severn Trent sewerage company (OFWAT, 2007). The industry can then utilise the transport distance to treat the water for reduced costs and co-produce energy. The implementation calculation is based on some assumption that firstly, the power production rate of this MFC is 13.3 mW/m^2 and after anode material thermal treatment, the power density has been improved to 26.6 mW/m^2. Secondly, the COD removal rate is based on the experimental data in Section 4.3 and corrected with the 50 % increasing based on the anode carbon thermal treatment. Thirdly, the COD removal rate is consistent for each meter of treatment.

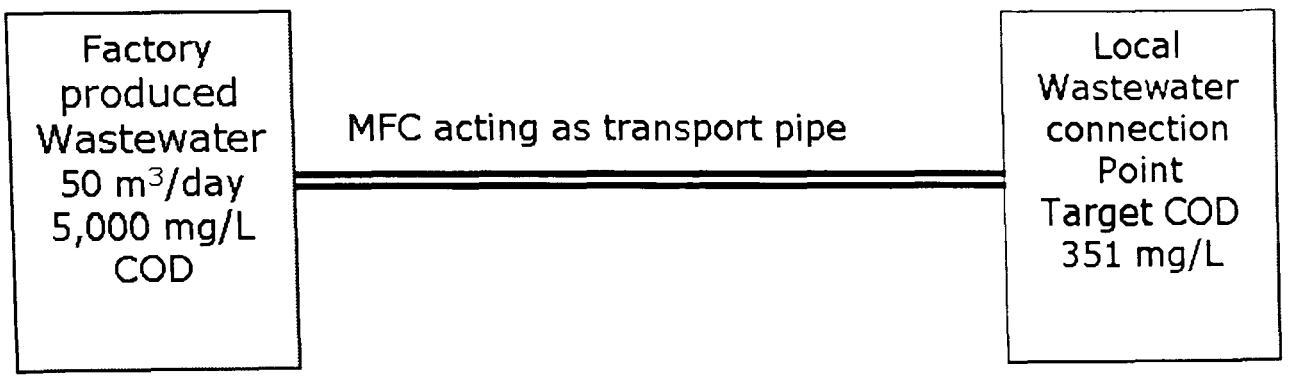

Figure 7.1 Outline of typical industrial setting

7.4.2 Mass balance

Since the food production plant is producing 50 m^3/day of process water where the COD is around 5000 mg/L, it produces about 2083 L/h and 250 kg COD per day. With a COD removal rate of 1.5 % per meter using a flow rate of 5.4 L/h as outlined in Section 7.1, the length of MFC treatment transport pipe can be calculated as following Equation (23):

$5000*(100\ \%-1.5\ \%)^x = 351$

$x = 176$ m

As the whole 50 m^3 of process water needed to be treated in one day (i.e. 24 hours) and the flow rate is 2 meter per hour, this means the 48 meter of transport pipe MFC needs to contain 50 m^3. So the pipe radius can be calculated as:

$\Pi r^2 * 48\ m = 50\ m^3$

$r = 0.6$ m

So the effective diameter needs to be 1.2 m. From Section 7.2 it was estimated that the MFC could contain 875 m^2 of anode material per m^3 of MFC. Since the length of MFC pipe should be 176 m, the total volume of MFC can be calculated as 199 m^3. Based on the power density of 23.3 W/m^3 in Section 7.2, the electricity that can be produced is 4.6 kW or about 110.4 kWh per day. Based on a hydrogen production yield of 11.6 mg H_2/g-COD in Section 7.3, the wastewater will yield about 11.6 mg H_2/g-COD * (5-0.351) g COD /L * $5*10^4$ L = 2.7 kg H_2 produced each day. Figure 7.2 is outlining the overall mass balance for the MFC transport line.

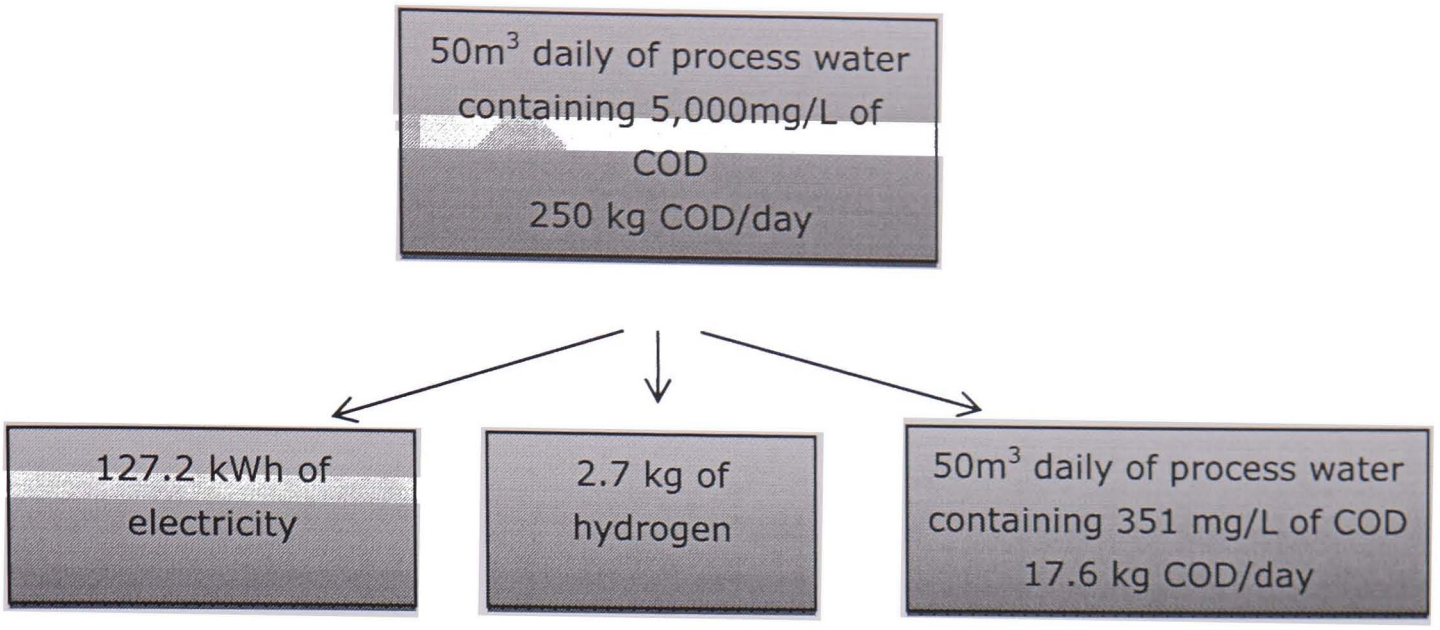

Figure 7.2 Daily mass balances for MFC

7.4.3 Energy balance

Figure 7.3 outlines the overall energy balance for the industrial MFC. The energy contained in the COD is around 9.5 MJ/kg according to Section 4.3.3.2, so the total energy that is potentially contained in the industrial process water is 50 m^3 * 5kg/ m^3 *9.5 MJ/kg =2.4 GJ per day, 1MWh equal to 3.6 GJ, so it is about 667 kWh. As calculated in Section 7.4.2, 127.2 kWh of electricity is produced in this case per day. The hydrogen production is 2.7 kg, the energy contained in hydrogen is 155 kJ/g, so it is 418.5 MJ, equal to 116.3 kWh. The total energy extracted from wastewater in this MFC pipe is 243.5 kWh per day. So the actual energy redeem is 243.5 kWh/ 667 kWh=36.5 %. The energy contained in the outlet of wastewater after MFCs treatment is around 46.4 kwh, which is equal to 7.3 % of energy in previous untreated wastewater. 56.2 % of energy was waste in the stream without any utilisation.

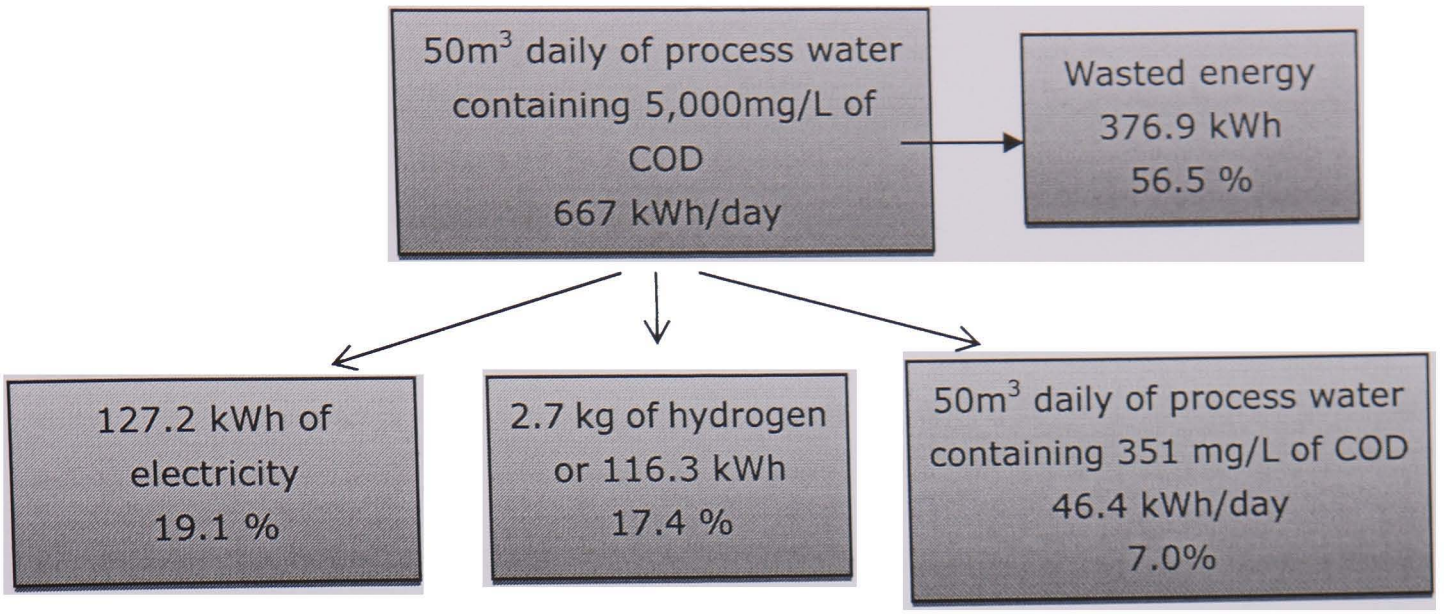

Figure 7.3 Daily energy balances for MFC

7.4.4 Cost balance

Figure 7.4 shows the estimated annual energy generation and cost savings from the MFC transfer pipe system. The energy contained in the initial process water is 667 kWh per day which around 243 MWh wasted per year. A MWh of electricity sells for around £60/MWh, so theoretically the energy is worth £14,580. However, the MFC is adding significant value to the stream. Firstly, it converts the COD in hydrogen which is worth about 2.7 kg/day *365 days * £6/kg = £5,913, and also there is produced electricity worth about 127.2 kWh* 365 days* £60/MWh =£ 2,784. Secondly, and more importantly, there is a large water disposal cost reduction due to the Mogden Formula. Since the COD can be treated to around 351 mg/L before going to traditional wastewater treatment company such as Severn Trent in the Nottingham area, about £4.24 /m^3 can be saved (OFWAT, 2007). So the total cost saving per day is £4.24 /m^3 * 50 m^3= £212 with annual savings of £77,380. So totally the company can gain about £86,077 annually excluding any green credit.

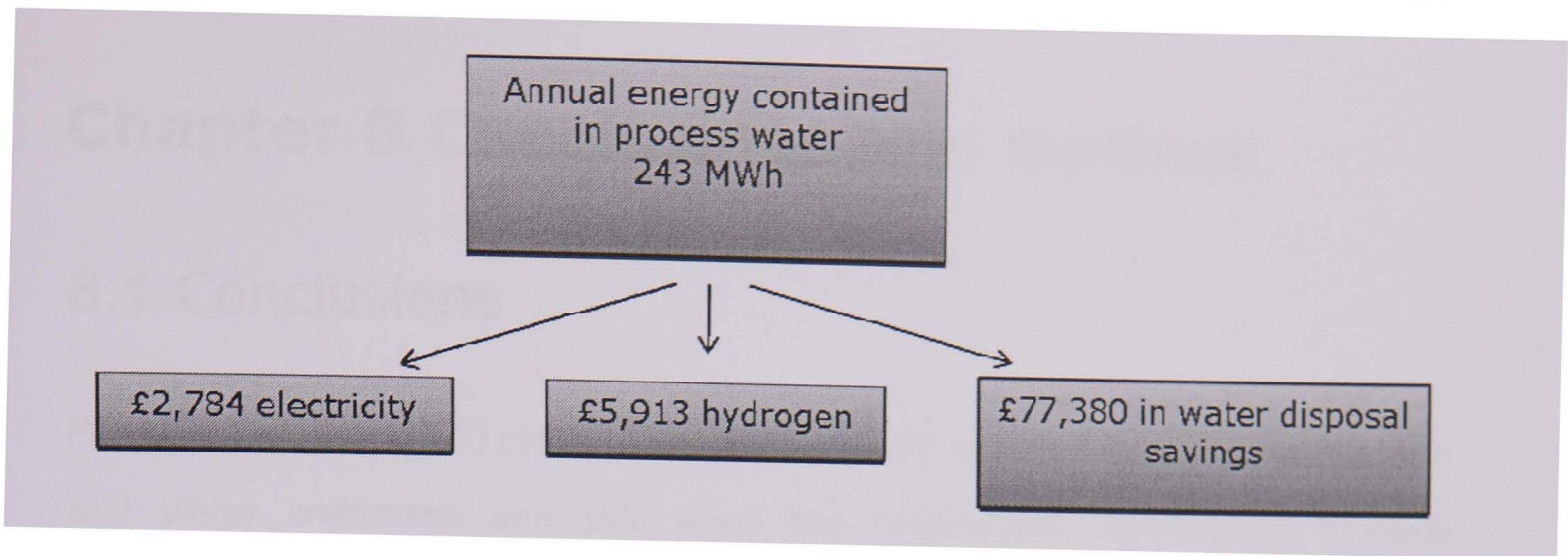

Figure 7.4 Annual estimated energy generation and cost savings from MFC transfer pipe

Considering the construction and materials cost of MFC setup, the anode material needed is about 19.9 m^3 based on the 10% of the volume of the hexagonal MFC filling with anode material. According to Section 4.5.1., the carbon cloth can be replaced using graphite granules, carbon clothy cost around £ 2000 /m^3 for the low cost solution. However, the alternative anode cost is £9,000. The cost for thermal treatment of the anode carbon material probably would be £20,000. Several possibilities exist to increase the performance of the MFC system. Increases the effective volume and surface of the anode materials, and hence increases the amount of substrate that can be treated per tube of MFCs is crucial to increase the power redeem, but it enhances the total investment costs as well. The Cathode material needed in this setup can be estimated as 10 cm wide with 176 m in length, which is 17.6 m^2. The Cathode material containing 0.5 g/m^2 of platinum costs roughly £1000 /m^2, so the cathode cost is £17,600. The piping should already be an integral part of the industry, but a typical cost is about £200/m and for this system would be about £35,200. There will also be cost of piping energy gases and connecting the electrical system. A total capital investment cost for the MFC process water treatment system would probably be around £100-120 k. Additional energy will be needed to power peripherals and the influent pumps. Post-treatment to remove residual sludge and nutrients may on the other hand increase the operational costs. In this case the annual cost saving and benefit is £80-90 k after MFC installation, which can pay for the MFC investment cost in 1-2 years.

Chapter 8 Conclusions and Outlook

8.1 Conclusions

Microbial Fuel Cell (MFC) carries a great promise for sustainable energy generation and water treatment and this work has contributed significantly towards developing innovative engineering solutions for industrial applications. Especially, continuous flow solutions and optimisations of anode materials were developed that can promote the general employment of the MFC technology as outlined below.

Several novel MFC reactor designs were developed through this study and discussed in Chapter 4. A Micro-channel MFC was developed with the advantage of a small reactor volume. A hexagonal tube MFC was further developed that was suitable for high-flow continuous operation. Both these MFC were developed using the flow as a barrier between the anode and cathode part of the MFC. A stacked MFC, developed at University of Gent, was also introduced based on the collaboration work. It had a proton exchange membrane, relatively low flow but a high coulombic efficiency. Based on the performances and experiment data for these three individual MFCs, Micro-channel MFC, stacked MFC and the hexagonal tube MFC, the conclusion can be made that all of these three MFC designations are capable to generate electricity, produce hydrogen as well as remove significant amount of organic matter from the waste water. Depending on the MFC structures, electrode materials and other environmental and experiment conditions, their MFC performances were quite similar. The highest power density based on actual application with data logger was Micro-channel MFC which was 29.5 mW/m^2, while the stacked MFC had the maximum power production of 24.6 mW/m^2 and the hexagonal MFC showed a max of 13.3 mW/m^2. The coulombic efficiencies of these MFCs were all very low and in the range from 0.7 % to 6.9 %, which showed that

the efficiency of organic matter converting to electricity was very low based on these reactors. This study has shown for the first time that the coulombic efficiency is virtually a linear function of the rate of effective anode surface area with the volume of anode chamber on a log to log basis. The relationship can be crucial towards developing engineering solutions where the coulombic efficiency can be scaled towards the flow restrictions in the MFC system.

The COD removal rates of the MFCs were 0.14 % for the Micro-channel MFC, 0.33% for the stacked MFC and 2.9 % for the Hexagonal-tube MFC per pass of MFC process with flow rate of 0.12L/h, 1.4L/h and 2.7L/h, respectively. But the coulombic efficiency showed that most of the substrate loss was not transformed into electric energy in these systems. From the hexagonal –tube MFC showed in Section 4.3.3.3.1, it was found that the COD removal rate is a function of flow rate that higher flow rates reduced the COD removal rate.

Production of H_2 was observed in MFCs. For the Micro-channel MFC, the H_2 recovery rate based on the theoretical H_2 production from supplied substrate was 0.02 %. The H_2 yield based on COD removed was 0.0115 mg/g COD. For the Hexagonal-tube MFC, the maximum production rate of H_2 was 36 mmol/min at the peak point and the overall H_2 recovery rate was 13.8 %. The H_2 yield was 11.6 mg/g COD. Chapter 4 indicates that continuous flow with no membrane can be used as an effective MFC technology for industry in terms of COD reduction and H_2 generation.

Electrode materials treatments were explored in Chapter 5, where several novel and simple chemical and physical treatment methods were applied to improve the performance of the MFC based on these treated electrode materials. For the anode materials treatment, two methods were introduced. The first was physical treatment using a high temperature CO_2 gas oxidation in the range of 400 to 800°C. The data showed that the anode materials after physical treatment improved the

cell voltages in a simplified two-chamber MFCs. It was observed that the best power performance was achieved at 600°C CO_2 treatment for the B carbon cloth material and 800 °C CO_2 treatment for the D carbon cloth material. The 600°C B material had an improvement of around 195% in power density compare to plain B materials and the 800 °C D material had an improvement of around 78% in power density compare to the plain D material based on polarization curves data. Further examination using SEM demonstrated that the increased performance of the high temperature treated anode was attributed to the exfoliation of the carbon fibres, where exfoliation helps the bacteria to fasten and grow on the surface of fibre. Nitrogen adsorption analysis of plain and treated materials showed that the macropore pore volumes for the 600 °C treated B and the 800 °C treated D materials were increased to 2.79 cm^3/g and 5.33 cm^3/g, respectively, compared to 0.66 cm^3/g and 2.27 cm^3/g, respectively, for plain B and D materials. The enlarged macropore pore volumes after gas oxidation treatment might attract more bacteria to attach onto the fibre resulting in increased electron transfer as well as the power performance.

The second anode material treatment involved common acids and alkalis to treat the carbon materials. The data suggest that the materials before and after treatment had very similar power densities, or even that the untreated material had higher power densities. This indicates chemical treatment does not improve MFC power performance. From the SEM photos of KOH treated B and D materials, it is clear that there is almost no change in the fibre surfaces compare to the plain B and D materials. It can be concluded that, rather than change anode materials structure and surface functional groups, acid and alkaline treatments may have the effect of cleaning the surface of anode fibre to prevent the bacteria growth on the surface. Further, it was shown that pure graphite granules without Pt catalyst can be used as cathode materials for MFC. The stacked MFC showed a maximum power density and current density of 2.3 W/m^3 and 15.7 A/ m^3, respectively, using pure graphite granules. Although the power density and current density are around 50%

lower than that of MFC with Pt as cathode catalyst, the cost of graphite granules is about 1/1000 that of Pt catalyst contained cathode materials making it a very attractive option. The removal of Pt catalyst removes one of the major economic barriers for the further industrial applications of MFCs technology. Chapter 5 indicates that CO_2 oxidation is quick and a low cost technique to improve anode performance for MFCs and pure graphite granules is a viable cathode option.

The rate limiting steps of the MFCs process were identified and tested for significance in Chapter 6. The focus was on optimization of barriers towards optimized engineering solutions and the individual bacteria activities were not tested. Four major barriers were identified. Firstly, it was found that the MFC cell voltage was not proportionate to the initial amount of active sludge added into the system, indicating that the sites on the anode surface available for the bacteria for electron transfer is a key limiting factor. Increasing these sites, such as through CO_2 activation, is pivotal for electron successfully transferred to the anode. Secondly, several chemicals with higher reduction potentials such as KNO_3 and O_2 can act as super electron acceptors instead of anode electrode to produce current. Thus in order to improve the power production and the electrons transfer to the anode, these chemicals needed to be controlled and can be a major barrier. Thirdly, proton transfer from anode chamber to cathode chamber is a major barrier that affects the MFCs performance. It was established that when the proton concentration in the cathode was kept within the window range of 0.35 mmol to 0.5 mol, a significant improvement in the cell power performance was observed. This indicates the importance of rapid transfer of protons to the cathode. Continuous flow was identified as a suitable engineering solution to obtain the transfer. Fourthly, the potential of the cathode was a key factor to control the yield and the recovery rate during cathodic H_2 production. The optimal applied voltage was found to be 0.4 to 0.8 V, and this can be supplied externally or, at certain conditions, internally be the MFC itself. Chapter 6 successfully identified the main barriers and suggested routes towards improving the performance for the MFCs studied in this work.

A possible implementation of MFC towards an industrial site was outlined in Chapter 7 using the optimised data from Chapters 4 though 6. This was based on the hexagonal tube MFC design for a long transport pipe design as identified in Chapter 4 and combined with the anode material with the 195% of power improvement after thermal treatment of Chapter 5. A typical industrial food production plant that produces 50 m^3/day of wastewater where the COD is around 5000 mg/L was chosen, and it was found that 36.5 % of the total energy contained in the waste water can be generated into renewable energy in the form of electricity (19.1 %) and hydrogen (17.4 %) leaving a residual COD energy content of 7.0 % in the remaining wastewater. For this case, the total annual estimated MFC energy generation is around 464.3 MWh of electricity and 985.5 kg of hydrogen. The wastewater disposal savings is probably the main industrial driver, which in this case is about £77,380 saved each year in the form of reducing effluent COD level before go to the wastewater treatment sites. The case study for industrial implementation of MFC in Chapter 7 clearly show the considerable amount of energy generation and cost savings achieved for the implementation of MFC.

In summary, this work has introduced novel MFC reactor designs that have identified new solution to deal with wastewater treatment and sustainable energy production. Novel, albeit simple, methods for anode and cathode materials treatment were applied that significantly improved MFC performance. The rate limiting steps of the MFC process was investigated and the limitation points were depicted to identify solutions for the crucial factors that effect on the performance of MFCs. Further research to develop low cost solutions to optimize these key steps might contain the key for the MFC technology to be applied in many areas.

8.2 Suggestions for further development

MFCs still have a long way to go to reach application at large scale. Real use is much

more complex than can be assessed at this stage and demonstrator units will need to be employed to go forward. This section suggests future potential research areas and directions that are worth study to reach this goal. Many factors need to be set up before reaching large scale demonstrator and eventually commercialisation and have been summarized below.

8.2.1 Reactor designs and electrodes structures

Virtually all published research has so far been based on the bench and laboratory scale MFC. Although the hexagonal tube MFC in this study, with an effective volume of 2.7 L, is one of the largest reactors reported, it is still far below actual water flow in industry as highlighted in Chapter 7. Reactor design for possible scale-up is essential and some solutions have been outlined in this work. Besides the handling capacity issue, other areas of reactor design need to be investigated, including the issue of a two-chamber design with membrane for separation versus a single chamber design. The two-chamber MFC design has a clear reaction route for electrons and protons transfer between anode and cathode chamber, but the drawbacks are low handling capacity. Single chamber MFCs using air oxygen as cathode electrode acceptor might be efficient solution but the efficiency needs to be improved. Totally anaerobic single chamber MFC studies also show great promise in terms of COD reduction potential and energy production. However, also here efficiency improvements need to be addressed.

The electrode material and morphology are two significant areas to study further where significant efficiency improvements can be achieved, particularly for continuous flow single chamber systems. The anode research should be focussed on the materials array in the anode chamber, low cost conducting materials that have large surface area with surface roughness and suitable sites that the bacteria will attach to and thrive on. The cathode studies need to be focused on the choices

of electron acceptors in cathode chamber, where some higher redox potential chemicals need to be considered to replace platinum.

8.2.2 Electrode materials treatment

The characteristics of MFC electrodes include both the presence of catalysts, functional groups and/or extra surface charges in or on the electrode surface, and the presence of mediators in the surrounding solution. Although external mediators can help the electron transfer and yield valuable research data, their unsustainable and uneconomic aspects prevents their use. A significant step towards large scale application might be to identify possible functional groups that can be attached to the electrode materials to improve efficiency. For the anode materials, the electrocatalytic properties of anodes have been modified by applying catalysts such as CNTs/polyaniline composite, Tungsten carbide or Fluorinated polyaniline polymerized on Pt sheet on the electrode matrix (Niessen, J. et al., 2004; Rosenbaum, M. et al., 2007). Further, ammonia treated or Fe_2O_3 coated carbon materials have shown to bring extra positive surface charge onto the anode surface, attracting more electrons onto the anode for electricity production (Cheng, S. and Logan, B.E., 2007). Also, Mn^{4+}, Ni^{2+}; Fe_3O_4, Ni^{2+}; Fe_3O_4 or neutral red modified graphite materials incorporated some functional groups which imitate the biological mediators and redox materials to act as assistant mediators on the surface of anode to help electron transfer (Park, D.H. and Zeikus, J.G., 2003; Kim, J.R. et al., 2005; Lowy, D.A. et al., 2006). The influence of such additions on a continuous single chamber MFC has not been tested and can all substantially increase the power densities and overall efficiency. Limited research has thus far been performed with regard to cathode materials. There are roughly two areas of concerns. Firstly, the choice of electron acceptors in cathode to function under MFC conditions, and secondly, alternative catalyst integration instead of the precious Pt catalyst that virtually all MFC designs currently depend on.

8.2.3 Bacteria behaviour

Currently the use of single species of bacteria or mixed culture in Microbial Fuel Cell is more or less showing the same efficiency. As mentioned in chapter 2, there are limitations and advantages for both approaches and both options are worth studying further. Especially for the electron transfer, which is one of the most important factors that affects the power performance of MFCs, the bacteria behaviour from organic metabolism, the release of electrons, possible production of electron mediators, as well as the electron transfer onto anode surface are all crucial topics for the breakthrough development of MFCs.

8.2.4 Combining MFC with other technologies

Future large scale employments of MFC will generate large amount of low voltage electricity and diluted hydrogen gas. Versatile designs that can (i) concentrate the power output, (ii) concentrate the hydrogen gas, and (iii) storage solutions for both electricity and hydrogen gas will need to be identified. There is potential for the MFC technology to combine with the H_2 bioreactor to produce hydrogen gas for further storage or fuel cells applications, just simply adding a small voltage to the system from a separate MFC, or together with the anaerobic digestion to produce methane in the system (Clauwaert, P. et al., 2008), and then separate and purify the biogases.

References

Aelterman, P., Rabaey, K., Pham, H. T., Boon, N. and Verstraete, W. (2006) Continuous Electricity Generation at High Voltages and Currents Using Stacked Microbial Fuel Cells. *Environ. Sci. Technol,* 40, 3388 - 3394.

Agilent (2006) Cerity Sofeware of Micro GC 3000.

Angenent, L. T., Karim, K., Al-Dahhan, M. H., Wrenn, B. A. and Domíguez-Espinosa, R. (2004) Production of bioenergy and biochemicals from industrial and agricultural wastewater *Trends in Biotechnology,* 22, 477-485.

AWAG (2008) Wastewater Treatment Process Diagram, Arkansas Watershed Advisory Group.

Barrett, E. P., Joyner, L. G. and Halenda, P. P. (1951) The Determination of Pore Volume and Area Distributions in Porous Substances. I. Computations from Nitrogen Isotherms. *Journal of the American Chemical Society,* 73, 373-380.

Bilen, K., Ozyurt, O., BakIrcI, K., KarslI, S., Erdogan, S., Yilmaz, M. and ComaklI, O. (2008) Energy production, consumption, and environmental pollution for sustainable development: A case study in Turkey. *Renewable and Sustainable Energy Reviews,* 12, 1529-1561.

Bockris, J. O. M., Reddy, A. K. N. and Gamboa-Aldeco, M. (2000) *Modern Electrochemistry: Fundamentals of Electrodics,* New York, Kluwer Academic Publishers.

Bond, D. R., Holmes, D. E., Tender, L. M. and Lovley, D. R. (2002) Electrode reducing microorganisms that harvest energy from marine sediments. *Science,* 295, 483-485.

Bond, D. R. and Lovley, D. R. (2003) Electricity production by Geobacter Sulfurreducens attached to electrodes. *Applied and environmental microbiology,* 69, 1548-1555.

Brunauer, S., Emmett, P. H. and Teller, E. (1938) Adsorption of Gases in Multimolecular Layers. *Journal of the American Chemical Society,* 60,

309-319.

Bullen, R. A., Arnot, T. C., Lakeman, J. B. and Walsh, F. C. (2006) Biofuel cells and their development. *Biosensors and Bioelectronics,* 21, 2015-2045.

Catal, T., Li, K., Bermek, H. and Liu, H. (2008) Electricity production from twelve monosaccharides using microbial fuel cells. *Journal of Power Sources,* 175, 196-200.

Chaudhuri, S. K. and Lovley, D. R. (2003) Electricity generation by direct oxidation of glucose in mediatorless microbial fuel cells. *Nature Biotechnology 21, (2003)* 21, 1229 - 1232.

Cheng, H., Scott, K. and Ramshaw, C. (2002) Intensification of Water Electrolysis in a Centrifugal Field. *Journal of The Electrochemical Society,* 149, D172-D177.

Cheng, S., Liu, H. and Logan, B. E. (2006a) Increased performance of single-chamber microbial fuel cells using an improved cathode structure. *Electrochemistry Communications* 8, 489-494

Cheng, S., Liu, H. and Logan, B. E. (2006b) Power Densities Using Different Cathode Catalysts (Pt and CoTMPP) and Polymer Binders (Nafion and PTFE) in Single Chamber Microbial Fuel Cells. *Environ. Sci. Technol,* 40, 364 - 369.

Cheng, S. and Logan, B. E. (2007) Ammonia treatment of carbon cloth anodes to enhance power generation of microbial fuel cells. *Electrochemistry Communications,* 9, 492–496.

Chiao, M., Lam, K. B. and Lin, L. (2003) Micromachined microbial fuel cells. *Micro Electro Mechanical Systems, IEEE The Sixteenth Annual International Conference on.* MEMS-03 Kyoto.

Choi, Y., Kim, N., Kim, S. and Jung, S. (2003) Dynamic Behaviors of Redox Mediators within the Hydrophobic Layers as an Important Factor for Effective Microbial Fuel Cell Operation *Bulletin of the Korean chemical society,* 24, 437-440.

Clauwaert, P., Toledo, R., van der Ha, D., Crab, R., Verstraete, W., Hu, H., Udert, K. M. and Rabaey, K. (2008) Combining biocatalyzed electrolysis with

anaerobic digestion. *Water Science & Technology,* 57, 575–579.

Cohen, B. (1931) The bacterial culture as an electrical Half-cell. *Journal of Bacteriology,* 21, 18.

Davis, F. and Higson, S. P. J. (2006) Biofuel cells—Recent advances and applications. *Biosensors and Bioelectronics,* 22, 1224-1235.

Ditzig, J., Liu, H. and Logan, B. E. (2007) Production of hydrogen from domestic wastewater using a bioelectrochemically assisted microbial reactor (BEAMR). *International Journal of Hydrogen Energy* Article in Press, Corrected Proof.

Dumas, C., Mollica, A., F´eron, D., Basseguy, R., Etcheverry, L. and Bergel, A. (2007) Marine microbial fuel cell: Use of stainless steel electrodes as anode and cathode materials. *Electrochimica Acta,* 53, 468-473.

EIA (2008) International Energy Outlook 2008, Energy Information Administration.

EPA (2002) Managing manure with biogas recovery systems improved performance at competitive costs, U.S. Environmental Protection Agency.

EPA (2008) Sustainable Infrastructure for Water & Wastewater. U.S. Environmental Protection Agency.

ESD (2003) English partnerships sustainable energy review, Energy for Sustainable Development.

Fang, H. H. P., Liu, H. and T. Zhang, T. (2002) Characterization of a Hydrogen-Prodducing granular sludge. *Biotechnology and bioengineering,* 78.

Forster, C. F. (2003) *Wastewater treatment and technology*, Thomas Telford Publishing.

Freguia, S., Rabaey, K., Yuan, Z. and Keller, J. (2007) Non-catalyzed cathodic oxygen reduction at graphite granules in microbial fuel cells. *Electrochimica Acta,* 53, 598–603.

Goldstein, J., Newbury, D. E., Joy, D. C., Lyman, C. E., Echlin, P., Lifshin, E., Sawyer, L. and Michael, J. R. (2003) *Scanning Electron Microscopy and X-ray Microanalysis*, Springer.

Gorby, Y. A., Yanina, S., McLean, J. S., Rosso, K. M., Moyles, D., Dohnalkova, A., Beveridge, T. J., Chang, I. S., Kim, B. H., Kim, K. S., Culley, D. E., Reed, S. B., Romine, M. F., Saffarini, D. A., Hill, E. A., Shi, L., Elias, D. A., Kennedy, D. W., Pinchuk, G., Watanabe, K., Ishii, S., Logan, B. E., Nealson, K. H. and Jim K. Fredrickson, J. K. (2006) Electrically conductive bacterial nanowires produced by Shewanella oneidensis strain MR-1and other microorganisms. *Proceedings of the National Academy of Sciences of the United States of America (PNAS),* 103, 11358-11363.

Grove, W. R. (1839) On voltaic series and the combination of gases by platinum. *Phlosophical magazine and journal of science, series 3,* 14, 127-130.

Habermann, W. and Pommer, E. (1991) Biological fuel cells with sulphide storage capacity. *Applied Microbiology and Biotechnology,* 35, 128-133.

Hammer, M. J. and Hammer, M. J. J. (2008) *Water and wastewater technology* Pearson/Prentice Hall.

Hasvold, Ø., Henriksen, H., Melvr, E., Citi, G., Johansen, B., Kjønigsen, T. and Galetti, R. (1997) Sea-water battery for subsea control systems *Journal of Power Sources* 65, 253-261.

He, Z., Minteer, S. D. and Angenent, L. T. (2005) Electricity Generation from Artificial Wastewater Using an Upflow Microbial Fuel Cell. *Environ. Sci. Technol,* 39, 5262 - 5267.

He, Z., Shao, H. and Angenent, L. T. (2007) Increased power production from a sediment microbial fuel cell with a rotating cathode. *Biosensors and Bioelectronics,* 22, 3252–3255.

Hoggers, G. (2002) *Fuel cell technology handbook*, CRC Press.

Ieropoulos, I. A., Greenman, J., Melhuish, C. and Hart, J. (2005) Comparative study of three types of microbial fuel cell. *Enzyme and Microbial Technology* 37, 238-245.

Ileleji, K. E., Martin, C. and Jones, D. (2008) Basics of Energy Production through Anaerobic Digestion of Livestock Manure. *Purdue Extension BioEnergy series*, ID-406-W.

IPCC (2001) IPCC 2001 b: Emissions scenarios: A special report of working group III of the Intergovernmental Panel on Climate Change.

Jang, J. K., Phama, T. H., Changa, I. S., Kanga, K. H., Moona, H., Chob, K. S. and Kim, B. H. (2004) Construction and operation of a novel mediator- and membrane-less microbial fuel cell. *Process Biochemistry,* 39, 1007–1012.

Jensen, K. F. (2001) Microreaction engineering - is small better? *Chemical Engineering Science,* 56, 293-303.

Kim, H. J., Park, H. S., Hyun, M. S., Chang, I. S., Kim, M. and Kim, B. H. (2002) A mediator-less microbial fuel cell using a metal reducing bacterium, Shewanella putrefaciens *Enzyme and Microbial Technology* 30, 145-152.

Kim, J. R., Min, B. and Logan, B. E. (2005) Evaluation of procedures to acclimate a microbial fuel cell for electricity production. *Appl.Microbiol. Biotechnol,* 68, 23-30.

Korneel Rabaey, W. V. (2005) Microbial fuel cells: novel biothechnology for energy generation. *Trends in Biotechnnology,* 23, 291-298.

Larminie, J. and Dicks, A. (2003) *Fuel Cell Systems Explained* John Wiley & Sons.

Liu, H., Cheng, S. and Logan, B. E. (2005a) Power Generation in Fed-Batch Microbial Fuel Cells as a Function of Ionic Strength, Temperature, and Reactor Configuration. *Environ. Sci. Technol,* 39, 5488 - 5493.

Liu, H., Cheng, S. and Logan, B. E. (2005b) Production of Electricity from Acetate or Butyrate Using a Single-Chamber Microbial Fuel Cell. *Environ. Sci. Technol,* 39, 658 - 662.

Liu, H. and Fang, H. H. P. (2003) Hydrogen production from wastewater by acidogenic granular sludge. *Water Science & Technology* 47, 153–158.

Liu, H., Grot, S. and Logan, B. E. (2005c) Electrochemically Assisted Microbial Production of Hydrogen from Acetate. *Environ. Sci. Technol,* 39, 4317 - 4320.

Liu, H. and Logan, B. E. (2004) Electricity Generation Using an Air-Cathode Single Chamber Microbial Fuel Cell in the Presence and Absence of a Proton Exchange Membrane. *Environ. Sci. Technol,* 38, 4040 - 4046.

Liu, H., Ramnarayanan, R. and Logan, B. E. (2004) Production of Electricity during Wastewater Treatment Using a Single Chamber Microbial Fuel Cell. *Environ. Sci. Technol,* 38, 2281 - 2285.

Liu, Z.-D., Lian, J., Du, Z.-W. and Li, H.-R. (2006) Construction of Sugar-based Microbial Fuel Cells by Dissimilatory Metal Reduction Bacteria. *Chinese Journal of Biotechnology,* 22, 131-137.

Logan, B. E. (1999) *Environmental Transport Processes*, John Wiley &Sons, Inc.

Logan, B. E. (2004) Extracting hydrogen and electricity from renewable resources. *Environmental science & technology,* 38, 161A-1667A.

Logan, B. E., Hamelers, B., Rozendal, R., Schröder, U., Keller, J., Freguia, S., Aelterman, P., Verstraete, W. and Rabaey, K. (2006) Microbial Fuel Cells: Methodology and Technology *Environ. Sci. Technol,* 40, 5181-5192.

Logan, B. E., Murano, C., Scott, K., Gray, N. D. and Head, M. (2005) Electricity generation from cysteine in a microbial fuel cell *Water Research* 39, 942-952.

Logan, B. E., Oh, S., Kim, I. S. and Ginkel, S. V. (2002) Biological Hydrogen Production Measured in Batch Anaerobic Respirometers. *Environ. Sci. Technol,* 36, 2530 - 2535.

Logan, B. E. and Regan, J. M. (2006) Microbial fuel cell- challenges and applications. *Environmental Science & Technology,* 40, 5172-5180.

Lovley, D. R. (2006a) Bug juice: harvesting electricity with microorganisms. *Nature reviews. microbiology,* 4, 497-508.

Lovley, D. R. (2006b) MIcrobial fuel cells: novel microbial physiologies and engineering approaches. *Current Opinion in Biotechnology* 17, 327-332.

Lowy, D. A., Tender, L. M., Zeikus, J. G., Park, D. H. and Lovley, D. R. (2006) Harvesting energy from the marine sediment–water interface II Kinetic activity of anode materials. *Biosensors and Bioelectronics,* 21, 2058–2063.

Madigan, M. T. and Martinko, J. (2006) *Brock Biology of Microorganisms*, Prentice Hall.

Martinot, E. (2006) Renewable energy gains momentum: Global markets and

policies in the spotlight. *Environment,* 48, 26-43.

Martinot, E., Chaurey, A., Lew, D., Moreira, J. R. and Wamukonya, N. (2002) Renewable energy markets in developing countries. *Annual Review of Energy and the Environment,* 27, 309-348.

McIntyre, D. R., Burstein, G. T. and Vossen, A. (2002) Effect of carbon monoxide on the electrooxidation of hydrogen by tungsten carbide. *Journal of Power Sources,* 107, 67-73.

McKinlay, J. B. and Zeikus, J. G. (2004) Extracellular Iron Reduction Is Mediated in Part by Neutral Red and Hydrogenase in Escherichia coli. *Applied and environmental microbiology,* 70, 3467–3474.

Min, B., Cheng, S. and Logan, B. E. (2005a) Electricity generation using membrane and salt bridge microbial fuel cells *Water Research* 39, 1675-1686.

Min, B., Kim, J., Oh, S., Regan, J. M. and Logan, B. E. (2005b) Electricity generation from swine wastewater using microbial fuel cells *Water Research,* 39, 4961-4968.

Min, B. and Logan, B. E. (2004) Continuous Electricity Generation from Domestic Wastewater and Organic Substrates in a Flat Plate Microbial Fuel Cell. *Environ. Sci. Technol,* 38, 5809-5814.

Moon, H., Chang, I. S. and Kim, B. H. (2006) Continuous electricity production from artificial wastewater using a mediator-less microbial fuel cell. *Bioresource Technology* 97, 621-627.

Morris, J. M., Jin, S., Wang, J., Zhu, C. and Urynowicz, M. A. (2007) Lead dioxide as an alternative catalyst to platinum in microbial fuel cells. *Electrochemistry Communications,* 9, 1730–1734.

Nevin, K. P. and Lovley, D. R. (2002) Mechanisms for Accessing Insoluble Fe(III) Oxide during Dissimilatory Fe(III) Reduction by Geothrix fermentans. *APPLIED AND ENVIRONMENTAL MICROBIOLOGY,* 68, 2294–2299.

Niessen, J., Schröder, U., Rosenbaum, M. and Scholz, F. (2004) Fluorinated polyanilines as superior materials for electrocatalytic anodes in bacterial fuel cells. *Electrochemistry Communications* 6, 571-575.

OFWAT (2007) Water and sewerage charges 2007-08 report. Birmingham, Water Services Regulation Authority.

Oh, S. E. and Logan, B. E. (2005) Hydrogen and electricity production from a food processing wastewater using fermentation and microbial fuel cell technologies *Water Research,* 39, 4673-4682

Oh, S. E. and Logan, B. E. (2006) Proton exchange membrane and electrode surface areas as factors that affect power generation in microbial fuel cells. *Appl Microbiol Biotechnol,* 70, 162–169.

Oh, S. E., Min, B. and Logan, B. E. (2004) Cathode Performance as a Factor in Electricity Generation in Microbial Fuel Cells. *Environ. Sci. Technol,* 38, 4900 - 4904.

Palanker, V. S., Gajyev, R. A. and Sokixsky, D. V. (1977) On adsorption and Electro-oxidation of some compounds on Tungsten Carbide- their effect on hydrogen electro-oxidation. *Electrochim Acta,* 22, 133-136.

Park, D. H. and Zeikus, J. G. (1999) Utilization of Electrically Reduced Neutral Red by Actinobacillus succinogenes: Physiological Function of Neutral Red in Membrane-Driven Fumarate Reduction and Energy Conservation. *Journal of Bacteriology,* 181, 2403-2410.

Park, D. H. and Zeikus, J. G. (2002) Impact of electrode composition on electricity generation in a single-compartment fuel cell using Shewanella putrefaciens. *Applied microbiology and biotechnology* 58-61.

Park, D. H. and Zeikus, J. G. (2003) Improved Fuel Cell and Electrode Designs for Producing Electricity from Microbial Degradation. *BIOTECHNOLOGY AND BIOENGINEERING,* 81.

Phung, N. T., Lee, J., Kang, K. H., Chang, I. S., Gadd, G. M. and Kim, B. H. (2004) Analysis of microbial diversity in oligotrophic microbial fuel cells using 16S rDNA sequences. *FEMS Microbiology Letters,* 233, 77-82.

Prasad, D., Sivaram, T. K., Berchmans, S. and Yegnaraman, V. (2006) Microbial fuel cell constructed with a micro-organism isolated from sugar industry effluent. *Journal of Power Sources,* 160, 991-996.

Qiao, Y., Li, C. M., Bao, S. and Bao, Q. (2007) Carbon nanotube/polyaniline composite as anode material for microbial fuel cells. *Journal of Power Sources,* 170, 79–84.

Rabaey, K., Boon, N., Hofte, M. and Verstraete, W. (2005a) Microbial Phenazine Production Enhances Electron Transfer in Biofuel Cells. *Environ. Sci. Technol.,* 39, 3401-3408.

Rabaey, K., Boon, N., Siciliano, S. D., Verhaege, M. and W., V. (2004) Biofuel Cells Select for Microbial Consortia That Self-Mediate Electron Transfer *Appl. Environ. Microbiol. 2004 70: ,* 70, 5373-5382.

Rabaey, K., Clauwaert, P., Aelterman, P. and Verstraete, W. (2005b) Tubular Microbial Fuel Cells for Efficient Electricity Generation. *Environ. Sci. Technol,* 39, 8077 - 8082.

Rabaey, K., Lissens, G., Siciliano, S. D. and Verstraete, W. (2003) A microbial fuel cell capable of converting glucose to electricity at high rate and efficiency. *Biotechnology Letters,* 25, 1531–1535.

Rabaey, K., Ossieur, W., Verhaege, M. and Verstraete, W. (2005c) Continuous microbial fuel cells convert carbonhydrates to electricity. *Water Science & Technology,* 52, 515-523.

Rabaey, K. and Verstraete, W. (2005) Microbial fuel cells: novel biothechnology for energy generation. *Trends in Biotechnnology,* 23, 291-298.

Rao, J. R., Richter, G. J., Sturm, F. V. and Weidlich, E. (1976) The Performance of Glucose Electrodes ,and the Characteristics of Different .Biofuel Cell Constructions. *Bioelectrochemistry and Biobzergetics,* 3, 139-150.

Rao, M. L. B. and Drake, R. F. (1969) Studies of electrooxidation of dextrose in neutral media. *Journal of electrochemical society,* 116, 334-337.

Reguera, G., McCarthy, K. D., Mehta, T., Nicoll, J. S., Tuominen, M. T. and Lovley, D. R. (2005) Extracellular electron transfer via microbial nanowires. *Nature,* 435, 1098-1101.

Reguera, G., Nevin, K. P., Nicoll, J. S., Covalla, S. F., Woodard, T. L. and Lovley, D. R. (2006) Biofilm and Nanowire Production Leads to Increased Current in

Geobacter sulfurreducens Fuel Cells. *APPLIED AND ENVIRONMENTAL MICROBIOLOGY,* 72, 7345–7348.

Reimers, C. E., Tender, L. M., Fertig, S. and Wang, W. (2001) Harvesting Energy from the Marine Sediment-Water Interface. *Environ. Sci. Technol,* 35, 192 - 195.

Ringeisen, B. R., Henderson, E., Wu, P. K., Pietron, J., Ray, R., Little, B., Biffinger, J. C. and Jones-Meehan, J. M. (2006) High Power Density from a Miniature Microbial Fuel Cell Using Shewanella oneidensis DSP10. *Environ. Sci. Technol,* 40, 2629 - 2634.

Rodrigo, M. A., Cañizares, P., Lobato, J., Paz, R., Sáez, C. and Linares, J. J. (2007) Production of electricity from the treatment of urban waste water using a microbial fuel cell. *Journal of Power Sources,* 169, 198-204.

Roller, S. D., Bennetto, H. P., Delaney, G. M., Mason, J. R., Stirling, J. L. and Thurston, C. F. (1984) Electron-transfer coupling in microbial fuel cells.1.Comparison of redox-mediator reduction rates and respiratory rates of bacteria. *J. Chem. Technol. Biotechnol. B Biotechnol. ,* 34, 3-12.

Rosenbaum, M., Schröder, U. and Scholz, F. (2005) In Situ Electrooxidation of Photobiological Hydrogen in a Photobioelectrochemical Fuel Cell Based on Rhodobacter sphaeroides. *Environ. Sci. Technol,* 39, 6328 - 6333.

Rosenbaum, M., Zhao, F., Quaas, M., Wulff, H., Schro¨der, U. and Scholz, F. (2007) Evaluation of catalytic properties of tungsten carbide for the anode of microbial fuel cells. *Applied Catalysis B: Environmental,* 74, 261–269.

Rozendal, R. A., Hamelers, H. V. M., Euverink, G. J. W., Metz, S. J. and Buisman, C. J. N. (2006) Principle and perspectives of hydrogen production through biocatalyzed electrolysis. *International Journal of hydrogen energy,* 31, 1632-1640.

RSC (2007) Sustainable Water: Chemical Science Priorities Summary Report, Royal Society of Chemistry.

Schroder, U., Niessen, J. and Scholz, F. (2003) A generation of microbial fuel cells with current outputs boosted by more than one order of magnitude.

Angewandte Chemie-International Edition, 42, 2880-2883.

Scottish-Executive (2006) Promoting and accelerating the market penetration of biomass technology in Scoltland.

Shukla, A. K., Suresh, P., Berchmans, S. and Rajendran, A. (2004) Biological fuel cells and their applications. *CURRENT SCIENCE,* 87, 455-468.

Stojic´, D. L., Marc´eta, M. P., Sovilj, S. P. and Miljanic´, S. S. (2003) Hydrogen generation from water electrolysis-Possibilities of energy saving. *Journal of Power Sources,* 118, 315-319.

Tsuchiya, H. and Kobayashi, O. (2004) Mass production cost of PEM fuel cell by learning curve. *International Journal of Hydrogen Energy,* 29, 985-990.

USDA (2007) An Analysis of Energy Production Costs from Anaerobic Digestion Systems on U.S. Livestock Production Facilities. The U.S. Department of Agriculture.

WBCSD (2004) Facts and trends to 2050 energy and climate change. World Business council sustainable development.

WBCSD (2005a) Collaborative actions for sustainable water management. Conches-Geneva, World Business council sustainable development.

WBCSD (2005b) Facts and trends Water. Conches-Geneva, World Business council sustainable development.

White, S., Fowler, H., Blenkinsop, S., McDonald, A., Parson, S., Jefferson, B. and Christopher, N. (2007) Sustainable Water: Chemical Science Priorities Summary Report IN J., H. (Ed. london, Royal Society of Chemistry).

Wiesmann, U., Choi, I. S. and Dombrowski, E.-M. (2007) *Fundamentals of biological wastewater treatment*, Weinheim: Wiley-VCH.

Woodward, J., Orr, M., Cordray, K. and Greenbaum, E. (2000) Biotechnology - Enzymatic production of biohydrogen. *Nature,* 405, 1014-1015.

Xia, Y. and Whitesides, M. G. (1998) Soft Lithography. *Angew. Chem. Int. Ed.,* 37, 550 ± 575.

Yao, S. J., Appleby, A. J., Geisel, A., Cash, H. R. and Wolfson, S. K. (1969) Anodic oxidation of carbonhydrates and their derivatives in neutral saline solution.

Nature, 224, 921-922.

You, S., Zhao, Q., Zhang, J., Jiang, J., Wan, C., Du, M. and Zhao, S. (2007) A graphite-granule membrane-less tubular air-cathode microbial fuel cell for power generation under continuously operational conditions. *Journal of Power Sources,* 173.

You, S., Zhao, Q., Zhang, J., Jiang, J. and Zhao, S. (2006) A microbial fuel cell using permanganate as the cathodic electron acceptor. *Journal of Power Sources,* 162, 1409–1415.

Yu, E. H., Cheng, S., Scotta, K. and Logan, B. E. (2007) Microbial fuel cell performance with non- Pt cathode catalysts. *Journal of Power Sources,* 171, 275-281.

Zhang, E., Xu, W., Diao, G. and Shuang, C. (2006) Electricity generation from acetate and glucose by sedimentary bacterium attached to electrode in microbial-anode fuel cells

Journal of Power Sources, 161, 820-825.

Zhao, F., Harnisch, F., Schroder, U., Scholz, F., Bogdanoff, P. and I., H. (2006) Challenges and Constraints of Using Oxygen Cathodes in Microbial Fuel Cells. *ENVIRONMENTAL SCIENCE & TECHNOLOGY,* 40, 5193-5199.